6 November 1976

7.7-10.16.7

CR-152668

THEMATIC MAPPING, LAND USE, GEOLOGICAL STRUCTURE AND WATER RESOURCES IN CENTRAL SPAIN

Project no. 28760

FINAL REPORT

28760

PRINCIPAL INVESTIGATOR: Dr. Núñez de las Cuevas

AGENCY: Instituto Geográfico y Catastral

General Ibáñez de Ibero, 3 - MADRID-3 (Spain)

6 November, 1976

THEMATIC MAPPING, LAND USE, GEOLOGICAL STRUCTURE AND
WATER RESOURCES IN CENTRAL SPAIN

Project. no.28760

FINAL REPORT

CONTRIBUTING ORGANIZATIONS

- Centro de Estudios Hidrográ
  ficos del Ministerio de
  Obras Públicas.

- Instituto de Geografía Apli
  cada del Consejo Superior
  de Investigaciones Científi
  cas.

- Instituto de Edafología del
  Consejo Superior de Investi
  gaciones Científicas

- Servicio de Fotogrametría y
  Fotointerpretación de la
  Universidad Politécnica de
  Madrid.

- Cátedra de Geodinámica In
  terna de la Universidad
  Complutense de Madrid.

- Cátedra de Geografía de
  la Universidad Compluten-
  se de Madrid.

- Centro de Investigación
  UAM-IBM de la Universidad
  Autónoma de Madrid.

- Laboratorio de Teledetec-
  ción del Instituto Geográ
  fico y Catastral.

I N D E X

CARTOGRAPHY

DIGITAL PROCESSING

EDAPHOLOGY

FORESTRY

THEMATIC MAPPING, LAND USE, GEOLOGICAL STRUCTURE AND WATER
RESOURCES IN CENTRAL SPAIN.

Project no. 28760

I. INTRODUCTION

This Final Report is submitted to NASA as result of one year
of investigations carried out in multidisciplinary mode by
the participant organizations in project no. 28760, for the
purpose of studying applications of LANDSAT -2 data to
several scientific fields in Central Spain.

This project involved the participation of various official
agencies and working groups related to the problem of surveying
the earth surface for their own scientific application. Ins-
tituto Geográfico y Catastral is the agency that holds the
coordinative function in project no. 28760, with the contribution
of the following organizations:

- Center of Hydrographic Studies, of the Ministry of Public
  Works

- Institute of Applied Geography, of the Head Council of
  Scientific Research

- Institute of Edaphology, of the Head Council of Scientific
  Research

- Service of Photogrammetry and Photointerpretation, of the
  Polytechnic University of Madrid

- Department of Internal Geodynamics, of the Complutense
  University of Madrid

- Department of Geography, of the Complutense University of
  Madrid

- IBM-Scientific Center, of the Autonomous University of Madrid

In spite of political changes occurred in the country during
the last year, the basic team of research has been maintained
as participant in the project, although some working groups
had to resign their contribution, mainly because variations
arose in their scientific and technical staff able to conduct
it. On the other hand, several new organizations have joined
the multidisciplinary group which, as result of its reinforced
capability for analysing LANDSAT-2 data, was ready to envisage
new applications of the satellite multispectral information,
although such new scientific works had not been considered
in the proposal submitted to NASA for approval of this project
in January 1973.

The items of investigation studied have been the following:

- cartography
- digital processing
- edaphology
- forestry
- geology
- geomorphology
- land use
- remote sensing techniques
- water resources

As general objective was defined the research in various
disciplines by means of LANDSAT-2 data taken over Central
Spain, for the purpose of developing an operational methodology
able to contemplate future space programs as a valuable working
tool in the knowledge of the earth disciplines. Every working
group has conducted the investigation applied to his own area
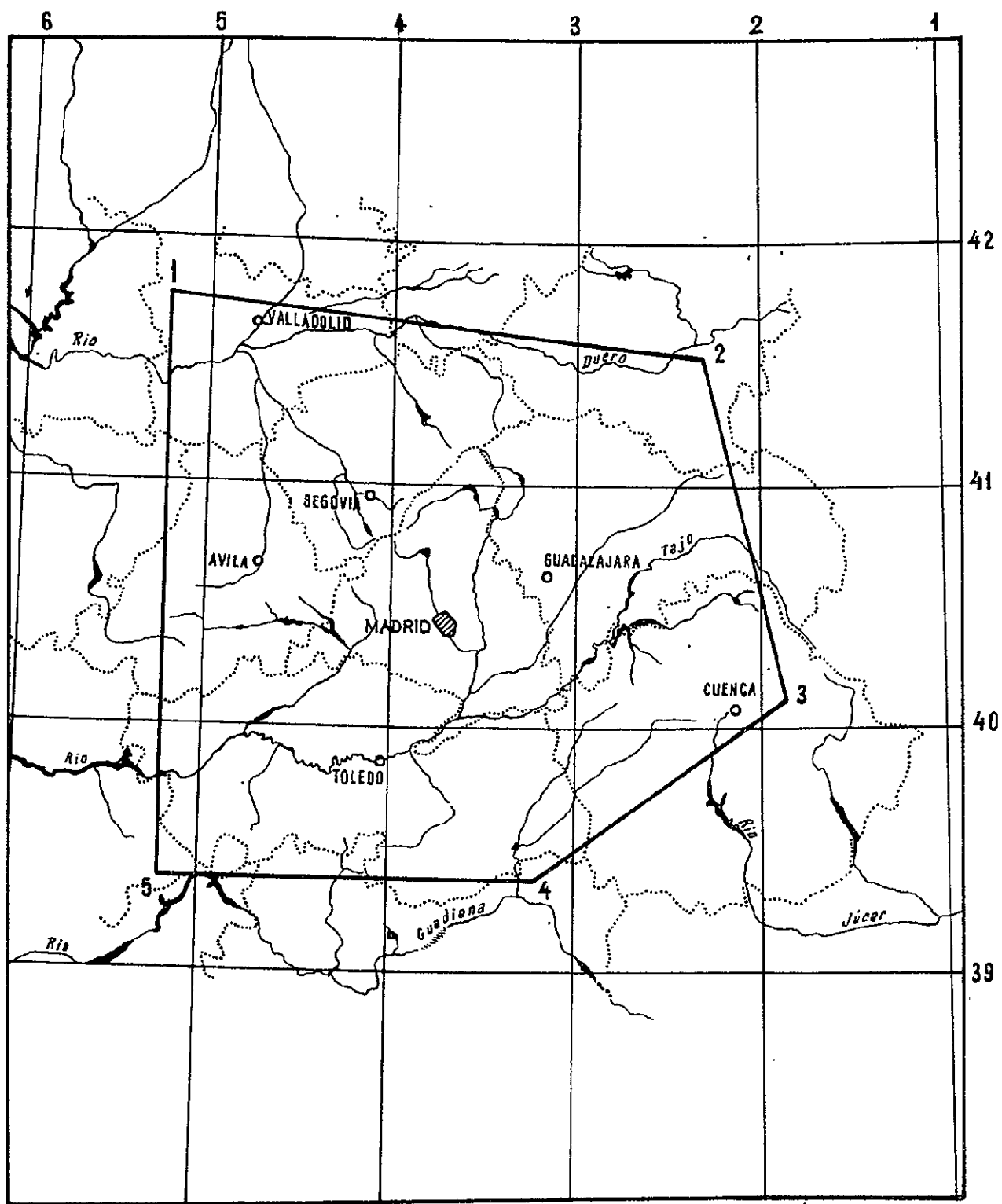
point no.	LATITUDE DEG		MIN		DIR	LONGITUDE DEG			MIN		DIR
1	4	1	5	6	N	0	0	5	1	1	W
2	4	1	3	2	N	0	0	2	1	0	W
3	4	0	0	8	N	0	0	1	5	2	W
4	3	9	4	3	N	0	0	9	1	2	W
5	3	9	2	2	N	0	0	5	1	3	W

Area of study in Central Spain
selected in project no. 28760

of interest, but all the participant organizations have the
benefit of an exchange of know-how and a continuous contact
between their scientific personnel. Furthermore, the techniques
and equipment available have been exploited in common, in a
joint effort to carry out this NASA supported project for the
benefit of all the national community.

As principal result of this project can be stated that a group
of investigators has worked together during one year, attending
various results in the applications of LANDSAT information to
their own area of scientific interest. In this case, LANDSAT-2
satellite has been the agglutinant which made possible the
success of the multidisciplinary group formed.

In the adjoining figure is represented the area of Central Spain
which was selected to carry out this project.

2. OBJECTIVES

Because the heterogeneous nature of the multidisciplinary
group in charge of this project, various specific objectives
have been defined in each application. They are the following:

Cartography. As a first step it was intended to determine
whether or not LANDSAT MSS data could be used for updating
maps at small scale in Central Spain, with enough cartographic
accuracy. Once established such capability, the purpose of the
investigation was focused in defining what kind of data could
be extracted (or updated) from LANDSAT information. As a third
step it was determined the application of the above mentioned
possibilities to the specific case of small scale Maps in the
country, producing an updated at scale 1:200.000 of the
Central Region.

Digital processing. In this field it was intended to study radiometric enhancement methods when applied to LANDSAT MSS data, for the purpose of obtaining improved images through a DICOMED D-47 film recorder. Research was focused to the analysis of NASA CCTs when converted to tapes in 8-bit at linear mode.

As a second objective it was defined the need of obtaining uncorrelated bands of the MSS sensor, in order to exclude redundant information used as input to an automatic classifier. Such objective was accomplished by study of linear combinations of channels in an image with an arbitrary number of them.

As a third objective it was intended to obtain relevant information from MSS data by the use of band ratioing techniques. Such procedure has been applied to eliminate light cloud cover and in geological studies.

Edaphology. This item has been studied with digital MSS data for the purpose of selecting, by clustering techniques spectral classes which could be representative in Central Spain of certain types of land use and soils, allowing their automatic classification in computer.

Forestry. The application of LANDSAT data to forestry had the purpose of differentiating several types of conifers species in Central Spain by means of a supervised classification in computer. Species selected have been the most common in the area: Pinus pinaster Sol., Pinus pinea L. and Pinus sylvestris L.

Geology. Two main objectives were defined in this scientific field. First, it was evaluated the capability of LANDSAT images to detect ample geological structures in Central Spain by photointerpretation techniques. Secondly, an analysis of band ratios of MSS digital data was done with the purpose of defining the best combinations to be applied in geology.

Geomorphology. In this field some analysis was conducted for
evaluating the geomorphological characteristics of LANDSAT
images when studied by photointerpretation techniques,
reviewing their capability for stereoscopic vision and
various morphostructural aspects.

Land use. It was intended to do thematic cartography of land
use by photointerpretation of LANDSAT images to small scales.
As result of this work two maps have been produced at scales
1:250.000 and 1:500.000 of the Province of Madrid.

Remote Sensing techniques. A multispectral survey was conducted
in Aranjuez test site with the purpose of applying aerospace
remote sensing techniques to various disciplines in a multidis-
ciplinary approach. LANDSAT information was used in the intent
of correlating it to the data obtained by means of airborne
photographic cameras and a multispectral scanner Daedalus.

Water resources. In this work an evalutation of LANDSAT data
has been carried out in multidisciplinary mode for determining
their real applications in hydrology. The area of study as
test site has been the Guadarrama basin. Agronomic, forestry,
hydrological and geological photointerpretation of the area
was conducted, as well as digital processing of LANDSAT data.

3. PARTICIPANT ORGANIZATIONS

Since the date of submission of proposal for this project, in
January 1973, several participant organizations have left
behind their contribution. They are the following:

- Instituto Geológico y Minero de España
- Comisión de Planeamiento y Coordinación del Area Metropolitana
  de Madrid (COPLACO).

- Cátedra de Botánica de la Universidad Complutense de Madrid.
- Cátedra de Ecología de la Universidad de Sevilla.

As stated before, such situation was forced by political changes occurred in the country during the last year, and because these working groups did not maintain their original staff of scientists and technicians able to conduct the project. The new participants who joined the multidisciplinary group in the last four years are the following:

- Centro de Investigación UAM-IBM de la Universidad Autónoma de Madrid.
- Servicio de Fotogrametría y Fotointerpretación de la Univer_. sidad Politécnica de Madrid.

The IBM-Scientific Center provided in this project all the required digital processing of LANDSAT data, carrying out a multidisciplinary work in connection with all the participants. During the year 1974 an IBM 360/65 computer (1024 K) was installed in the Center, interfaced to an interactive TV terminal RAMTEK. The software used was ERMAN-II program, which is the commercial version of ERIPS program developed by IBM-FSD for NASA in Houston. The capabilities of ERMAN-II program are the following:

- Pattern Recognition
- Image Registration
- Load
- Image composition
- Image manipulation and display
- Delog

Acting of the IBM-Scientific Center in the project was possible because its dedication to support research programs in the country contributing to the benefit of the national community.

EQUIPMENTS	IGC REMOTE SENSING LABORATORY/PHOTOINTERPRETATION FACILITY							
	INPUT				OUTPUT			
	PRODUCT	IMAGE	FORMAT	SCALE	PRODUCT	FORMAT	IMAGE	SCALE
LIGHT TABLES	ROLL FILM CUT FILM	COLOR (+) COLOR (-) B & W (+) B & W (-) IR B&W IR COLOR	FROM 35 mm TO 9¼"	LANDSAT MAXIMUM 1:1.000000 AERIAL ANY	SAME AS INPUT	SAME AS INPUT	SAME AS INPUT	SAME AS INPUT
ADDITIVE COLOR COMPOSITE VIEWER	ROLL FILM CUT FILM	POSITIVE B & W	70 mm	LANDSAT 1:3369.000 AERIAL ANY	HORIZONTAL SCREEN PROJECTION	B&W COLOR IR B&W IR COLOR	20"x20"	LANDSAT 1:500.000 AERIAL 6'74 x ENLARGEMENT

Table 1.

HARDWARE	IGC REMOTE SENSING LABORATORY/COMPUTER FACILITY						
	INPUT		SOFTWARE	OUTPUT		
	PRODUCT	FORMAT		PRODUCT	FORMAT	IMAGE
FILM RECORDER INTERFACED TO PDP 11/45 COMPUTER	LANDSAT CCT REFORMATED AERIAL MSS REFORMATED	9 TRACK 800 BPI	DICOMED	CUT FILM 4"x5"	70 mm	COLOR (+) COLOR (-) B & W (-)
IBM 360/65 & IBM 370/145 REMOTE TERMINAL	DIGITAL TAPES	9 TRACK 800 BPI	LARSYS	PATTERN RECOGNITION	PAPER PRINTOUT	-

Table 2.

Table 3

EQUIPMENTS	IGC REMOTE SENSING LABORATORY/PHOTOGRAPHIC FACILITY								
	INPUT				PROCESS	OUTPUT			
	PRODUCT	FORMAT	SCALE	IMAGE		PRODUCT	FORMAT	SCALE	IMAGE
DURST COLOR ENLARGER	CUT FILM	MAXIMUM 13x18cms	LANDSAT 70 mm	B&W (+)	COLOR COMPOSITE GENERATION	CIBACHROME PAPER	MAXIMUM 20"x20"	LANDSAT MAXIMUM 1:500.000	COLOR(+)
				B&W (-)	ENLARGEMENT	AGFA PAPER			B&W (+)
				COLOR(+)		CIBACHROME PAPER			COLOR(+)
			AERIAL ANY	COLOR(-)		KODAK PAPER		AERIAL ANY	COLOR(+)

Table 3.

Table 4

| EQUIPMENT | IGC REMOTE SENSING LABORATORY/FIELD TEST FACILITY | | | |
	ENVIRONMENTAL MEASUREMENT	PARAMETER	RANGE	OUTPUT
MOTOR BOAT	WATER	TRANSPORTATION	-	-
TRUCK	LAND	TRANSPORTATION	-	-
CONTACT THERMOMETER	LAND WATER/AIR	SURFACE TEMPERATURE	$-10^{o} + 60^{o}$	REGISTER
SOIL THERMOMETER	LAND	TEMPERATURE 30 cms DEPTH	$-10^{o} + 65^{o}$	INDICATOR
WATER THERMOMETER	WATER	TEMPERATURE UNTIL 15m DEPTH	$-10^{o} + 60^{o}$	INDICATOR
pH-METER	WATER LAND	ACIDITY	$0 - 14$	INDICATOR
AUTOMATIC METEOROLOGICAL STATION	AIR	WIND SPEED WIND DIRECTION RELATIVE HUMIDITY TEMPERATURE	0'75mph $0^{o} - 360^{o}$ $0 - 100\%$ $-35^{o} + 49^{o}C$	REGISTER
SPECTROPHOTOMETER	WATER	COLOR TURBIDITY SUSPENDED SOLIDS 57 TESTS ON LABORATORY	VARIABLE	INDICATOR
SPECTRORADIOMETER	LAND WATER	PERCENT DIRECTIONAL REFLECTANCE	400 nm 1350 nm WAVELENGTH	COMPUTER PRINTOUT
CONDUCTIVITY METER	WATER LAND	SALINITY CONDUCTIVITY	$0 - 100$	INDICATOR
NOT DECIDED	LAND	HUMIDITY	$0 - 100\%$	INDICATOR

Table 4.

EQUIPMENTS	IGC REMOTE SENSING LABORATORY/LIBRARY FACILITY	
	PRODUCTS	FORMAT
MICROFICHE READER	NTIS MICROFICHES	4" x 5"
MICROFILM READER	LANDSAT MICROFILMS	16 mm
BIBLIOGRAPHY	BOOKS REVIEWS NEWSLETTERS	ANY
ARCHIVE	IMAGES	ANY
AUDIOVISUAL	FILMS	ANY

Table 5.

As a non profit organization the Center is governed by a Board
of Trustees under the presidence of the Autonomous University
of Madrid rector.

The Service of Photogrammetry and Photointerpretation has
conducted in this project basic field work during the
multispectral survey of Aranjuez test site, mainly focused
to the identification of different types of farming crops.
The Service has phtointerpretation facilities and conducts
every year several courses on photogrammetry, photointerpretation
and related applications.

4. TECHNIQUES

LANDSAT information was studied in this project in two
different modes:

- photographic images: most of them in black and white paper
  prints at scale 1:500.000.
- digital tapes: which have been provided by NASA upon request
  to the EROS Data Center.

MSS information over Central Spain was multispectral and
multitemporal, covering all the area with 25 images from October
1975 ot April 1976.

In an effort to provide to all participants in the project
with their needed LANDSAT imagery and digital processing
capability, Instituto Geográfico y Catastral (I.G.C.) has
installed during the year 1975 a Remote Sensing Laboratory
which was intended also for developing other national programs
on remote sensing. Although the Laboratory can conduct research
in various scientific fields in multidisciplinary mode, its
major participation in the project has been focused to the
following activities:

- reproduction work of LANDSAT 70 mms transparencies (-) and
  enlargement to operational scales in photointerpretation.
- evaluation of the cartographic applications of LANDSAT
  imagery and production (or updating) of maps at small scale.
  This activity was carried out in connection with the
  Cartography Division of I.G.C.
- Support to the IBM-Scientific Center. of the Autonomous
  University of Madrid for developing a digital processing
  capability of LANDSAT data, and conversion of tapes to
  images by means of a DICOMED D-47 film recorder.

The Remote Sensing Laboratory has carried out also the relations
with NASA in this project, as well as the submission of Quarterly
and Final Reports, upon receipt of them from the multidisci-
plinary group. Printing work was done by the Cartographic
Division of I.G.C. In tables 1 to 5 is presented the structure
and facilities of the Laboratory, as they were submitted in the
First Quarterly Report.

As the project was multidisciplinary every participant has
used the techniques required for his own scientific application,
and such techniques have shown very different from one group
to the other. Because they are indicated in the various
contributions, none comment is included in this section on
such subject.

Some remarks are exposed here on the photographic processing
of LANDSAT data conducted by the Remote Sensing Laboratory of
I.G.C. This activity has been divided in two part, each one
requiring different techniques:

1. Black and white processing. The original 70 mms transparencies
   (-) have been used in two ways:

   a) contact reproduction to positive 70 mm transparency. This

product was required as input working document for the
additive color composite viewer, which shows false color
images enlarged at scale 1:500.000 on horizontal screen.
The reproductions showed problems because the critical ·
density requirements, in the gray level scale, of the
viewer. Original negatives had to be reduced in their
maximum density to 0.2 units lower. Reproduction was
done on Agfa Gevarex GO 21P film.   values were also
obtained, in the straight part of the relative logE
curve, for each developing time. Densitometric analysis
were made on a Densichron Welch equipment:

b) enlargement on paper print at scale 1:500.000. A total
of 880 copies, including all four bands MSS, have been
distributed to participants. Reproduction was done on
Agfa Copyline Projection P150 WP paper, automatically
processed on a PAKO film processor.

2. Color processing. This capability was developed as result
of the need for reproducing and enlarging images obtained
through the DICOMED D-47 film recorder. The film obtained
from the recorder, in cut sheets 4"x 5", was not processed
at the I.G.C., but this was done by commercial photographic
laboratories in Madrid.

The types of color films used were the following:
·- Kodak Ektachrome Daylight 6115 (+)
- Kodak Vericolor II 4107 (-) .

Once the film processed, enlargement was conducted by the
following techniques:
- Negative to positive on Kodak color paper RC37 and 2 step
Besseler chemicals
- Positive to positive on Cibachrome color paper and P-18
chemicals.

Enlargements had a maximum size of 40x50 cms in both cases, being able to provide part of LANDSAT images at scale 1:200.000. Processing in color at such scale was done only with subscenes corresponding to the Province of Madrid for cartographic purposes, and no distribution was intended of the images to the contributing organizations.

5. DATA QUALITY

Images received from EROS Data Center were bulk photographic products and enlarged copies at scale 1:1.000.000. Enclosed is in table 6 the minimum and maximum value of densities in each original negative received, corresponding to all LANDSAT images taken over Central Spain in bands 4,5,6 and 7. As it can be seen from table 6, the extreme values of the gray level scale have strong variations, which made difficult the reproduction work and corresponding photointerpretation based on changes in tonalities. Measurement of densities has been done on a Macbeth densitometer by transparency.

6. DATA DELIVERY

Delivery of information was done following the flow-diagram enclosed, through the Air Attachee to the Spanish Embassy in Washington to the Comisión Nacional de Investigación del Espa_ cio (CONIE). From that point LANDSAT information was forwarded to the Principal Investigator for reproduction and distribution to the participant organizations.
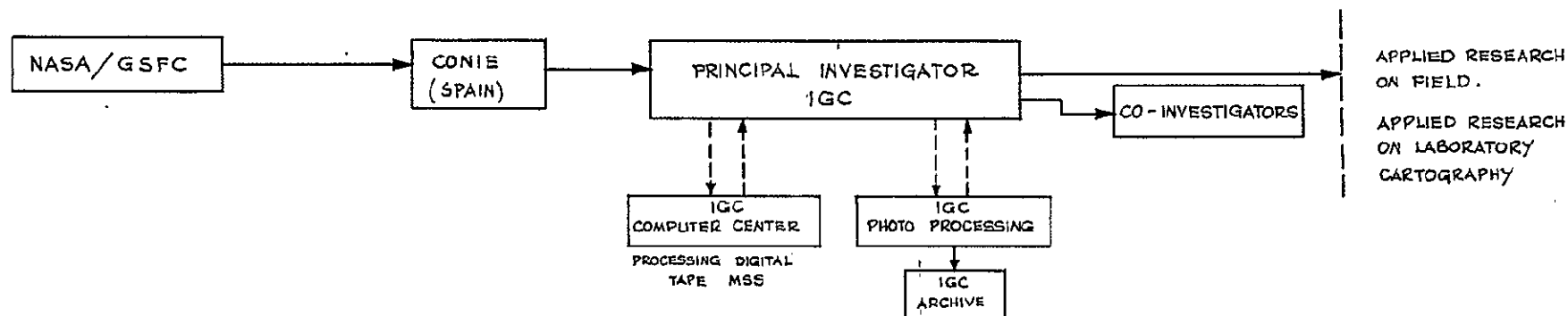
Although information received was satisfactory and none delay was observed in delivery, the first images supplied for this project have been sent in October 1975; which represented a

no.	band 4		band 5		band 6		band 7	
Image	min.	max.	min.	max.	min.	max.	min.	max.
2008-10081	0.10	2.11	0.10	2.11	0.10	2.12	0.10	2.11
2010-10243	0.08	1.90	0.08	1.92	0.07	1.81	0.06	1.78
2010-10245	0.06	1.90	0.06	1.89	0.06	1.79	0.06	1.81
2168-10091	0.04	0.86	0.04	0.87	0.03	0.82	0.04	0.86
2187-10141	0.21	2.21	0.16	2.18	0.15	2.13	0.15	2.14
2169-10143	0.10	2.11	0.09	2.07	0.08	2.07	0.09	2.11
2187-10143	0.17	2.18	0.11	2.03	0.15	2.16	0.16	2.16
2169-10145	0.09	2.07	0.09	2.11	0.08	2.06	0.09	2.10
2187-10150	0.17	2.19	0.16	2.16	0.15	2.15	0.16	2.14
2170-10204	0.13	2.01	0.14	2.03	0.13	2.04	0.14	2.03
2171-10255	0.09	2.10	0.09	2.08	0.08	2.10	0.09	2.10
2188-10195	0.15	2.16	0.15	2.14	0.12	2.10	0.14	2.12
2188-10201	0.13	2.13	0.12	2.12	0.13	2.12	0.12	2.12
2189-10253	0.15	2.14	0.13	2.08	0.13	2.15	0.13	2.10
2240-10080	0.07	2.04	0.06	2.04	0.07	2.04	0.07	2.05
2223-10135	0.12	2.18	0.11	2.17	0.10	2.18	0.11	2.17
2223-10141	0.13	2.19	0.11	2.16	0.13	2.15	0.11	2.18
2314-10190	0.10	2.07	0.09	2.05	0.08	2.00	0.10	2.08
2333-10235	0.08	2.06	0.09	2.01	0.09	2.03	0.09	2.02
2333-10241	0.11	2.11	0.11	2.10	0.11	2.12	0.10	2.10
2350-10182	0.07	2.04	0.05	1.70	0.04	1.65	0.04	1.67
2441-10215	0.04	1.66	0.04	1.56	0.03	1.55	0.04	1.62
2477-10202	0.08	2.09	0.07	2.07	0.07	2.03	0.07	2.06

Table 6. Minimum and maximum densities of the original bulk
negatives received from EROS Data Center, corresponding
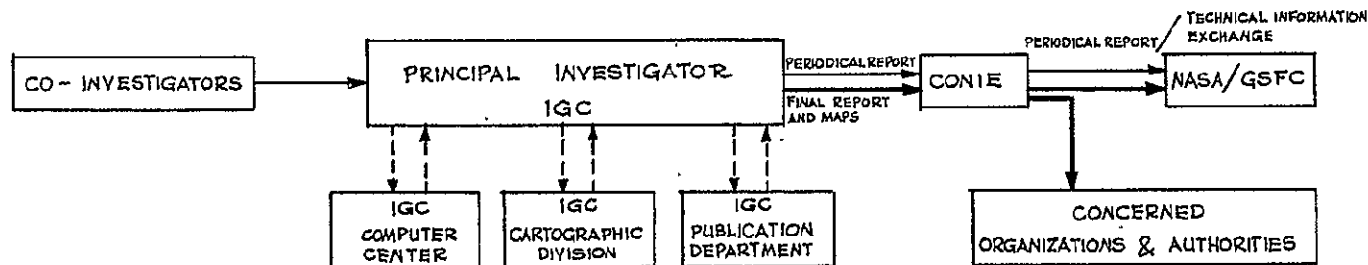to LANDSAT-2 images taken over Central Spain.

DATA FLOW FROM NASA TO P.I.

```
NASA/GSFC  ──────►  CONIE     ──────►  PRINCIPAL INVESTIGATOR  ──────►  APPLIED RESEARCH
                    (SPAIN)             IGC                               ON FIELD.
                                                          └──►  CO-INVESTIGATORS   APPLIED RESEARCH
                                                                                   ON LABORATORY
                                                                                   CARTOGRAPHY
```

IGC
COMPUTER CENTER

PROCESSING DIGITAL
TAPE MSS

IGC
PHOTO PROCESSING

IGC
ARCHIVE

DATA FLOW FROM P.I. TO NASA

ANALYSIS OF
RESEARCH RESULTS
AND MAPS

```
CO-INVESTIGATORS  ──────►  PRINCIPAL INVESTIGATOR  ── PERIODICAL REPORT ──►  CONIE  ── PERIODICAL REPORT ──►  NASA/GSFC
                            IGC                    ── FINAL REPORT
                                                      AND MAPS                      TECHNICAL INFORMATION
                                                                                    EXCHANGE
```

IGC
COMPUTER
CENTER

IGC
CARTOGRAPHIC
DIVISION

IGC
PUBLICATION
DEPARTMENT

CONCERNED
ORGANIZATIONS & AUTHORITIES

retard in the commencement of the investigation and a
lengthening in the date of submission of this Final Report,
after one year of active work with LANDSAT data over Central
Spain.

7. PUBLICATIONS

A Remote Sensing Newsletter has been published since September
1975. It included continuous references to the development of
this project, images received from NASA, remote sensing
equipments available in Spain, publications, congress, etc.
This Newsletter is being distributed free of charge to persons
directly related to remote sensing technology or applications,
both domestic and foreing. Other scientific publications are
included in the bibliography presented by participants.

8. FELLOWSHIP

In the intent of training scientists and technicians in the
new tecnology of remote sensing, several fellowship have been
given by IBM-Scientific Center to participants in this project.

At the request of the Center, the Institute of International
Education (IIE) has administered a fellowship training program
which will continue in the following years. This program provides
two six-month fellowship per year, at U.S. universities or
institutions such as Purdue, EROS Data Center, U.S. Geological
Survey and NASA facilities.

Completed fellowship

Grantee: José Luis Labrandero Sanz
Spanish Institution: Department of Soils, Institute of Edaphology,
Head Council of Scientific Research.

Education and training program has been carried out at Purdue
University during six months under the supervision of Professor
M.F. Baumgardner

Grant: $ 11.500

Present fellowship

Grantee: Laura Muñoz

Spanish Institution: Department of Internal Geodynamics.
                     Complutense University of Madrid.

Education and training program is being carried out at:
· U.S. Geological Survey, Reston, Virginia/7th. International
Remote Sensing Workshop. EROS Data Center, Sioux Falls, S.D./U.S.
Geological Survey, Flagstaff, Arizona.

End of this grant in March 1977.

Grant: $11.000

Future fellowship

The following candidates have been nominated

Ramón López Muñiz
Spanish Institution: Instituto Geográfico y Catastral

Antonio Carceller Loras
Spanish Institution: Instituto Geográfico y Catastral

Education and training Center: Jet Propulsion Laboratory/Cali-
                               fornia Institute of Technology.

C A R T O G R A P H Y

EVALUATION OF LANDSAT MSS DATA FOR UPDATING CARTOGRAPHY
AT SMALL SCALES IN CENTRAL SPAIN.

Germán L. Lemos and Jesús Roca Novoa

Remote Sensing Laboratory
Geographic and Cadastral Institute
Madrid
SPAIN.

CARTOGRAPHY

EVALUATION OF LANDSAT MSS DATA FOR UPDATING CARTOGRAPHY AT
SMALL SCALES IN CENTRAL SPAIN.

By Germán L. Lemos and Jesús Roca Novoa
Laboratorio de Teledetección
Instituto Geográfico y Catastral
Madrid.

1. INTRODUCTION

Although cartography was not defined as the main application
of LANDSAT satellites, after the malfunction of the RBV cameras
with their 81 reseau marks, cartographers turned the attention
to the use of MSS data as a document for mapping. As cartographic
requirements are subject to limits of tolerance more strict
than the Earth science disciplines, the information supplied
by LANDSAT has to be studied in a highly strict way for such
application.

After the geometric correction of MSS data done by NASA, they
have to be positioned by reference to a geodetic system for
defining whether or not they can be used as a cartographic
document.

As there is a need of information for updating maps at small
scales, and such information is normally obtained by genera-
lization of maps at larger scale, LANDSAT data are contemplated
here as a valuable tool for updating existing cartography in
central Spain. Once defined that MSS data are able to update
items of interest in a map, the following questions come
inmediately: what items of interest can be updated? is LANDSAT
able to define all of them?, how? Answer to these points are
reviewed here.

The method here envisaged for updating maps at small scales
has been applied in Central Spain to the Provincial Map of
Madrid made by Instituto Geográfico y Catastral at scale
1:200.000.

2. ACCURACY OF LANDSAT MSS DATA

MSS data furnished by NASA for this project were both in
photographic and digital form. In the first case 70 mm negative
transparencies were available in a multitemporal coverage over
Central Spain; in the second case, magnetic tapes requested
have been provided to the investigator in standard CCT format,
9 track, 800 bpi. This material was analyzed for determining
and improving its cartographic accuracy.

2.1. Photographic analysis

Bulk LANDSAT transparencies can be positioned in an absolute
reference system by means of the indicators they contain in
the margin. Such marks, although being able to serve for
posi ioning any point in latitude/longitude geographical
coordinates, do not seem to achieve the required cartographic
accuracy for mapping purposes at small scales. If errors as
large as 2 kms can be easely commited, the value of LANDSAT
images by themselves as cartographic document should only be
appl ed at scales smaller than 1:5.000.000 (according to the
U.S. National Mapping Accuracy Standards - NMAS). As example
in figure 1 is presented the grid of reference in image 2187-
10143, which could be used as a mapping system independent of
ground control. The image has also marginal indicators which
allor to position it in polar stereographic coordinates.

In the intent to refer one single LANDSAT image to a conventional
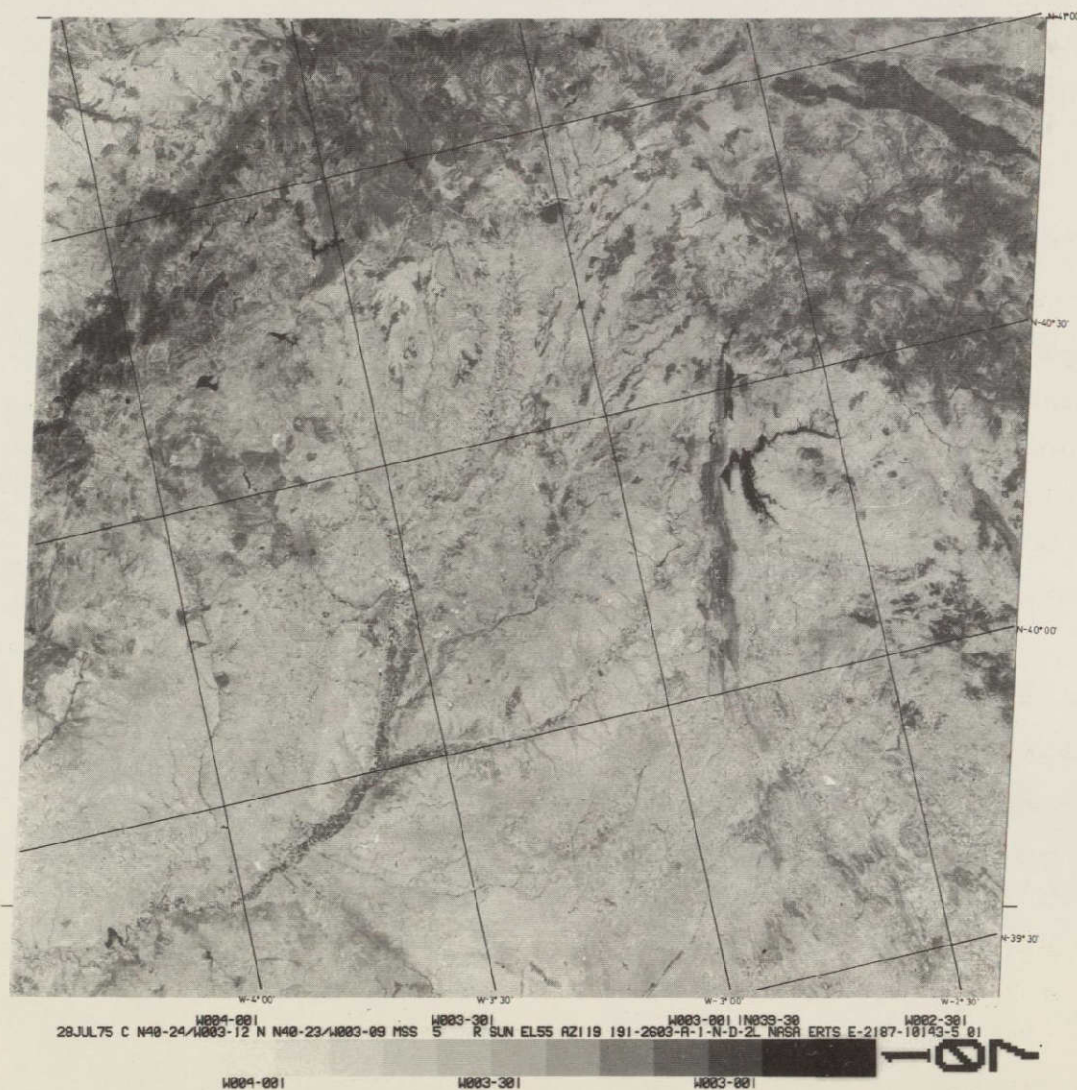map projection the Universal Transverse Mercator (UTM) grid

Figure 1.—Absolute reference system existing on LANDSAT images by means of marginal indicators of geographical coordinates

was adopted for this analysis, with the purpose of defining positional errors. As it is known, such error have a value in the order of 200 to 450m. The selection of control points for this purpose was done according to criteria of good identification in enlarged LANDSAT images and in the basic reference system used. Also, measurements were done on the Provincial Map of Madrid at scale 1:200.000, with the intention of determining its cartographic accuracy or need for being updated.

As basic reference system it was used the National Topographic Map (N.T.M.) at scale 1:50.000, where control points have been identified in geographical coordinates (λ, φ). This map has 1.130 sheets covering all the country and it is finished since the year 1958.

The N.T.M. was done in polyedric projection with every sheet limited by 20 minutes of arc of meridian and 10 minutes of arc of parallel, by reference to the ellipsoid of Struve. Recently, the UTM grid referred to the international ellipsoid of Hayford was adopted for the N.T.M. Such map, being produced and printed by Instituto Geográfico y Catastral, has allowed an accuracy in location of control points of 1" of arc for the longitude and 0.5" of arc for the latitude.

Typical control points were dams in reservoirs, intersection of roads and rivers, etc. In figure 2 is presented the spatial distribution of such points around Madrid province.

Conversion of geographical coordinates to U.T.M. was done before obtaining real distances between control points. Such calculation was effected by the known formulas:

$$X = 500.000 \pm (IV)p + (V)p^3 + B_5$$

$$Y = (I) + (II)p^2 + (III)p^4 + A_6$$

$$p = 0,0001 \Delta M''$$

28JUL75 C N40-24/W003-12 N N40-23/W003-09 MSS 5 R SUN EL55 AZ119 191-2603-A-1-N-D-2L NASA ERTS E-2187-10143-5 01

Figure 2.—Spatial distribution of control points around Madrid province

which are referred to the international ellipsoid of Hayford. The value of each term can be found in reference 1, being X and Y the UTM coordinates of the control point.

The transfer of control points to the image presented problems of scaling in the different images tested at 1:500.000. As a multitemporal coverage of the area of control points was available, the following images have been measured:

$$E - 2403 - 10113$$
$$E - 2187 - 10143$$
$$E - 2169 - 10145$$
$$E - 2223 - 10135$$

Table 1 summarizes the results obtained from this analysis, with indication of the control points positioned in figure 2 and explanation of their nature. The computations were done by measurement of the following distances:

MAP - REAL

or   LANDSAT - REAL

The absolute values in LANDSAT measurements indicate RMS (root-mean square) errors in each observation done on the four images above mentioned. Distances to points J_1 and J_2 could not be measured on the Provincial Map, because their location out of it.

As it can be seen from table 1, the Provincial Map of Madrid has a need for being updated, because the high values of the errors obtained by measurement of distances between control points located in rivers intersections or meanders. Such points (in the lower part of the table F_7, K_5, E_5, G_7, H_5, B_6, E_6, C_6 and H_6) produce an error much larger than the tolerance of the map; thus their position is not accurately represented on it, as they correspond to natural features with dynamic change.

POINTS	ERROR DISTANCES(m) MAP-REAL	ERROR DISTANCES(m) LANDSAT-REAL	CONCEPT
$C_1 - B_1$	35	46	C_1= dam reservoir Pinilla B_1= dam reservoir Riosequillo
$C_1 - D_1$	21	308	C_1= dam reservoir Pinilla D_1= dam reservoir Vellón
$B_1 - D_2$	53	274	B_1= dam reservoir Riosequillo D_2= rivers intersection
$A_2 - D_2$	33	477	A_2= rivers intersection D_2= rivers intersection
$D_4 - F_4$	62	139	D_4= dam reservoir Los Arroyos F_4= river intersection
$F_4 - H_4$	18	159	F_4= rivers intersection H_4= river/road intersection
$D_7 - F_7$	93	348	D_7= river/road intersection F_7= rivers intersection
$K_5 - E_5$	431	349	K_5= rivers intersection E_5= rivers intersection
$C_7 - G_7$	413	199	C_7= hill of Los Angeles G_7= river meander
$D_5 - H_5$	409	444	D_5= lake of Retiro H_5= riv ers intersection
$B_6 - E_6$	231	233	B_6= river meander E_6= river meander
$C_6 - H_6$	103	103	C_6= river meander H_6= river meander
$J_1 - J_2$	---	417	J_1= rivers intersection J_2= dam reservoir Buendía
$J_2 - C_1$	---	476	J_2= dam reservoir Buendía C_1= dam reservoir Pinilla
$J_1 - C_1$	---	218	J_1= rivers intersection C_1= dam reservoir Pinilla

TABLE 1: Comparison of results obtained by measurement of real distances between control points in U.T.M. corrdinates, in the Provincial Map of Madrid at scale 1:200.000, and in LANDSAT images at scale 1:500.000 without correction (bulk data).

When control points in the map correspond to man made features, like dams in reservoirs or intersections with roads, the errors appearing on the map are much lower and they meet the carto-graphic requirements at such scale.

LANDSAT images can benefit from selection of the control points above rejected, assuming that they have a good indentification on the basic cartographic reference system (in this case, the N.T.M. at scale 1:50.000).

According to NMAS requirements, mapping planimetric data has to be done with an error minor than 0,5 mm (0.02 inch), measured on the publication scale in 90% of well-defined features. Thus, for scale 1:1.000.000 the 90% accuracy value is therefore ∿ 500m on the ground, ∼ 250m at scale 1:500.000 and ∼ 100m at scale 1:200.000. As map errors may not be normally distributed, for practical purposes the RMS error of position for points tested should be less than 300 m at 1:1.000.000 scale, 150 m at 1:500.000, and 60 m at scale 1:200.000 to meet NMAS.

If this is so, from table 1 it can be established that bulk LANDSAT MSS images do not meet the requirements of NMAS if being referred to a U.T.M. projection for mapping purposes at small scales. Bulk images could only meet such requirements at scales of 1.000.000 or smaller.

2.2. Digital analysis

Once determined that bulk LANDSAT enlarged images at scale 1:500.000 over Central Spain do not meet the NMAS requirements for planimetric mapping in U.T.M. projection, an analysis of digital data was carried out for defining the necessary geometric corrections to be done on them before being applied to cartography at small scales. This procedure needed computer programming and associated hardware, as well as electronic printing of the corrected CCTs.

2.2.1. Registration: This work was conducted through IBM-Scientific Center of the Autonomous University of Madrid, where ERMAN-II program is available on an IBM 360/65 computer interfaced to an interactive television terminal RAMTEK. This powerful software has the capability of geometrically correcting an original NASA CCT, supplying with an output tape where the pixel is positioned in U.T.M. coordinates and it is converted from rectangular to square format representing 80 m x 80 m at the earth surface. This is done through the REGISTRATION program, which was used for the purpose of this investigation.

Registration program needs control points of well known geographical coordinates to be introduced through the television terminal via cursor. As the program adjusts only a maximum matrix of 1000 x 1000 pixels at one time, the original CCT E-2187-10143 (3240x2340 pixels) was divided in the subscenes indicated at figure 3; where all together cover the province of Madrid in mosaic and each one has at least a 10% overlap.

In each subscene were obtained geographical coordinates of well known control points (a minimum of 6 in each one), taken from the N.T.M. at scale 1:50.000.

As input information to the program were also used the geographical coordinates of the corners of each subscene and its digital coordinates (by digital coordinates it is understood here line and pixel at the upper left corner of the subscene, number of lines and number of pixels to be loaded). Digital coordinates were approximately obtained by interpolation in b&w LANDSAT images at scale 1:500.000, while geographical coordinates were also approximately extracted from the same photographic document, once drawn its grid of parallels and meridians (figure 1). Both types of coordinates are required only approximately as indicator of the area of study to display
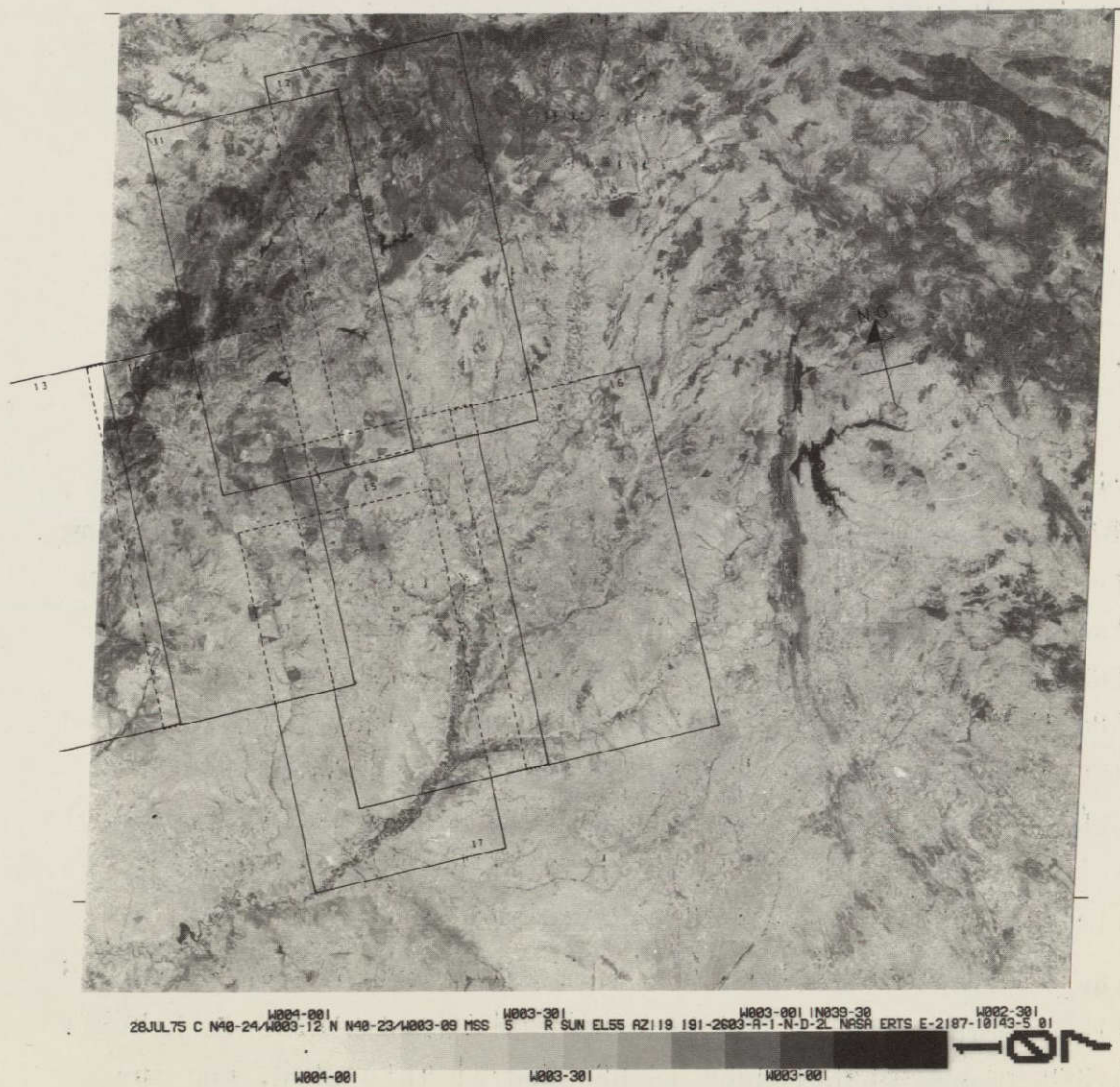
28JUL75 C N40-24/W003-12 N N40-23/W003-09 MSS 5 R SUN EL55 AZ119 191-2603-A-1-N-D-2L NASA ERTS E-2187-10143-5 01

Figure 3.—Subscenes selected in Madrid province for geometric correction of MSS digital data

through TV terminal, because the corners of the subscenes never enter as control points in the registration programs.

Geographical coordinates of control points were entered in the computer through the RAMTEK terminal by conversational console via cursor, once the subscene had been displayed in false color at the TV screen and the control points has been identified on it.

Identification of control points was done following some practical rules for reducing errors in their location at the TV terminal, which seems to be critical if an accurate registration is required.

The identification of control points in the TV screen has to be done before locating them in the reference map and obtaining their geographical coordinates. At this point, a magnification factor of the display can be used for selecting those points of good definition (this concept envolves considerations on the contrast and texture of the area under study). It is agreed that man made features produce much accurate identification of control points than natural phenomenal, namely if the points correspond to intersections of linear structures, like highways, airfields, corner of dams in reservoirs, etc.

As the TV display can be done at an scale comparative to the reference map used for positioning control points, bulk LANDSAT enlarged images do not need to be used at this step, and the definition of the points benefits from a much better accuracy than the obtained by positioning them on the satellite photographic product.

All these considerations apply only to the area of study in this project; the Central Region of Spain, where a good geodetic network exists, the basic reference map has good cartographic

accuracy being maintained up to date, and where there are many
man made features to be taken as control points. In a remote
area without cartography, the overall accuracy of this digital
analysis should be reduced.

Before doing registration of a LANDSAT CCT, the instantaneous
field of view of MSS sensor represent a nominal 79 m square,
even though it prints out at about 79 m by 56 m due to a pixel
overlap in the cross-track direction. After the registration
is run, the output pixel is squared at 80x80 m (on the ground).

Registration program applies a polynomial algorithm $F(x,y)$ to
correct original pixels to their new position in lines, and a
second polynominal algorithm $G(x,y)$ is used for positioning
them in columns, according to an U.T.M. grid adjusted to the
subscene by means of the entered control points. The degree of
the polynomial depends on the number of control points used
for each subscene. Table 2 shows their minimum number in each
case.

polynomial degree	minimum control points
1	4
2	7
3	11
4	16
5	22
6	29

Table 2.

Geometric correction of a matrix of 1000x1000 pixels requires
about 15 minutes of C.P.U. At the end of such operation geo-
graphical coordinates of control points are displayed at the
TV screen, with indication of their residual values after the

```
CONSOLE
   0    0   1   1   2   3   3   4   4   5   6   6   7   7   8   9    9  10
   0    6   2   8   4   0   6   2   8   4   0   6   2   8   4   0    6   2
   0    0   0   0   0   0   0   0   0   0   0   0   0   0   0   0    0   0
**********************************************************************************
1008                                                                       ------
984*                                         *  12A23A55 1                  I   I
960*        REGISTRATION-  POINT EVALVATION DISPLAY FOR RUN      7      PAGE   1 ------
936*                                                                       I   I
912*     POINT       INPUT              REFERENCE             RESIDUAL    IN  ------
888*      ID       LINE,PIXEL       LATITUDE , LONGITUDE .    .X    Y   R  FIT  ARDC  I   I
864*                                                                       ------
840*                                                                       I   I
816* H6          999, 1516   40001059.99N,003018012.99W   .0    0   0.0 *   --   ------
792* F6         1101, 1675   40005018.99N,003010029.99W    0    0   0,0 *   --   I   I
768* E6         1216, 1795   40009027.99N,003004001.99W    0    0   0.0 *   --   ------
744* C6         1618, 1606   40027017.99N,003005045.99W    0    0   0.0 *   --   I   I
720* B6         1580, 1225   40028007.99N,003021021.99W    0    0  .0.0 *   --   ------
696* A6         1723, 1350   40033017.99N,003014020.99W    0    0   0.0 *   --   I   I
672* D6         1260, 1370   40013043.99N,003020010.99W    0    0   0 0 *   --   ------
648*                                                                        --   I   I
624*                                                                        --   ------
600*                                                                        --   I   I
576*                                                                        --   ------
552*                                                                        --   I   I
528*                                                                        --   ------
504*                                                                        --   I   I
480*                                                                        --   ------
456*                                                                        --   I   I
432*                                                                        --   ------
408*                                                                        --   I   I
384*                                                                        --   ------
360*                                                                        --   I   I
336*                                                                        --   ------
312*                                                                        --   I   I
288*                                                                        --   ------
264*                                                                        --   I   I
240*                                                                        --   ------
216*                                                                        --   I   I
192*                                                                        --   ------
168*                                                                        --   I   I
144*                                                                        --   ------
120*                                                                        --   I   I
096*                         XDDAMMASS.TH     XDDDAMMASS,TH                      ------
072* TYPE IN NEW LATALONGO   ---------------  ---------------                I   I
048*                                                                         EOF--
024*   '                                                                     I   I
000*-                                                                        EOT--
```

Figure 4.—Computer printout of geographical coordinates of control points used for correcting geometrically the subscene I5.
Value of residuals are also indicated

registration was run. The residuals are digitally measured in
X and Y directions, as well as in radius vector. Figure 4 shows
a computer printout of the goegraphical coordinates of control
points introduced for -correcting geometrically the tape I5
(see figure 2). In figure 4 residuals are zero; which means
that an accurate identification and positioning of points has
been obtained. If residuals were not null, the instantaneous
field of view of MSS sensor does not allow an error of one
pixel when the information is required for small scales mapping,
specially at 1:200.000.At such scale residuals must be zero in
order to meet NMAS planimetric requirements. In this situation
a new registration could be run on the resulting tape, with
new control points, until errors elliminated. Such interactive
mode of operation provides at the end to the investigator with
a tape geometrically corrected by reference to UTM projection
system.

As it can be seen in figure 4, a total of 7 control points and
a second order algorithm were used for tape I5. The registration
program assumes that the mean latitude of the image under study
is N40 degrees. This value was introduced in the program as
being the parallel of Madrid, and it was taken as mean value
for all LANDSAT images over Central Spain. Figure 5 shows a
flow-diagram of the registration program here applied for
cartographic purposes.

In general more geometric accuracy was obtained in the regis-
tration process when control points were located near the
borders of the image. It is more exact to register with a few
points near the corners than with many points in the center of
the image. More accuracy was also obtained by the use of a first
order polynomial algorithm than by a second order algorithm.
Residual errors seem to be smaller in the first case.
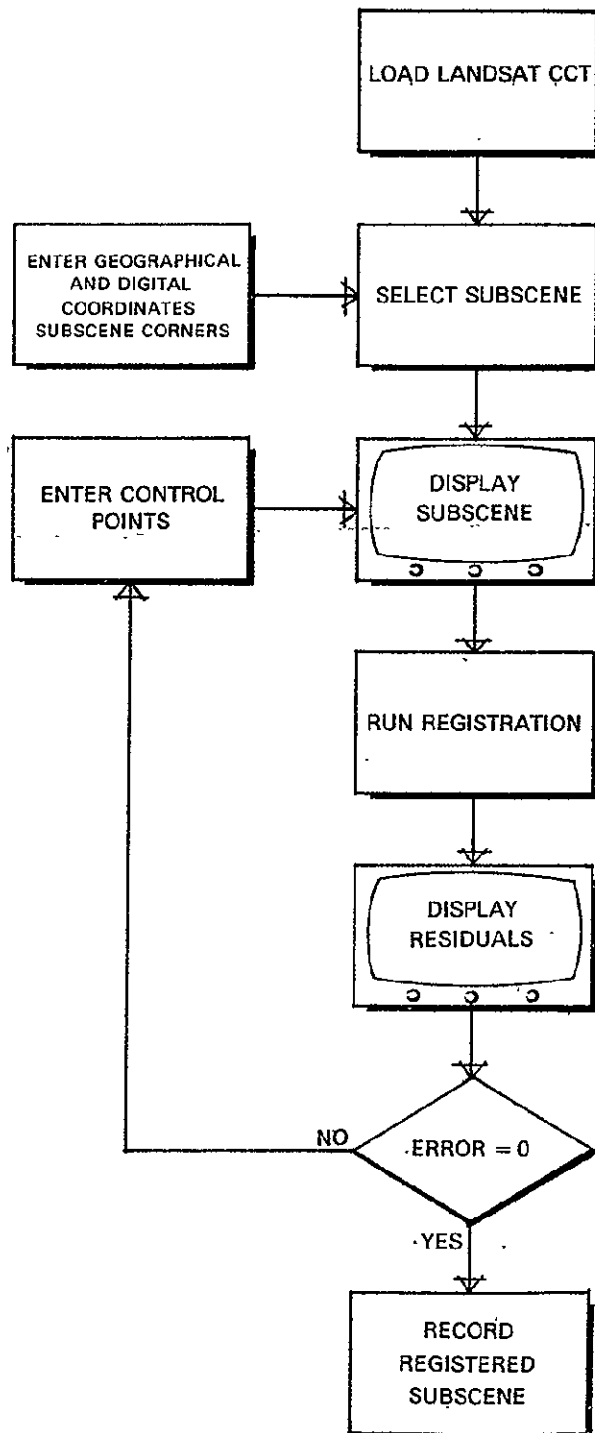
Figure 5.—Flow-diagram of the registration program used in cartography

Continuing with the digital analysis of LANDSAT information
applied to cartography, as an option of the registration
program a mapping movement vector menu was obtained through
TV terminal display for all the subscenes. In figure 6 is
shown the menu corresponding to tape I5. Such menu presents
the displacements of 16 regularly distributed pixels of the
subscene under study, once their position has been obtained
in U.T.M. coordinates through registration program. As it can
be seen in figure 6 there is a general movement of pixels in
the image looking like a rotation once registered. Although
it cannot by defined any accurate measurement of distances or
angles through the television display presented in figure 6,
the value of the longest vector on the display (19 lines and
23 pixels long) could be indicator, as well as the general
movement of rotation-like, of any systematic error in the
recording of the original CCT. In any case, it can be seen
from figure 6 that the geometry of MSS data presents linear
and angular anamorphosis when referred to a mapping projection
system. This result is in accordance with the errors obtained
by photographic analysis of LANDSAT information.

As the output pixel size is square of 80 m side, and the NMAS
requirement for mapping at scale 1:200.000 is a RMS error of
about 60 m, assuming that a perfect registration was done
LANDSAT data do not guarantee at such scale the necessary
cartographic accuracy; however, when a basic topographic
location of the items in the map to be updated exists LANDSAT
information can be used for updating works with cartographic
accuracy at such scale. Also, LANDSAT registered data referred
to U.T.M. projection do meet the NMAS requirements for planimetric
mapping at scales 1:500.000.

THE LONGEST VECTOR ON THIS DISPLAY IS 19 LINES AND 23 PIXELS LONG

Fig. 6.—Mapping movement vector menu

RT

EOF

EOT

34

X651

IMD LATITUDE / LONGITUDE TABLE

IMAGE NAME _____

ENTER POINTS
  VIA CURSOR - CURSOR POINTS THEN EOF, EOT
    OR
  VIA KEYBOARD - EOF THEN ENTER POINTS, EOT

POINT LINE	PIXEL	LINE	PIXEL	LATITUDE	LONGITUDE
1		15	1	39 59.33 25N	003 51 07.99W
2		467	3	40 19:03 90N	003 51.02 82W
3		825	123	40.34 31 09N	003 45 52 02W
4		745	597	40 31 03 90N	003.25.24 40W
5		11	593	39.59 22.89N	003 25 34 76W
6					
7					
8					
9					
10					
11					
12					
13					
14					
15					
16					
17					
18					
19					
20					
21					
22					
23					
24					
25					

SCR

PET

EOF

EOT

Fig. 7.—Geographical coordinates of the corners of the subscene I5, once geometrically corrected

As random angular and linear anamorphosis exist in the original
geometry of MSS data, when two original overlaping CCTs were,
intended to be geometrically positioned by reference to each
other, this should not be possible unless the tapes wese also
registered and referred to a geodetic conformal projection.
In such case, a digitally controled mosaic of an area could
be obtained, although the convergence of meridians could be
influencing the accuracy of registration if the latitude of
the images varied.

Finally, in figure 7 is indicated the menu corresponding to
geographical coordinates of the corners of the subscene I5,
once geometrically corrected.

2.2.2. Conversion to image. After referencing the original CCT
to a geodetic projection, a new tape (or subscene) is obtained,
which has to be converted into image. This could be done by means
of CRTs, Electron Beam Recorders, Laser Beam Recorders or other
electronic devices. In any case, the photographic product
obtained can be considered as having the conformality of the
geodetic projection and it does not present degraded quality,
being able for reproductions larger than 1:500.000.

In this project tape to image conversion was done with a DICOMED
D-47 film recorder operational at Instituto Geográfico y Ca-
tastral, interfaced to a PDP 11/45 computer (32K). The output
products were 70 mm format transparencies in false color
representing subscenes of nominal 1000 x 1000 pixels once
registered to UTM projection (see figure 8).

Before entering the film recorder tapes must be reformated
to be made compatible with it, which accepts either of both
6 or 8 bits. Also, recording of channels is done in one file
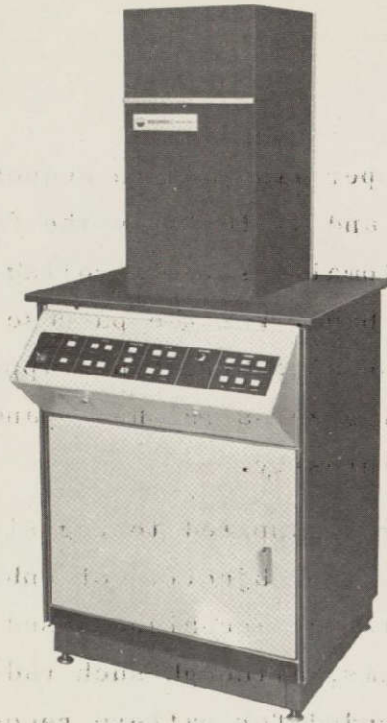
Figure 8.—DICOMED D-47 film recorder

ARRAY GEOMETRICS

H_1 = Length of top horizontal line
H_c = Length of horizontal major axis
H_2 = Length of bottom horizontal line
V_1 = Length of left vertical line
V_c = Length of vertical major axis
V_2 = Length of right vertical line
M_1 = Length of matrix diagonal (0,0 to max., max.)
M_2 = Length of matrix diagonal (0, max. to max., 0)
L = Direction of scan line
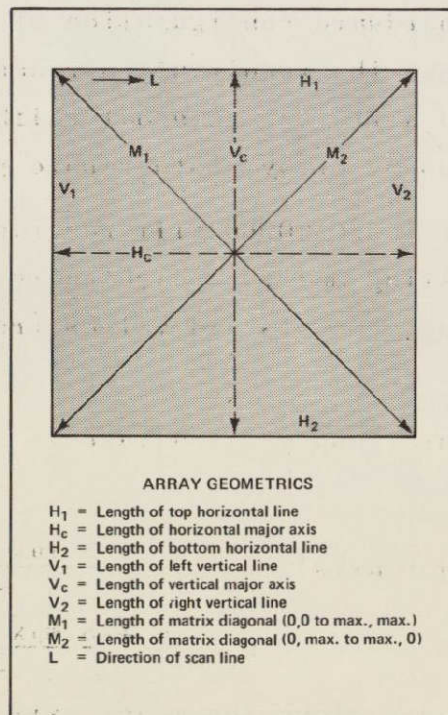
Figure 9.—Plotting matrix measurement definitions

each, with one register per line and in sequential mode for
bands 4, 5 and 7 or 7,5 and 4. That way the film recorder
runs the color image automatically controling the color
filters applied to each band. For the purpose of this project
registered tapes were run at 8 bits (this applies to all four
channels), by interleaving zeros in the expanded radiometric
range to 255 levels of intesity.

The radiometric corrections applied to registered tapes before
conversion to image have the objective of enhancing the output
image to be photointerpreted. Techniques used normally envolve
equalization of histograms, although such radiometric
corrections are not intended for pattern recognition because
the change introduced in the radiometric balance of the data.
This subject is discussed in another section of this final
report (see Digital Processing, references 2).

Tapes converted to images have been run in linear mode according
to NASA original recording, although they could be run in
logarithmic mode by hardware configuration of the DICOMED
reocrder. In such case, the resultant increase in contrast
could be reduced by a different internal calibration according
to the type of film used, or by photographic processing.

Geometric accuracy of the DICOMED film recorder is defined by
reference to the plotting matrix indicated in figure 9. It
concerns the following concepts and values (reference 3):

- Orthogonality (0)
  ($\pm$ 0,25% of horizontal and vertical axes)% $= \pm \left| \frac{M_1 - M_2}{M_1 + M_2} \right| \times 100$

- Linearity (L)
  ($\pm$ 0,35% of the major axis) $\quad L_H(\%) = \pm \frac{Svmax - Svmin}{2Hc} \times 100$

  $$L_V(\%) = \pm \frac{Svmax - Svmin}{2Vc} \times 100$$

  S = length of segments along the major axis

- Line curvature (P)

  ($\pm$ 0,15% of the major axis) $\qquad P(\%) = \pm \dfrac{d}{L}$ x 100

  d = deviation from best fit straight line

  L = length of the major axis (Hc or Vc)

- Trapezoiding (T)

  ($\pm$ 0,3% of the major axis) $\qquad T_H(\%) = \pm \left[\dfrac{H_1 - H_2}{H_1 + H_2}\right]$ x 100

  $\qquad\qquad\qquad\qquad\qquad\qquad\qquad T_V(\%) = \pm \left[\dfrac{V_1 - V_2}{V_1 + V_2}\right]$ x 100

  T_H and T_V are the horizontal and vertical axes respectively.

- Rectangularity (R)

  ($\pm$ 0,3% of the major axis) $\qquad R(\%) = \pm \left[\dfrac{H_c - V_c}{H_c - V_c}\right]$ x 100

- Spatial repeatability (S)

  ($\pm$ 0,05% of each major axis $\qquad S(\%) = \pm \dfrac{d}{L}$ x 100
  at 20 minutes interval)

  d is the deviation of a point and L is lenght of the major
  axis (H_c or V_c)

In this project several images have been obtained through the
film recorder provinding valuable data to be photointerpreted
in multidisciplinary mode. Some of them are shown in the section
of digital processing (reference 2)or herein enclosed (figure 12).
In none of them was observed a geometric distorsion of the film
recorder. On the contrary, such images have been used as a
valuable cartographic document in the analysis of LANDSAT data
over Central Spain. In any case, analog input signals generated
by the D/A converters (figure 10), can be appropriately modified
and then be sent to the deflection control circuits for complying
with the geometric requirements above mentioned (in parenthesis
is shown their maximum relative value).

Scale of the image obtained is result of the resolution mode
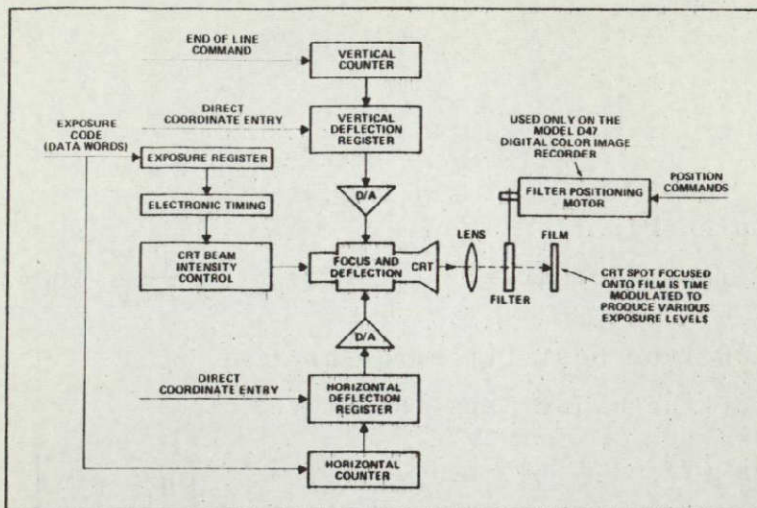
Figure 10.—Simplified block diagram of the DICOMED D-47 film recorder
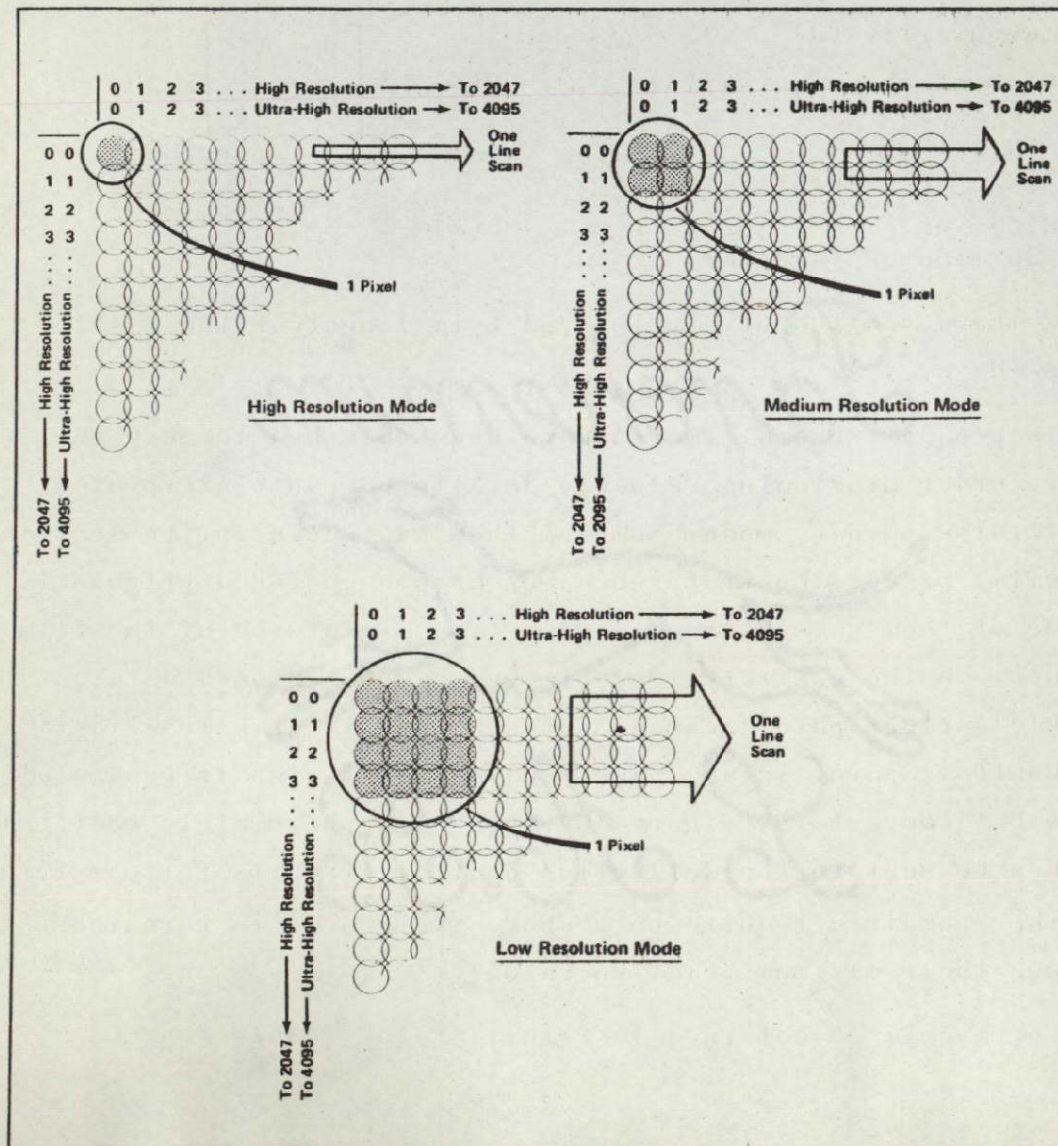
Figure 11.—Resolution modes available in the DICOMED D-47 film recorder

used in the film recorder, which has three operational modes: high, medium and low (figure 11). High resolution assigns one pixel to a single point, medium resolution assigns one pixel to four points of equal intesity and low resolution provides an assignment of 16 points. Thus, the various resolutions provide either a 1 by 1,2 by 2, or 4 by 4 points per pixel format. This feature permits a small scale image array to be recorded at a larger scale.

Although registered tapes could be run in any of such modes, for cartographic purposes there is a need of enlarging the image obtained, and the enlargement factor depends on the mode of resolution used. As the LANDSAT photographic document was intended to be enlarged at scale 1:200.000, the high resolution option could not be used in this project because the limit imposed by the enlargement factor. If the size of the registered subscenes has a maximum nominal value of 1000 x 1000 pixels, (80 x 80 kms on the ground), at scale 1:200.000 the enlargement factor should be about 40X. Thus, the film recorder was run at low resolution, although such mode degrades the image because the overlap existing between pixels (in that way enlargement factor to scale 1:200.000 was reduced to 10X).

When printing a LANDSAT registered image through the film recorder every pixel is square and the recorded tape represents a rectangular area on the ground of sides parallel to the X - Y axes in the UTM projection. The output image obtained through the DICOMED recorder has its X - Y local axes also parallels to the axes of U.T.M. projection. If the LANDSAT tape to be recorded was not registered or it was an original NASA CCT (conveniently preprocessed to be compatible with the CRT format), its conversion to image should destroy the geometric fidelity of the bulk scene, because the image skew for compensation of
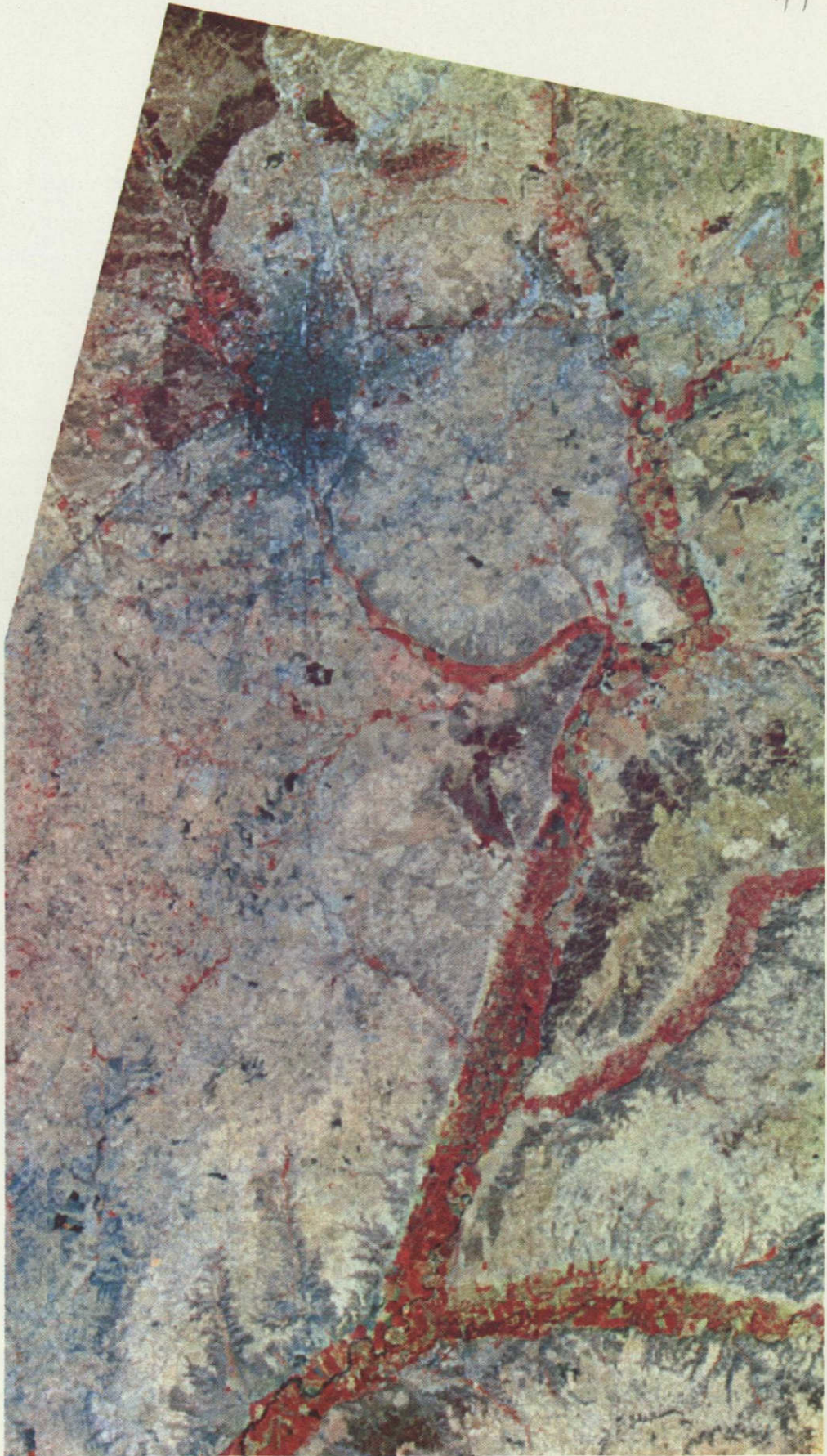
Fig. 12. —False colour image of Madrid-Aranjuez, corresponding to subscene I5. Original at scale 1:200.000, here reproduced at 60% of size. This image is geometrically corrected in U.T.M. projection. Coordinates of corner points are indicated in figure 7

Earth rotation would disappear in the output product. This
effect can be eliminated by internal reformat of the digital
tapes.

Although pixels are squares of 79 m in MSS data, they are
printed out in bulk processing as rectangules of 79 x 56 m.
Such requirements can be accomplished when an original CCT
(conveniently reformated) is converted to image by the film
recorder. This is possible with an optional hardware configu-
ration of the equipment (manually changed), which is called
"ERTS Aspect Ratio Option". It maintains the spot size circular
at high resolution; but separates the printing distance of
horizontal lines in a mode which produces a 54 x 54 mm square
format of the exposed area representing 3240x2340 pixels (a
full CCT).

As result of these above mentioned modes of operation with the
film recorder, all the subscenes indicated in figure 3 were
converted to a photographic document in false color, on positive
color Ektachrome Daylight 6115 film. Processing of this film is
not envisaged by Instituto Geográfico y Catastral, but it was
done by PIX Laboratories S.A. in Madrid. Every subscene was
recorded on a color transparency of cut film 4" x 5" at low
resolution. Such document, representing on the ground a nominal
area of 80 x 80 kms in UTM projection, was used as the basic
document to be photointerpreted for cartographic purposes.
When the transparency was enlarged at scale 1:200.000 it was
not possible to find out errors in the positioning of control
points when referred to UTM projection. In figure 12 is observed
the subscene I5 registered and enlarged. It represents in false
color (4= blue, 5 = green, 7 = red) the city of Madrid and the
irrigation lands of Jarama, Tajo and Tajuña rivers, once the
MSS data contained on it had been digitally positioned, by

means of ground control points, in UTM projection. Documents like this one have been used for updating the Provincial Map of Madrid at scale 1:200.000. The geographical coordinates of the five corner points of figure 12, once geometrically corrected, were indicated in figure 7.

As result of this digital analysis of LANDSAT data it has been defined their capability to be geometrically corrected and referenced to an UTM projection by means of well known ground control points; being the new image able to be used· as a cartographic document for updating maps at small scales.

3. UPDATING MAPS AT SMALL SCALES

In paragraph 2 it was confirmed the capability of LANDSAT · digital data for meeting the cartographic requirements of maps at small scales, once the images had been geometrically corrected and positioned in a geodetic reference system by means of control points. As result of the digital analysis of data, a methodology was established for updating maps at small scales. Figure 13 represents the diagram of operations used with LANDSAT information when being applied to updating maps at scale 1:200.000. All steps indicated in figure 13 have been widely commented before, and only the photointerpretation work is considered here.

Once the original transparencies had been registered and obtained through the film recorder, their enlargement to scale 1:200.000 could be done by optical projection or by photographic processing. In the first case it was used a DOT additive color composite viewer with change scale option, which projected on horizontal screen the enlarged image. The map was directly updated by transparency when positioned on
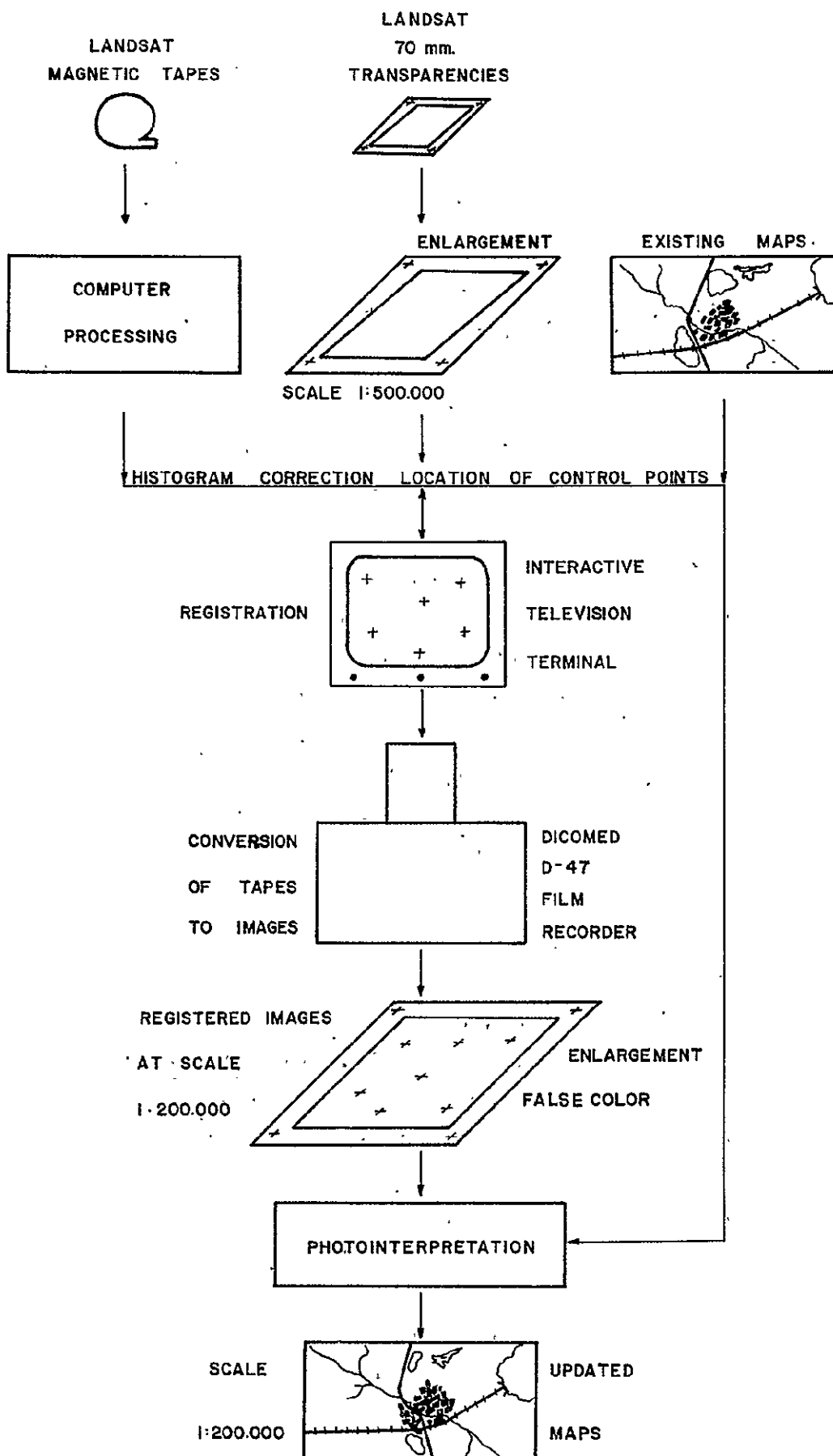
Figure 13.—Diagram of operations used for updating maps at scale 1:200.000

the screen. In the second case, photographic enlargement of
the false color original transparency obtained through the
DICOMED film recorder was done on Cibachrome color paper and
P-18 chemicals.

Both methods have shown the same accuracy for small scale
mapping purposes, although the color composite viewer eliminates
the need of photographic enlargement of the original transpa-
rency. Furthermore, the viewer permits obtaining a rough draft
of the map to be delineated at a later stage by conventional
cartographic techniques.

It is considered that producing and updating maps at small
scales should require registration of each image at one time
(3240x2340 pixels), with control points mainly located in the
corners, and a first or second order algorithm of transfor-
mation. This work will be done in the future through IBM-
Scientific Center of the Autonomous University of Madrid. At
the moment registration was done for this project, taking the
Province of Madrid as target, by 6 control points every subscene
of 1000x1000 pixels, which is a prohibitive way of work in
the future if a national coverage of LANDSAT registered tapes
is required for small scales working purposes.

Although the need of using LANDSAT data in digital form as
input to a cartographic system in Spain, some comparative
considerations are indicated here, showing the goodness of
such space acquired imagery as a valuable working tool. Let
us consider a photogrammetric survey at scale 1:30.000 by
conventional aerial techniques. Every image, in format of
21'5 x 21'5 cms, should have a 60% overlap along the flight
direction and 30% side overlap. In the case of Spain a total
of 35.000 photograms should be required for a total coverage
of the national territory. The same coverage could be obtained

Main surficial features		Best bands				
		4	5	6	7	F.C.
MAN MADE.	large cities		X		X	X
	transportation network		X		X	X
	airports			X	X	
	ports			X	X	
	excavations			X	X	X
WATER	coast profiles	X		X	X	
	reservoirs, lakes	X			X	X
	rivers, channels			X	X	X
	snow		X		X	X
	pollution	X	X			
	irrigation network		X			X
VEGETATION	Coniferae					X
	Quercus					X
	fertile lowlands		X			X
	rangelands		X			X
GEOMORPHOLOGY	drainage patterns				X	X
	bare soils			X		X
	sediment transport	X				X
	marshlands	X				X
F.C.= false color SUM		5	7	6	10	15

Table 3. Main surficial features identified by LANDSAT.

with less than 100 LANDSAT images, allowing a much more rapid
updating of cartography at small scales, at a very lower price,
and with the possibility of maintaining the information up to
date.

In the case of Spain (504.750 kms^2), considering for a satellite
mosaic covering the country the necessary images to be obtained
over Portugal, Balearic and Canary Islands, South of France
and North of Africa, and considering the side overlap of
LANDSAT images at N40 degrees latitude, a total of 50 false
color images should be required for a complete coverage of
the National Map.

Once agreed that there is a need of LANDSAT data for cartographic
purposes at small scales, an analysis was carried out for
determining what can be detected on the satellite image that
should be represented on the map. At this point, many scientific
works have been done in the last years (in what could be called
the early times of LANDSAT program), trying to identify by
photointerpretation techniques "all" the information contained
in a satellite image. And this is an exhaustive work, time
changing, dependent of multitude of parameters, varying with
the geographical location, etc. For cartographic purposes at
small scales the working approach for determining what can be
detected is a question of generalization of LANDSAT information.

Such generalization is intended for the purpose of defining
what the cartographer has to look for in a LANDSAT image, with
guarantee that the information "will be thear" and it will be
as invariant as possible. Factors like atmospheric conditions,
sun angle elevation, date of observation, etc., will always
modify the output product of a remote sensing system; but
for operational purposes such modifications need to be centered
around mean invariant values. Let us take as example of this
invariant approach done by the cartographer the following

Topographic items	LANDSAT detection	Topographic items	LANDSAT detection
Roads		Hydrography	
highways		rivers	yes
in service	yes	dams, cascades	no
in construction	yes	lakes	yes
in project	no	marshlands	yes
one roadway	no	channels	no
main tolls	no	seashore	yes
principal roads	no	Habitated places	
secondary roads	no	isolated houses	no
others	no	industrial plants	no
Railroads		airfields	no
two roads	no	cities	
one road	no	more than 5.000 h.	yes
narrow-gages	no	from 3.000h. to 5.000h.	no
stations	no	less than 3.000 h.	no
tunnels	no	Vegetation	
grade crossing	no	forests	yes
teleferics	no	Altimetric data	no
		Administrative limits	no

Table 4. Topographic items appearing in a map at scale 1:500.000 and their identification by means of LANDSAT data.

case: it is scientifically recognized as a merit that a
geologist says "I have discovered a fault in a LANDSAT image";
but a cartographer cannot say". I have discovered a highway",
because highways must be positioned on his maps even before
they are constructed. In other words, LANDSAT can provide
valuable data of many surficial features, but only those data
invariant and sustematically identifiable can be considered
by the cartographer.

In the intent of applying LANDSAT data to updating maps at
small scales, a list has been established in table 3 containing
the main surficial features identified at LANDSAT images when
studied in Spain. Such table is based in experienced criteria
of photointerpreters and gives a comparison of the capabilities
of each spectral band and their false color combination for
identifying the most relevant natural and artificial (man made)
features.

As it can be seen from the sum of applications in each band,
false color information is unique for identification of the
natural cover of the earth surface, while band 7 is specially
indicated when artificial features (man made) have to be located.

When talking about false color, it has to be understood as a
combination of MSS bands 4,5 and 7, which gives information
in the spectral regions of the green, red and infrared;
providing data not only in the visible spectrum but farther
than the conventional color infrared photographic images.

Table 4 represents existing topographic items in a map at
scale 1:500.000. Such information is agreed that "has to be on
the map", no matter how LANDSAT data are able to identify it
at the earth surface. Topographic items in table 4 were
obtained from the existing european specifications for maps
at scale 1:500.000, according to which the National Map of

Topographic items	Time invariant	Best band				False color
		4	5	6	7	
highways	:					
in service	yes		X		X	X
in construction	yes		X		X	X
rivers	yes			X	X	X
lakes	yes	X			X	X
marshlands	yes	X			X	X
seashore	yes	X		X	X	
cities						
more than 5.000h.	yes		X		X	X
forests	yes					X
Sum		3	3	2	7	7

Table 5. Combination of tables 3 and 4 showing topographic
items identified by LANDSAT in any season (multi-
temporal detection).

Spain will be produced (reference 4). From the analysis of
table 4 it can be defined in a certain way the capability
of LANDSAT for supplying topographic data at the scale under
study. The limitation of the satellite for defining many of
the items indicated in the table comes from the MSS sensor
resolution, which is not enough to provide many of the basic
data required in the map at such scale. Resolution of
corrected images is 80 x 80 m.

Continuing with the intention of defining invariant values to
look at in a LANDSAT image, a combination of tables 3 and 4
was studied, looking for topographic items identifiable
during the four seasons of the year. The result is shown in
table 5, where cartographic information indicated is multi-
temporal invariant. The meaning of this term multi-temporal
has to be understood here in the way that, although changes
occurring in the nature, such changes are always detectable
by at least one of the MSS spectral bands at any time. As this
research project was NASA supported, a multitemporal coverage
of images over Central Spain was available for the purpose of
this work.

Analysis of table 5 gives the following results:

1 - All items appearing in table 4 as detectable by LANDSAT
show a multi-temporal capability for being identified. The
reason is that resolution of the MSS sensor imposed in
table 3 a much stronger limitation than the seasonal
variation studied in table 5. From this, it can be stated
that resolution is a more limitative factor than the
temporal change of the surface cover for LANDSAT data
applied to cartography at small scales.

2 – Band 7 shows the same detection capability than false
color composites, according to the sum of different
conventional signs identified. This result is different
to the one presented in table 3, where false color
information, when applied to cartography in general
(including thematic mapping), was more able to discrimi-
nate natural phenomena. When the area of analysis is
limited to topographic mapping, band 7 shows as good
capability as false color information for discriminating
different types of cartographic items.

3 – Band 7 and false color information can detect by themselves
altmost all the topographic items that MSS data can
position in a map at scale 1:500.000. In the case of
forests, better information is achieved from the color
composite, while the infrared band gives more accuracy
in the delineation of seashores. Except for these two
items, their content of information seems to be similar,
and both band 7 and the false color composites together
can detect all the MSS information applicable to topographic
mapping in Spain.

A comment must be given to the high capability of band 4 for
detection of interrelations between water and land. From a
topographic point of view border lines can be better recognized
in band 7, as in the cases of sheashores, marshlands and lakes.
But band 4 is able to provide bathymetric information at low
depths, while the infrared absorption of radiation in the water
does not allow band 7 to give any data of the underwater
configuration.

Another topographic item for interest is the detection of cities
of more than 5.000 inhabitants. When a map at scale 1:500.000
is produced, the urban area has to be generalized from
information at larger scales. Such generalization can be done

by means of LANDSAT data, as shown in the false color composite
of Madrid appearing in figure 12. Bulk data in false color at
scale 1:500.000 or larger do not allow by themselves to
determine with cartographic accuracy the contours of even
large cities. As an example of this can be indicated the
land use map at scale 1:250.000 submitted within this final
report, which was done by an experienced photointerpreter
(reference 5). Comparing in the map the city of Madrid with
the topographic map at scale 1:200.000 also enclosed herein
(where the city was drawn by generalization of information
at scale 1:25.000), it can be stated that LANDSAT does not
offer enough information for determining urban contours
with cartographic accuracy. Only if the urban area is
represented schematically or by a conventional sign, should
LANDSAT give enough accuracy for indentification of cities.
As such schemes or conventional signs are well represented
in a map at small scale LANDSAT information was considered
time invariant and able to detect cities in tables 5 and 4.

Cartography at small scales from LANDSAT data can be accomplished
in three stages: ·
- acting of automatic cartography
- acting of LANDSAT information
- acting of conventional cartography

They are analyzed below.

3.1. Acting of automatic cartography.

Three main activities are indicated for this method of work:
- Drawing of the parallel and meridian canevas, and its exterior
  limit or frame
- Positioning of the main geodetic network, with its
  corresponding sign.

- Positioning of the main geodetic network, with its corres-
  ponding sign.

- Positioning of all urban areas which might be·located in
  the map and definition of their conventional sign, corres-
  ponding to their relative administrative importance and/or
  number of·inhabitants.

3.2. Acting of LANDSAT information.

As defined in paragraph 2, LANDSAT data have to be geometri-
cally corrected and referenced to a geodetic projection for
achieving cartographic accuracy. Corrected images can be used
for mapping the positively indentified items by LANDSAT indicated
in table 5: highways in service, highways in construction, rivers
lakes, marshlands, seashore, large cities and forests. All
such items can be detected in any season from LANDSAT informa-
tion and, what makes really useful the data, these cartographic
items show a rapid change in the nature and they are able to
be kept constantly up to date by means of multi-temporal MSS
recordings.

Band 7 and false color composites can be used as unique working
documents for topographic mapping, although every item could
be better identified by different radiometric enchancement
methods (reference 2).

3.3. Acting of conventional cartography.

All item indicated in table 4 which did not show enough resolu-
tion or real pattern for LANDSAT detection have to be mapped
by means of conventional cartographic techniques. At this
point, ancillary information is required. in the form of existing
maps, field work, conventional aerial photography, etc. The

list of such items is indicated in table 6. Their position
in a map cannot be sistematically defined from LANDSAT satel-
llites, unless resolution of the MSS sensor increased in the
future.

roads	dams, cascades
main tolls	channels
railroads	isolated houses
stations	industrial plants
tunnels	airfields
teleferics	small cities
grade crossing	altimetric data
	administrative limits

Table 6.

Updating maps at small scales can benefit from the use of
LANDSAT information, which can be considered as a powerful
working tool existing in the space. Such information has several
advantages, when applied to cartography, that guarantees its
value and uniqueness. They are the following:

- possibility of a multitemporal coverage of the earth surface,
  providing the capability of maintaining the information up to
  date.
- more economic production and updating of cartography at small
  scales than by the use of conventional techniques.
- rapid way of work, with a strong reduction in the number of
  basic information other than LANDSAT required; allowing a
  faster mapping of large areas than by conventional techniques.
- invariance of the space information compared to the aerial
  images obtained by photogrammetric surveying. Such invariance

is concerned with format, scale, projection, distorsion,
orientation, etc.

- elimination of progressive errors generated by conventional
  techniques, when maps at small scales are obtained by
  generalization of large scale maps (1:25.000   1:50.000
        1:200.000   1:500.000   1:1.000.000).

Because the limited resolution of the MSS sensor, only some
topographic items can be identified sistematically from LANDSAT
data. Such items are important to be periodically recognized
because their rapid natural (or artificial) change. The capa-
bility of LANDSAT information for defining topographic items
of interest in a map at small scale is summarized in table 7.

highways in service	marshlands
highways in construction	seashore
rivers	large cities
lakes	forests

Table 7.

Although MSS information is unique in the world, it cannot
be used as the unique input for mapping at small scale;
requiring ancillary information by conventional techniques
in order to overcome the following limitative factors:

- not enough resolution for defining all the topographic items
  to be positioned in a map at small scale. Such not detectable
  items were indicated in table 6.
- absence of altimetric data, because the lack of a photogra-
  mmetric base in the observation system.

- none indication of political or administrative limits,
  which have to be in the map and cannot be envisaged by any
  remote sensing system because their absence of physical
  patterns.
- need of geometric correction of the MSS data by reference
  to a geodetic projection before achieving the necessary
  cartographic accuracy.

4. THE NATIONAL MAPS AT SMALL SCALE.

LANDSAT information could be applied in Spain to updating the
following small scale maps produced by Instituto Geográfico
y Catastral:

- Provincial Maps at scale 1:200.000
- National Topographic Map at scale 1:500.000
- National Topographic Map at scale 1:1.000.000

At each scale the input LANDSAT information should be different,
as it should be also the processing technique used and the
cartographic work.

4.1. National Topographic Map at scale 1:1.000.000.

The interest of this scale is evident, and it is enough to
remember that Spain was one of the ten countries attending
the First International Conference of the World Map at scale
1:1.000.000, held at London in 1909.

Instituto Geogrъafico y Catastral has published several maps
at such scale in basic topographic versions and for the purpose
of thematic cartography. The last editions correspond to 1963
and 1974. In the edition of 1963, it was used a conformal conical
projection of Lambert with two automecoic parallels at N36°40'
and N39°20'. In the edition of 1974, it was used the same pro
jection and the automecoic parallels used were at N37°10'41"058
and N42°49'18"942. Printing is done in six colors with twelve
hypsometric inks. The map has level curves every 100 meters

and shading relief. The basic work was done by photographic
reduction and generalization of the National Topograhic Map
at scale 1:50.000.

According to the NMAS requirements, for practical purposes .the
RMS error of position in a map at such scale should be less than
300 m on the ground. From Table 1 it was obtained a mean value
of the RMS errors in 90% of control points, when referencing
LANDSAT images to UTM projection; being such value 278 m, which
is of the same magnitude that the tolerance of the map.

As the mean value obtained has the same magnitude than the
allowable RMS error, it can be said that LANDSAT bulk images
referred to a UTM projection, when used for mapping purposes
at scale 1:1.000.000, do not offer absolute guarantee of accu-
racy.

The most appropiate band for mapping at such scale should be
band 7, as well as the false color composite. The items to be
updated have been indicated in table 7.

As the National Map is in Lambert projection some scale correc-
tions are needed on LANDSAT images, although in the case of
Spain they would not be of influence at the mean latitude of
N40^o, with the automecoic parallels choosen. It is not intended
in this report to present the mathematical corrections that a
Lambert projection should impose in the LANDSAT image, but some
general remarks are indicated.

As the flight direction of the satellite is given as 9° west of
south (being cos 9° = 0,0988), assuming a north-south track for
this report, 184 kms of side in each photograph represents 1°40'
of latitude. Along adjacent flight strips the east and west
edges of the images would match because their same scale in north-
south dimension(assuming that exposure positions would be at
the same latitudes), being the maximum mismatches, therefore,

in the east-west direction at the joining edges of successive
images in a flight strip.

In the image center at N40^0 latitude it could be obtained the
scale factor and be compared to the factors of the upper and
lower images in the same orbital pass, thus obtaining the scale.
factors of the northern and southern edges of each image and
the expected errors in imagery matching at each join edge.

4.2. National Topographic Map at scale 1:500.000.

The National Topographic Map of Spain at scale 1:500.000 will
be updated in the year 1977 with the sheet distribution indicated
in figure 14. Such map will be produced extracting information
from LANDSAT MSS data in digital tape when geometrically corrected
by reference to the U.T.M. projection. The methods here indicated
in paragraphs 2 and 3 will be used for this work.

The National Map will be produced according to the european
specifications, although such standard procedure presents some
problems in the particular case of Spain; like the color distri-
bution of elevations and the location of the isohypse of 75 m.
The light color distribution (yelowish-greenish tones) has been
calculated according to the european mean elevation above sea
level, which is lower than the existing in Spain. As result of
this, the dominant color in the new map would be the dark brown,
with low contrast of the cartographic information represented
on it.

The scale 1:500.000 seems the most appropiate for cartographic
application of LANDSAT data.

4.3. Provincial Maps at scale 1:200.000.

The Provincial Maps at scale 1:200.000 were made by generalization
of information and reduction of the N.T.M. at scale 1:50.000,
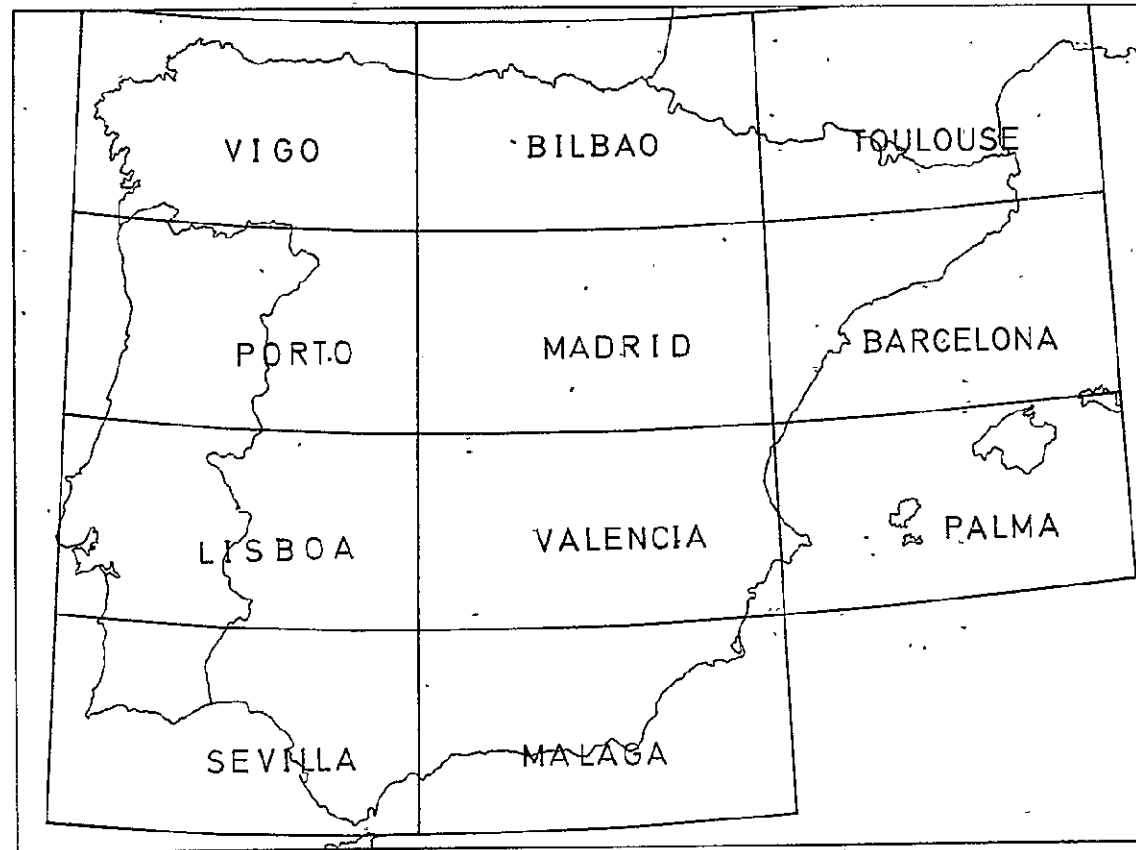
Fig. 14.—Sheet distribution of the National Map at scale 1:500 000

which is in polyedric projection. Such map, as it was demons-
trated from Table 1, does not meet the standard cartographic
requirements, mainly because the wrong position of rivers and
natural features which have changed in the last years.

The methodology for updating Provincial Maps should be the same
that it was mentioned for the National Map at scale 1:500.000,
by means of corrected LANDSAT digital data. As part of this
project the Provincial Map of Madrid was updated from MSS
digital information, and in this final report is presented
the new edition of the map (folded in the back cover).

Several modifications have been introduced in the new map as
compared to the old one. As new topographic and thematic items
identified on it by means of LANDSAT can be indicated the
following:
- one new urbanization (Tres Cantos)
- two golf course (Puerta de Hierro and Club de Campo)
- forests (with differentiation of conifers and leafy trees)
- irrigation lands (along Manzanares, Tajo, Tajuña and Jarama
  rivers)
- one new reservoir

Also, several main roads have been modified, the rivers layout,
the toponymy and several other conventional signs. This map
was made in a fast mode of operation by photointerpretation of
the geometrically corrected images generated from MSS digital
data.

5. CONCLUSIONS

In this report it has been evaluated the capability of LANDSAT
MSS data for updating maps at small scales in Central Spain.

As stated in the analysis of cartographic accuracy done with
LANDSAT data, the images themselves can be positioned in an

absolute reference system (geographical coordinates or polar
stereographic coordinates) by means of their marginal indicators./
Errors in this case do not allow a higher accuracy in positioning
a point than 2 kms; which is a value only able to use the images
for mapping purposes at scale 1:5.000.000 or smaller.

By reference to a UTM projection, the errors (RMS), in bulk
images could be in the order of 250 to 450 m. Such measurements
were done by means of control points located in the images, and
they do not allow MSS data to be used in cartography at such
scale.

By digital analysis of LANDSAT data and geometric positioning
of pixels·in UTM projection, it was achieved and accuracy of the
corrected MSS information which could be used for updating maps
at scale 1:200.000 or smaller. The results here obtained show
that adjustement of the UTM grid is better obtained by a first
order, or even second order, algorithm of geometric correction.

In the selection of control points man made features exhibit
better capability for an accurate registration than natural
phenomena, which are normally wrongly positioned on small scale
maps (as the Provincial Map of Madrid at scale 1:200.000) and
present dynamic changes. The number of control points has influen
ce in the accuracy of registration with a CCT. Also, their posi-
tion near the border of images reduces residuals and the proce-
ssing time of C.P.U. required in registration. If results do·not
meet the NMAS requirements for mapping purposes (which force an
error of zero· pixels at the current MSS resolution), the geometric
correction of CCTs could be run interactively until a good result
is achieved.

Positioning of independent·CCTs to a common geodetic projection
· is required for elimination of the anamorphosis existing in
their bulk data, and for having benefit of the conformal proper-
ties of the projection. Such relative image to image geometric

relationship is possible by registration of the original MSS
data, mainly with the purpose of constructing digitally controled
mosaics. Bulk data by themselves do not allow establishing this
relative geometric relationship between independent CCTs.

Conversion of registered CCTs to image is a need if the informa-
tion referred to UTM projection is to be photointerpreted for
cartographic purposes. Geometric correction of the output false
color image can be done by hardware configuration of the film
recorder. Some limitations exist in the enlargement of the image,
when it is going to be used for mapping at small scales, mainly
concerned with degraded printing or enlarging factors. The output
image maintains the cartographic fidelity of the registered CCT.
As an option the false color image could be enlarged by projec-
tion. In that case better operational results can be obtained if
projection is done on horizontal screen, allowing not only the
photointerpretation but the drawing of the rough draft transpa-
rency of the map to be updated.

LANDSAT information is needed when a map at small scales is
desired to be kept up to date. MSS data allow a faster and more
economic cartographic work, being limited by the resolving
power of the sensor. For cartographic purposes only clearly
and sistematically detectable features can be taken into
consideration when using LANDSAT data as input. In any case,
it is required ancillary information when producing or updating
a map. Such information concerns conventional cartography and
aerial photography. Table 7 summarizes the items able to be
updated by LANDSAT.

Band 7 and false color composites exhibit the best capability
in cartography, being their content of information for such
application very similar, except in the case of water features
detection (band 7 gives better results) and in forest identifi
cation (false color is required).

When applying these considerations to the National Topograhic
Maps, the goodness of LANDSAT information shows dependent on
the scale. At scale 1:1.000.000 a use of bulk data referred to
an UTM projection system could be done, providing data of all
the national territory, although the cartographic accuracy of
such MSS data is not guaranteed. The use of a conformal Lambert
projection should not modify significantly the application at
this scale.

The methodology for updating maps at scales 1:500.000 and
1:200.000 is similar and there is only a difference in the enlar
gement factor applied to the geometrically corrected image to be
photointerpreted. As example of this operational use of LANDSAT
data it has been updated the Provincial Map of Madrid at scale
1:200.000. This procedure required geometric correction of
digital data by means of control points referred to UTM projection.

Finally, from this evaluation of MSS information applied to
updating cartography, it can be stated the need of better reso-
lution and spectral bands in the sensor, if LANDSAT program will
follow-on in the future with the objective of providing systema-
tic data to be used, not only in an experimental stage, but for
operational purposes.

References.

1 - Servicio Geográfico del Ejército. "Tablas de la Proyección
    UTM", Sección de Geodesia, Madrid, 1974.

2 - A. Santisteban. "Study of radiometric enhancement méthods applied to LANDSAT MSS images"; Final Report, NASA project no. 28760, IBM - Scientific Center, Madrid, 1976.

3 - Dicomed Corp. "Dicomed color image recorder operation and programming manual (12M042)", Minneapolis, Minnesota.

4 - Instituto Geographique National. "Specifications de la série World 1404", Paris.

5 - E. Chicharro Fernández. "Application of LANDSAT-2 data to land use mapping in Central Spain", Final Report, NASA project no.28760, Universidad Nacional de Educación a Distancia, Madrid.

D I G I T A L   P R O C E S S I N G

STUDY OF RADIOMETRIC ENHANCEMENT METHODS APPLIED
TO LANDSAT MSS IMAGES.

A. Santisteban

DETERMINATION OF UNCORRELATED BANDS IN A LANDSAT
MSS IMAGE.

A. Santisteban

THE BAND RATIOING TECHNIQUE APPLIED TO LANDSAT
MSS IMAGES.

A. Santisteban

IBM — Scientific Center
Autonomous University of Madrid
SPAIN.

DIGITAL PROCESSING

STUDY OF RADIOMETRIC ENHANCEMENT METHODS APPLIED TO LANDSAT MSS IMAGES

Antonio SANTISTEBAN

Centro de Investigación UAM-IBM
Universidad Autónoma de Madrid
Madrid - 34

1. INTRODUCTION

It is well known that the human eye can not discriminate too many grey levels. In fact not so many as a microdensitometer, a multispectral scanner or any other image digitizing device can. Hence a digital image can show up quite a lot of information when studied numerically (for instance by some automatic classification computer program) while appearing nearly uniform or blurred to a photointerpreter who studies it as an output of a film recorder. Then some processing is needed in order to obtain from the original digital image a photographic printout more suited to the analytic capabilities of the human observer. This processing, known in general as radiometric enhancement, can be done either photographically or digitally. We will cover in this paper only the latter which is clearly a more versatile and powerful method[1].

Most digital images are recorded on 9-track magnetic tapes and, for that reason, every picture element (pixel) is represented by 8-bits even if data actually consists of less bits. For instance[2][3]. LANDSAT MSS images delivered by NASA have 8 bits per pixel in every band althogh bands 4,5 and 6 contain 7-bit data and band 7 contains 6-bit data. We must point out that the LANDSAT multispectral scanner gathers data of bands 4, 5 and 6 in 6-bit logarithmic scale; NASA translates them into a 7-bit linear scale according to colibration data: The differences of calibration among the six sensors of each band, along with the overall differences of calibration over a frame are responsible of the fact that more than 64 levels are occupied in the output bands.

In this paper we discuss the most useful methods of radiometric enhancement of digital images. In particular we apply these methods to LANDSAT multi-spectral scanner images[3], preparing them for recording using a DICOMED D-47 film recorder. This instrument accepts 6-bit and 8-bit data and can consider them as either linear or logarithmic scale data. We will consider only 8-bit linear output data because images delivered by NASA contain linear scale data and we take advantage of the greater number of output grey levels. We will also discuss briefly the use of the CONRAC RHN19 colour TV screen included in the RAMTEK GX 100B interactive display system as output device. It has only 16 levels in each electron gun, hence only 16 grey levels are available for the output.

In Section 2 of this paper we consider radiometric enhancement functions in general, while in Section 3 we mention the most useful practical cases that we apply to a practical example in Section 4. In Section 5 we discuss the application of different enhancement functions at the same time. Finally we make some considerations about colour images in Section 6.

2. RADIOMETRIC ENHANCEMENT FUNCTIONS

Let
$$J_n = \{i \mid i \epsilon Z, \ 0 \leq i \leq 2^n - 1\}, \ n \epsilon N \tag{1}$$
be the subset of the integer numbers that can be written with n binary digits (bits). Then a (single band) digital image is a two-dimensional array of elements of some J_n; the numbers $i \epsilon J_n$ represent the radiometric intensity levels of the corresponding pixels.

Any radiometric transformation of a digital image is a mapping
$$F : J_n \rightarrow J_m \tag{2}$$
of its set of radiometric levels into another (possibly different) set of levels. In particular we are concerned with a special kind of radiometric transformations: the so called radiometric enhancement[1] that are not characterized by any mathematical property but by a subjective fact: they tend to facilitate the analysis of the image by a photointerpreter by means of a redistribution of the most relevant radiometric levels in a way more suited to the human eye tonal response, taking into account the performance of the image producing devices. The only mathematical condition that we impose is that the mapping must preserve an order relation of its original set in
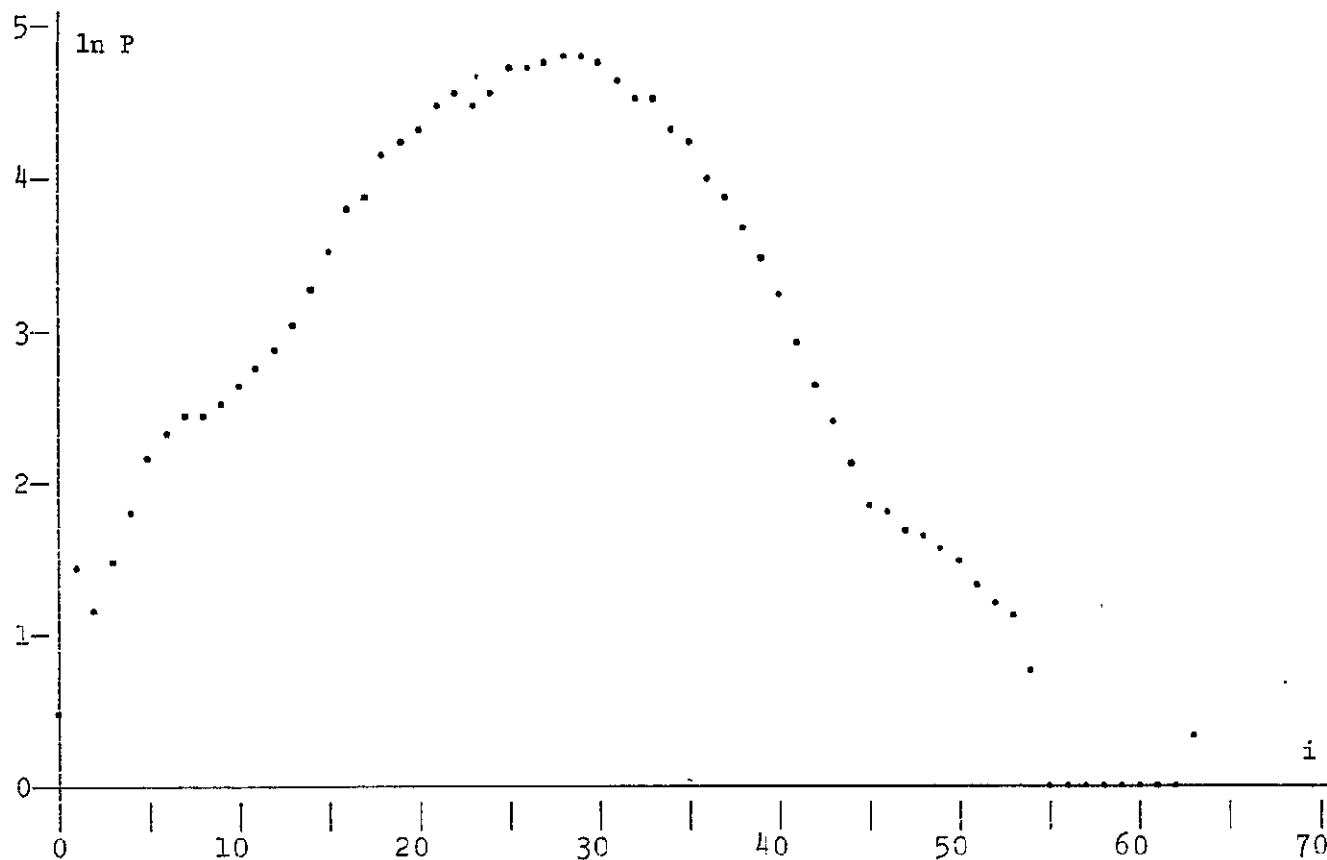
Fig. 1. Histogram of the example image in logarithmic scale.
(When P(i) = 0 is plotted P(i) = 1).

its image $F(J_n) \subset J_m$, namely either

$$\forall \; i, j \in J_n, \quad i \leq j \Rightarrow F(i) \leq F(j) \tag{3a}$$

or

$$\forall \; i, j \in J_n, \quad i \leq j \Rightarrow F(i) \geq F(j) \tag{3b}$$

or, what amounts to the same, thay must be monotonous mappings. In case of a decreasing monotonous mapping we say that we get a negative of the original image.

Despite its psychophysiological improving effect, radiometric enhancement usually degrades the image in the sense that increases its entropy or, conversely, loses information. Only when F is a biunivocal mapping of

$$J_n' = \{i \mid i \in J_n, \; P(i) \neq 0\} \subset J_n \tag{4}$$

onto its image $F(J_n') \subset J_m$, $P(i)$ being the number of pixels with radiometric level i, the transformation is isoentropic.

To proof the previous assertions we remember that the entropy S and the unformation I of an image are defined as[4]

$$S = -I = \sum_{i \in J_n} p(i) \log p(i) \tag{5}$$

where

$$p(i) = \frac{P(i)}{\sum_{i \in J_n} P(i)} \tag{6}$$

log stands for logarithm of base 2 and $p(i) \log p(i)$ is taken as zero whenever $p(i) = 0$. Then, if $F(i) = F(j)$ with $i \neq j$, the fact that

$$p(i) \log p(i) + p(j) \log p(j) < [p(i)+p(j)] \log[p(i) + p(j)] \tag{7}$$

implies that the entropy increases when $p(i) \neq 0$, $p(j) \neq 0$.

3. SPECIAL ENHANCEMENT FUNCTIONS

Now we are going to discuss the most useful enhancement functions F (see eq. (1)).

We consider that the histogram of the original image is the function

$$P : J_n \longrightarrow \{0\} \cup N \tag{8a}$$

and the histogram of the output image is the function
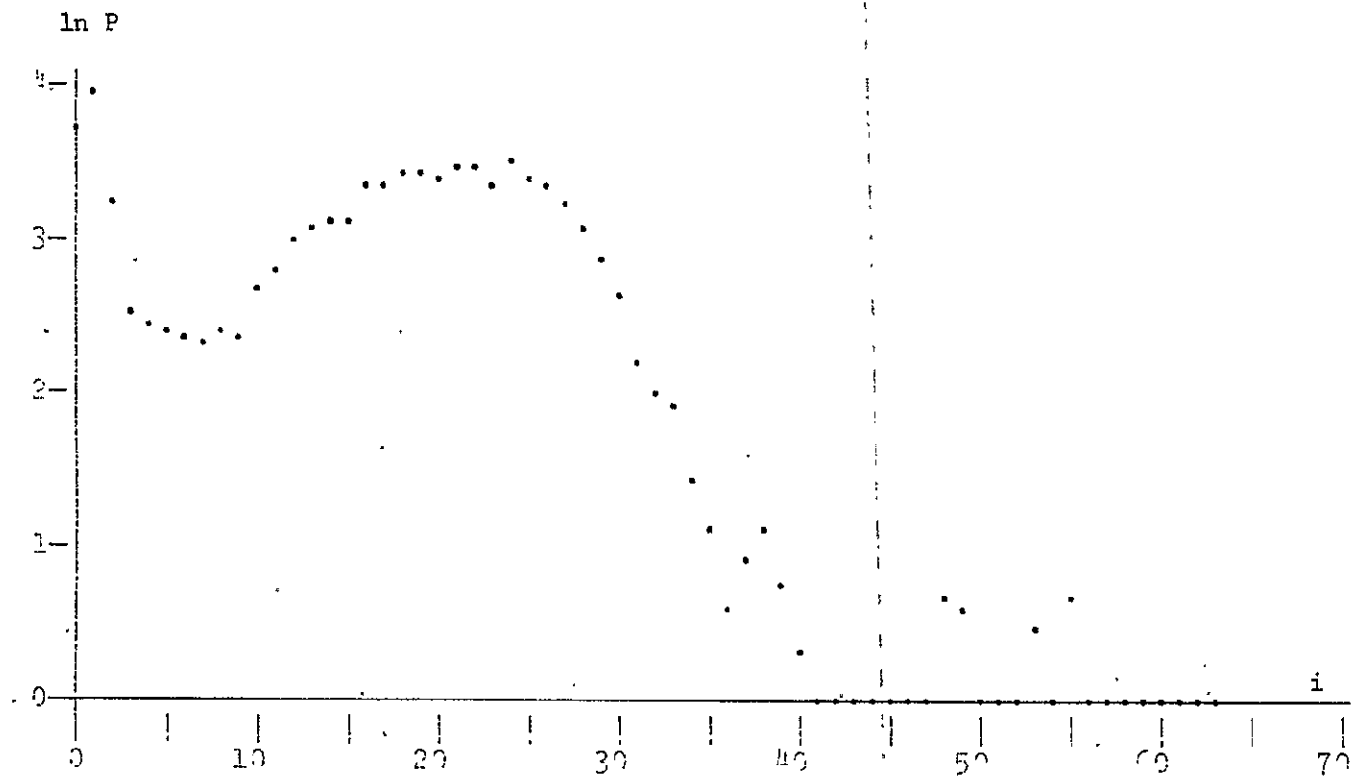
Fig. 2. Histogram of the image of a reservoir and its surroundings in logarithmic scale. There are two well separated lobes, one corresponding to the water and the other to the dry land.
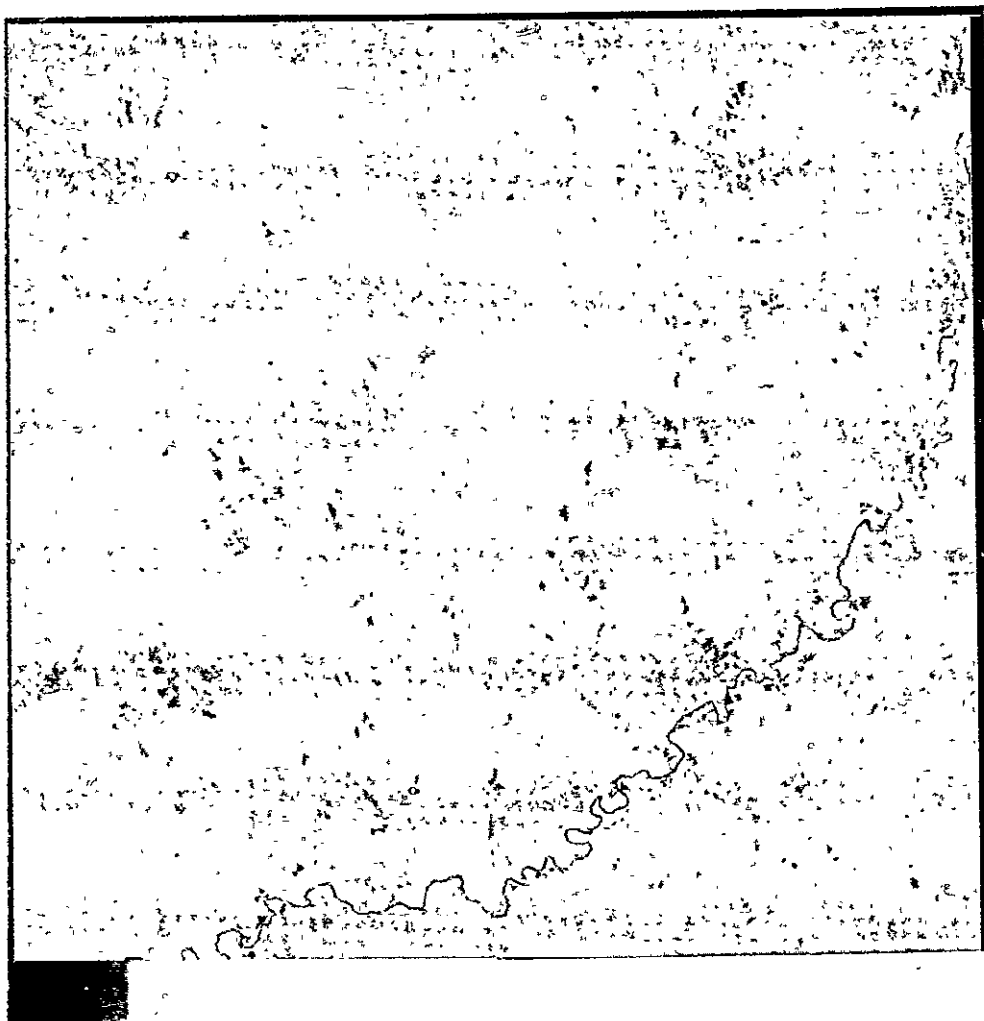
Fig 3.—The original example image (In fact the 6 bits of data are assigned the 6 more significative bits of the 8-bits scale of the film recorder)
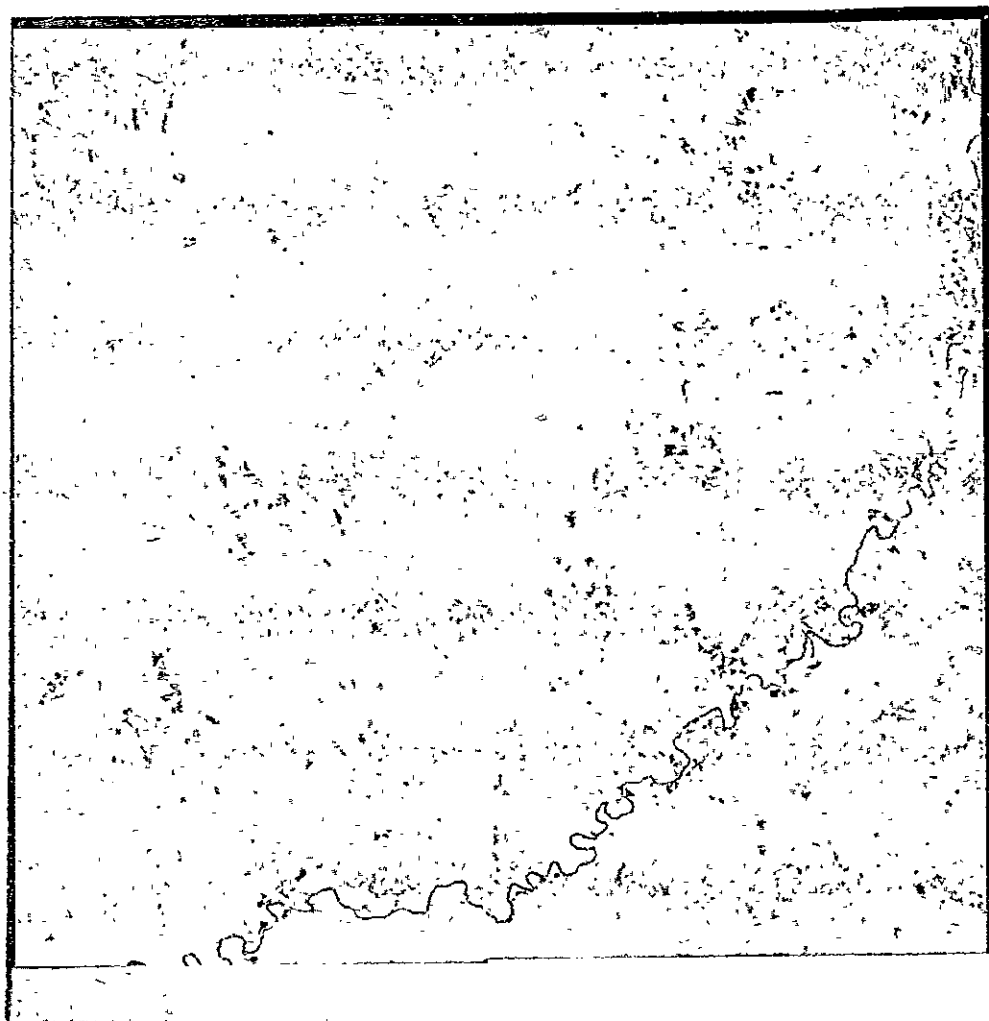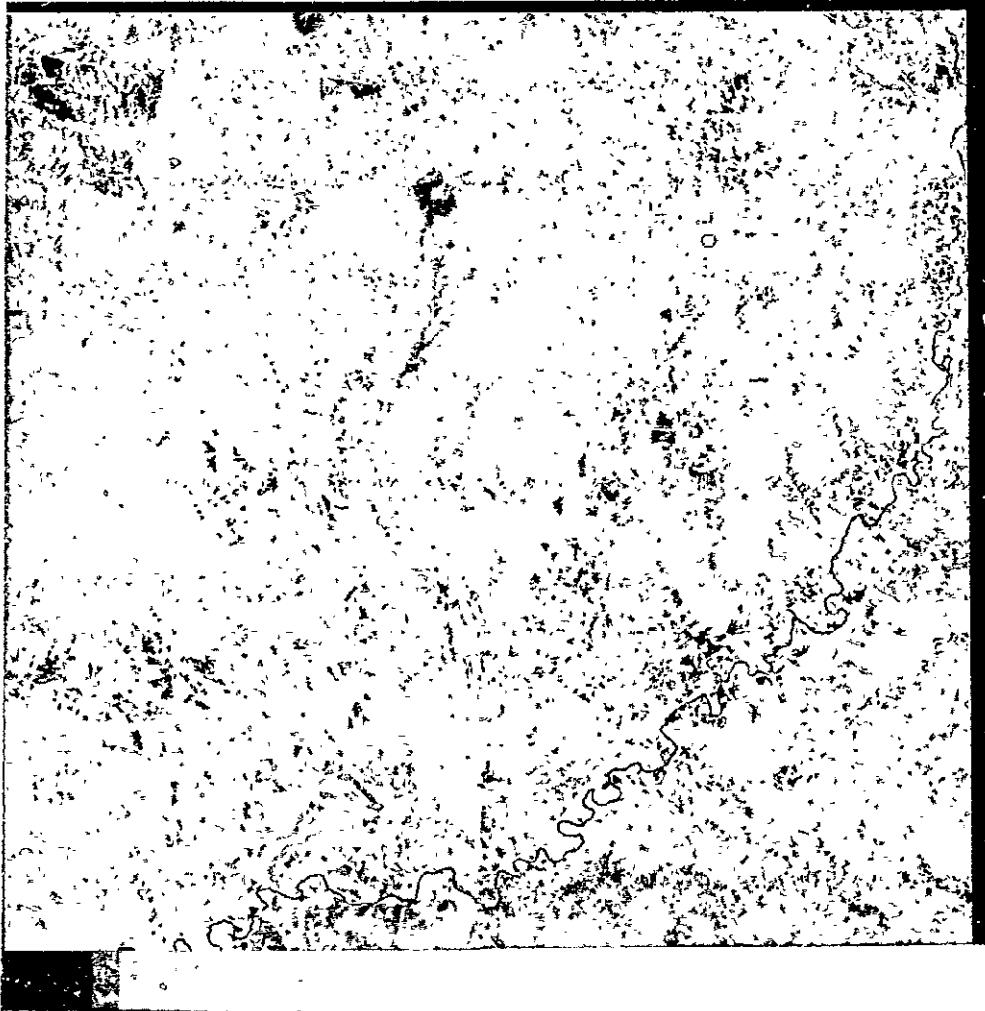
Fig 4.—Example image enhanced with $v = 4$

Fig 5.—Example image enhanced with $\nu = 3$

$$Q : J_m \longrightarrow \{0\} \cup N. \qquad \qquad (8b)$$

and call μ and σ the mean and standard deviation of the histogram $P(i)$:

$$\mu = \frac{\sum\limits_{i \in J_n} i \, P(i)}{\sum\limits_{i \in J_n} P(i)} \qquad \qquad (9a)$$

$$\sigma^2 = \frac{\sum\limits_{i \in J_n} i^2 \, P(i)}{\sum\limits_{i \in J_n} P(i)} - \mu^2 \qquad \qquad (9b)$$

To simplify notation we introduce the rounding function

$$e : R \longrightarrow Z \qquad \qquad (10a)$$

defined as

$$e(x) \equiv Int(x + 0.5) \qquad \qquad (10b)$$

i.e. $e(x)$ is the bigest integer number smaller than or equal to $x + 0.5$.

3.1. Linear Function

The simplest enhancement function, and nearly the only one used, is the truncated linear (usually referred simply as linear), defined as

$$L_1(i) = \begin{cases} 0 & \text{if } ai + b \leq 0 \\ e(ai + b) & \text{if } 0 \leq ai + b \leq 2^m - 1 \\ 2^m - 1 & \text{if } 2^m - 1 \leq ai + b \end{cases} \qquad (11)$$

If we take

$$a = \frac{\alpha}{\sigma} \quad , \qquad \qquad b = \beta - \alpha \frac{\mu}{\sigma} \qquad \qquad (12)$$

we obtain an image that, apart from the effect of the truncation due to the function e and the cut off of the histogram tails, has mean β and standard deviation α.

This enhancement transformation gives very good results when the histogram (empty levels excluded) approaches a normal distribution or, at least, is approximately bell shapped (see Fig. 1).

A good parameter selection may be
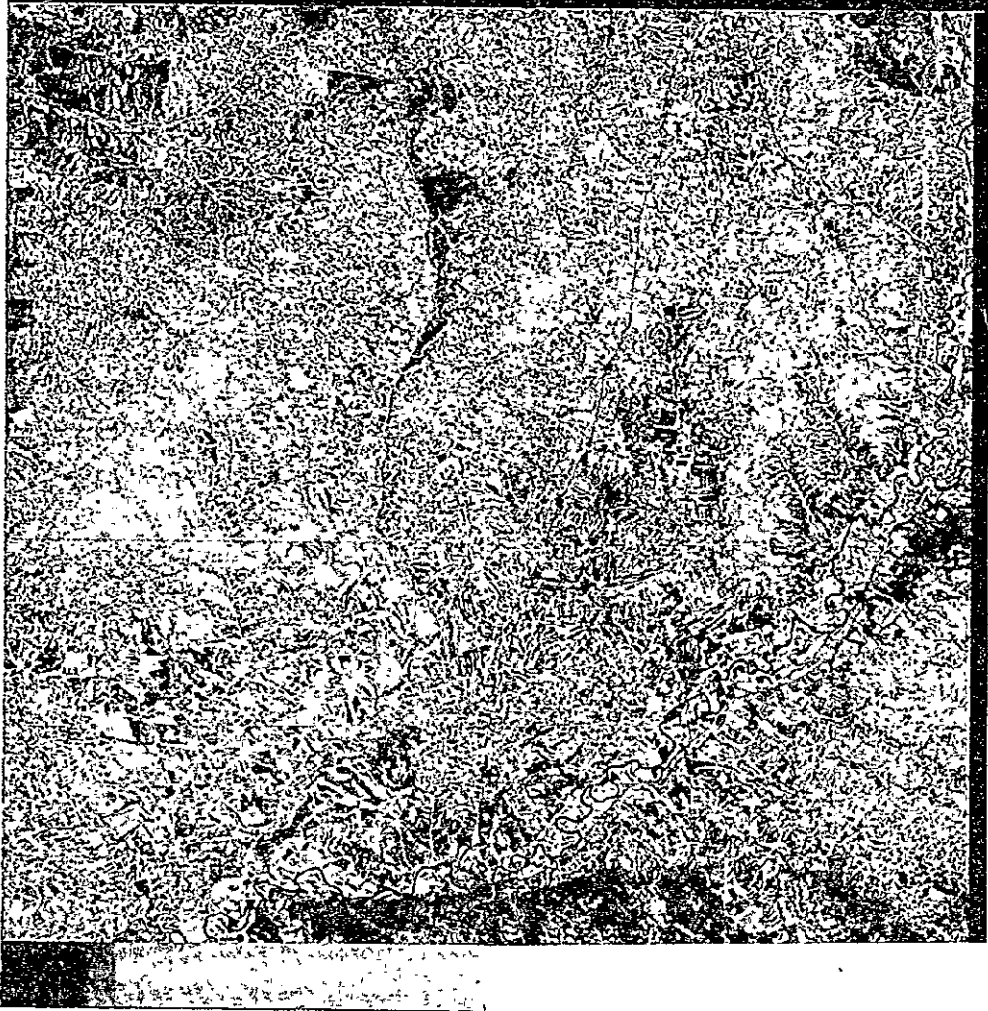
Fig. 6 —Example image enhanced with $\nu = 2$

Fig. 7.—Example image enhanced with $v = 1$

$$\alpha = \frac{2^m - 1}{2\nu} \quad , \quad \beta = \frac{2^m - 1}{2} \quad , \tag{13}$$

then

$$a = \frac{2^m - 1}{2\nu\sigma} \quad , \quad b = \frac{2^m - 1}{2} \left(1 - \frac{\mu}{\nu\sigma}\right) \tag{(14)}$$

and the output image has its mean at the center of the tonal range and the central peak of width $2\nu\sigma$ of the histogram is assigned the whole range. All levels more than ν standard deviations far from the mean are accumulated on the end values 0 and $2^m - 1$. The value of ν is a compromise between the need of high contrast (small ν) and limitation of the degradation produced by the tail-cut off (big ν).

3.2. Piecewise linear function.

When the histogram is not bell shapped at all but has several lobes (see Fig. 2) the linear transformation (11) may deteriorate the image, mainly if we want a high contrast. Then we can try a piecewise linear function. We may use a stiff segment for each lobe and a flatter one for the interlobe part:

$$L_3(i) = \begin{cases} 0 & \text{if } a_1 i + b_1 \le 0 & \text{and } 0 \le i \le c_1 \\ e(a_1 i + b_1) & \text{if } 0 \le a_1 i + b_1 \le 2^m - 1 & \text{and } 0 \le i \le c_1 \\ e(a_2 i + b_2) & \text{if } 0 \le a_2 i + b_2 \le 2^m - 1 & \text{and } c_1 \le i \le c_2 \\ e(a_3 i + b_3) & \text{if } 0 \le a_3 i + b_3 \le 2^m - 1 & \text{and } c_2 \le i \le 2^n - 1 \\ 2^m - 1 & \text{if } 2^m - 1 \le a_3 i + b_3 & \text{and } c_2 \le i \le 2^n - 1 \end{cases} \tag{15}$$

Obviously there are many (8 in this example) degrees of freedom in the construction of piecewise enhancement function: the gain and biass of each segment (remember that, though condition (3) must be satisfied, all gain and biass parameters are independent) and the break points (c_1 and c_2 in equation (15)).

3.3. Approaches to the optimal information display

Taking into account that J_n and J_m are sets of symbols for image codding, and the well known result of information theory[4] that states that the optimum codding is the one in which all symbols have the same frequency, we are going to consider an approach to the optimal information transmission to the photointerpreter.

Figure	v	a	b	Left tail		Right tail	
				levels	% pixels	levels	% pixels
4	4	6.27	−42.35	0 − 6	0.07	48 − 63	0.02
5	3	8.37	−89.97	0 − 10	0.24	42 − 63	0.16
6	2	12.55	−212.20	0 − 16	2.19	38 − 63	1.39
7	1	25.10	−551.91	0 − 22	19.22	33 − 63	13.66

T A B L E   1

Parameters concerning figures 4 to 7

It is obvious that no mapping of J_n into J_m can induce the transformation of the histogram $P(i)$ into a flat histogram $Q(j)$ because

$$Q(j) = \begin{cases} P(F^{-1}(j)) & \text{if } j \in I_m(J_n) \\ 0 & \text{if } j \notin I_m(J_n) \end{cases} \tag{16}$$

Nevertheless we can distribute the continuous tonal range, i.e. the continuous interval $[0, 2^m - 1] \subset R$, in 2^n ordered parts of lengths $d(i)$ proportional to $P(i)$;

$$d(i) = \frac{2^m - 1}{\sum\limits_{j \in J_n} P(j)} P(i), \tag{17}$$

and construct the radiometric enhancement function H that assigns to each $i \in J_n$ the integer number nearest to the middle point of the corresponding subintervals of $[0, 2^m - 1]$, namely

$$H(i) = e\left(\frac{d(i)}{2} + \sum\limits_{\substack{j \in J_n \\ j < i}} d(j) \right) \tag{18}$$

This transformation produces an image whose grey levels have a tonal difference proportional to the number of pixels in each level. Then there is the same number of pixels in any tonal interval of suitable width.

When 2^m is greater than (or even equal to) the cardinal of J'_n (see eq. (4)), there are empty levels in the output image; more empty levels in general than the difference between 2^m and the cardinal of J'_n because, in general, the less populated initial levels group together, This used to happen when we have a film recorder to print the image.

When we display the image on the colour television screen of the RAMTEK GX 100B interactive terminal that has only 16 grey levels, this method produces a flatter histogram by accumulation of several initial levels on the same output level.

4. EXAMPLES OF RADIOMETRIC ENHANCEMENT OF LANDSAT MSS IMAGES

Let us apply the previous ideas to a practical example. We consider a sub-image of a LANDSAT multispectral scanner image: the band 7 of frame 2223-10132. The subimage has 1024 pixels of width, starting in pixel 51, and 714 lines of length, starting in line 1266, and corresponds to a region of
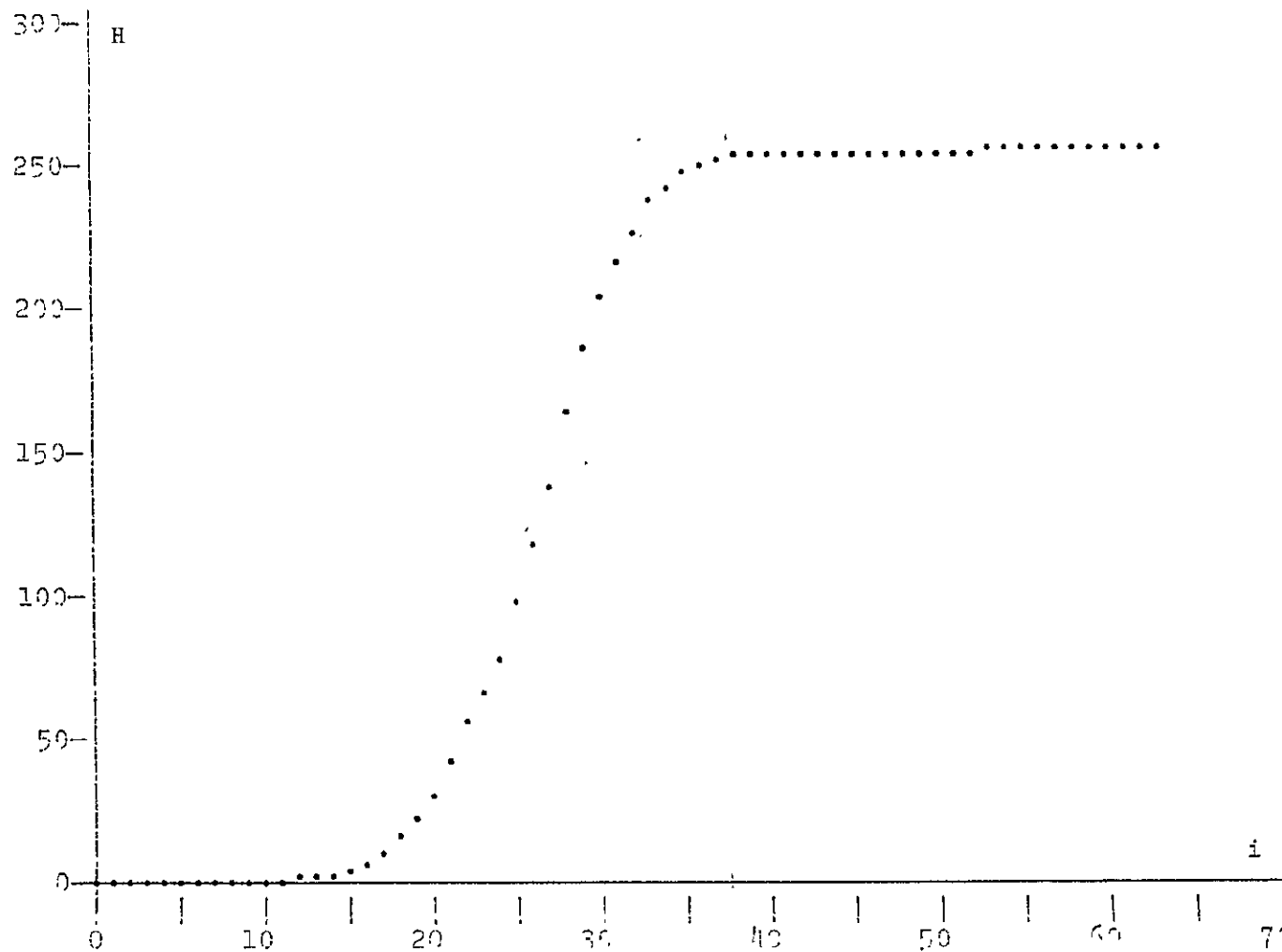
Fig. 8. Equalizing enhancement function for the example image.

approximately 58,4 Km by 56,4 Km just south of Madrid.

We have added at the botton left side of every image we are going to show up a grey wedge for the sake of reference. It contains 17 grey levels (namely 0, 16, 32, 48, 64, 80, 96, 112, 128, 144, 176, 192, 208, 224, 240 y 255) hence one can check the influence of development and/or printing in order to do comparisons among the pictures. The lenght of the grey wedge corresponds to 29 Km in the image. The images are not registered but the DICOMED D-47 film recorder is able to correct the distortion due to the rectangular shape of LANDSAT MSS image pixels.

In Fig. 1 we show the histograms P(i) of the above mentioned subimage in logarithmic scale (*) values of i greater than 63 are omitted because this band actually contains 6-bit data. Obviously it is far from a normal distribution, but seems to be more similar to a superposition of several gaussian distribution. Nevertheless, as they appear not clearly separated, the overall aspect of the histogram is quite bell-shapped at variance to Fig. 2.

In fact Fig. 2 is the histogram of an image representing a reservoir and its surroundings. It shows up two clearly separated peaks, the one at low levels corresponding to the water and the other to the dry land. This always happens when we deal with an image that includes a big area of water or snow covered (that produces a peak at the highest levels). As we pointèd out in Section 3.2., we must use a piece-wise linear enhancement function (15) or the equalized function (18) if we want to see the structure in the two regions.

Let us come back to Fig. 1. The histogram has mean $\mu=27.07$ and standard deviation $\sigma=5.08$. Fig. 3 shows the original image enhanced using eq. (11) with a=4 and b=0. As a matter of fact such an enhancement is simply the adaptation of the grey level range of the input to the grey level range of the output: ignoring the grey wedge, the output would have been the same if we had recorded the original data using the 6-bit scale of the film recorder.

The poor visual effect of Fig. 3 clearly indicates the need for a real radiometric enhancement. We will try the linear enhancement of eq. (11) with a and b given by eq. (14) using several values of ν. Hence

$$a = \frac{127.5}{\nu\sigma} = \frac{25.10}{\nu} \tag{19a}$$

(*) When P(i) = 0 we plot the value 1.
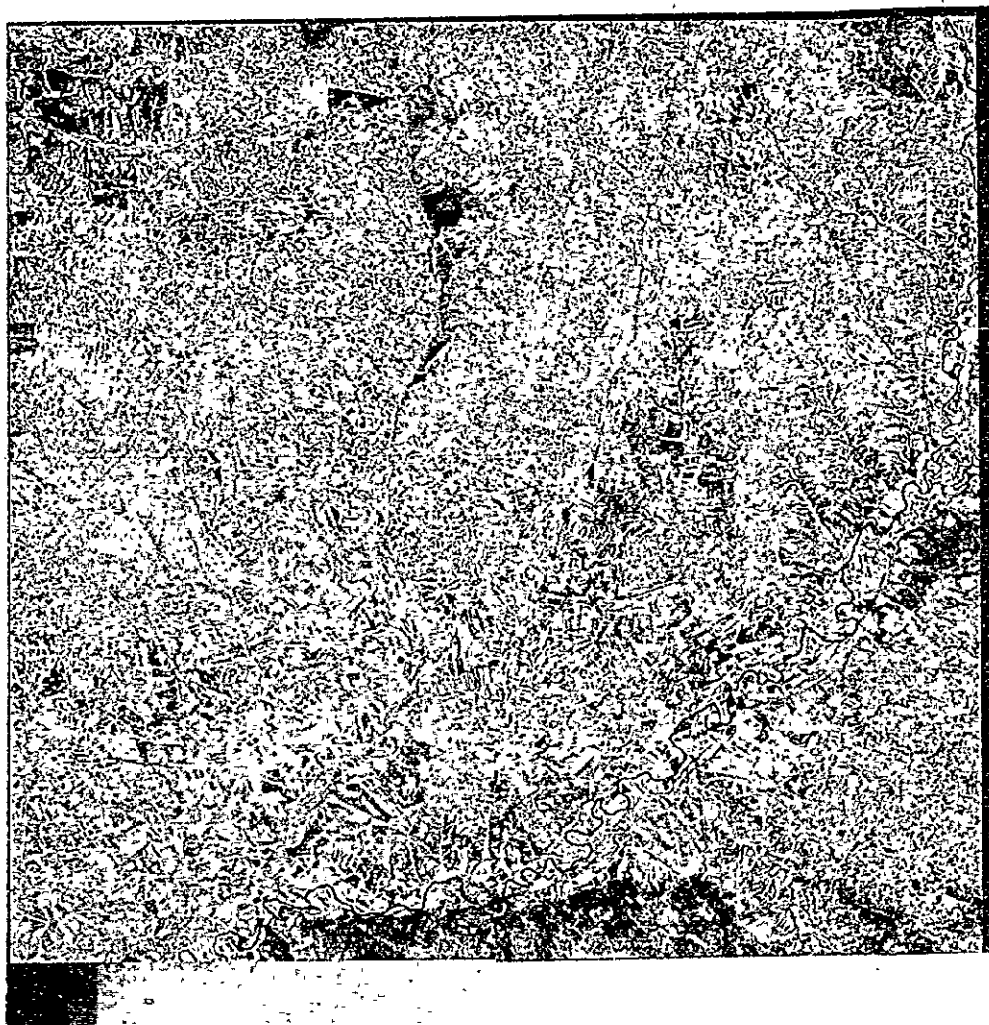
Fig 9 —Example image enhanced with the function of Fig 8

$$b = 127.5 \left[1 - \frac{\mu}{\nu\sigma}\right] = 127.5 - \frac{679.41}{\nu} \qquad (19b)$$

Table 1 summarizes the parameters used to obtain Fig. 4-7. We indicate under "left tail" the original levels that are mapped onto level 0, and under "right tail" those mapped onto 255, along with the corresponding percentages of pixels of those values.

It is appearent that $\nu=4$ produces a too poor contrast and $\nu=1$ a exceedingly high contrast with too many pixels accumulated in the end values. Between $\nu=2$ and $\nu=3$, may be the best value; possibly more near than $\nu=2$. This must be though of only as a hint. Every image is a particular problem whose histogram must be studied prior to any decision not only about the value of ν but even about whether a linear function may be used or not.

In Fig. 9 we show the same image enhanced with the equalization function H of eq. (18) that is represented in Fig. 8. This is a good method that gives good contrast in general (the more populated the levels the more separated), does not produce an important accumulation of pixels in the end levels and can be applied to all images. Nevertheless this enhancement methods is not used (except when m is smaller than n, see eq. (2)): it is usually prefered the (conceptually) more simple linear enhancement.

5. COMBINATION OF SEVERAL RADIOMETRIC ENHANCEMENT FUNCTIONS

The techniques so far described are intended to improve the appearance of the whole image. It is obvious that often a smaller subimage may be better displayed using a different enhancement function, but the use of this function to enhance the whole image implies a poorer aspect of other areas.

To show this with a practical example we take a subimage of band 4 of LANDSAT frame 1028-10200. The subimage has 1050 pixels of width, starting on pixel 2171, and 900 lines of length, starting on line 1 and corresponds to an area of 59.9 Km by 71.1 Km at the NE of Zaragoza and including it. A grey wedge has been added as before.

This subimage has mean $\mu_1=46.46$ and standard deviation $\sigma_1=10.69$. Fig. 10 shows it linearly enhancement with eq. (11) being the gain $a_1=5.96$ and the bias $b_1=-149.56$. These values correspond to $\nu=2$. Levels 0 to 25, which include 0.96% of the pixels, are mapped onto level 0 and levels 70 to 127,
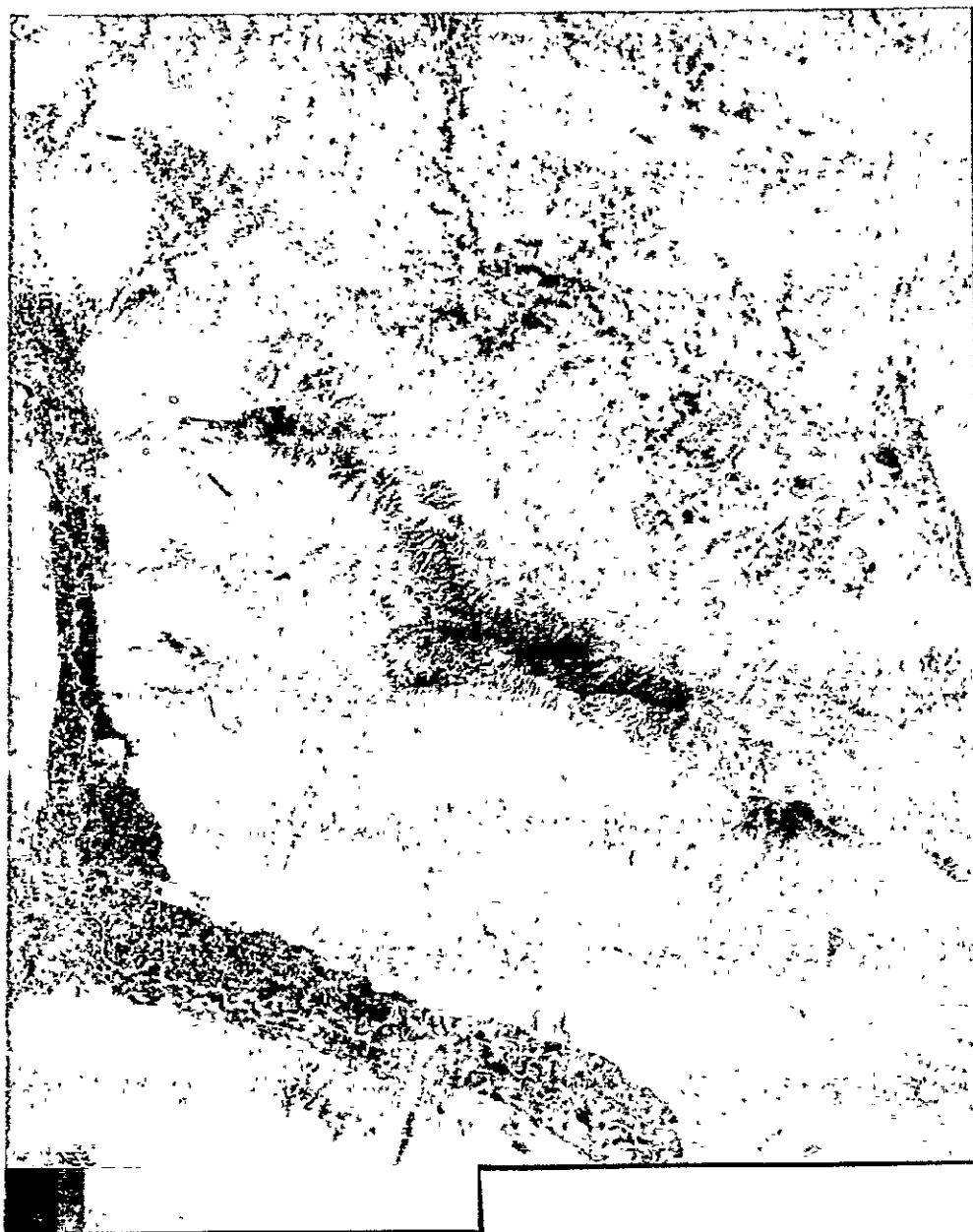
Fig. 10 —Zaragoza image enhanced with $v = 2$

Fig. 11.—Zaragoza image enhanced with a function adapted to enhance Los Monegros obtained from the sub-image data with $v = 2$

Fig. 12 —Zaragoza image enhanced with $\nu = 2$ (as in Fig 10) in which Los Monegros subimage has been enhanced with a more suitable function (as in Fig 11)

with 2.49% are mapped onto level 255.

Let us consider a subimage of the previous one with 400 pixels, starting on pixel 2361, by 100 lines, starting on line 589. It corresponds to an area of 22.8 Km by 7.9 Km on Los Monegros, a very arid region N.E. of Zaragoza. This smaller subimage has mean $\mu_2=56.99$ and standard deviation $\sigma_2=8.80$: it is brighter than most of the bigger image and has less relevant radiometric levels. To enhance this subimage using eq. (11) and $\nu=2$ we take a gain $a_2=7.24$ and a bias $b_2=-285.34$. Levels 0 to 39 with 0.88 % of the pixels are mapped onto 0 and levels 75 to 127 with 2.34% of the pixels are mapped onto 255.

Using the latter enhancement 27.44% of the pixels of the bigger image are assigned the value 0 and 0.66% the value 255. Hence the overall image, as shown in Fig. 11, is badly deteriorated by this enhancement that optimizes the appearance of Los Monegros.

A solution to the problem of having a good display of a subimage being, at the same time, able to see properly its surroundings is the one shown in Fig. 12. A enhancement function with a_2 and b_2 is applied to Los Monegros subimage while another enhancement with a_1 and b_1 is applied to the remainder of the image. The only obvious drawback is that we see a discontinuity on the border of the subimage.

6. RADIOMETRIC ENHANCEMENT OF COLOUR IMAGES

The best way to enhence a colour image is to apply one of the methods so far studied to each band separately as if they were black and white images.

This is also what we do when using the RAMTEK GX-100B display system. Nevertheless we must point out that, given that its refresh memory has only 8 bits per pixel to be distributed among the three bands we usually are compelled to take J_3 for two of the colours and J_2 for the other as the set of output grey levels instead of J_4 which can be used for single band images.

REFERENCES

1. A. Rosenfeld, "Image Processing by Computers", Academic Press (1969).

2. NASA Earth Resources Technology Satellite, "Data User Handbook", N71 - 75587 (1971).

3. R. Bernstein, "Digital Image Processing of Earth Observation Sensor Data", IBM J. Res. & Dev., 20, 40 (1976).

4. L. Brillouin, "Science and Information Theory", Academic Press (1971).

DETERMINATION OF UNCORRELATED BANDS IN A LANDSAT MSS IMAGE

Antonio SANTISTEBAN

Centro de Investigación UAM-IBM
Universidad Autónoma de Madrid
Madrid-34

1. INTRODUCTION

When we want to produce a false colour print with a LANDSAT MSS image that has four bands we must first determine which one will be excluded. The usual convention is to omit. band 6. But we do not know how much information we are disregarding with that choice. On the other hand, all four bands are correlated and we are introducing some redundant information with the three bands kept.

Thus it would be desirable to have a method to extract the real information content of all bands and put it in some way in no more than three new bands (to be assigned the three fundamental colours). Automatic classifiers would also take advantage of such a method because they would avoid the expensive processing of redundant data.

The best way to solve this problems is to obtain uncorrelated bands,i.e. bands that have no correlation when we compute statistics all over the image. These bands are linear combinations of the original ones and their amounts of information decrease very rapidly from the first to the last.

In Section 2 we present the mathematical method to obtain uncorrelated bands for an image with an arbitrary number of them. It is based on the calculation of the eigenvectors of the covariance matrix. In Section 3 we discuss a practical example.

It is obvious that this method will be even more usefull when we deal with
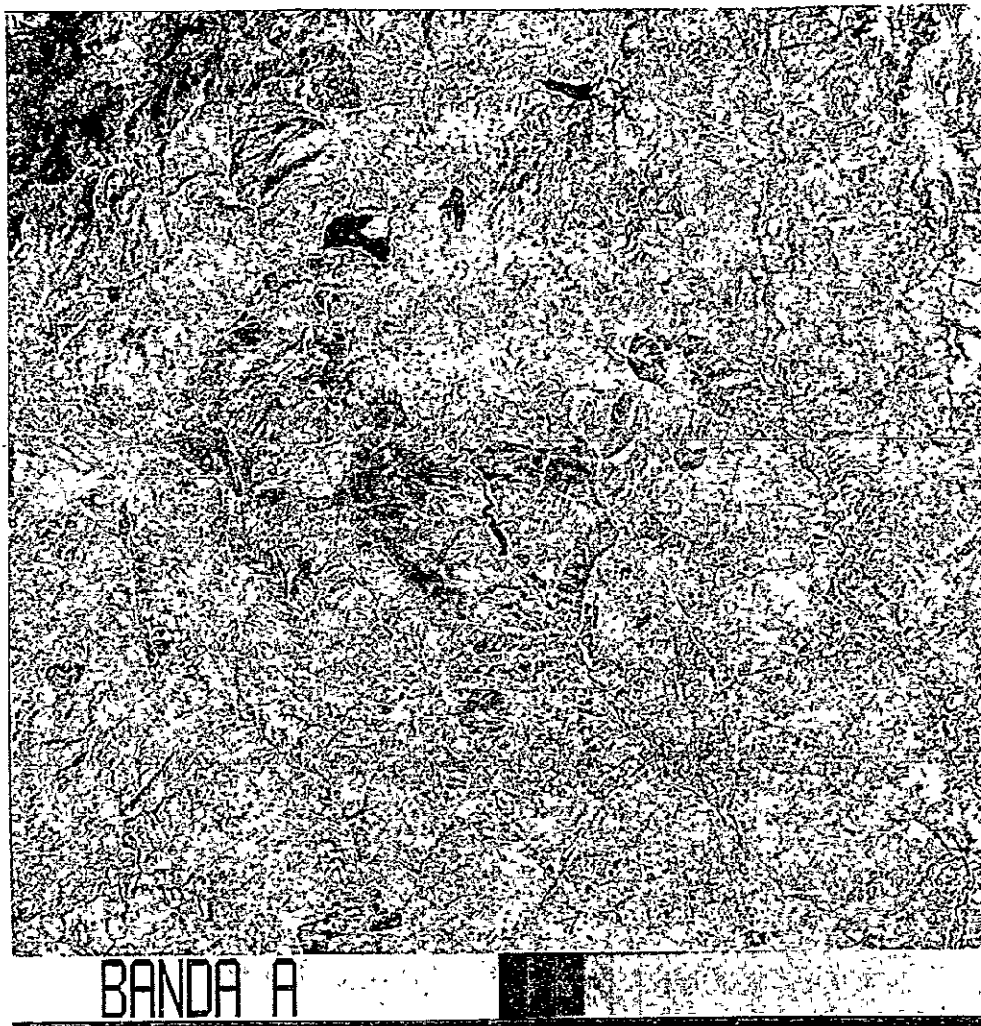
BANDA A

Fig. 1.—Band A enhanced

C.2

images containing more than four bands. In that case we will be interested in the three more significant bands in order to display a false colour image (even if there are more than three bands with a relevant amount of information). In automatic classification we will be able to supply the classifier with an image with nearly the same information as the original but with less bands.

2. DETERMINATION OF THE UNCORRELATED BANDS

Let us consider any pixel of a n-band multispectral image as an element $\vec{x}$ of the n-dimensional vector space on the real numbers R^n, being the radiometric intensity levels in the n bands, x_i, $i=1,\ldots,n$, its n coordinates on a given orthonormal base $\{\vec{e}_i, i=1,\ldots,n\}$. Hence, using Einstein summation convention.

$$\vec{x} = x_i \, \vec{e}_i \tag{1}$$

As a matter of fact pixels are very special elements because their coordinates on the base $\{\vec{e}_i\}$ are integer numbers that can be written with m binary digits, i.e.

$$x_i \epsilon J_m = \{a \,|a\epsilon Z\subset R, \ o\leq a\leq 2^m - 1\} \tag{2}$$

We allow during the following calculation pixel coordinates to take on real values and only in the last step of the process we will approximate them by integer numbers of m bits provided that they represent intensity levels of digital images.

Let us also consider a n-band digital image as a vectorial random variable[1] $\vec{X}$ (whose components refered to the base $\{\vec{e}_i\}$ are X_i, $i=1,\ldots,$ n) on the space of events R^n.

The variance of $\vec{X}$ is the matrix C of covariance of its coordinates

$$C = E(\vec{X}\otimes\vec{X}) - E(\vec{X}) \otimes E(\vec{X}), \tag{3}$$

where E denotes expectation and $\otimes$ the tensor product. It is a symmetric matrix so it can be diagonalized. Let us call λ_i its eigenvalues, i.e. the roots of the secular equation

$$|\, C - \lambda 1 \,| = 0, \tag{4}$$

being 1 the identity matrix, in decreasing order, i.e., $\lambda_1\geq\lambda_2\geq\ldots\geq\lambda_n$. We assume
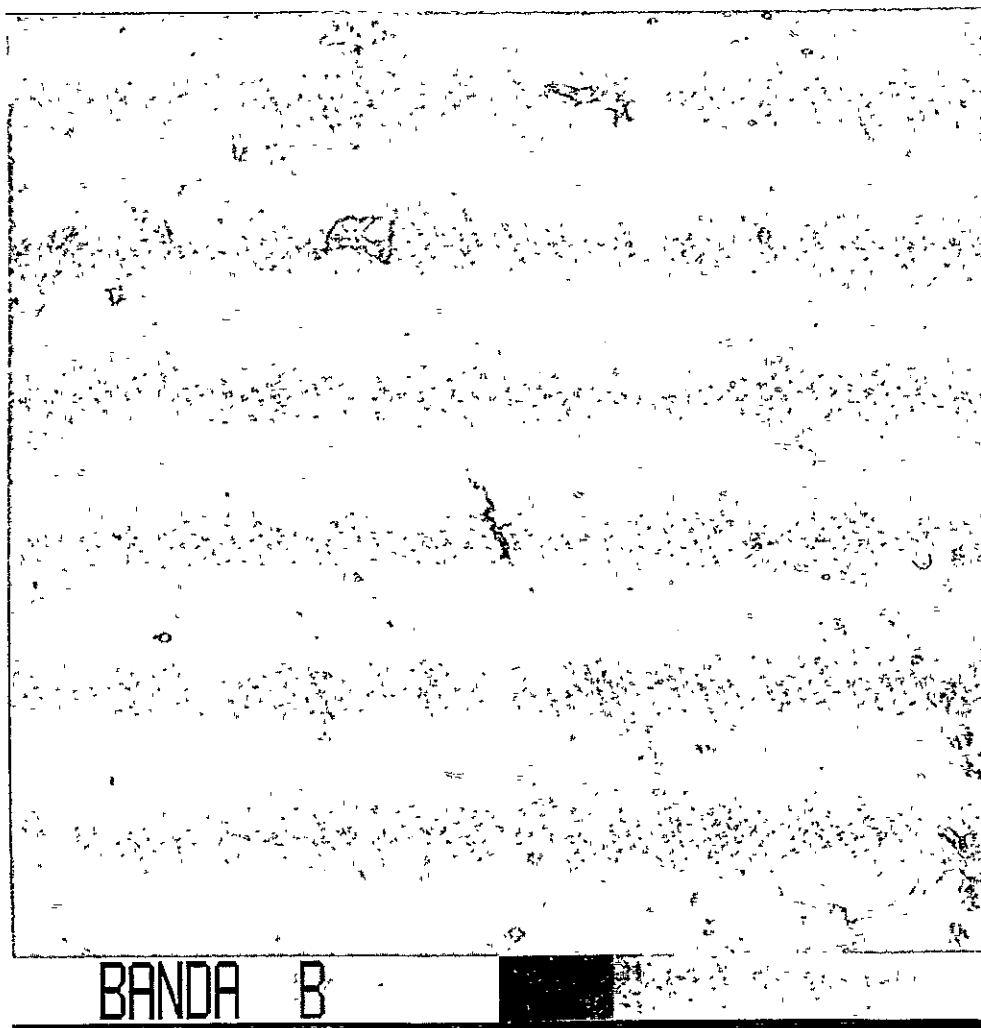
Fig. 2:—Band B enhanced proportionally to band A

that these is no degeneracy, although this assumption is not essential to the calculation but only makes it simpler; farthermore it is true in all practical cases. Let us call $\vec{f}_i$ the eigenvectors of C :

$$C\vec{f}_i = \lambda_i \vec{f}_i \tag{5}$$

and F the orthogonal matrix that diagonalizes C :

$$FCF^{-1} = \Lambda \tag{6}$$

being

$$\Lambda_{ij} = \lambda_i \delta_{ij} \tag{7}$$

The columns of F are the eigenvectors $\vec{f}_i$:

$$F_{ji} = (\vec{f}_i)_j \tag{8}$$

The new random variables

$$Y_i = F_{ij} X_i, \quad i=1, \ldots, n, \tag{9}$$

which are the coordinates of $\vec{X}$ on the base $\{\vec{f}_i\}$, are then uncorrelated variables provided that their covariance matrix is Λ. The standard deviation of the probability distribution of Y_i is then $\sqrt{\lambda_i}$.

Only when $\vec{X}$ has a normal probalility distribution can we assure that Y_i are independent random variables and not simply uncorrelated.

Hence the pixel $\vec{x}$ has coordinates in the base $\{\vec{f}_i\}$, i.e. intensity levels in the new uncorrelated bands

$$y_i = F_{ij} x_j \tag{10}$$

As we want pixels to take values on J_m, we must approximate their values. Then we finally construct n new quasi-uncorrelated bands in which the intensity levels are

$$z_i = \text{Int} (a \, y_i + b_i) \tag{11}$$

The parameters a and b_i, i=1,...,n are introduced to guarantee that $z_i \in J_m$.

Taking into account that the maximum length of the interval y_i can take values on is $(2^m - 1) \sqrt{n}$, i.e. the length of the diagonal of the n-dimensional hy-
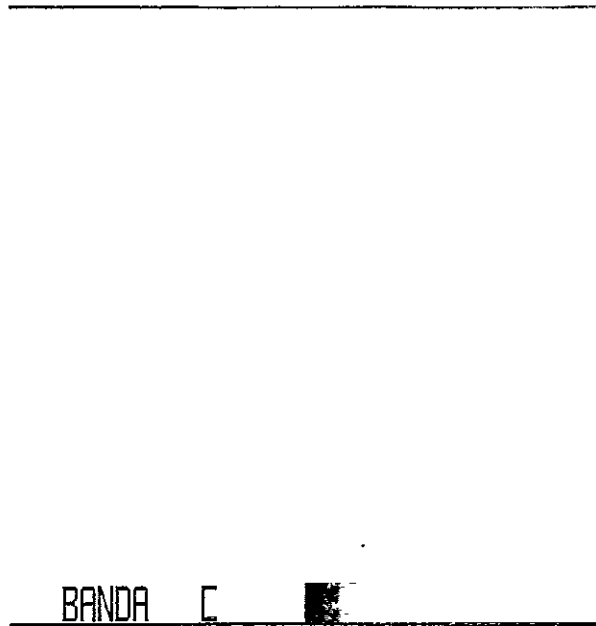
BANDA   C   ■

Fig. 3 —Band C enhanced proportionally to band A
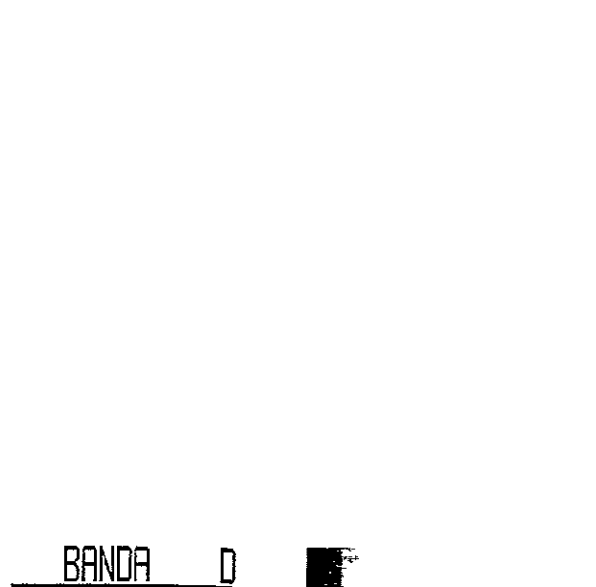
BANDA   D   ■

Fig 4.—Band D enhanced proportionally to band A

percube, we take

$$a = \frac{1}{\sqrt{n}} \qquad (12)$$

to reduce to a lenght 2^n-1 the range of z_i. We also take

$$b_i = \frac{2^m-1}{2} - E(Y_i) = \frac{2^m-1}{2} - F_{ij} \ E(X_j) \qquad (13)$$

to center the probability distribution of z_i in the middle point of its range.

The bands thus constructed are approximately uncorrelated (although we usually refer them simply as uncorrelated bands) whose probability distributions have means and standard deviations approximately equal to $(2^m-1)/2$ and $\sqrt{\lambda_i/n}$ respectively.

3. DISCUSSION OF A PRACTICAL EXAMPLE

We are going to apply this technique to LANDSAT MSS images, so now n=4 (the four bands are called 4,5,6 and 7) and we take m=8, the fact that these data have actually 7 or 6 bits being taken into account by the values of b_i. We will call the new quasi-uncorrelated bands, A,B,C and D.

The eigenvalues λ_i are ordered in decreasing order so that band A has the greatest standard deviation and band D the smallest one.

As a practical example we take a subimage of frame 2223-10132 (of September the 2nd, 1975) of 1024 pixels of width, starting on pixel 51, by 715 lines of length, starting on line 551. It corresponds to an area of 58.4 Km. by 56.5 Km. around Madrid. A grey wedge with 17 levels (16^k, k=0,1,...,15 and 255) is added at the botton of the pictures that we will show; it can be used as a reference to take into account the possible differences introduced by the development and printing processes. The length of the wedge corresponds to 29 Km on the image. We use a DICOMED D-47 film recorder to produce the photographs through its 8-bit linear scale and non square pixel compensation facilities.

Table 1 lists the means and standard deviations of the original image. The
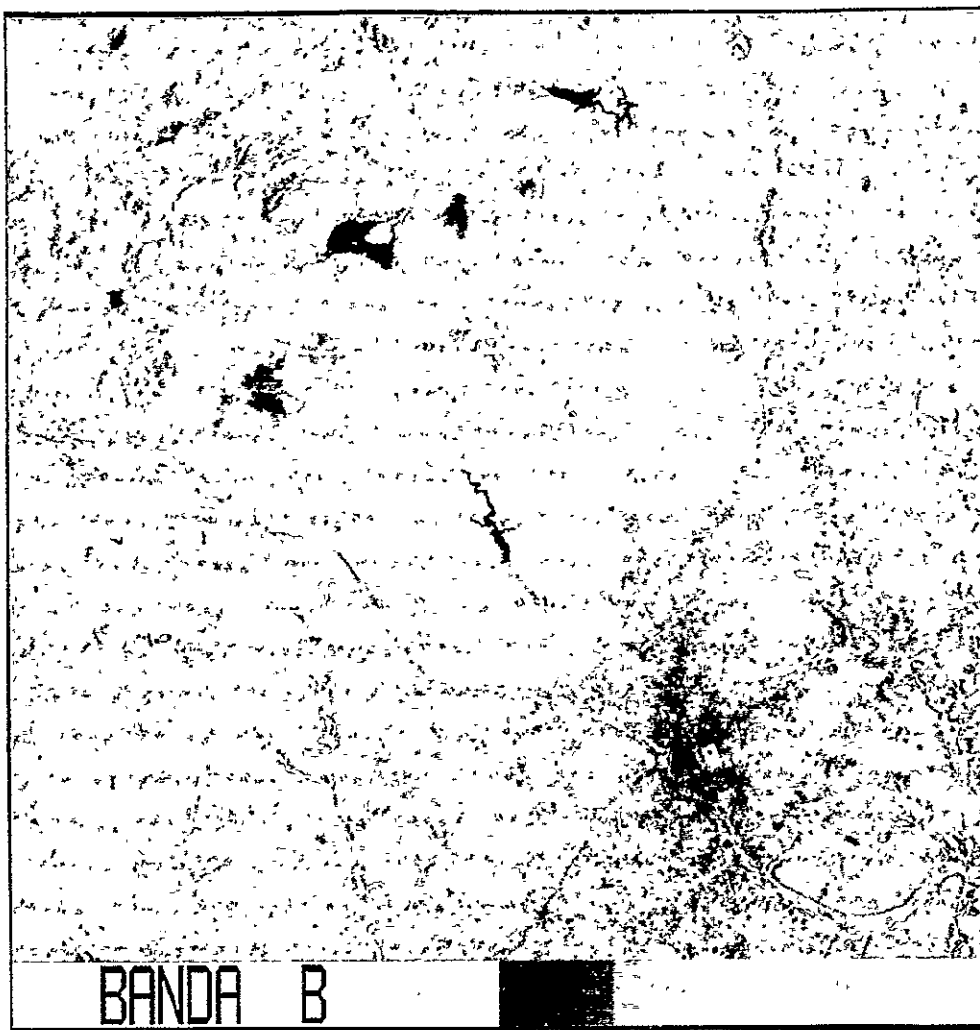
Fig. 5.—Band B with a maximum enhancement

covariance matrix is

$$\begin{pmatrix} 59.88 & 106.51 & 84.00 & 28.60 \\ 106.51 & 201.11 & 157.82 & 54.50 \\ 84.00 & 157.82 & 150.02 & 58.08 \\ 28.60 & 54.50 & 58.08 & 25.59 \end{pmatrix} \qquad (14)$$

and the correlation matrix, defined by

$$\rho_{ij} = \frac{C_{ij}}{C_{ii}C_{jj}} \qquad (15)$$

is :

$$\begin{pmatrix} 1.000 & 0.971 & 0.886 & 0.731 \\ 0.971 & 1.000 & 0.909 & 0.760 \\ 0.886 & 0.909 & 1.000 & 0.937 \\ 0.731 & 0.760 & 0.937 & 1.000 \end{pmatrix} \qquad (16)$$

Table 2 indicates the eigenvalues of C that correspond to the new bands A, B, C and D, the actual standard deviation of these bands (the differences between these values and $\sqrt{\lambda_i}$ /2 being produced by the round-off error) and the values of the transformation coefficients.

TABLE 1

Original Image

Band	Mean	Standard deviation
4	29.03	7.74
5	41.28	14.18
6	50.87	12.25
7	22.43	5.06

With this examples we realize a very general fact: there is a high correlation between the two visible bands and between the two infrared bands, while the correaltion between a band of the first pair and a band of the last pair is smaller although rather big.

Band	λ_i	Standard deviation	Projection over bands			
			4	5	6	7
A	409.36	10.12	0.368	0.689	0.586	0.214
B	23.27	2.43	−0.314	−0.515	0.617	0.505
C	2.69	0.85	0.859	−0.502	0.076	0.071
D	1.27	0.62	0.169	0.093	0.519	0.833

T A B L E   2

Uncorrelated band image

Bands C and D of the new image have very small information contents, most of the information of the original image having been accumulated in bands A and B.

Provided that even the standard deviation of band A is small we must radiometrically enhance the images before showing them to a photointerpreter. Of course this step must be omitted when we want the image for an automatic classifier. In the latter case we should give to it bands A and B only because bands C and D do not add relevant information.

We apply to band A a linear enhancement[2] such that the central peak of its distribution of semiwidth equal to two standard deviations is assigned the whole range of ourput levels [0,255], being its mean at the middle point approximately. Fig. 1 shows band A so enhanced with a gain factor of 6.30.

We show in Figs. 2-4 bands B, C and D respectively enhanced with the same gain 6.30 and appropriate bias factors so that we can realize the relative amount of information of each band.

In order to know with more detail how bands B, C and D look like, we show in Figs. 5-7 these bands linearly enhanced in such a way that their distribution's central peak of semiwidth equal to two standard deviations are assigned the whole range [0,255]. The gain factors applied are respectively 26.23, 75.00 and 102.82.

It is appearent that bands C and D contain nearly only noise. The noise sources in LANDSAT MSS images are mainly two: i) the round-off error produced in the quantization of the(analog) original signal and ii) the differences in calibration among the six sensors of each band. The former is approximately white noise and amounts at most to one radiometric level. The latter produces the typical stripping evident in many images which can amount to several levels. Both noise components are evident in bands C and D although stripping obviously dominates. The underlying signal in band C (see Fig. 6 in which this band is enhanced as much as possible) shows mainly structural features as reservoir limits, roads and rivers or more properly the vegetation besides them (remember that the image corresponds to summer time). The underlying signal of band D hardly shows some uniform bodies as the city,
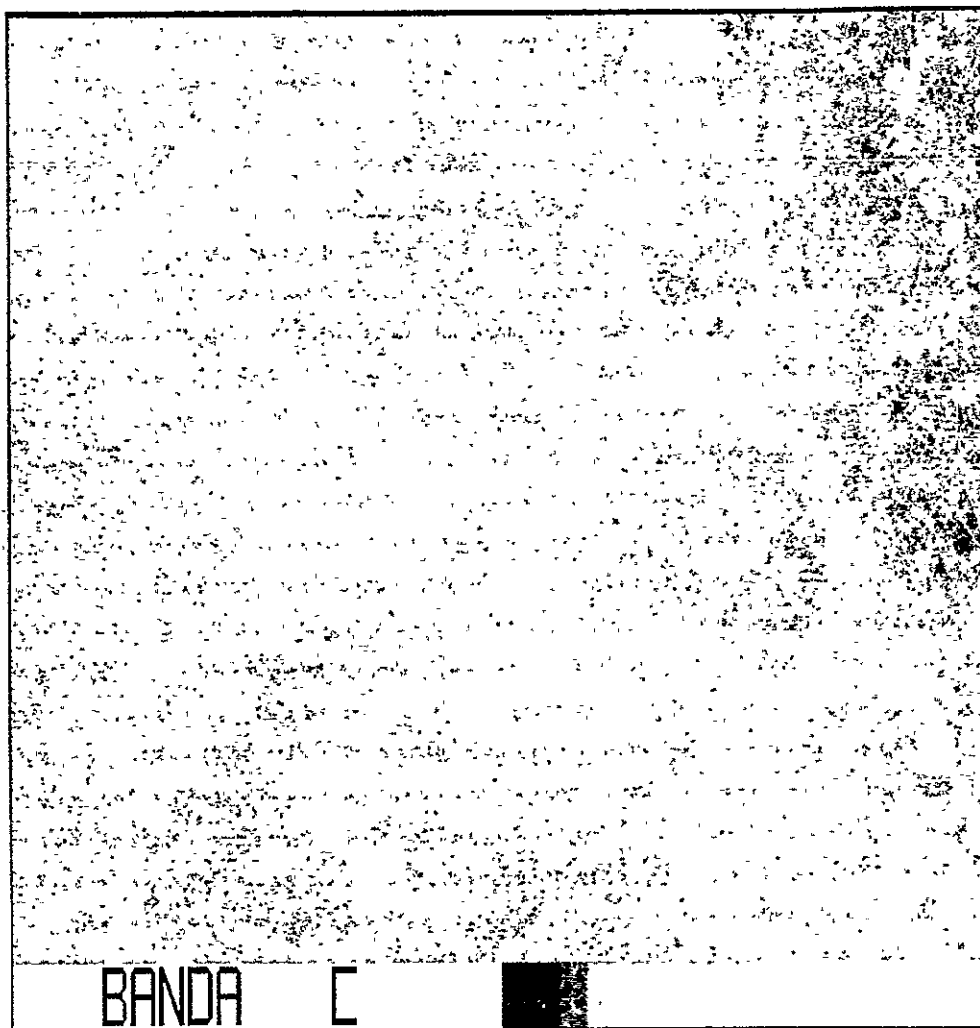
Fig 6 —Band C with a maximum enhancement

Fig 7 —Band D with a maximum enhancement

reservoirs or forests (see Fig. 7).

We have anticipated that because of the high degree of correlation among the four bands of LANDSAT MSS image (see eq. (16)) we really have not four bands with information. In fact we have two bands with relevant information, namely bands A and B (see Figs. 1 to 4).

Comparing bands A and B (see Fig. 5 in which band B is more enhanced) we rea-lize that one complements in some way the other so that both together have nearly all the information existing in the four original bands. Band A con-tains a lot of information concerning both structural features (as rivers and roads) and different land areas (urban, forests, water, etc.). Band B · makes more emphasis on structural features (the dendritic aspect of Guada-rrama river network is clearly visible).

Hence bands A and B alone may be used to produce false colour images (see Fig. 8) or to perform automatic classification. In fact Fig. 8 is a composite of band A (enhanced as in Fig.1) in green and band B with a maximum enhan-cement (as in Fig. 5) in red. Note that the name of each band appears in the complementary colour of that in which it is recorded and the botton wedge is obviously yellow. Despite its unusual aspect, this picture may be really va-luable for photointerpretation. This colour assignment has been selected in order for vegetation to appear red (as is usual in LANDSAT false colour images).

Finally in order to clearly understand the real meaning of the uncorrelated bands A, B, C and D we consider the four dimensional histogram P of the ori-ginal image: $P(\vec{x})$, $\vec{x} \epsilon R^4$, is the number of pixels with intensity levels x_1 in band 4, x_2 in band 5, x_3 in band 6 and x_4 in band 7. Thinking of it as a mass distribution in the four dimensional euclidean space we realize that it is very flat along the directions $\vec{f}_4$ (that corresponds to band D) and $\vec{f}_3$ (corres-ponding to band C). Hence it is quite a two dimensional "object" longer along · direction $\vec{f}_1$ (band A) than along $\vec{f}_2$ (band B).
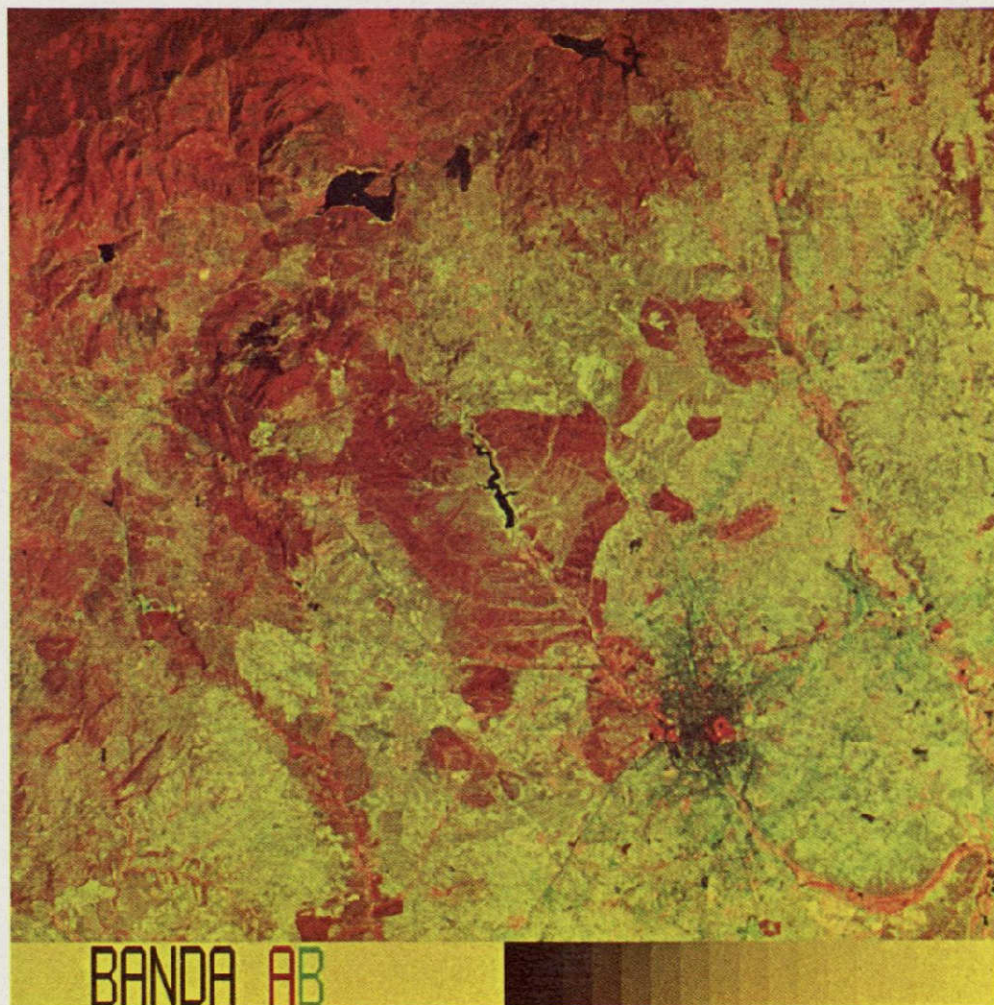
Fig. 8.—Two colour composite of band A (green) and band B with maximum enhancement (red)

REFERENCES

1) L. Breiman, "Probability", Addison-Wesley (1968).

2) A. Santisteban, "Study of Radiometric Enhancement Methods Applied to
    LANDSAT MSS Images" in this report.

THE BAND RATIOING TECHNIQUE APPLIED TO LANDSAT MSS IMAGES

Antonio SANTISTEBAN

Centro de Investigación UAM-IBM

Universidad Autónoma de Madrid

Madrid – 34

1. INTRODUCTION

Band ratioing is becoming one of the best known digital techniques to obtain new bands with relevant information from a multispectral image. The reason is the following: Being the light intensity measured in each band by a multispectral device (a multispectral scanner for instance) approximately the product of the light intensity impinging the viewed object by its reflectivity, the quotient of the measures in two bands is expected to be independent of the ilumination.

This technique turns out to be very usefull to enhance certain features in LANDSAT MSS images. It has been used to eliminate light cloud coverage [1] and in geological applications [2,3] with relative success. On the other hand this process is very sensitive to noise, specially to the typical stripping (see Section 3 below).

In Section 2 we present three formulae to obtain quotient images. The first one (see Section 2.1) gives good displays in systems with few grey levels (as television screens for instance) but is not suited to film recorders if we do not perform an equalizing enhancement [4] prior to recording. The other two formulae (see Sections 2.2 and 2.3) perform an enhancement at the same time that they compute the ratio. The last one of them (Section 2.3) uses the logarithm of the quotient in order to transform multiplications and divisions into additions and subtractions thus yielding a symmetric distribution.

In Section 4 we apply the methods described in Sections 2.2 and
2.3 to a particular example aimed to show up the gallery vegetation
beside narrow rivers.

2. IMAGE RATIOING METHODS

Let us call x and y the radiometric level of a pixel in the two
bands that participate in the ratio and z the resulting level of the
pixel in the new quotient band. We assume that $0 \leq x, y, z \leq 255$ for the
sake of generality although LANDSAT MSS image data actually contain
7 bit in bands 4, 5 and 6 and 6 bit in band 7.

2.1. The nonparametric formula of ERMAN II

The earth resources management interactive program ERMAN II [5] performs
ratios of LANDSAT MSS images. The output image contains the four
original bands plus the twelve possible ratios. The formula used is

$$z = \begin{cases} \text{Int } (K_{ij} \frac{x}{y+1}) & \text{if} \quad K_{ij} \frac{x}{y+1} \leq 255 \\ \\ 255 & \text{if} \quad K_{ij} \frac{x}{y+1} \geq 255 \end{cases} \qquad (1)$$

where Int stands for integer value.

The addition of a unit to the denominator prevents it from vanishing.
i and j denote the numerator and denominator bands and the constant
K_{ij} has the values $K_{45} = K_{46} = K_{54} = K_{56} = K_{64} = K_{65} = 32$,
$K_{47} = K_{57} = K_{67} = 16$, $K_{74} = K_{75} = K_{76} = 64$.

Hence $z \simeq 32$ when both bands have the same radiometric level (thinking
of band 7 as multiplied by 2 in order for all bands to have the same
range of levels). There is an obvious lack of symmetry because 32
levels are assigned to the case in which $x \leq y$ and 224 to that in
which $x > y$ and half the output pixels take value on a number of
levels of the order of 32 (sometimes even much less) while the other
half take values on much more levels. The distribution of pixels is

very concentrated on rather low levels and the contrast of the picture
that we can produce with a linear scale film recorder will be very poor.
But the application of a radiometric enhancement to the quotient using
an equalizing function [4] overcomes this drawback. As a matter of fact
this is the way in which ERMAN II operates: the transformation of levels
is such that in each one of the 16 levels available in black and white
(or the 8 or 4 levels available in false colour) using the RAMTEK GX-100 B
interactive display units, it tends to be approximately the same number
of pixels.

2.2. Parametric ratioing formula

When we are going to display the quotient image by means of a film
recorder with 8-bit linear scale we must radiometrically enhance the
data. This enhancement may be done at the same time that we calculate
the ratio simply through the use of suitable parameters.

Let us define the quotient by

$$
z = \begin{cases}
0 & \text{if } 0 \geq a \dfrac{x+1}{y+1} + b \\[2em]
\text{Int} \left(a \dfrac{x+1}{y+1} + b \right) & \text{if } 0 \leq a \dfrac{x+1}{y+1} + b \leq 255 \\[2em]
255 & \text{if } 255 \leq a \dfrac{x+1}{y+1} + b
\end{cases}
\tag{2}
$$

The addition of 1 to the numerator is a simple matter of symmetry.
The parameters a and b control the contrast and brightness of the
output image and, at the same time, the range of values of $(x+1)/(y+1)$
that are assigned the whole interval [0, 255] excluding the tail
cut-offs.

To determine a and b we can follow many criteria but in general the
more useful are the following:
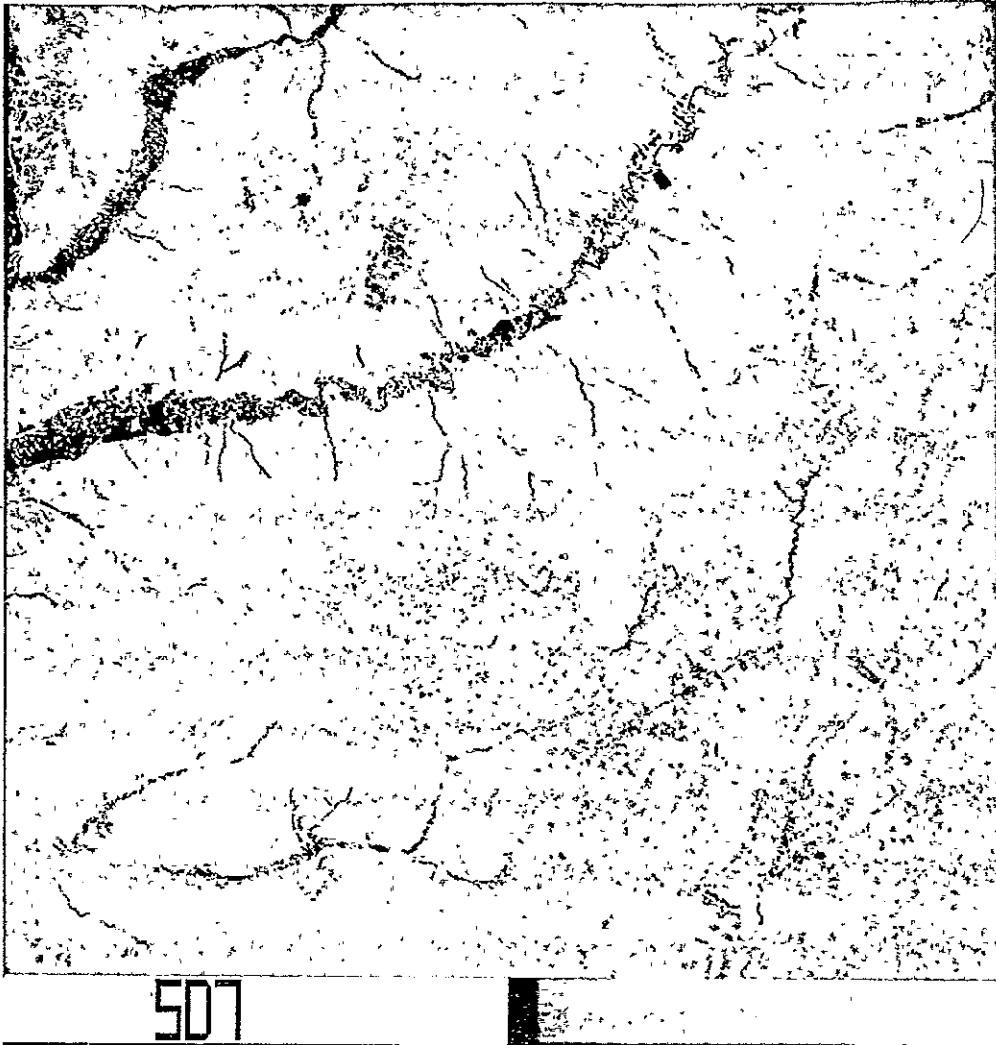
Fig. 1.—Quotient image 5D7 obtained with c = 1.5

i) Take $1/c$ and c as cut-off points. Hence the quotient values

$$\frac{1}{c} \leq \frac{x+1}{y+1} \leq c \tag{3}$$

are assigned the whole range of levels while smaller values are assigned 0 and bigger values 255. Then

$$a = \frac{255\ c}{c^2 - 1} \qquad\qquad b = - \frac{255}{c^2 - 1} \tag{4}$$

and the value

$$\text{Int}\ (\frac{255}{c+1}) \tag{5}$$

is assigned when $x=y$. It remains to determine the parameter c that limits the ratio values allowed. Obviously we can determine a good value of c if we know beforehand the distribution of quotients otherwise c must be estimated by trial and error.

ii) Take the cut-off points at $\tilde{z}/c$ and $\tilde{z}\ c$ being

$$\tilde{z} = \frac{\overline{x+1}}{\overline{y+1}} \tag{6}$$

and $\overline{x}$ and $\overline{y}$ are the mean values of the numerator and denominator bands. Hence the whole range of output levels is assigned to

$$\frac{\tilde{z}}{c} \leq \frac{x+1}{y+1} \leq \tilde{z}\ c \tag{7}$$

and

$$a = \frac{255\ c}{\tilde{z}\ (c^2-1)}\ , \qquad\qquad b = - \frac{255}{c^2-1} \tag{8}$$

and the value of eq. (5) is assigned to $\tilde{z}$. The determination of c rises the same problems as before.

The second method has an obvious advantage with respect to the other one. Even though $\tilde{z}$ is not the mean value of the quotient, it is in general a good estimate of it, actually the only one we have before calculating the quotient image. Therefore this method assigns the whole range of levels to a (logarithmically) symmetric interval around a point near to the actual mean.

2.3. Logarithmic ratioing formula

Images obtained by means of the parametric ratioing formula with a (logarithmically) symmetric interval are usually dark: their means are smaller than 127.5. The lack of linearity that implies that fact desappears when we use a logarithmic scale to record the image.

If instead we use directly a logarithmic ratioing formula as eq. (9) below and record images using a linear scale we have more flexibility and keep full control of the calculation. Furthermore the computation time may be reduced by the use of a look-up table with the logarithms of the integer numbers from 1 to 256.

Thus we define the logarithmic quotient image whose pixels have intensity levels given by

$$
z' = \begin{cases}
0 & \text{if } 0 \geq \alpha\log(\frac{x+1}{y+1})+\beta \\
\text{Int } [\alpha\log(\frac{x+1}{y+1})+\beta], & \text{if } 0 \leq \alpha\log(\frac{x+1}{y+1})+\beta \leq 255 \\
255 & \text{if } 255 \leq \alpha\log(\frac{x+1}{y+1})+\beta
\end{cases}
\tag{9}
$$

Where log stands for logarithm of base 2.

To determine α and β we can follow many criteria but we point out again the two more useful:
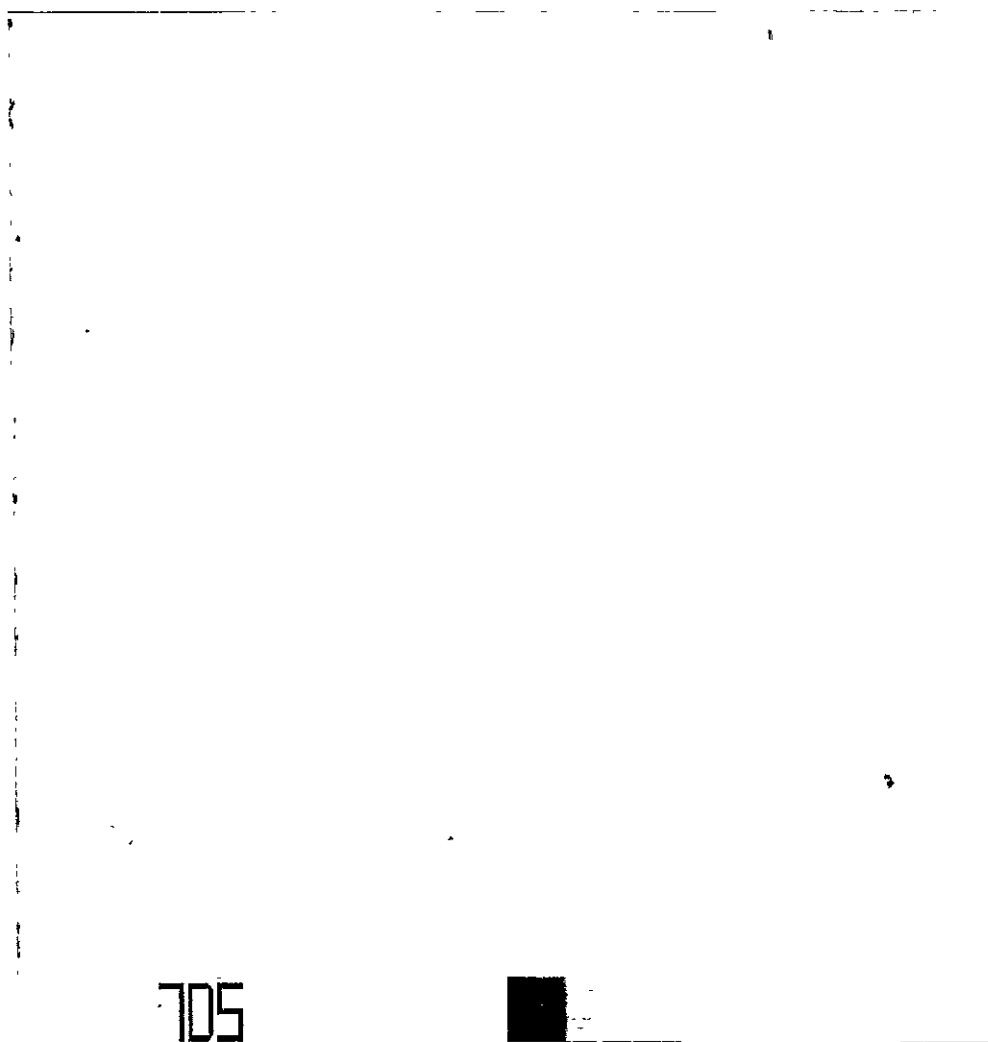
Fig. 2.—Quotient image 7D5 obtained with c = 1.5

i) Take $1/c$ and c as cut-off points i.e.

$$-\log c \le \log \frac{x+1}{y+1} \le \log c \tag{10}$$

We must assign the intensity 127.5 when $x=y$ and

$$\alpha = \frac{127.5}{\log c} , \qquad \beta = 127.5 \tag{11}$$

ii) Take $\tilde{z}/c$ and $\tilde{z} c$ as cut-off points (see eq.(6)). Then

$$\log \tilde{z} - \log c \le \log \frac{x+1}{y+1} \ge \log \tilde{z} + \log c \tag{12}$$

We want to assign the intensity 127.5 when $(x+1)/(y+1)=\tilde{z}$ hence

$$\alpha = \frac{127.5}{\log c} , \qquad \beta = 127.5(1- \frac{\log \tilde{z}}{\log c}) \tag{13}$$

Notice that the use of the logarithm of the quotient implies a complete symmetry between the cases $x \ge y$ and $x \le y$ and therefore the mean of the distribution of z' is higher than the mean of z.

3. THE EFFECT OF NOISE IN QUOTIENT IMAGES

Quotient images are very sensitive to noise. To see it let us consider eq.(2) in the simplified non-integer form.

$$z = a \frac{x+1}{y+1} + b \tag{14}$$

We do not take into account the round-off error noise introduced by the ratioing method but only the noise already existing in the original images. As we are mainly concerned with LANDSAT MSS images the dominant noise is the well known stripping introduced by the differences in calibration among the six sensors of each band, that can amount to several grey level units.
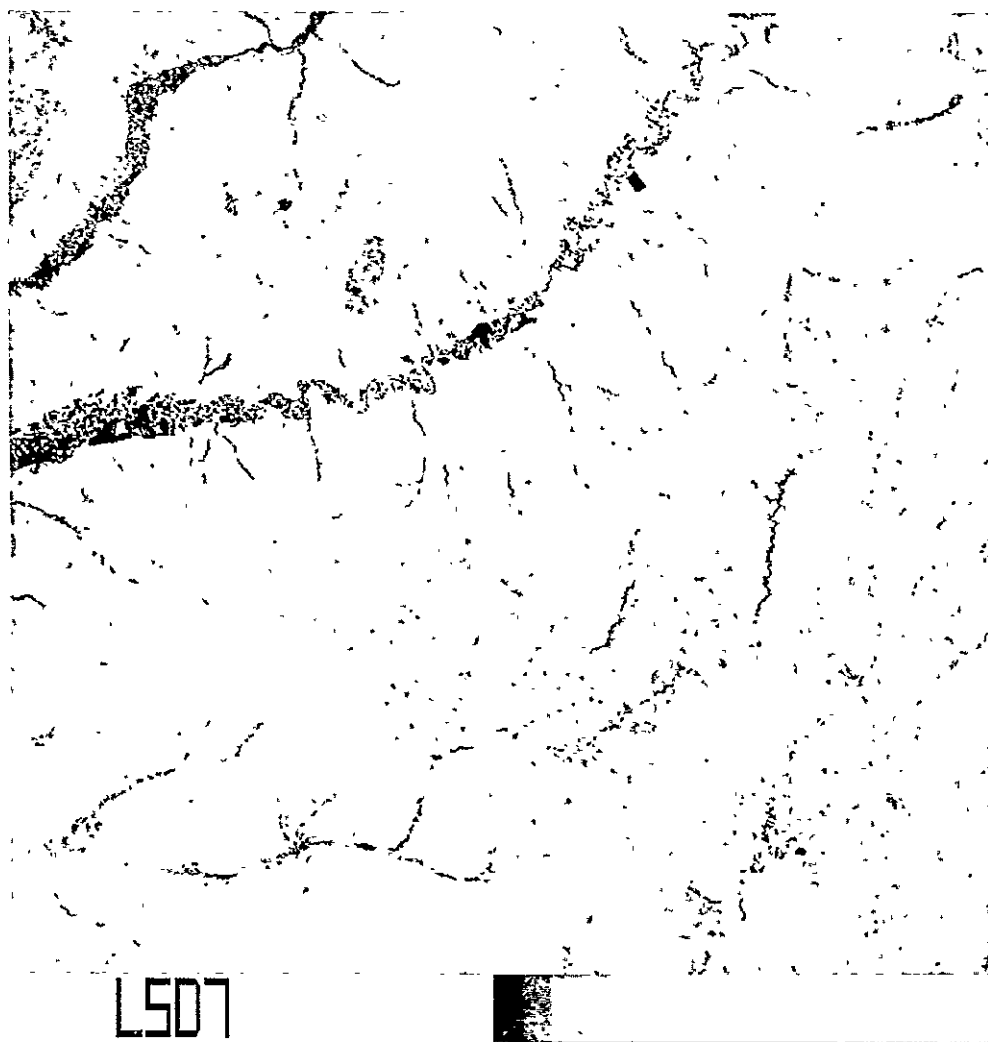
Fig. 3.—Quotient image L5D7 obtained with c = 1.5

Imagine that the values of a pixel in the two bands to be divided are

$$x = x_o + \varepsilon$$

$$y = y_o + \delta \qquad\qquad (15)$$

being x_o and y_o the values that correspond to the pure signal, ε and δ the noise components and

$$z_o = \frac{x_o+1}{y_o+1} \qquad\qquad (16)$$

The noise component of the output image is

$$n(\varepsilon,\delta) = z - z_o = a\left(\frac{x_o+1+\varepsilon}{y_o+1+\delta} - \frac{x_o+1}{y_o+1}\right) \qquad\qquad (17)$$

defined as a function of the input noise components ε and δ. It obviously increases with the gain factor a.

The noise in the quotient image induced by noise in the numerator image is

$$n(\varepsilon,o) = a\,\frac{\varepsilon}{y_o+1} \qquad\qquad (18)$$

that is independent of the pixel's grey level of the numerator image and increases when the denominator decreases. Then it is more apparent in the brighter areas of the quotient image. The noise caused by noise in the denominator image is (*)

$$n(o,\delta) = a\,\frac{x_o+1}{y_o+1}\,\frac{\delta}{y_o+1+\delta} \qquad\qquad (19)$$

that increases as the numerator image becames brighter and the denominator one becames darker.

The same conclusions may be drawn from the logarithmic formula (9) although calculations are more involved.

_____

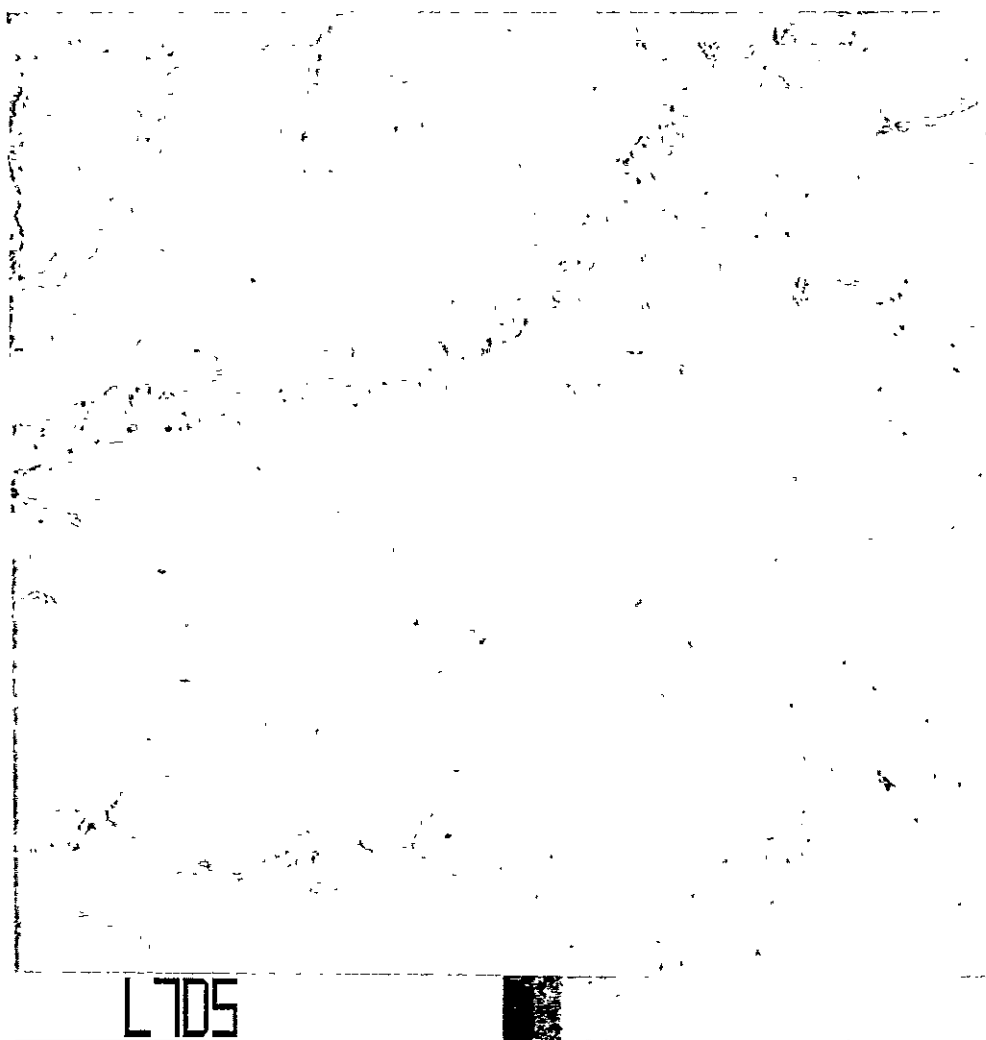(*) Remember that $y_o+1+\delta=y+1\geq1$ and the denominator never vanishes.

Fig 4 —Quotient image L7D5 obtained with c = 1.5

As a matter of fact the stripping in water areas may be enormous, completely masking out any other information. Because of this important drawback, the ratio of two images with considerable amounts of noise may be a useless image for nearly all purposes. Therefore this technique must be applied with care, making a previous selection of suitable images.

4. APPLICATION TO A PARTICULAR EXAMPLE

We take a subimage of LANDSAT MSS frame 2223-10132 in order to apply the parametric ratioing methods discussed in Sections 2.2 and 2.3. This subimage has 1024 pixels of width, starting on pixel 1057, by 714 lines of length, starting on line 1266. It was taken on summer-time (September the 2nd, 1975).

This image corresponds to an area of 58.4 km by 56.4 km around Tajo river, East of Aranjuez, between its tributaries Tajuña (top) and Cedron (botton). This area is rather arid and with scarce vegetation during the summer, the rivers being too narrow to be directly seen in LANDSAT imagery.

We are going to take bands 5 and 7 and calculate both quotient images, namely 5/7 and 7/5. This is a good method to detect rivers in conditions similar to those of the considered area. Actually what we visualize is no the water but the gallery vegetation beside the rivers that ranges from wide irrigation areas in the main rivers to two rows of trees in the smaller tributary rivers.

To begin with we study both bands separately and realize that they are good images in the sense that their signal to noise ratios are high. We list in Table 1 their means and standard deviations.
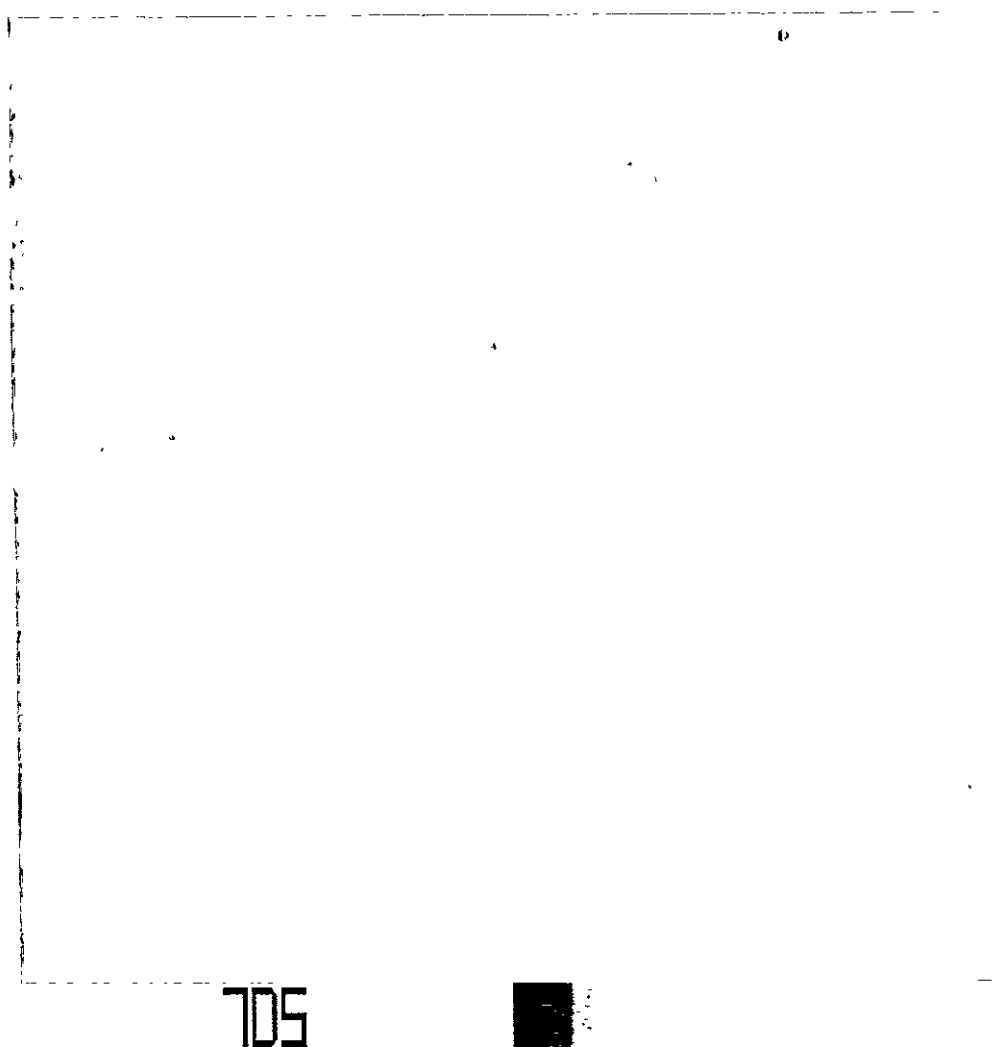
Fig 5 —Quotient image 7D5 obtained with c = 3.0

Table 1

Original   Bands

Band	Mean	Standard Deviation
5	57.26	12.81
7	28.39	5.28

We compute the value of $\tilde{z}$ (see eq.(6)) for the quotient of bands
5/7 being $\tilde{z}$ = 1.98, and for the quotient of bands 7/5 where $\tilde{z}$ = 0.50.
Now we can obtain the quotients using criterion ii) (see Sections 2.2
and 2.3 above) to determine a (or α) and b (or β). We will try three
values of c, namely c = 1.5, 2.0 and 3.0

Table 2 summarizes all data about these quotient images. In the first
column we indicate the kind of quotient image. 5D7 and 7D5 are the
quotients 5/7 and 7/5 respectively computed through the formula of
eq.(2) with a and b given by eq.(8). L5D7 and L7D5 indicate the same
quotients as before but computed through the logarithmic formula of
eq.(9) with α and β given by eq.(13). The second column indicates the
value c used. The third and fourth columns give respectively the values
of a and b for images obtained using eq.(2) and give the values of
α and β when the quotient image have been got by using eq.(9). The fifth
and sixth columns give the means and standard deviations of the quotient
images. The seventh and eighth columns give the percentages of pixels
that are acumulated on the end point levels 0 and 255, i.e. the per-
centages of pixels that do not satisfy respectively the first or second
unequalities of eq.(7) (in case of 5D7 and 7D5 images) or eq.(12) (in
case of L5D7 and L7D5 images). Finally the last column indicates which
one of the figures show the image (note that not all of them are shown).

The first fact that we observe is that the greater is c (i.e. the wider
is the range of quotient values allowed the greater is the gain factor
a or α and hence the greater are the standard deviation and the contrast

Quotient Band	Parameter Values Used			Mean	Standard Deviation	Pixels at end levels		Figure
	C	a/α	b/β			% at 0	% at 255	
5D7	1.5	154.55	-204.00	102.87	33.16	2.23	0.02	1
5D7	2.0	85.85	-85.00	84.81	19.94	0.97	0.00	
5D7	3.0	48.70	-31.88	64.13	11.69	0.17	0.00	
7D5	1.5	612.00	-204.00	107.40	38.89	0.02	2.27	2
7D5	2.0	340.00	-85.00	89.03	27.49	0.00	0.91	
7D5	3.0	191.25	-31.88	66.15	18.66	0.00	0.15	5
L5D7	1.5	217.96	-86.80	126.88	36.40	2.21	0.02	3
L5D7	2.0	127.50	1.85	125.88	24.48	0.86	0.00	
L5D7	3.0	80.44	48.22	128.04	16.72	0.15	0.00	6
L7D5	1.5	217.96	341.80	128.12	36.40	0.02	2.21	4
L7D5	2.0	127.50	253.15	129.12	24.48	0.00	0.86	
L7D5	3.0	80.44	206.78	126.96	16.72	0.00	0.15	

T A B L E   2

123

of the quotient image. Consequently the percentage of pixels accumulated on the end values decreases as c increases.

The means of the quotient images 5D7 and 7D5 decrease and then the images became darker as c increases (see eq.(5)). The differences between these means and the value $255/(c+1)$ (namely 102.20 when c=1.5, 85.00 when c=2.0 and 63.75 when c=3.0) are mostly due to the fact that $\tilde{z}$ is not the mean of $(x+1)/(y+1)$, and can be thought of as an estimate of the amount by which $\tilde{z}$ differs from the actual mean. The same can be said of the differences between the means of images L5D7 and L7D5 and 127.5. We realize that all those differences are small and then our guess of estimating the quotient mean by $\tilde{z}$ turns out to be completely justified.

To understand the very high values of the gain a in 7D5 images, remember that $\tilde{z} = 0.50$ for this quotient while $\tilde{z} = 1.98$ for the 5D7 images whose gain factors are obviously much smaller. (see eq.(8)). In the L5D7 and L7D5 images this fact is accounted for by the bias β much higher in L7D5 than in L5D7 (see eq.(13)).

The images L5D7 and L7D5 obtained with the same c are positive-negative pairs. In fact, their intensity levels are related by (see eq.(9)).

$$z'(L7D5) = 255 - z'(L5D7) \tag{19}$$

On the other hand, image 7D5 is no longer the negative of image 5D7 for the lack of symmetry already discussed (see eq.(2)).

To obtain the photographs for display we use the DICOMED D-47 film recorder with its 8-bit linear scale and non-square pixel compensation facilities. We also add at the botton right side of our photographic displays, a grey wedge in order for the reader to be able to account for the possible printing deficiencies. Its 17 levels are 16^k, k=0,1,...,15 and 255. The length of this wedge corresponds to 29 km on the image.

Fig. 6.—Quotient image L5D7 obtained with c = 3.0

Looking at Fig.1-6 we realize the absence of relevant stripping as
was expected from the quality of the originals. These images clearly
show up the vegetation near the rivers, although other kind of
information is not very appearent in part because of the homogeneity
of the depicted area.

Let us compare Fig. 2 with Fig. 5 that are 7D5 images obtained with
different values of c. Fig. 1, with a smaller value of c, has higher
contrast and contains more information about the irrigation areas near
the main rivers. It also shows more clearly the narrower rivers and
gives some information about structures on the more homogeneous region
between the rivers. The same conclusions are drawn from a comparison
between the two L5D7 images of Fig.3 and Fig.6.

Nevertheless c may not be decreased to much because it induces an
accumulation of pixels on the levels 0 and 255 than, when it becames
too big, reduces the actual information content of the image.

The comparison between Fig. 3 and Fig. 4, that are negative of each
other, confirms that they have the same information.

Images 5D7 and 7D5 on the other hand (see Fig. 1 and 2) do not have
the same information. The brighter parts of each one have more
information than their (darker) counterparts of the other. This owe
to the fact that a certain interval of quotient values greater than
one is assigned more levels than the interval subtended by its
(smaller than one) inverses. Hence there is more information about the
neighbourhood of the rivers in 7D5 than in 5D7.

The brighter parts of images 5D7 and 7D5 also have more information
than those of images L5D7 and L7D5 respectively. Nevertheless the
latter images have more overall information than the former (compare
Figure 1 with Fig. 3 and Fig. 2 with Fig. 4)..

Our final conclusion is that image ratioing, using suitable parametric formulae to perform a radiometric enhancement at the same time, is a good tool to emphasize certain special features in LANDSAT MSS images though it must be used with care because of its noise sensitivity. The bands to be divided and the particular formula to be used are to be selected ad hoc, while the determination of parameter values rests a trial and error question.

ACKNOWLEDGEMENT

I acknowledge L.Montoto of Centro de Investigación UAM-IBM for his suggestion of using the quotients of bands 5 and 7 as an example of our image ratioing methods, pointing out that this is the best way to show up the gallery vegetation that signals the presence of narrow rivers in Central Spain. I also acknowledge G.López de Lemos of Instituto Geográfico y Catastral for the recording and development of photographs.

REFERENCES

1) G.Kritikos, B.Sahai and E.Triendl, "Mapping of Water Bodies in Northern Germany", Symposium on European Earth Resources Satellite Experiments. (Frascati, 1974).

2) T.G.Longshaw, R.P.Viljoen and M.C.Hodson, "Photographic Display of LANDSAT-1 CCT Images for Improved Geological Definition", IEEE Trans. Geosc. Elec. GE-14, 66 (1976).

3) L. Muñoz, "Possibilities of Application of Band-Ratio Technique to the Geological Features of the Western Limit of the Tajo Basin" on Thematic Mapping, Land Use, Geological Structure and Water Resources in Central Spain, Second Quarterly Report (1976).

4) A. Santisteban, "Study of Radiometric Enhancement Methods Applied to LANDSAT MSS Images" on this report.

5) "Earth Resources-Management II (ER-MAN II). User's Guide", SB11-5008-0 (IBM, 1976).

E D A P H O L O G Y

MADRID AND ITS ENVIRONMENT: LAND USE AND SOILS BY
DIGITAL ANALYSIS OF LANDSAT DATA.

J. L. Labrandero

Institute of Edaphology
Department of Soils
Head Council of Scientific
Research. Madrid.
SPAIN.

E D A P H O L O G Y

MADRID AND ITS ENVIRONMENT: LAND USE AND SOILS BY DIGITAL
ANALYSIS OF LANDSAT DATA.

By José L. Labrandero
Licenciado en Ciencias Geológicas
Instituto de Edafología, Dpto. de Suelos
Consejo Superior de Investigaciones Científicas
Madrid.

ABSTRACT

Digital analysis of LANDSAT data, when applied to the spectral
study of Madrid and its environment by means of LARSYS program,
developed at LARS/Purdue University, allows knowledge of urban
structure, models, typical mediterranean mountains and main
types of soils by computer classification.

The principal stages of this working program include grouping
of spectral classes of land use and soils by clustering
techniques.

Results obtained show that this line of investigation is
promising for automatic classification of LANDSAT data applied
to thematic cartography and soils identification.

1. INTRODUCTION

Digital analysis of LANDSAT-2 data taken over Madrid and its
environment, using LARSYS program, is the main objective of
this work, with special enphasis given to land use and soil
classification.

This geographic area is selected because it presents models
of varied urban structure, typical mediterranean vegetation

of Quercus ilex and, also, because the city is settled on a geo-edaphic unit known as "Facies Madrid"; of great interest and importance from an edaphologic point of view.

The main objective was classifying the spectral classes identified, taking into consideration the following points:

- main spectral classes (urban, rural, mountain)
- urban subclasses (vegetation, hydric, edaphic)
- inventory of the area
- thematic cartography by digital techniques
- applications

2. MATERIAL AND METHODS

LANDSAT image used for automatic classification was E-2187-10143, dated July 28th, 1975, taken at 9 h. 14 m. (local time). Each band included 7.619.040 pixels, from which a subscene geometrically corrected was generated taking lines 779 to 165'J and columns 337 to 1893. Output product was a registered tape of 710 lines x 1212 columns, which provided the basic data dealing with in this report (Fig.1)

As reference material were used:

- Topographic Maps of Instituto Geográfico y Catastral at scale 1:50.000 and Servicio Geográfico del Ejército at scale 1:25.000
- Charts of Madrid streets updated
- Soil map of Spain at scale 1:1.000.000
- Aerial images at scale 1:15.000.

The methodology used on this work was operational at the Laboratory for Application of Remote Sensing-LARS/Purdue University, where LARSYS program version 3 was available.
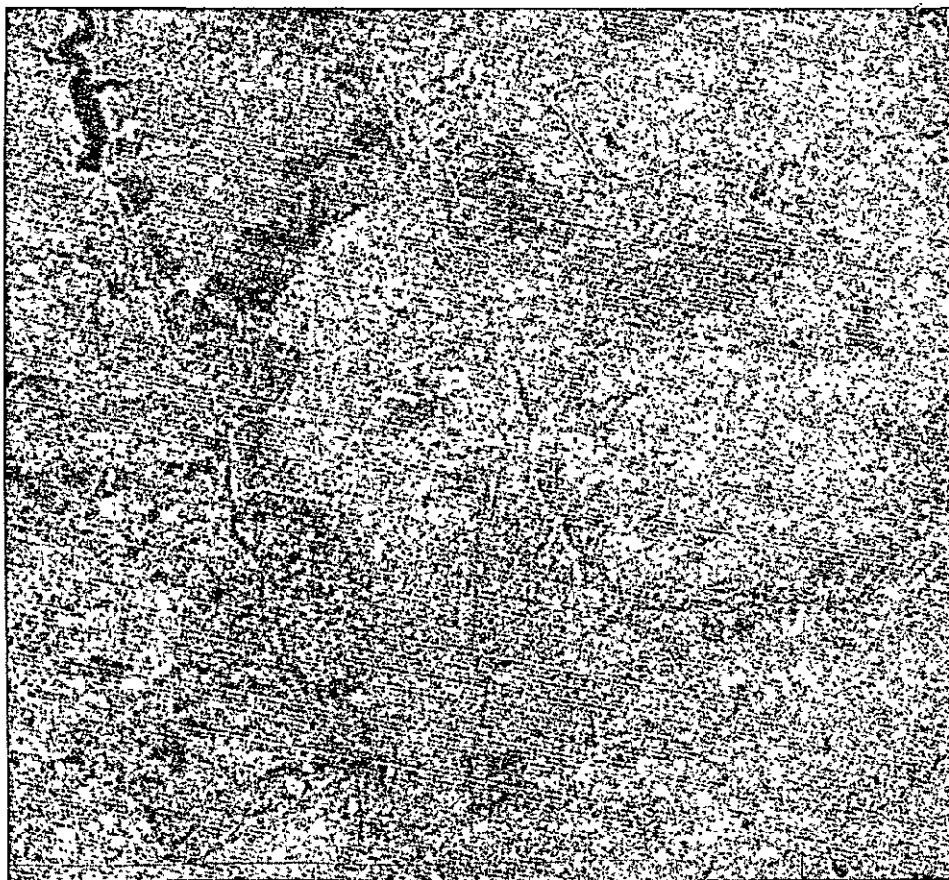
Fig 1.—Area of study: «Madrid and its environment». Date July 28, 1975

3. ANALYSIS AND STAGES

3.1. Identification of areas and points of interest

The first problem appearing to the investigator is identifying
the area to be selected for digital classification, recognizing
on it the most interesting points as reference. There are two
solutions in this stage.

a) Obtaining the PICTUREPRINT function in paper print with
   alphanumeric characters, representing 16 gray levels of
   intensity (reflectivity) values. It was selected band 5
   (0'6 - 0'7 μ) for the purpose of easely recognizing the
   communication network around Madrid; but because the date
   of observation (July 28th), no contrast appeared with soils
   and other types of vegetative cover. Band 6 showed the same
   difficulty and the second solution, consisting in an image
   display, was adopted.

b) IMAGEDISPLAY function, generated in television terminal.
   This function allowed identification of significative points
   as reference of the area under study.

3.2. Selection of test sites

Four different areas were selected as test sites for basic
model of calculation and classification, being the results
extrapolated to the area under study. LARSYS program evaluates
every point and assigns it to the most similar class.

Two areas called Retiro and Plaza de Castilla represent urban
structures. The area of Casa de Campo was selected for knowing
types of vegetation, water, urban classes and types of soils.
The area of El Pardo represents mountain, water and soils.

Retiro and Casa de Campo test sites have 3.000 pixels, or
50 lines x 60 columns. In Plaza de Castilla 2.000 pixels

were taken (40 lines x 50 columns), and the area of El Pardo
contained 4.800 pixels (80 lines x 60 columns).

3.3. Cluster of the selected areas

The spectral classes grouped in natural form were obtained
for each of the test sites by means of the CLUSTER function,
taking the decission of classifying with 12 classes. In the
same CLUSTER function is obtained for each class the value of
the mean vector and covariance matrix; which means a number
of absolute value representing the average of the mean vectors
correspondant to the total of class points, and a measure of
dispersion of data.

Tables no. 1, 2, 3 and 4 indicate absolute values of spectral
characteristics more relevant for each test site.

3.4. Separability between classes and cluster

In the function SEPARABILITY, the mean taken as reference by
LARSYS, based in the values of mean vector and covariance matrix,
is known as transformed divergence and its value is comprised
between 0 and 2.000 (perfect separability).

The twelve classes of cluster of Retiro are grouped considering
a maximum value of divergence equal to 1.700; however some
classes with minor divergence were rejected because their
different spectral characteristics (Figures 2 and 3).

In Plaza de Castilla, also urban area, the maximum value of
divergence was limited to 1.600, combining the classes with
those clusters of minor divergence than the above mentioned.

In the test site of El Pardo, divergence taken as limit was
1.500, also with the influence of the investigator as, for
example, classes 1 and 2, with divergence higher than 1.650
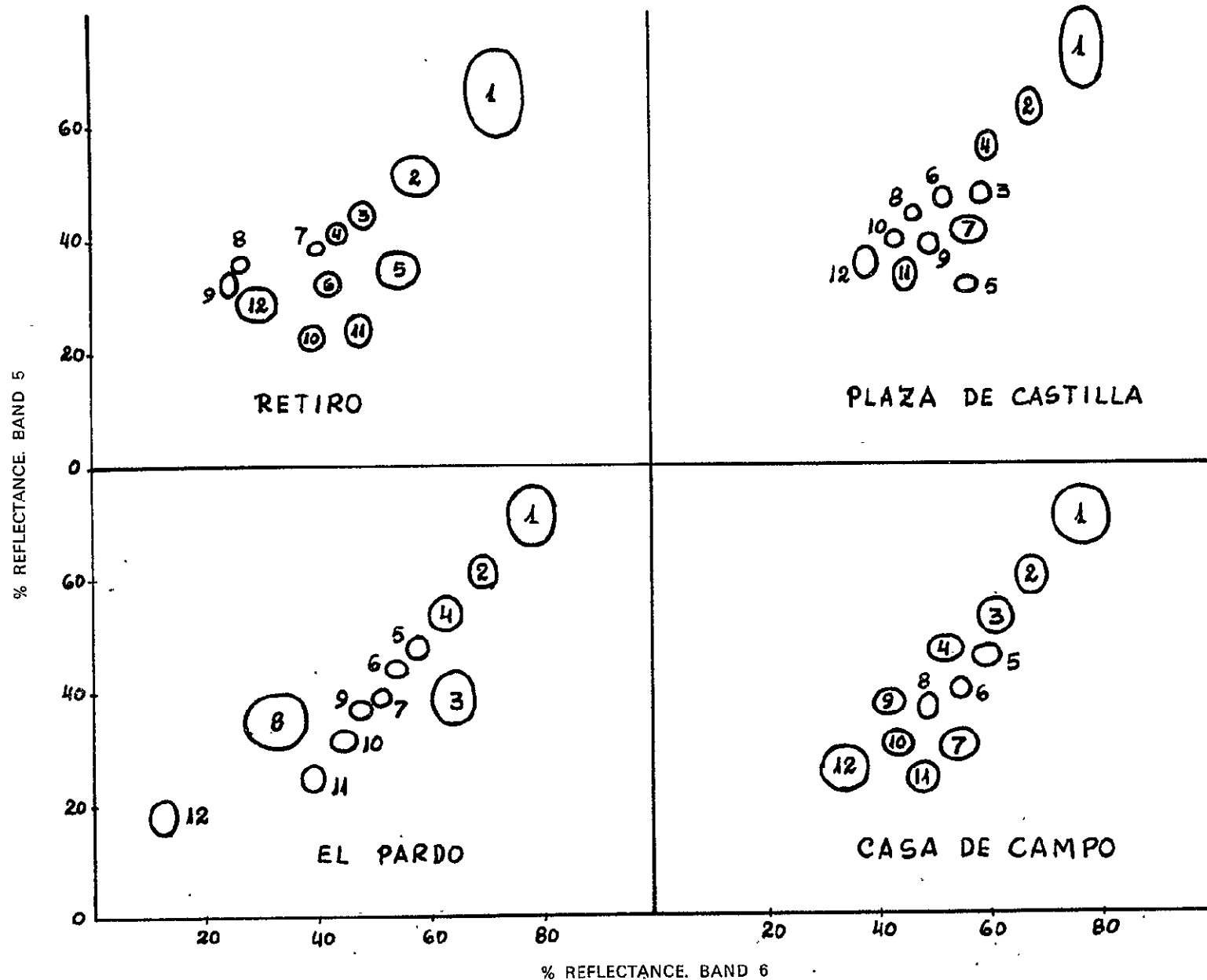but combined because their similar spectral responses.
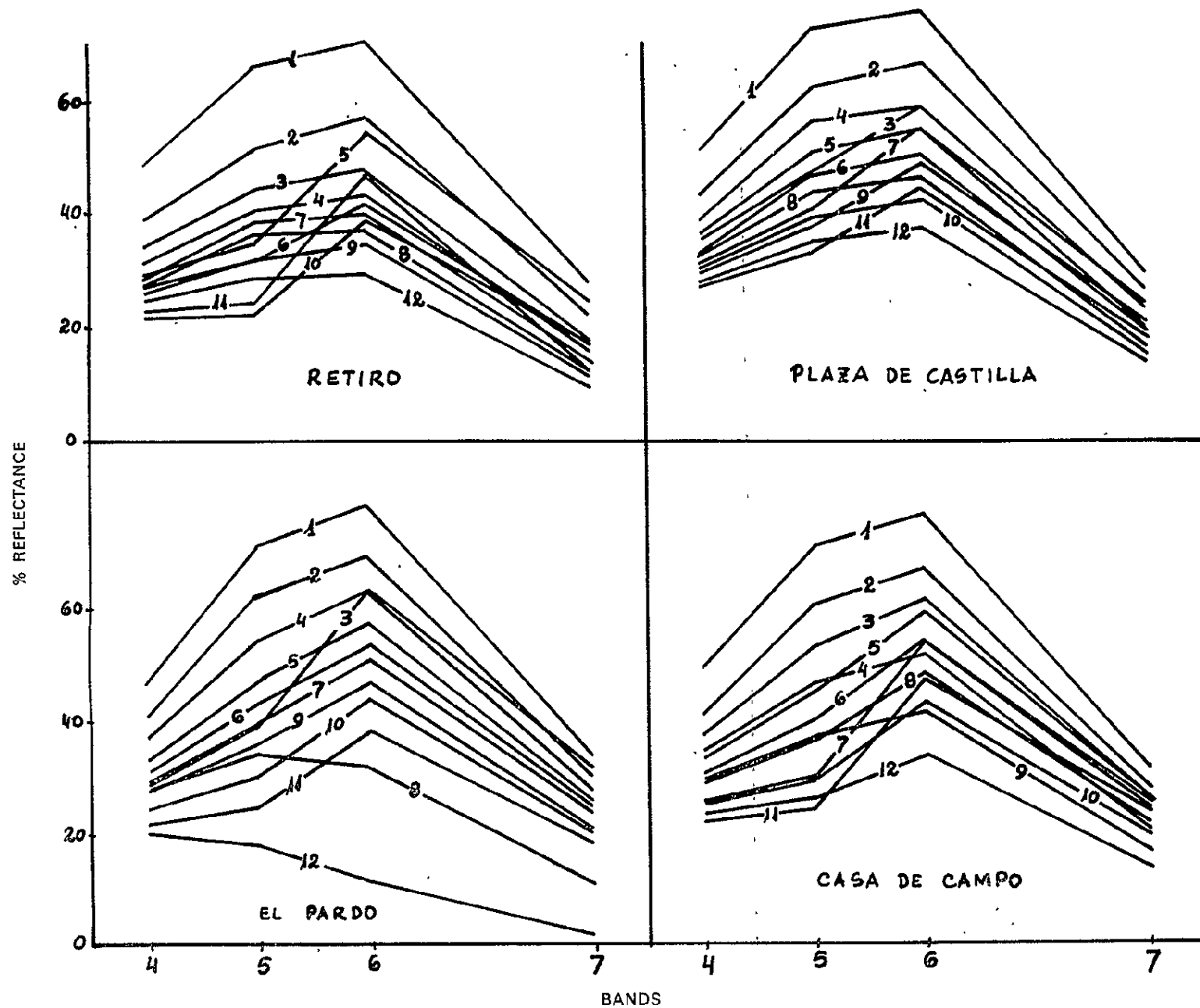
FIG. 3: MADRID AND ITS ENVIRONMENT: CLUSTER

FIG. 2: MADRID AND ITS ENVIRONMENT: CLUSTER

TABLE 1: CLUSTER: MADRID, RETIRO

MEAN   -VARIANCE _ RATIO VISIBLE/INFRARED

CLASSES	BAND 4	BAND 5	BAND 6	BAND 7	VIS/IR
1 CEMENT	48,31 -34,07	66,38 -59,26	71,31 -35,07	28,38 - 6,92	1,1505
2 NO BUILDINGS	38,10 - 7,71	51,81 -14,15	57,81 -19,17	23,07 -10,73	1,1116
3 NEW BUILDINGS	33,98 - 5,45	44,87 - 5,14	48,46 - 6,04	18,81 - 2,96	1,1723
4 NEW BUILDINGS	30,69 - 3,57	40,77 - 3,08	44,09 - 3,63	16,82 - 2,08	1,1732
5 COMPACT VEGET.	28,89 - 5,69	34,95 -12,61	55,00 -18,26	25,64 - 9,57	0,7917
6 GRASS	26,65 - 2,31	31,97 - 6,26	42,57 - 6,27	18,09 - 3,23	0,9666
7 OLD BUILDINGS	28,59 - 1,87	38,52 - 1,73	40,22 - 2,03	15,14 - 0,83	1,2122
8 OLD BUILDINGS	27,44 - 1,55	36,08 - 1,96	37,18 - 1,99	13,81 - 0,86	1,2458
9 WATER/STREETS	25,84 - 2,10	32,20 - 3,66	35,11 - 2,64	13,14 - 1,48	1,2029
10 PARKS	21,08 - 4,41	22,64 - 6,47	39,67 - 7,32	18,66 - 4,45	0,7495
11 PARKS	22,59 - 5,10	24,15 -10,70	48,22 - 7,08	23,29 - 3,55	0,6478
12 WATER/PONDS	24,88 - 4,92	28,55 -12,65	29,81 -14,27	10,91 - 3,59	1,3020

TABLE 2: CLUSTER: MADRID, PLAZA DE CASTILLA

MEAN   -VARIANCE   RATIO VISIBLE/INFRARED

CLASSES	BAND 4	BAND 5	BAND 6	BAND 7	VIS/IR
1 CEMENT	51,39 -46,38	73,81 -50,63	76,97 -12,17	30,58 - 3,59	1,1641
2 SQUARES/PARKING	43,64 - 8,41	63,53 - 9,38	67,17 -10,24	27,05 - 3,68	1,1374
3 URBAN/TREES	35,43 - 3,10	47,94 - 3,74	59,27 - 4,59	24,60 - 3,61	0,9941
4 NO BUILDINGS	34,45 - 3,74	56,73 - 4,95	59,73 - 5,19	23,58 - 2,92	1,1544
5 OLD BUILDINGS	36,94 - 3,44	51,70 - 3,50	55,39 - 2,55	21,45 - 1,05	1,1536
6 OLD BUILDINGS	34,73 - 3,48	47,47 - 2,94	51,68 - 2,95	20,14 - 1,36	1,1447
7 URBAN/TREES	31,52 - 3,10	41,45 - 7,43	56,20 -10,11	24,50 - 6,82	0,9043
8 OLD BUILDINGS	32,99 - 2,95	44,38 - 2,65	46,96 - 2,80	18,00 - 1,24	1,1909
9 RESIDENTIAL/TREES	29,91 - 3,28	38,82 - 4,34	49,69 - 3,54	21,23 - 2,32	0,9692
10 NEW BUILDINGS	30,63 - 2,45	39,93 - 2,83	43,13 - 2,99	16,64 - 1,45	1,1804
11 RESIDENTIAL/TREES	27,37 - 2,27	33,82 - 6,98	45,32 - 4,70	19,59 - 2,66	0,9428
12 NEW BUILDINGS	28,09 - 2,31	35,54 - 8,28	38,09 - 5,35	14,15 - 1,70	1,2089

TABLE 3: CLUSTER: MADRID, RETIRO

MEAN   −VARIANCE   RATIO VISIBLE/INFRARED

CLASSES	BAND 4	BAND 5	BAND 6	BAND 7	VIS/IR
1 BARE SOIL	46,52 − 8,75	71,05 −18,26	78,75 −21,38	33,93 − 4,73	1,0433
2 BARE SOIL	40,66 − 3,64	62,17 − 6,51	69,60 − 6,69	30,57 − 2,12	1,0265
3 COMPACT VEGET.	29,59 − 5,21	39,21 −19,24	63,98 −16,09	32,00 − 8,72	0,7167
4 XEROCHREPTS	36,98 − 2,86	53,89 − 6,87	62,87 − 7,13	28,18 − 2,78	0,9980
5 HAPLOXERALFS	32,90 − 3,19	47,48 − 3,78	57,92 − 4,22	26,52 − 1,79	0,9519
6 HAPLOXERALFS	30,73 − 2,21	43,53 − 2,70	53,99 − 3,39	25,01 − 1,84	0,9401
7 MOUNTAIN	28,47 − 1,40	39,53 − 2,89	51,27 − 2,89	24,00 − 1,45	0,9033
8 RESERVOIR BORDERS	28,10 − 8,28	34,21 −21,40	32,48 −30,20	11,84 −10,11	1,4058
9 MOUNTAIN	27,32 − 2,17	36,53 − 3,79	47,52 − 3,59	22,99 − 2,01	0,9147
10 VEGETATION	24,82 − 1,42	30,75 − 3,84	44,54 − 4,62	21,37 − 1,61	0,8432
11 VEGET./BRUSHWOOD	21,66 − 3,45	24,94 − 5,80	38,94 − 5,23	18,12 − 2,10	0,8167
12 WATER	20,23 − 4,28	18,29 − 8,67	12,28 − 7,99	2,55 − 1,69	2,5975

TABLE 4: CLUSTER: MADRID, CASA DE CAMPO

MEAN   −VARIANCE   RATIO VISIBLE/INFRARED

CLASSES	BAND 4	BAND 5	BAND 6	BAND 7	VIS/IR
1 PARKING	49,24 −18,23	71,08 −24,95	76,41 −23,79	31,27 − 6,03	1,1175
2 NO BUILDINGS	41,26 − 7,35	60,57 −10,24	66,99 − 9,54	28,10 − 6,11	1,0710
3 NO BUILDINGS	37,62 − 3,53	52,90 − 8,28	61,38 − 9,54	26,08 − 7,15	1,0350
4 OLD BUILDINGS	34,68 − 4,94	46,68 − 7,81	52,04 − 8,29	20,85 − 3,17	1,1165
5 HAPLOXERALFS	33,15 − 2,55	45,68 − 4,79	59,04 − 6,87	26,80 − 3,03	0,9182
6 HAPLOXERALFS	30,31 − 2,58	40,26 − 4,17	54,56 − 4,70	24,75 − 2,39	0,8898
7 PARKS	25,60 − 3,16	30,10 − 9,81	54,42 −10,11	26,63 − 5,14	0,6874
8 RESIDENTIAL	28,12 − 2,40	36,68 − 5,16	48,69 − 3,18	22,14 − 2,04	0,9149
9 NEW BUILDINGS	29,06 − 4,02	37,66 − 6,40	41,77 − 8,96	16,37 − 3,06	1,1474
10 RESIDENTIAL	25,13 − 2,49	30,14 − 4,75	43,17 − 6,08	19,56 − 2,64	0,8810
11 PARKS	22,20 − 3,39	24,11 − 8,09	47,70 − 7,42	23,90 − 3,75	0,6468
12 WATER	23,64 − 5,81	26,18 −14,45	33,95 −18,24	13,15 −11,90	1,0578

141

The fourth test site, located in Casa de Campo, had a limit divergence of 1.700. As final stage every class was correlated to existing cartographic information and aerial imagery for the purpose of·identification.

3.5. Individual classification of the areas

Following the methodology of LARS, after combining similar classes and identifying types of surface cover, a classification of the areas has to be done. Function MERGESTATISTICS can help in the combination of cluster classes, obtaining a new packet of cards used as input of the classification (Figures 4 and 5).

The classification is done by LARSYS program based on a maximum likelihood rule, comparing each data to all the classes and evaluating the minimum probability of error.

If after finished the individual classification, results do not agree with the objectives, it can be reviewed any phase of the analysis for correction. This happened in the area of Retiro, where a second classification was done until considered acceptable. Results obtained by means of function PRINTRESULTS are shown in tables no. 5, 6, 7 and 8.

3.6. Final classification

Once all the test sites have been classified, it is possible to obtain new absolute values of divergence in the final classes (in this case 16), for knowledge of their separability. If such problem does not appear, all the area under study can be classified with·the final number of classes by the·function CLASSIFYPOINTS, taking as basic data each class defined in the test sites.

Results of the final classification by PRINTRESULTS function give an idea of the spectral characteristics of the 16 classes used.
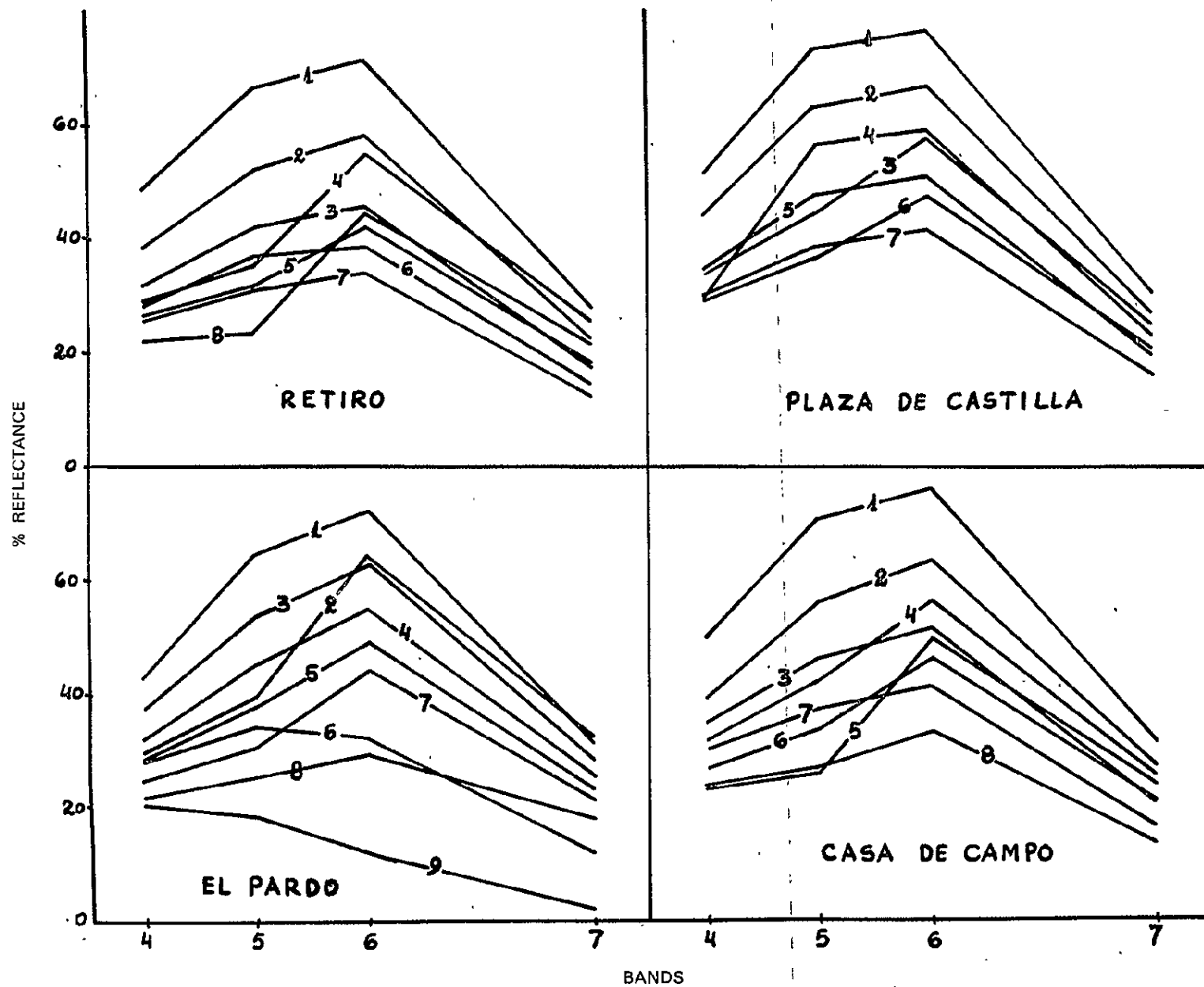
BANDS

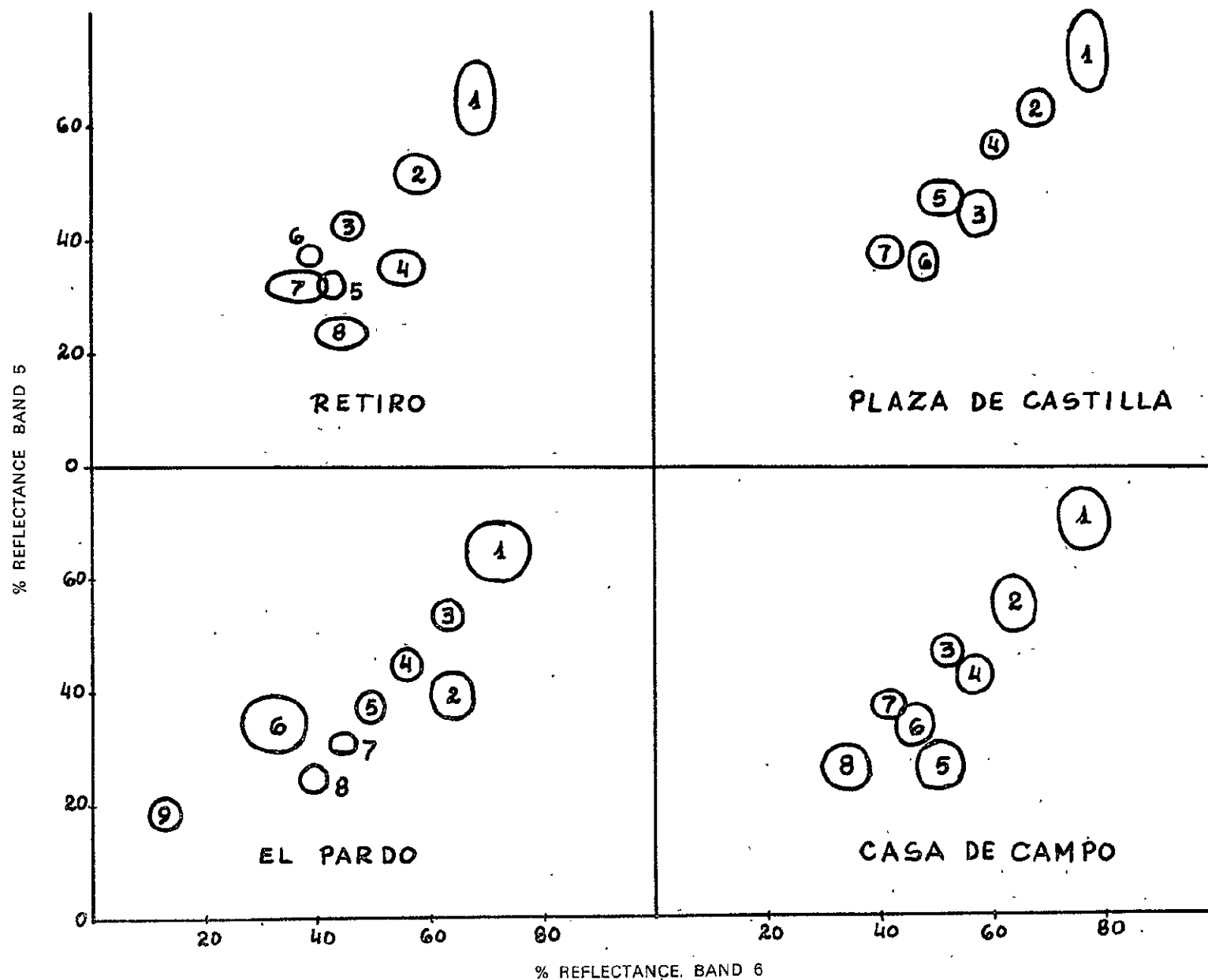FIG. 4: MADRID AND ITS ENVIRONMENT: CLASSIFICATION

FIG. 5: MADRID AND ITS ENVIRONMENT: CLASSIFICATION

TABLE 5: CLASSIFICATION: MADRID, RETIRO

MEAN   -VARIANCE   % OCCUPIED PER CLASS

CLASSES	BAND 4	BAND 5	BAND 6	BAND 7	%
CONCRETE	48,31 -34,07	66,38 -59,26	71,31 -35,07	28,38 - 6,92	0,5
NO BUILDING	38,10 - 7,71	51,81 -14,15	57,81 -19,17	23,07 -10,73	3,0
NEW BUILDING	31,77 - 6,60	42,12 - 7,45	45,53 - 8,64	17,47 - 3,24	22,0
COMPACT VEGET.	28,89 - 5,69	34,95 -12,61	55,00 -18,26	25,64 - 9,57	2,9
GRASS	26,65 - 2,31	31,97 - 6,26	42,57 - 6,27	18,09 - 3,23	7,2
OLD BUILDINGS	28,03 - 2,04	37,33 - 3,31	38,74 - 4,32	14,49 - 1,27	37,9
WATER/STREETS	25,57 - 2,95	31,47 - 7,61	34,04 - 9,48	12,69 - 2,68	16,6
PARKS	21,96 5,33	23,53 - 9,48	44,69 -25,00	21,75 -10,69	9,8

TABLE 6: CLASSIFICATION: MADRID, PLAZA DE CASTILLA

MEAN   -VARIANCE   % OCCUPIED PER CLASS

CLASSES	BAND 4	BAND 5	BAND 6	BAND 7	%
CONCRETE	51,39 -46,38	73,81 -50,63	76,97 -12,17	30,58 - 3,59	1,8
SQUARES/PARKING	43,64 - 8,41	63,53 - 9,38	67,17 -10,24	27,05 - 3,68	4,9
URBAN/TREES	33,44 - 6,91	44,64 -16,16	57,70 - 9,73	24,55 - 5,19	9,7
NO BUILDINGS	39,45 - 3,72	56,73 - 4,92	59,73 - 5,19	23,58 - 2,92	10,0
OLD BUILDINGS	34,74 - 5,76	47,58 -11,49	51,06 -14,28	19,75 - 3,20	35,0
RESIDENTIAL	28,80 - 4,41	36,64 -11,62	47,78 - 8,76	20,51 - 3,13	15,6
NEW BUILDINGS	29,73 - 3,88	38,38 - 9,12	41,35 - 9,61	15,91 - 2,52	22,8

TABLE 7: CLASSIFICATION: MADRID, EL PARDO

MEAN   -VARIANCE   % OCCUPIED PER CLASS

CLASSES	BAND 4	BAND 5	BAND 6	BAND 7	%
BARE SOIL	42,50 -11,97	64,65 -25,70	72,16 -27,66	31,51 - 5,10	6,5
COMPACT VEGET.	29,59 - 5,21	39,21 -19,24	63,98 -16,09	32,00 - 8,72	3,3
XEROCHREPTS	36,98 - 2,86	53,89 - 6,87	62,87 - 7,13	28,18 - 2,78	8,7
HAPLOXERALFS	31,67 - 3,80	45,23 - 6,96	55,69 - 7,50	25,66 - 2,37	28,3
MOUNTAIN	27,94 - 2,10	38,14 - 5,52	49,53 - 6,70	23,21 - 2,43	30,1
RESERVOIR BORDERS	28,10 - 8,28	34,21 -21,40	32,48 -30,20	11,84 -10,11	2,9
VEGETATION	24,82 - 1,42	30,75 - 3,84	44,54 - 4,62	21,37 - 1,61	10,6
VEGET./BRUSHWOOD	21,66 - 3,45	24,94 - 5,80	38,94 - 5,23	18,12 - 2,10	3,5
WATER	20,23 - 4,28	18,29 - 8,67	12,28 - 7,99	2,55 - 1,69	6,2

TABLE 8: CLASSIFICATION: MADRID, CASA DE CAMPO

MEAN   -VARIANCE   % OCCUPIED PER CLASS

| CLASSES	BAND 4	BAND 5	BAND 6	BAND 7	%
PARKING	49,24 -18,23	71,08 -24,95	76,41 -23,79	31,27 - 6,03	2,7
NO BUILDINGS	39,09 - 8,23	56,00 -23,23	63,64 -17,13	26,90 - 7,67	15,6
OLD BUILDINGS	34,68 - 4,94	46,68 - 7,81	52,04 - 8,29	20,85 - 3,17	7,8
HAPLOXERALFS	31,70 - 4,57	42,91 -11,83	56,75 -10,75	25,76 - 3,76	26,0
PARKS	23,72 - 6,15	26,79 -17,72	50,70 -19,80	25,12 - 6,20	11,2
RESIDENTIAL	27,03 - 4,49	34,29 -14,89	46,67 -11,28	21,19 - 3,80	25,2
NEW BUILDINGS	29,06 - 4,02	37,66 - 6,40	41,77 - 8,96	16,37 - 3,06	5,7
WATER	23,64 - 5,81	26,18 -14,43	33,95 -18,24	13,15 -11,90	5,9
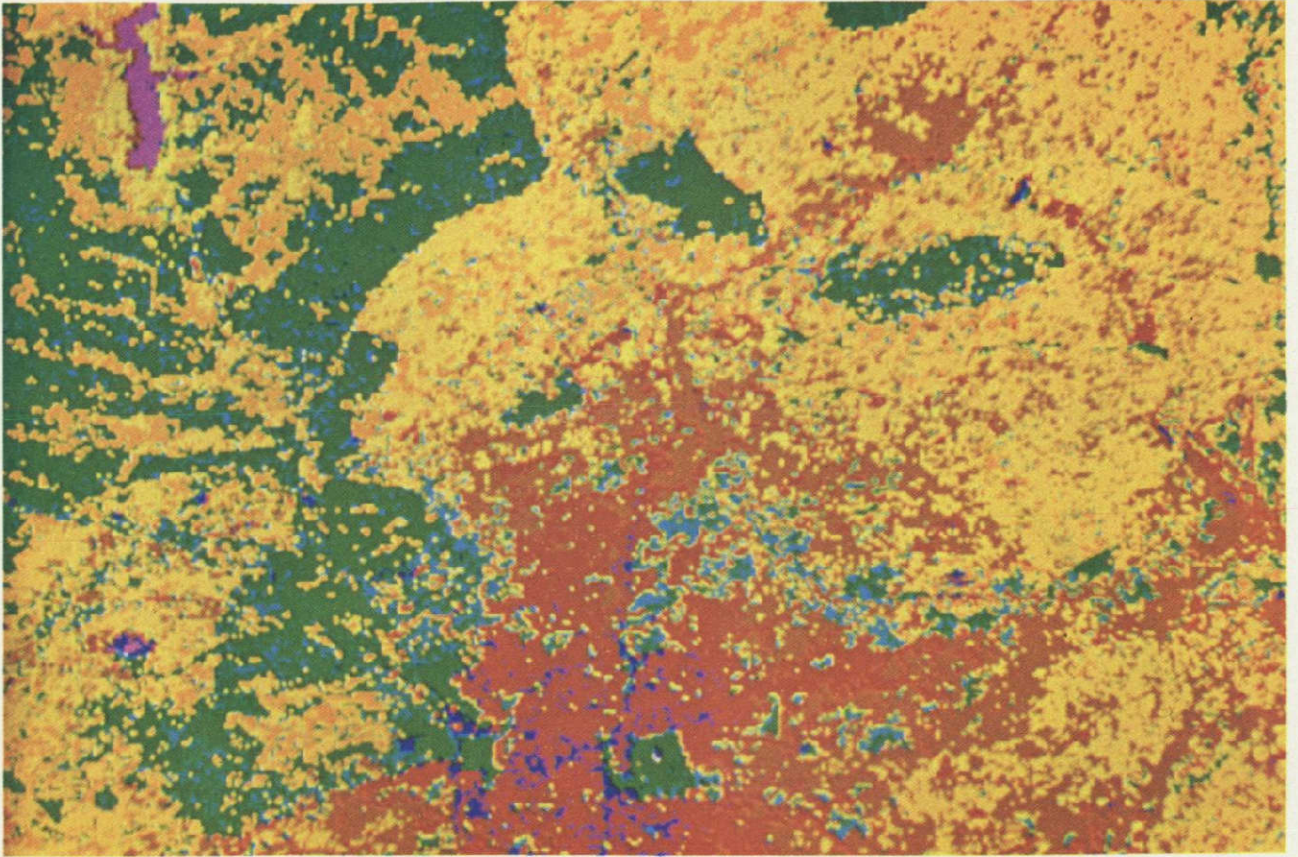
Fig. 6. — Madrid and its environment classified in 16 spectral classes by digital analysis of LANDSAT data. Date July 28, 1975

4. RESULTS AND DISCUSSION

Sixteen units spectrally different have been identified by digital analysis of LANDSAT data, as result of classifying four test sites (Retiro, Plaza de Castilla, El Pardo and Casa de Campo), which contained 32 classes (Fig. 6).

Functions MERGESTATISTICS and SEPARABILITY were used for the 16 classes, verifying that between class no. 2 ("no buildings") and class no. 13, representing Xerochrepts soils, existed a divergence of 862, which means that both classes are spectrally similar. In fact, urban areas without edifications in Madrid have soils of the Xerochrepts group in a strong proportion.

Class no. 6, defined as "Residential 1", with high density of trees (corresponding to the area of El Viso) and class no.9, called "grass, present low values of separability; both classes with similar characteristics by the influence of vegetation in the spectral responses. This same class 6 and the class represented by mediterranean "mountain" of Quercus ilex, have quite similar values, which shows their separability of 710.

The group of Haploxeralfs soils and the class "Residential 2" have a divergence of 772, indicating that their spectral parameters are similar. As known, Madrid capital is settled on Xerocrepts and Haploxeralfs soils.

Those classes representing certain types of cover with low values of separability cannot be differentiated being sure of accuracy in the classification, based only on LANDSAT data taken July 28, 1975.

Values of divergence between other classes is higher than 1.000, and a great amount of classes have the maximum value of 2.000, indicating a perfect separability. Tables 9 and 10 shows the mean values of reflectance for each class and its variance.

TABLE 9: CLASSIFICATION: MADRID AND ITS ENVIRONMENT

MEAN — VARIANCE

CLASSES	BAND 4	BAND 5	BAND 6	BAND 7
PARKING	49,83 -30,36	71,33 -42,77	75,88 -24,50	30,63 - 6,15
NO BUILDING	39,06 - 7,34	55,72 -20,16	62,17 -19,45	25,77 - 9,61
SQUARES	43,64 - 8,41	63,53 - 9,36	67,17 -10,24	27,05 - 3,68
OLD BUILDINGS	34,73 - 5,57	47,39 -10,89	51,26 -13,17	19,98 - 3,38
NEW BUILDINGS	29,39 - 6,15	38,82 - 9,73	41,19 -14,74	15,65 - 3,72
RESIDENTIAL 1	27,50 - 5,10	34,90 -15,13	46,96 -10,82	21,01 - 3,72
RESIDENTIAL 2	33,44 - 6,92	44,64 -16,16	57,70 - 9,73	24,55 - 5,19
PARKS	22,86 - 6,50	25,19 -16,32	47,76 -31,36	23,47 -11,22

TABLE 10: CLASSIFICATION: MADRID AND ITS ENVIRONMENT

MEAN —VARIANCE % OCCUPIED PER CLASS

CLASSES	BAND 4	BAND 5	BAND 6	BAND 7	%
GRASS	24,61 - 4,66	29,88 -10,95	42,99 - 9,73	19,19 - 4,66	7,3
COMPACT VEGET.	29,35 - 5,42	37,76 -20,97	60,93 -34,93	29,84 -18,06	4,2
MOUNTAIN	27,94 - 2,10	38,14 - 5,52	49,53 - 6,71	23,21 - 2,43	8,2
BARE SOIL	42,30 -11,97	64,65 -25,70	72,16 -27,66	31,51 - 5,10	15,9
XEROCHREPTS	36,98 - 2,85	53,89 - 6,86	62,87 - 7,12	28,18 - 2,78	10,9
HAPLOXERALFS	31,68 - 4,08	44,39 - 9,98	56,07 - 9,00	25,69 - 2,89	11,4
LAKES/STREETS	25,48 - 5,61	30,74 -16,40	33,84 -13,83	12,68 - 5,47	1,3
RESERVOIRS	20,23 - 4,28	18,29 - 8,70	12,28 - 8,00	2,55 - 1,69	0,3

149

TABLE 11. PERCENT COVER OF EACH CLASS

CLASSES	%	CLASSES	%
PARKING	4,7	GRASS	7,3
NO BUILDING	7,7	COMPACT VEGET.	4,2
SQUARES	7,2	MOUNTAIN	8,2
OLD BUILDINGS	5,9	BARE SOIL	15,9
NEW BUILDINGS	3,7	XEROCHREPTS	10,9
RESIDENTIAL 1	4,1	HAPLOXERALFS	11,4
RESIDENTIAL 2	5,2	LAKES/STREETS	1,3
PARKS	2,1	RESERVOIRS	0,3

TABLE 12. IDENTIFICATION OF EIGHT CLASSES

SIMPLIFIED CLASSES	INITIAL CLASSES	%	MAP SYMBOL
NO BUILDINGS		19,6	
	Parking		
	No building		
	Squares		
URBAN		9,6	0
	Old buildings		
	New buildings		
RESIDENTIAL		9,3	.
	Residential 1		
	Residential 2		
MOUNTAINS AND PARKS		21,8	*
	Parks		
	Grass		
	Compact Veget.		
	Mountain		
XEROCHREPTS		26,8	/
	Base soil		
	Xerochrepts		
HAPLOXERALFS		11,4	=
	Haploxeralfs		
LAKES/STREETS		1,3	+
	Lakes/streets		
RESERVOIRS		0,3	W
	Reservoirs		
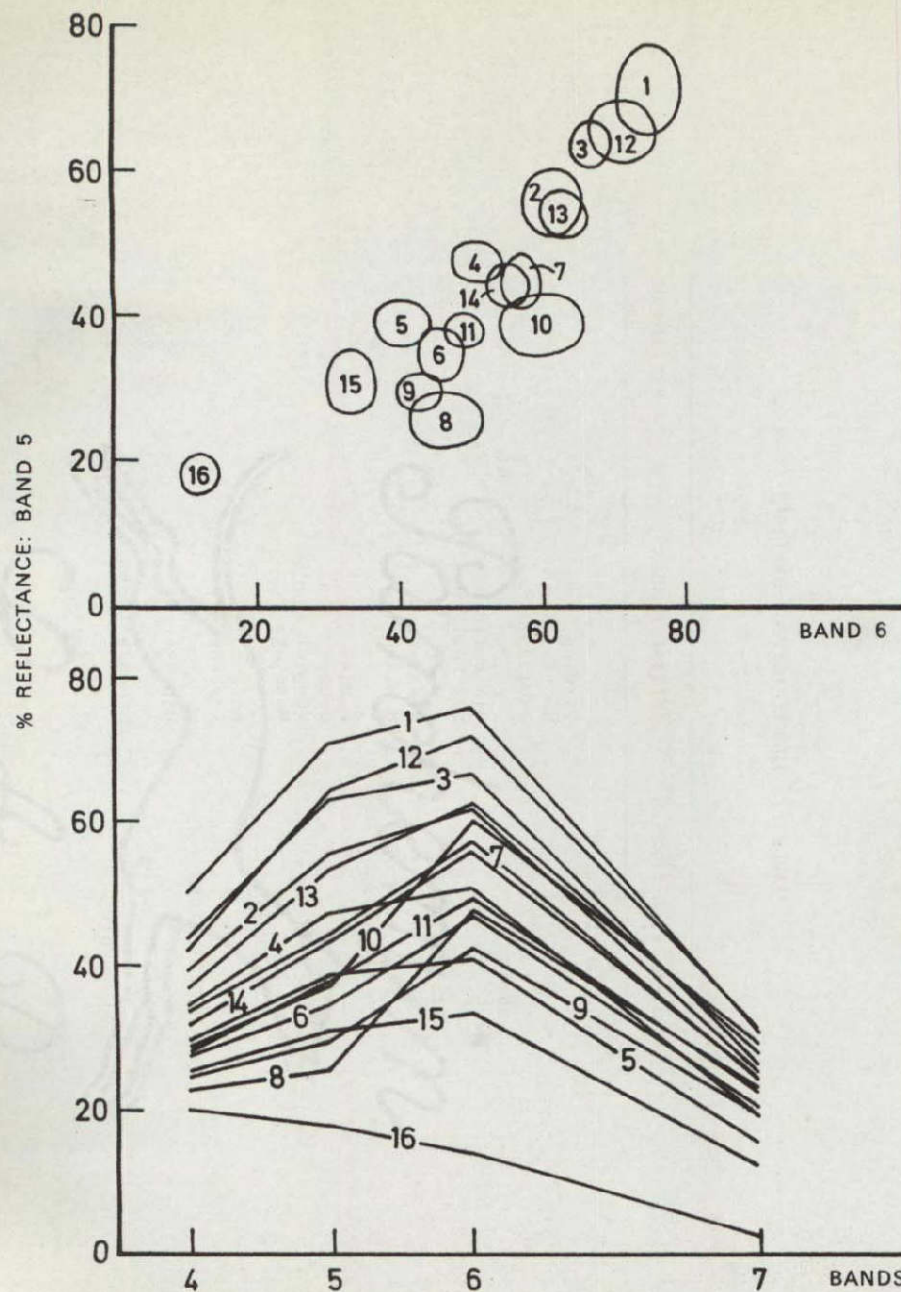
FIG. 7: MADRID AND ITS ENVIRONMENT

CLASSIFICATION

1   PARKING
2   NO BUILDINGS
3   SQUARES
4   OLD BUILDINGS
5   NEW BUILDINGS
6   RESIDENTIAL 1
7   RESIDENTIAL 2
8   PARKS
9   GRASS
10 COMPACT VEGET.
11 MOUNTAINS
12 BARE SOIL
13 XEROCHREPTS
14 HAPLOXERALFS
15 LAKES/STREETS
16 RESERVOIRS
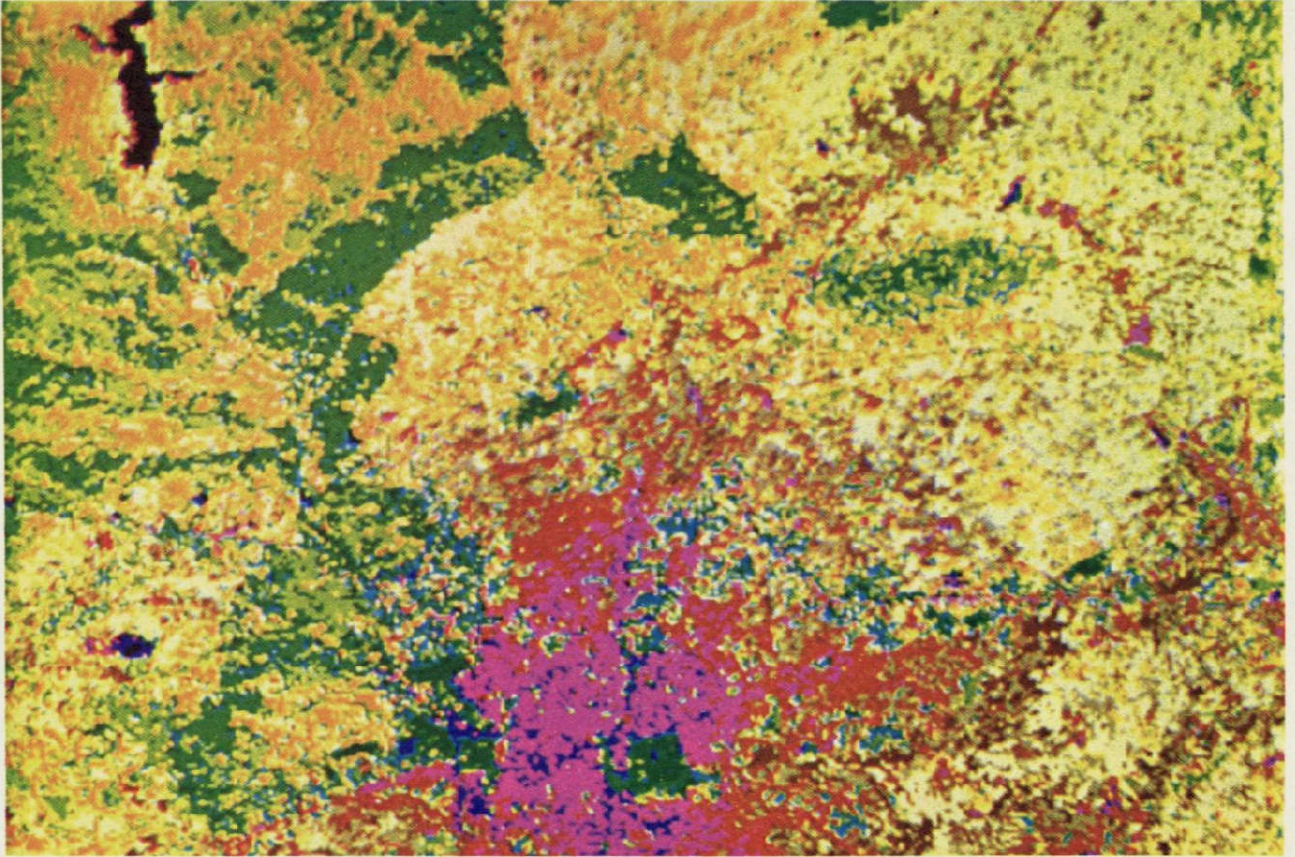
Fig. 8. Madrid and its environment classified in 8 spectral classes by digital analysis of LANDSAT data. Date July 28, 1975

As result of the classification, percentage covered by each class can be used as important data at the moment of applying results (Table 11).

In conclussion, there are 16 spectral classes with four main types of cover included in the categories: urban, forest (mountain-vegetation), edaphic and hydric. (Figure 7).

A reduction in the number of classes to eight simplifies the image of the area (Fig. 8) and its interpretation. The new eight classes identified are shown in table 12.

Printed images of "Madrid and its environment" show digital displays of the area under study, geometrically corrected, in false color, and classified. The equivalence tables of symbols of computer printout, color of display and significance of each class is given. (Tables 13 and 14).

The surface included in the images (fig. 9 and 10) has an extension of 12.267 hectares, and it represents the same area than fig. 11, where the symbols used by the computer can be seen. Each symbol represents a surface of 1.15 acres or 0.47 hectares at scale 1:25.000.

The map printed by the computer, with eight simplified classes is more clear and schematic, offering more advantages to the not specialized user.

Applications of a study of LANDSAT data done by computer can be established as function of the mentioned objectives in this report: land use and soils classification. With this digital analysis we have established the main spectral classes (urbans, edaphics, forests and hydrics) and subclasses of Madrid environment and its area of influence (or impact).

More detailed studies in this sense could be basic for a structural planning of urban and rural areas. In the urban areas
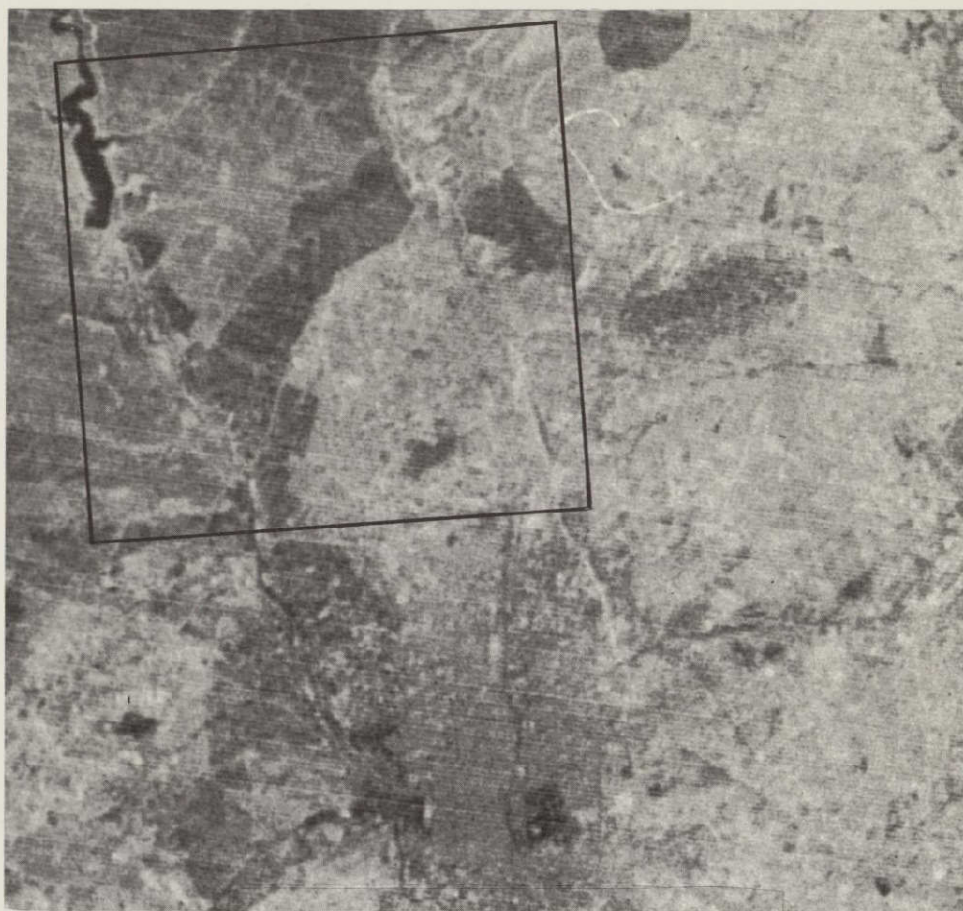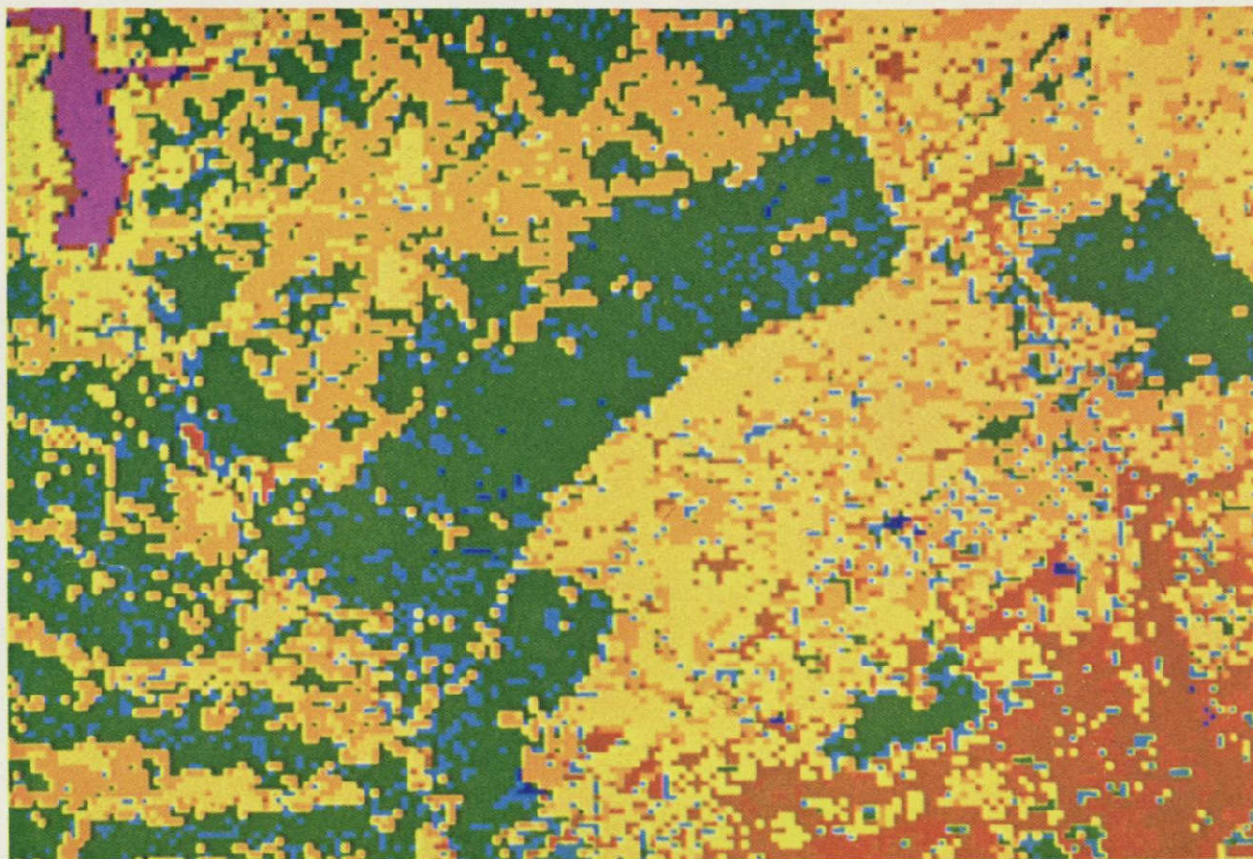
Fig. 9.—Area of El Pardo. Date July 28, 1975

Fig. 10. — Madrid and El Pardo. Classification in 8 classes. Date July 28. 1975
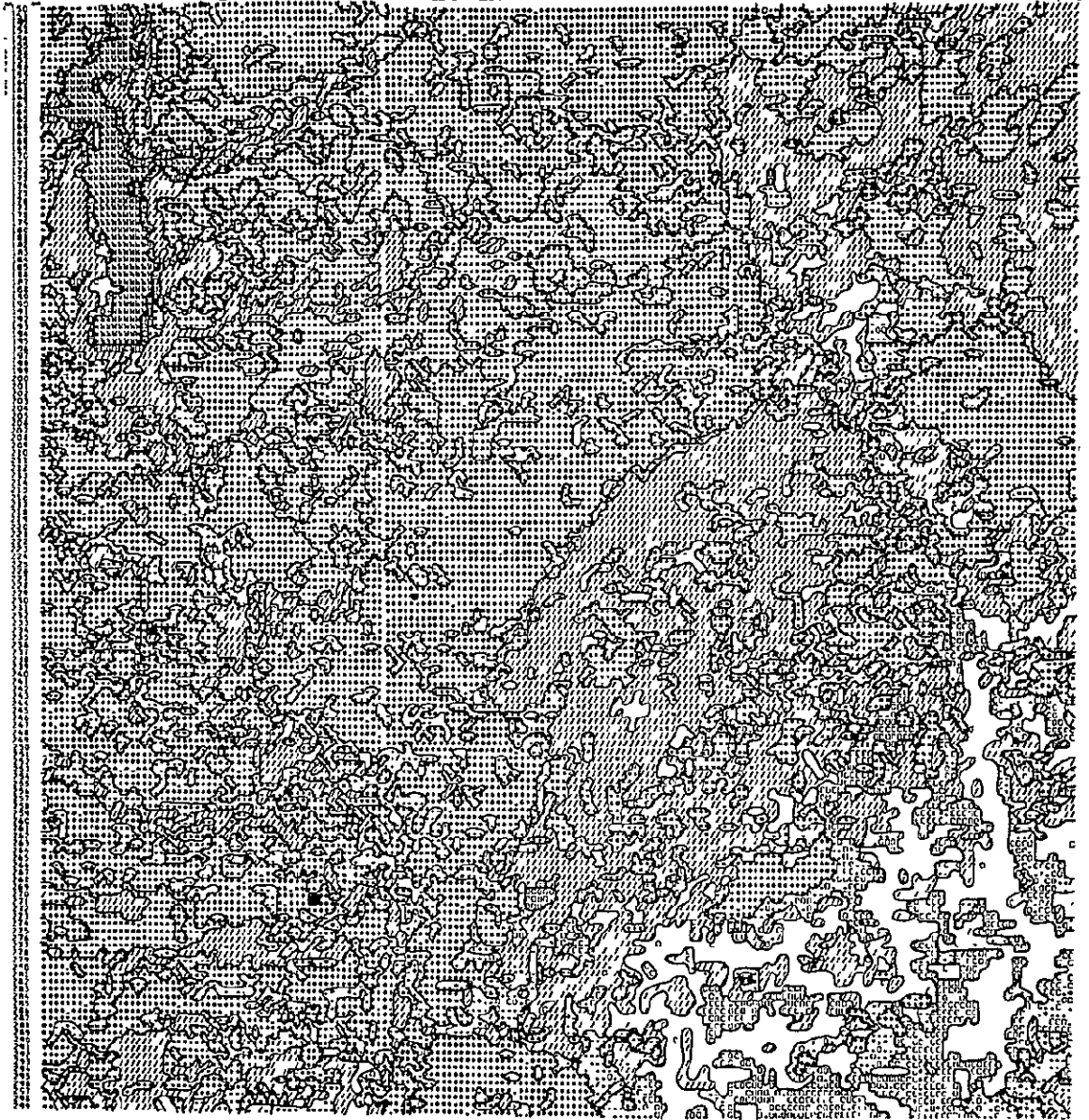
Figure 11. Madrid and El Pardo. Computer printout of 8 classes.

TABLE 13. COLOR IDENTIFICATION OF 16 CLASSES

COMPUTER SYMBOL	IMAGE COLOR	CLASS SIGNIFICANCE
P	Dark brown	Parking
o	Light brown	No buildings
ʃ	Light greenish grey	Squares
.	Red	Old buildings
0	Dark rose	New buildings
=	Dark blue	Residential 1
−	Light blue	Residential 2
*	Dark green	Parks
/	Light green	Grass
V	Yellowish green	Compact veget.
I	Greenish yellow	Mountain
S	Light Beige	Bare soil
X	Yellow	Xerochrepts
H	Mustard yellow	Haploxeralfs
+	Navy blue	Lakes/streets
W	Black	Reservoirs

TABLE 14. COLOR IDENTIFICATION OF 8 CLASSES.

COMPUTER SYMBOL	IMAGE COLOR	CLASS SIGNIFICANCE
‖	Dark brown	No buildings
0	Red	Urban
.	Light blue	Residential
ĸ	Light green	Mountains and Parks
/	Yellow	Xerochrepts
=	Mustard yellow	Haploxeralfs
+	Navy blue	Lakes/streets
W	Dark rose	Reservoirs

exists the possibility of a cyclic checking of urban changes, observing the direction and evolution of growth in the cities.

Concerning rural areas, LANDSAT data show the possibility of an inventory of crops (classes and surfaces); damages by plages and meteorological conditions and not cultivated surfaces classified by type of soils. Outside of knowing the land use in a certain moment, it can be known the variation of soils in time.

Advantages offered by digital analysis of LANDSAT data in the study and investigation of Earth Sciences can be translated as the possibility of selection of the date for study, cost economy per unit of surface area, easy correlation of classes and rapid development of a working program. These advantages and the possibility of studying the earth surface every 18 days justify the great number of projects envolved in the use of remote sensing technology.

F O R E S T R Y

DIFFERENTIATION OF CONIFERS SPECIES IN CENTRAL SPAIN
BY DIGITAL ANALYSIS OF LANDSAT DATA.

Joaquín D'Aubarede
Pilar Avizanda

Remote Sensing Laboratory
Geographic and Cadastral Institute
Madrid
SPAIN.

F O R E S T R Y

DIFFERENTIATION OF CONIFERS SPECIES IN CENTRAL SPAIN BY
DIGITAL ANALYSIS OF LANDSAT DATA.

By Joaquín D'Aubarede and Pilar Avizanda
Remote Sensing Laboratory
Instituto Geográfico y Catastral
Madrid.

1. INTRODUCTION

This work is carried out with the purpose of differentiating
conifers species in Central Spain, by means of digital
processing techniques applied to LANDSAT MSS information.

The analysis done pretends to establish spectral differences
in the responses of Pinus pinea L., Pinus pinaster Sol. and
Pinus sylvestris L. when studied in their natural habitats
of the forests around Madrid Province.

A supervised classification of different species, by selection
of training fields, is the technique applied in this report to
the test sites defined in Sierras of Guadarrama and Gredos.

2. BIOLOGICAL AND ECOLOGICAL BACKGROUND

In this work it is intended to differentiate the following
conifers species in Central Spain by means of digital,
analysis of LANDSAT data:
- Pinus pinaster Sol.
- Pinus pinea L.
- Pinus sylvestris L.

Such species are well represented in Central Spain, around
the Sierras of Guadarrama and Gredos, which are the areas of
study. They present thick masses of pinus in their natural
habitat (figure 1), with the following environmental conditions:

P. pinaster Sol. It covers in the Iberian Peninsula broad
extensions of mountains; namely in the Sierras of Guadarrama
and Gredos, living in soils of siliceous nature. The average
altitude where it can be found at the area under study is
1.000 m, forming mixed forests with the Pinus sylvestris in
Sierra of Guadarrama. It is an species of vigorous nature and
fast growing, according to the good lighting conditions that
requires. Flowering season is from March to May, depending on
the severity of the moderate climate. The sheated needles have
a length of 15-27 cms, being of a high dark-greenish colour.

P. pinea L. It is distributed all over the mediterranean coast,
living at an average height of 1000 m. In the Iberian Plateau
it can be found on sandy and deep soils, while in Central Spain
it does not surpass the altitude of 1000 m and forms mixed
forests with the Pinus pinaster. This is a tree of second
magnitude and fast growing which has a vigorous nature and
needs good lighting conditions. Flowering season is from March
to May. The needles have a length of 10 to 20 cms in greenish-
blue colour.

P. sylvestris L. In Spain it covers a broad area from the Piri-
neos mountains to Sierra Nevada, forming thick forests in the
Central ridge, with optimum growing conditions in Navafría
and Balsaín (area of study in this work). Living in siliceous
and clayish soils, its optimum altitude attended is 1.500 m.
This species requires medium lighting conditions and it has
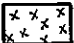a quite vigorous nature. Flowering season is from May to
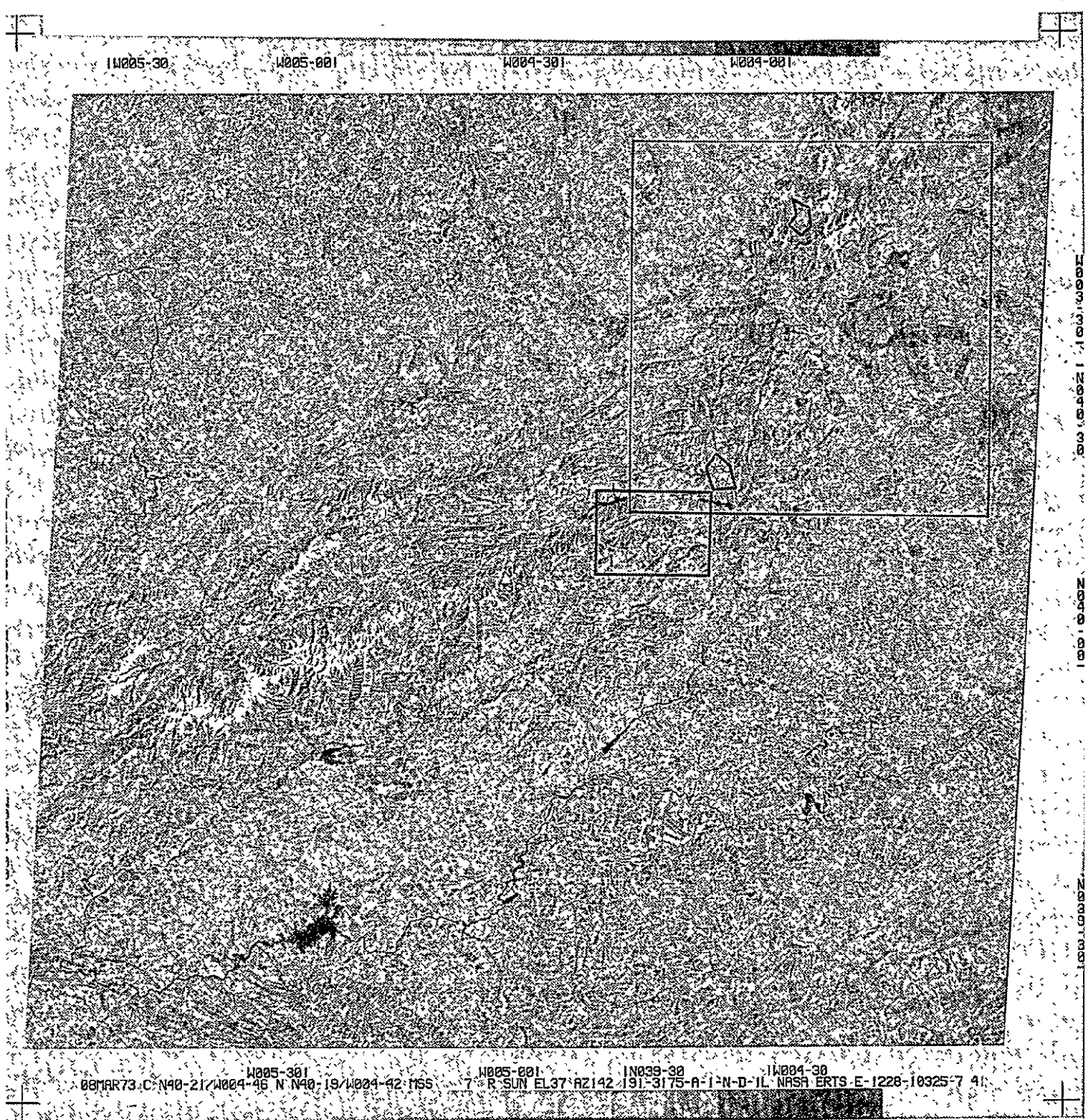
P pinea training field

P sylvestris training field

Fig. 1.—Test sites selected in Sierras of Guadarrama and Gredos for analysis of conifers species

June. Although needles have a normal length of 3 to 10 cms, in Spain they do not surpass 3 to 6 cms, being of greenish-gray to glaucous colour.

3. METHODOLOGY

Differentiation of the three main conifers species existing in Central Spain was intended by the use of digital MSS information as basic input. From the library of the Remote Sensing Laboratory was analyzed LANDSAT tape E-1228-10325, corresponding to the month of March 1973, which was taken at the time of the flowering period of species. Such image has a sun elevation angle of 37 degrees and no cloud cover.

As ancillary information it was used the Forestry Map of Spain, which is at scale 1:400.000 and has provided the basic ground truth over test sites. Some photointerpretation of recent LANDSAT images was also carried out through a DOT color composite viewer (reference 1) in an effort to keep up to date the information of the Forestry Map. Once defined the location of the working areas, according to criteria of good identification of representative training fields (figure 1), a digital analysis of the original LANDSAT tape was done.

The technique used was a supervised classification of the zones, taking as training class different species of conifers. This work was done at the IBM-Scientific Center of the Autonomous University of Madrid; where ERMAN-II program is available, operating on an IBM 360/65 computer interfaced to an interactive television terminal RAMTEK.

As a first stage was intended to establish a difference between both species Pinus pinaster Sol. and Pinus pinea L.
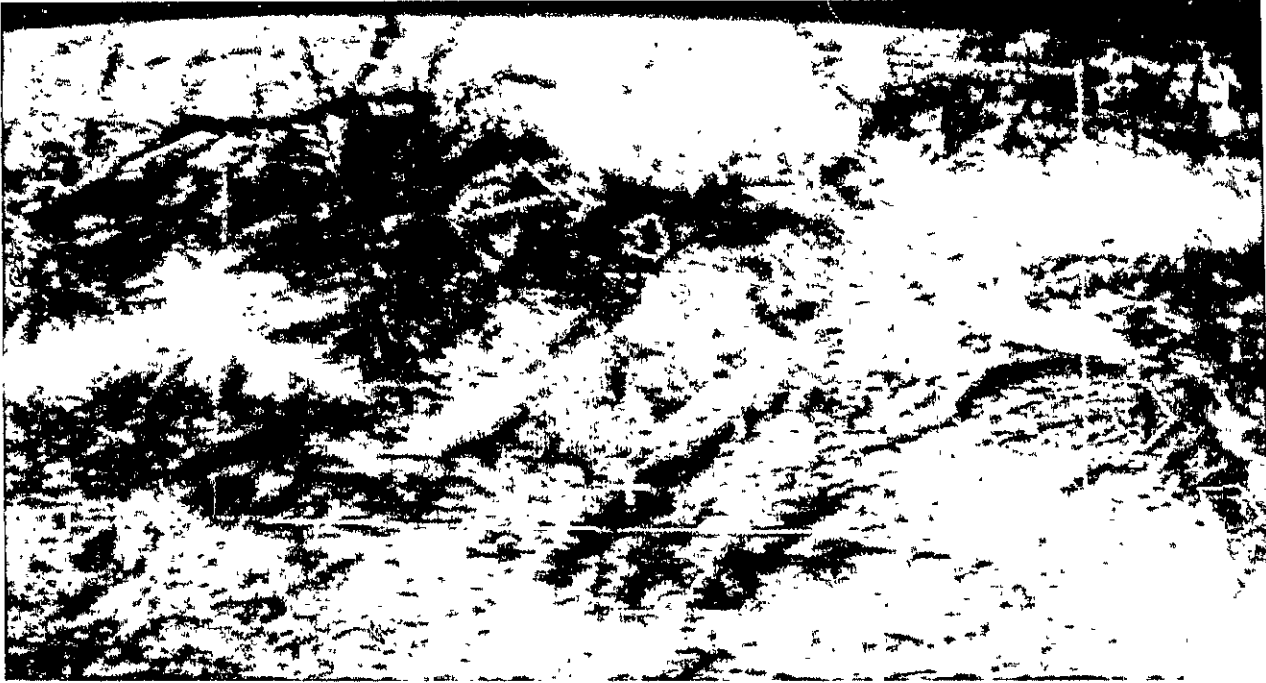
Fig. 2.—Training fields corresponding to test-site no. 1

Test site no.1 was selected for this purpose (figure 1), and four training field were chosen on it, representing the items indicated in table 1.

Field name	Class identification	Class symbol
NIEVE	Snow	NIEV
PINASTE	Sun exposed Pinus pinaster	PSOLSO
PINASTI	Pinus pinaster in shadow	PINBRA
PINEA	Sun exposed Pinus pinea	PNEA

Table 1. Correspondence of training fields name and classes identification.

In figure 2 is indicated the location of training fields. The calculation of statistics corresponding to such training fields in all four bands MSS produced the results indicated in figure 3; where the mean and standard deviation values are represented as output menu of the interactive television terminal.

From the analysis of figure 3 it can be anticipated that the spectral response of both species is very characteristic in band 4 (corresponding to channel 1), because the low value of their standard deviation. As the mean values show very similar in all four bands MSS, differentiation of the species seems to be difficult. At this point, histograms were obtained for the three classes identified in each LANDSAT spectral band (figures 4, 5, 6 and 7), corresponding to their training fields.

Although results expected were not very promising, because the strong overlap of spectral responses, a classification of the area under study was done by pattern recognition. The result of such classification is indicated in figure 8, where correspondence of colors and classes is represented at table 2.

MEAN AND STANDARD DEVIATION REPORT
FOR CLASSES AND TRAINING FIELDS
AND ALL AVAILABLE CHANNELS

CHANNEL NUMBER	FIELD NIEVE (400) CLASS NIEV		FIELD PINASTE (369) CLASS PSOLSO		FIELD PINASTI (184) CLASS PINBRA		FIELD PINEA (506) CLASS PNEA	
	MEAN	ST DEV	MEAN	ST DEV	MEAN	ST DEV	MEAN	ST DEV
1	106 34	29 95	18 79	1.83	15.82	1.01	20 53	1.96
2	104 66	30 89	14 40	3.02	9.43	1 49	15 77	2 53
3	95.71	28.60	26 62	3 26	16.10	2.33	22.97	3 42
4	36.40	11 05	15 70	2 03	8 72	1.60	12 64	2.15

Fig. 3.—Mean and standard derivation values of training fields

166

class symbol	color
NIEV	blue
PSOLSO	green
PINBRA	cyan
PNEA	red

Table 2.

Differentiation of Pinus sylvestris and Pinus pinea was intended on test site no. 2 (figure 1), with a new LANDSAT image dated March 7, 1973 (E-1227-10271), with sun angle elevation of 37 degrees similar to the previously used image (E-1228-10325) for test site no.1. As both images were taken with an interval of 24 hours, the vegetative status of conifers species was in similar conditions.

A supervised classification was done in the new area of study with two training fields of P. sylvestris and P. pinea.L. Computation of statistics conducted to the result indicated in table 3.

Band	Field PINEA		Field SILVES	
	Mean	St. dev.	Mean	St.dev.
4	24,26	2,16	18,08	1,26
5	21,33	3,16	11,89	1,73
6	31,57	4,07	20,77	2,75

Table 3. Mean and standard deviation values of training fields.

163

HISTOGRAMS FOR FIELDS AND/OR CLASSES
PINASTE (3691
PINASTI (184)
PINEA   (506)
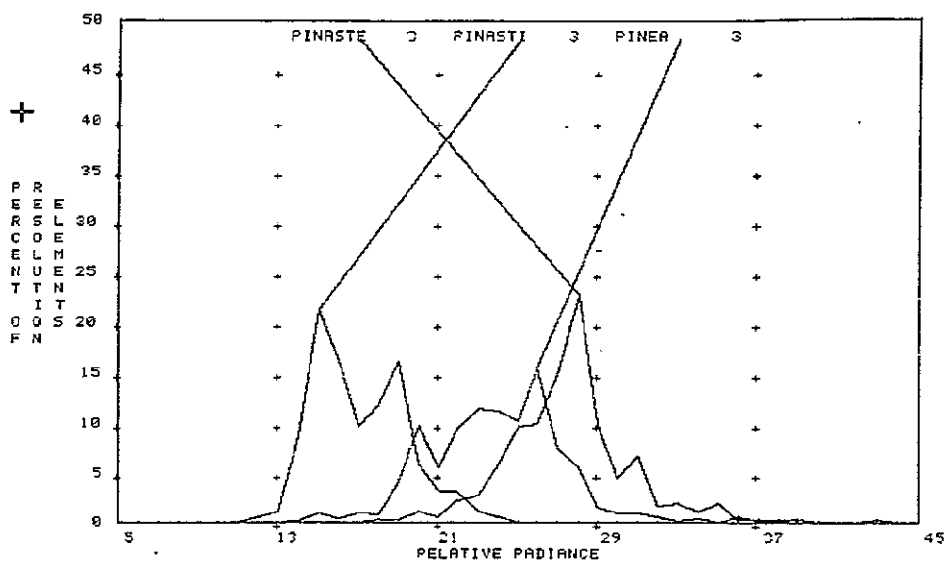
Fig. 4.—Histogram of classes in band 4

HISTOGRAMS FOR FIELDS AND/OR CLASSES
PINASTE (3691
PINASTI (184)
PINEA   (50t)

Fig. 5.—Histogram of classes in band 5

HISTOGRAMS FOR FIELDS AND/OR CLASSES
PINASTE (369)
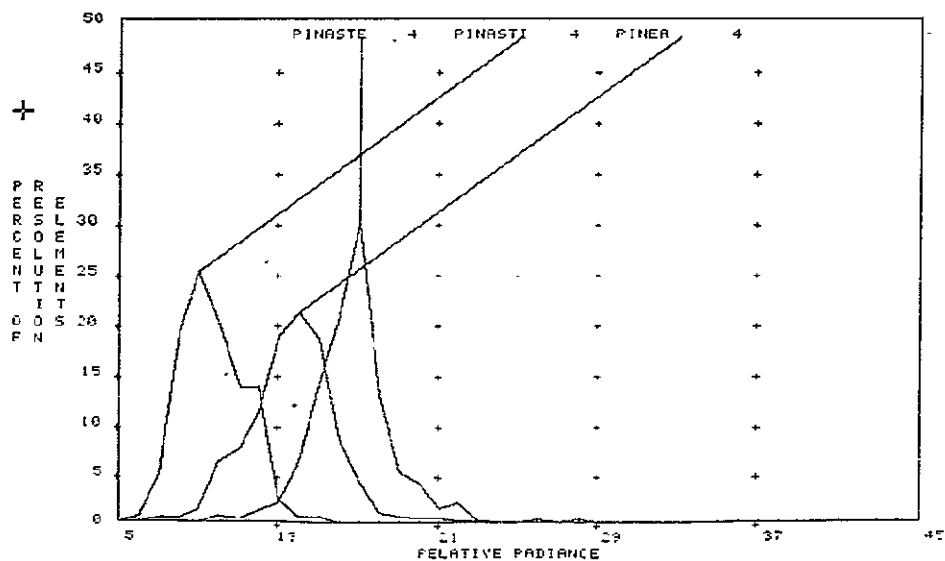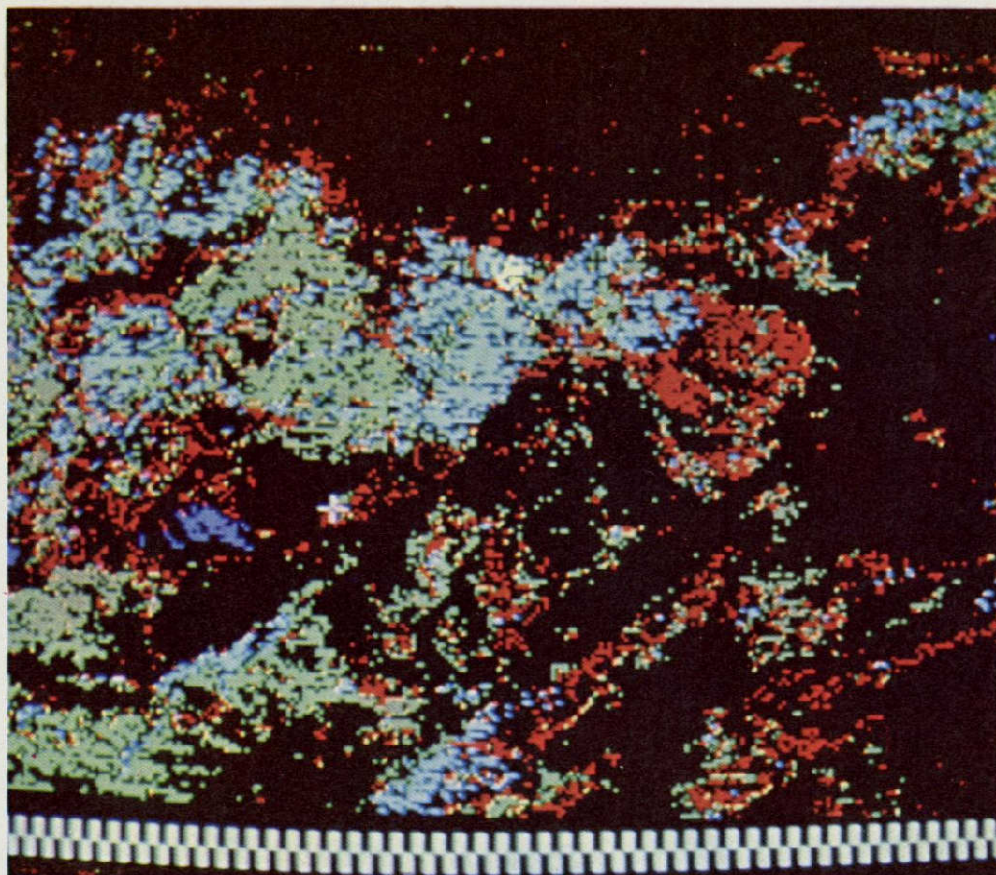PINASTI (184)
PINEA   (506)

PINASTE   3   PINASTI   3   PINEA   3

PERCENT OF RESOLUTION ELEMENTS

RELATIVE RADIANCE

Fig. 6 —Histogram of classes in band 6

HISTOGRAMS FOR FIELDS AND OR CLASSES
PINASTE (369)
PINASTI (124)
PINEA   (506)

PINASTE   4   PINASTI   4   PINEA   4

PERCENT OF RESOLUTION ELEMENTS

RELATIVE RADIANCE

Fig. 7.—Histogram of classes in band 7

Fig. 8. Result of the supervised classification in test-site no. 1. Black color represents threshold value

Band 7 was not available for this classification. The values
of mean and standard deviation obtained in the training fields
show that a differentiation of both species of conifers is
possible when based on a supervised classification of LANDSAT
data. In figure 9, 10 and 11 the histogram values for each
band are represented.

4. RESULTS AND DISCUSSION

At the flowering season of Pinus pinaster and Pinus pinea it
was not possible to differentiate both species in Central Spain
by digital analysis of LANDSAT data. Such result could be due
to the fact that both species have the same biotop. As both
pinus have a strong need of light for attending their
development and climax, their crowns and cortical systems
cannot afford a competition with other trees of the same
species. Their forests have to be open, with the number of
trees per hectare being low when compared to other species
of different nature, like the Pinus sylvestris in normal
closeness. Such circumstances force the existence of open
spaces between trees; soil or open space which, due to the
biological needs of both species and the geological nature
of the central region of Spain, is similar for them. These
reasons indicate that texture of the species as seen by
LANDSAT must be quite homogenous in both cases.

An individual analysis of each species shows that a certain
similarity is observed in their needles, of approximate
length, and in their greenish-blue color, which produces quite
similar reflectances in band 4 (green region of the spectrum).

The histograms of figures 4, 5, 6 and 7 show that a discrimination
of Pinus pinaster and Pinus pinea is not possible in the LANDSAT
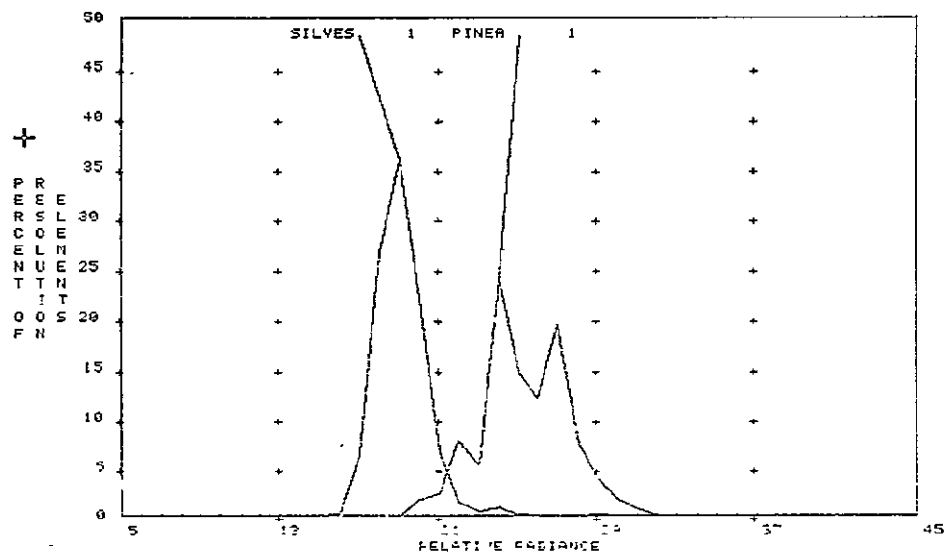
HISTOGRAMS FOR FIELDS AND/OR CLASSES
SILVES (1665)
PINEA (310)

Fig. 9.—Histogram of classes in band 4

HISTOGRAMS FOR FIELDS AND/OR CLASSES
SILVES (1665)
PINEA (310)
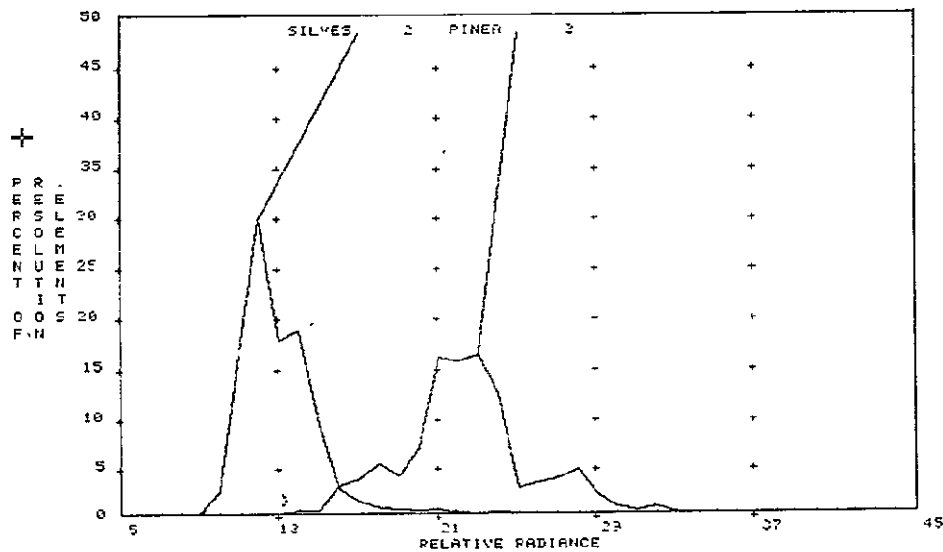

Fig 10.—Histogram of classes in band 5

HISTOGRAMS FOR FIELDS AND/OR CLASSES
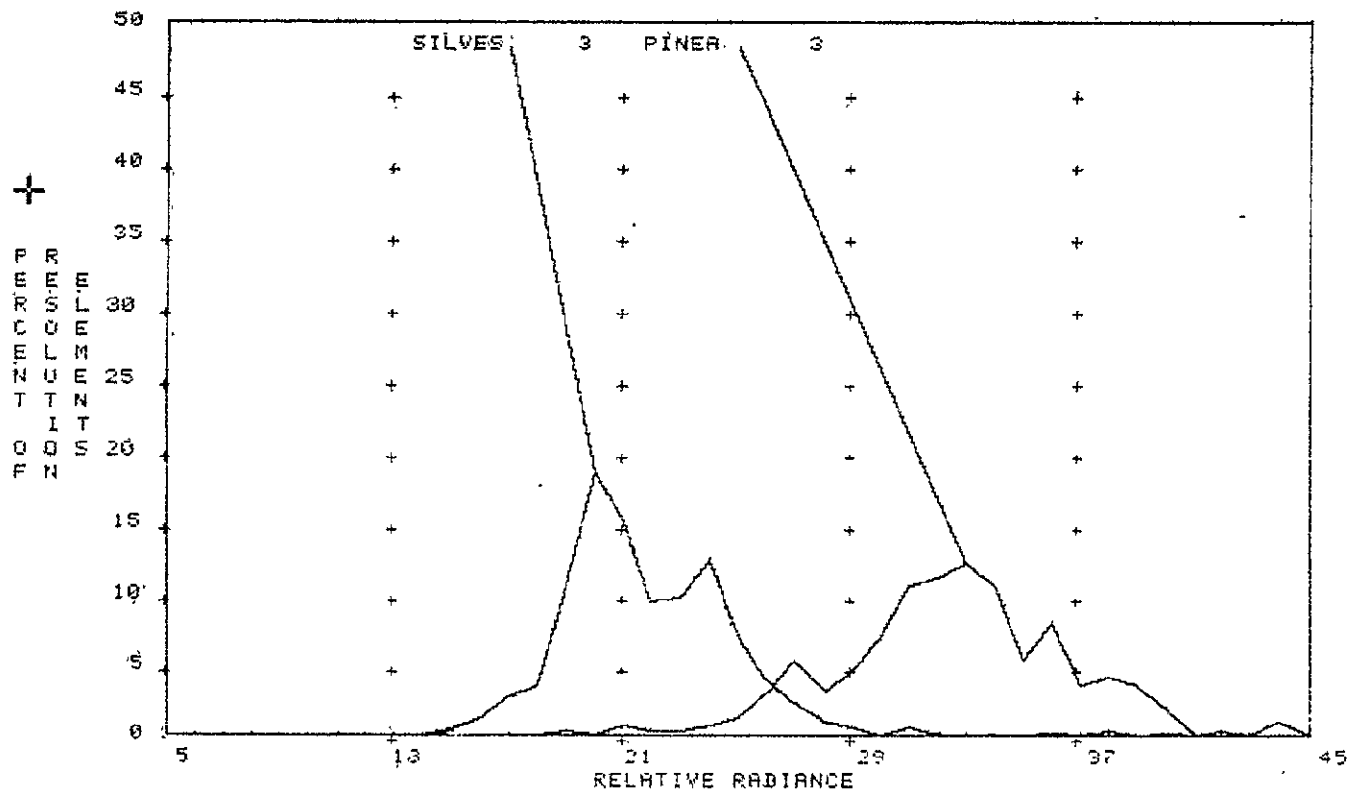SILVES   (1665)
PINER   (310)

Fig. 11.—Histogram of classes in band 6

image studied, because the high amount of pixels that belong
to both species and have similar values of reflectance. Such
mixed spectral response appears also in the training fields
of Pinus pinaster in shadow and in sun light, being in the
second case more difficult to find out a difference with
Pinus pinea class.

Differentiation of P. sylvestris and P. pinea was much better
achieved, because the biological and ecological needs of both
species are not the same. As the flowering period of P.
sylvestris is from May to June, and the movement of the sap
begins on it two months latter than in P. pinea, their
reflactance curves do not seem to be equal, nor it is their
color.

As P. sylvestris is a species with medium lighting conditions
requirements, it has a higher density of trees per hectare
than P. pinea; which should have an important effect in the
texture of the crowns when observed at satellite altitudes.
Band 4 seems to contain better MSS information than bands 5
and 6 for differentiation of both species.

The conclusions presented are only defined for Central Spain,
and they do not apply in general to P. sylvestris L. and P.
pinea L. species, because such species in other areas with
different factors (climatology, ecology and geology), could
have different spectral responses than here evaluated.

References

1 - J. D'Aubarede and P. Avizanda "Application of LANDSAT-2
    data to updating forestry maps in the central region of
    Spain". Third Quarterly Report, NASA project no. 28760,
    Instituto Geográfico y Catastral, Madrid.

G E O L O G Y

DETERMINATION BY MEANS OF LANDSAT IMAGES OF DIFFERENT
GEOLOGICAL STRUCTURES IN THE CENTRAL AREAS OF IBERIAN
PLATEAU.

M. Alía
C. Martín Escorza
A. G. Ubanell
L. Muñoz

Internal Geodynamics Department
Complutense University of Madrid.
SPAIN.

G E O L O G Y

DETERMINATION BY MEANS OF LANDSAT IMAGES OF DIFFERENT GEOLOGICAL
STRUCTURES IN THE CENTRAL AREAS OF THE IBERIAN PLATEAU.

By M. Alía, C. Martín Escorza, A.G. Ubanell and L. Muñoz
Cátedra de Geodinámica Interna
Universidad Complutense
Madrid.

SUMMARY

Starting with the observation of the LANDSAT images, new
structures of tectonic origin have been able to be determined
in the Iberian Plateau.

In the first place, we would point out the megastructure
"Bóveda Castellano-Extremeña", of eliptical form and which,
because of its amplitude (some 350 kms. as minimum in its
largest axis, orientated to the NE) should be considered as
lithospheric scale. Its origin (ALIA, M. 1976, b) can be
related to the interactive processes between the veins and
the crust which gave way to an arching initially, which was
followed by a distension process with the formation of valleys
and basins during the upper Terciary. In this great structure,
two areas are differentiated; one septentrional, which is
more complex and accidented, and the other, more homogenous,
meridional. Both are separated by the "Banda Estructural de
Toledo" (ALIA, M. 1972) of an E-W direction.

Forming part of the most heterogeneous septentrional unit,
and also by means of LANDSAT images, the "Halo Estructural de
Guadalix" has been differentiated; an annular structure of
concentric rings with a maximum radius of 40 kms. located North
of Madrid.

Distinct alineations localized in the granite-metamorphic
Basement of the Central System have also been differentiated
and evaluated with relation to the field data, with a diagram .
offered of the set of observations.

Also, the best band relations have been found to obtain optimum
results in areas of this type, and thus in a zone of the
Iberian Plateau, geological structures have been determined
and the different types of lithologies.

1. INTRODUCTION

The team studies being made by the members of the Department
of Internal Geodynamics of the Complutense University of Madrid
in the central areas of the Iberian Plateau include: analysis
of the structures in fayed veins, detections of alineations of
tectonic origin in zones covered by non-tectonized neogenic
sediments, raising maps from the ceilings of the basement in
these last zones by geophysical methods (magnetometrics and
gravimetrics, mainly) and gravimetric profiles through zones
with fayed and unfayed basement. These studies have allowed
obtaining a certain structural and tectonic conception of the
above mentioned areas.

These discoveries have been greatly enriched by the consequences
obtained from the observation of LANDSAT images, which were
provided by NASA through the Geographic and Cadastral Institute
of Spain in accordance with Project no. 28760 signed between
both agencies.

The geological results obtained from these images have allowed
integrating some of the facts observed in the field, to
facilitate the vision of the unit of some already known
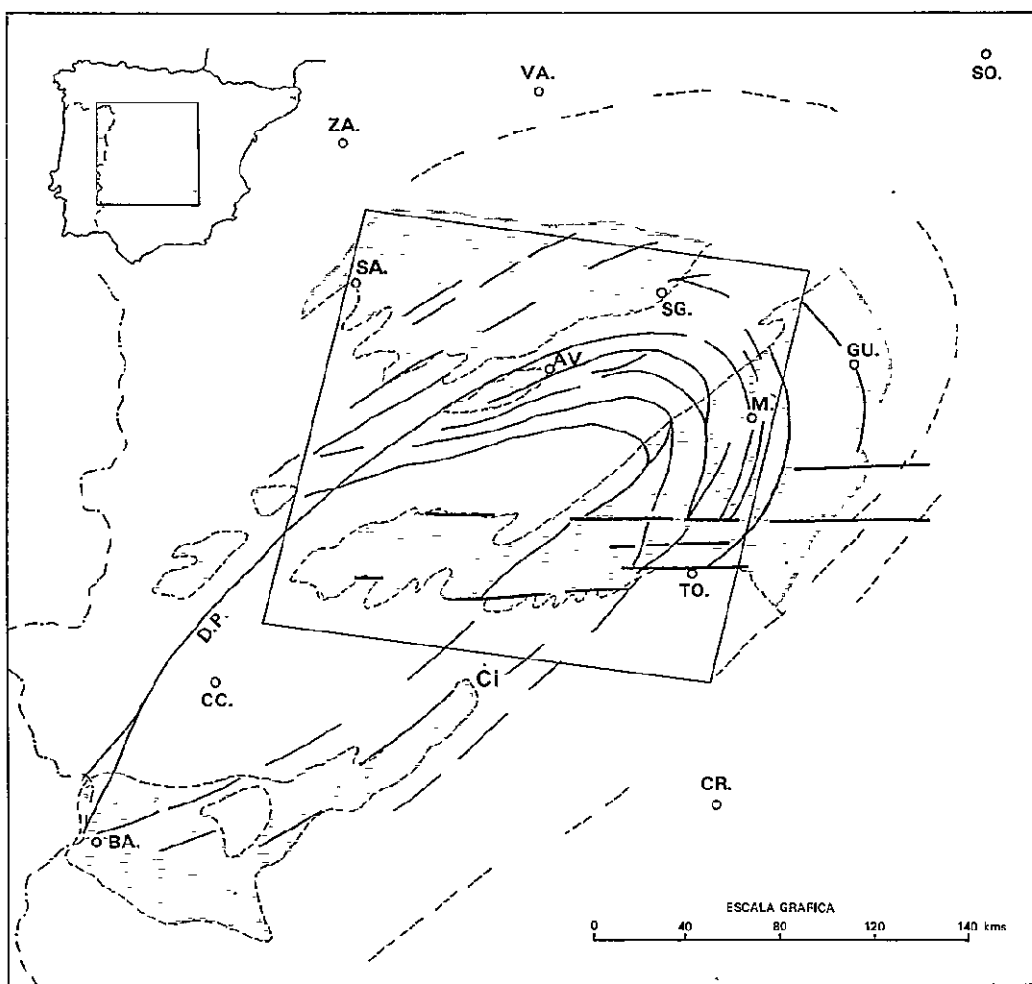structures, to make them coherent with others newly detected

Figure 1

175a

Figure 2

by LANDSAT images, and to make even more ample some of the preconceived investigation lines.

It has been very interesting to be able by means of such images to establish the existence of a cortical megastructure ("Extremenian-Castillian Vault", ALIA, 1976, a, b) which, with an eliptical form and the major axis orientated following a NE-SW direction, crosses a great part of the inside areas of the Iberian Plateau.

2. DESCRIPTION OF THE AREA STUDIED, MATERIAL, METHODS AND TECHNIQUES USED.

The area studied (figure 1) corresponds to the central regions of the Iberian Plateau and fundamentally include the Central System, the Mountains of Toledo and the two Valleys of the Tajo and the Duero. The Central System and the Mountains of Toledo are made up of granite and metamporphic rocks, formed in the Hercinian Cycle, and in the Valleys of Tajo and Duero crop up, in the majority, covering materials deposited during the Terciary.

In the Central System, two great alineations can be differentiated: The Sierra de Gredos, situated to the West and the Sierra del Guadarrama, on the oriental side. It should likewise be pointed out that the Valley of Tajo is limited in its meridional part by another large granite-metamorphic alineation of the Hercinian Cycle: The Mountains of Toledo.

All of these zones are covered by images E:1228-10325, 1229-10384; 1227-10271; 2170-10204; 2367-10122, of which the most frequently used channels were bands 5, 6 and 7, which have been found as the best for geological examination.

The interpretation and analysis has been made through the direct observation of images available in different sizes,
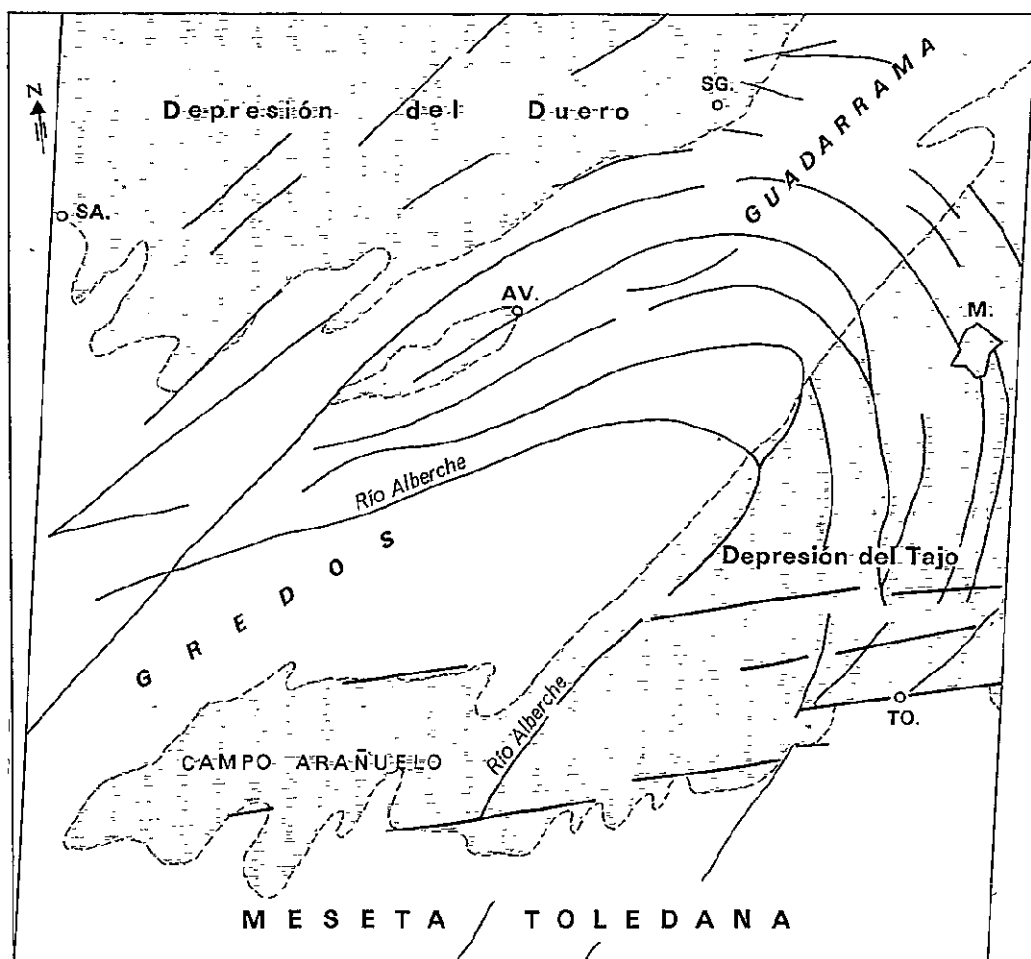
Figure 3

on which transparencies were superimposed and lines were
marked when due to geological accidents of tectonic origin.
The analysis, the ponderation, integration and coherence of
such structural lines with the observed and known facts of
the land, have made possible obtaining greater structures
with the results stated here.

In the zone of the Valley of Tajo an interactive RAMTEK
Terminal has been used, connected to an IBM 360-65 computer.
The terminal comprises a conversational screen and an image
display unit (color-TV), as well as a memory bank to accumulate
images at 8 bits, with 16 levels in each of the three tube.
The entire system is governed by the ERMAN-II programme
(L. MUÑOZ, 1976 - Second Quarterly Report, fig. 4).

3. RESULTS

3.1. Application of the above mentioned methods to a composite
of the images E-1228-10325 and E-1229-10384 in any of its
channels, but specially in bands 5 and 7, has allowed (ALIA
1976 a, b) to interpret that the dominant structures of the
unit observed in the images correspond to an ample arching
which affects the terrestrial coverage in the regions of the
Iberian Plateau, and which has been called "Extremenian-Cas-
tillian Vault" (op.cit. page 229). This megatructure (figure 1)
is equally developed in the regions where the materials of
the Hercinian basement are fayed (Central System and Mountains
of Toledo) as in those others where said basement stays hidden
under the coverings of posterior sediments.

The defining elements in the case of the fayed basement are
fundamentally provided by fractures which, with their preferent
alineations and continuity, sketch the greater structure to
which they belong. Many of these fractures are used by the
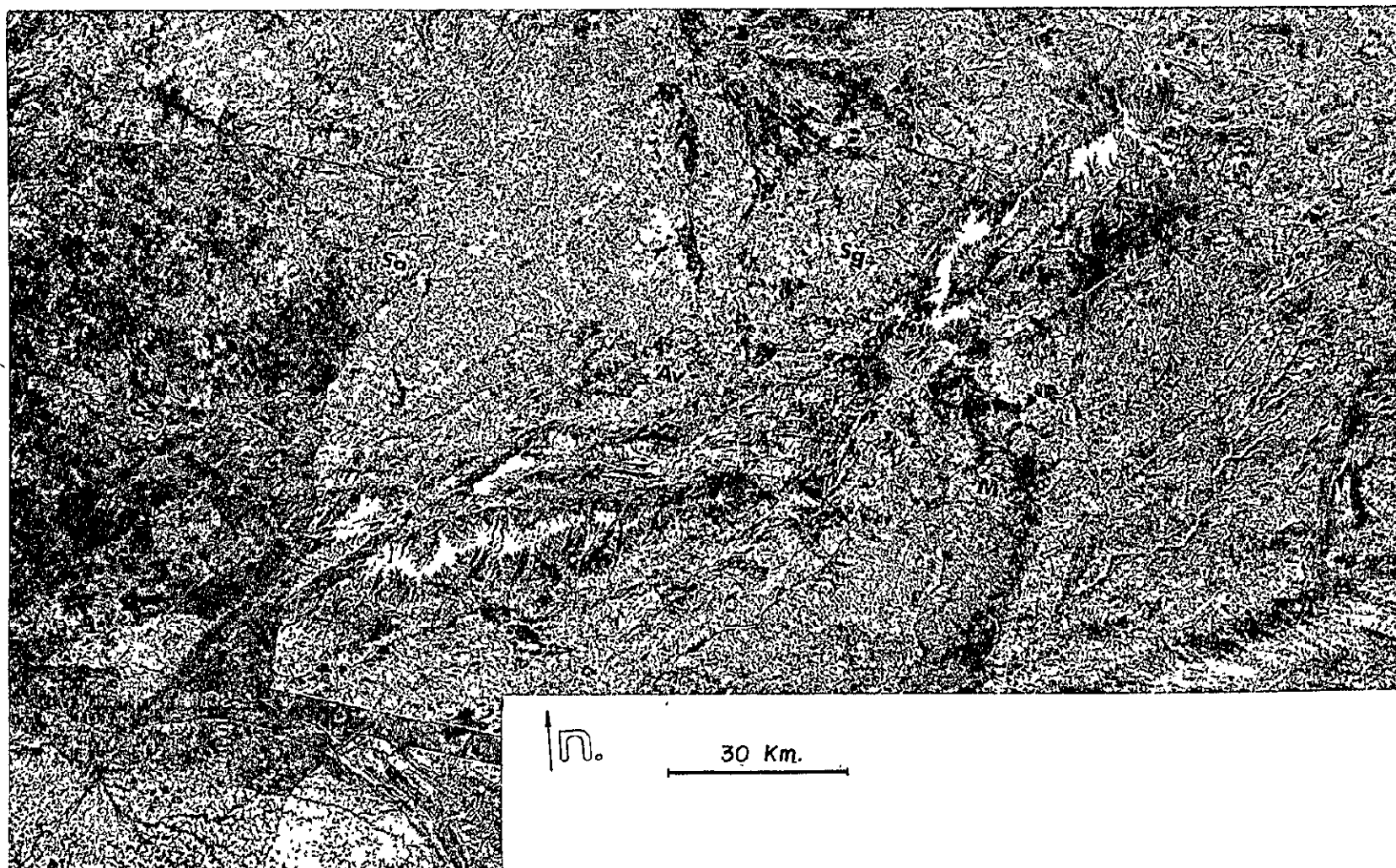
30 Km.

Figure 4

fluvial network at the present times. In the case of the zones
with sedimentary coverage, equally aligned elements are
presented which correspond to and are the surface reflection
of', through the covering, existing alineations in the hidden
basement, in accordance with correlations which have already
been established for the zones of the Valley or Tectonic
Depression of the Tajo (ALIA et al., 1973; CADAVID et al.,
1967; MARTIN ESCORZA, 1976 a, b; MARTIN ESCORZA et al., 1972,
1973). Such alineations under cover are generally expressed
by lateral changes of facies and powers which are also found
following the lines represented in the cartography. Some of
these lines are weakness bands which equally use the present
or subpresent fluvial network.

Figure 2 corresponds to the image E-1228-10325-7 taken by
LANDSAT-1 of the central region of Spain. Figure 3 squemati-
cally marked the main structural alineations which are
integrated for this region into the Extremenian-Castillian
Vault.

As observed in figures 1 and 3, the Extremenian Castillian
Vault is affected in the middle by structural alineations
with a parallel E-W direction, which belong to an important
existent alineation also on a Peninsular scale, already
detected by ALIA (1972) and known since then with the name
of "Banda Estructural de Toledo". The influence of this
tectonic structure on the "Extremenian-Castillian Vault"
is shown in its middle areas and thus divides it into two
large units: the septentrional, with visible and numerous
arched alineations (figures 1, 2 and 3) and the meridional
with a lesser proliferations of defining alineations (figure 1).
The "Banda Estructural de Toledo" interrupts the Southern
directed continuity of some main alineations of the
septentrional unit, others are slightly detoured and others

N

SALAMANCA

GUARDA

AVILA

MADRID

TOLEDO

☐ TERTIARY SEDIMENTS

☐ ORDOVICIAN

／ FAULTS or FRACTURES

／ IDEM. PROBABLE

⋯ APLITIC DYKE

0   Km   100
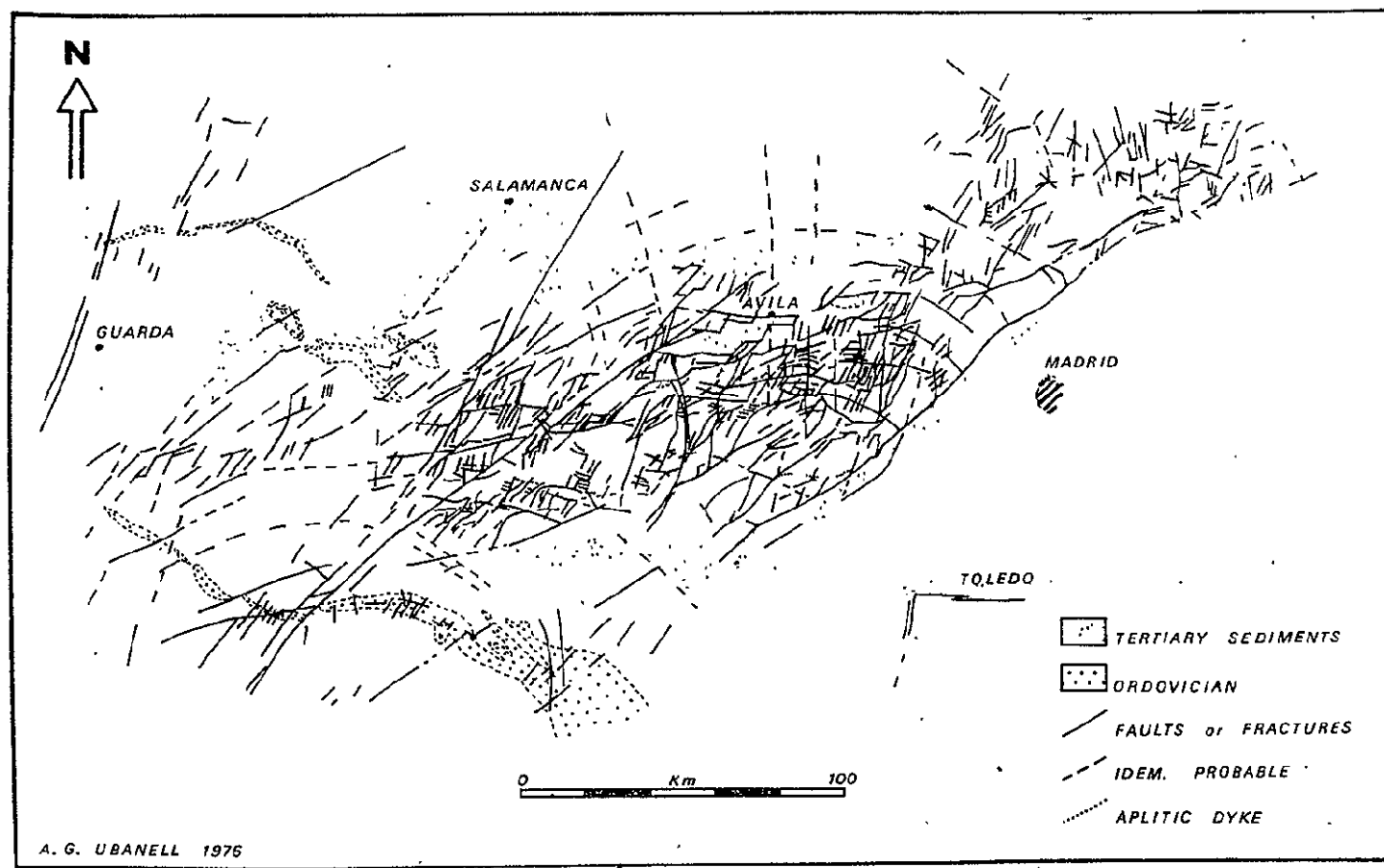
A. G. UBANELL   1976

Figure 5

such as that which limits the Vault on its northwestern border,
stays neatly marked on the North as well as the South. This
line, which in figure 1 is indicated by letters D.P.,
corresponds to the well-known and important Dique de Alentejo-
Plasencia (GARCIA DE FIGUEROLA, 1963, 1965; GARCIA DE FIGUEROLA,
et al., 1974).

In the southeastern part of the Vault, the most important
defining line is found to be in direct relation with the
presence of the sedimentary sub-basin Badajoz-Cijara (see
figure 1).

The megastructure thus defined as "Extremenian-Castillian
Vault" is a tectonic-structural element of prime importance
in the Iberian Plateau and by itself indicates, it seems to
us, a directing model, from which the investigations for
profiling and concreting the lesser structures and accompanantes
of this which we consider the main one, can be proceeded
with.

3.2. In this respect we offer here (figure 5) and as a result
of this Project, a promenorization of the observable alineations
in the unit of the hercinian flayed basement which constitutes
the Central System (UBANELL, 1976). In order to obtain this,
we have used the images E-1228-10325, E-1229-10384 and E-1227-
10271 in bands 5 and 7. (figure 4). The direct knowledge in
the field of these regions has permitted improving and giving
a greater significance to these structural ranges, in comparison
with the results offered by other aothors (as for example
BISCHOFF, 1975). With more recent images of the same zone it
is possible to extract a greater detail, and thus in the
structural scheme of alineations of figure 6, the E-2170-10204-7
has been used with a date of July 1975, obtained by LANDSAT-2
and which still covering the same area as that in figure 2,
gives a clearer view.

N

SALAMANCA

SEGOVIA

AVILA

MADRID

TOLEDO

TERTIARY SEDIMENTS

ORDOVICIAN

FAULTS or FRACTURES

IDEM, PROBABLE

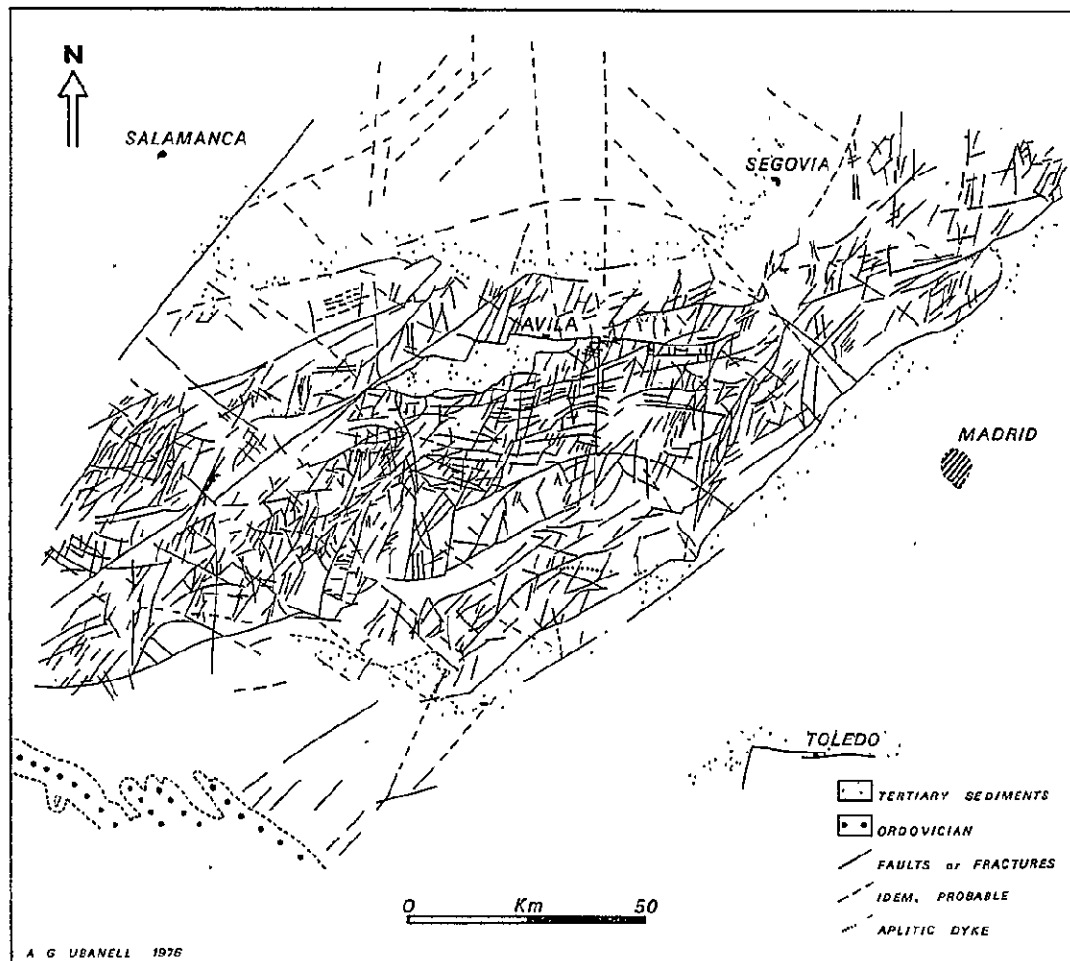APLITIC DYKE

0   Km   50

A G UBANELL   1976

Figure 6

183

The noticiable imporvement in the quality and clearness of
the LANDSAT images is appreciated, from the first ones
received up to the most recent ones, as they have permitted
differentiating other lesser structures, which would otherwise
have reamined undetected.

3.3. Such succeeds in the regions situated to the North of
Madrid, where the images E-2223-10135; 2187-10143; 2169-10145,
in their different bands 4, 5, 6 and 7, would not suggest
a marked structural form. Nevertheless, the careful observation
of the most recent image (July, 1976), the E-2367-10122-7, has
made it possible that in said regions an annular structure has
been determined which affects the materials of the hercinian
basement in the Central System as well as the sedimentary neogene
covering of the Valley of Tajo, in this case composed mainly
by arcosas (figure 7). This structure (Figure 8) has been named
the "Halo estructural de Guadalix" since the town of Guadalix
is the most central point of it. Its average radius is 30 to
40 km. and its outside ring reaches in effect the city of
Madrid. This structure is not a complete ring, since in its
most septetrional part, it is cut off by the larger fracture,
with a NE-SW direction which limits the meridional edge of
the Central System.

As can be directly observed in the zone of the studied image
(figure 9) many of these curved alineations correspond to
secondary sources of the present fluvial network, but the
clearest defining elements and also those which are most
numerous correspond to streams and fluvial interlickings of
even lesser order and importance (figure 10). Such streams
are arranged making up a unit which is only explicable by
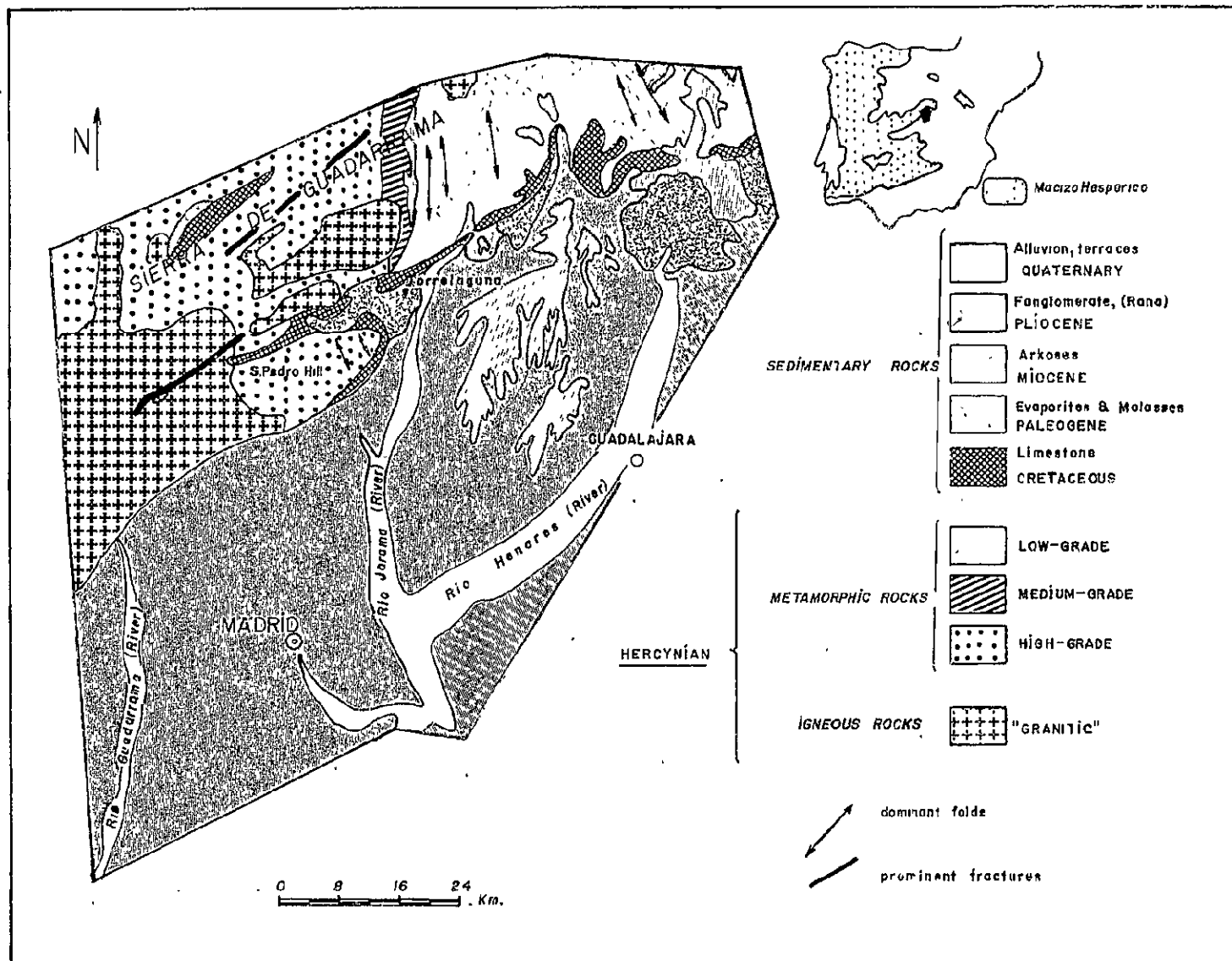the existence of the cited structure and in some concrete

Figure 7

areas they offer a good ecample of the influence of the "Halo Estructural de Guadalix" (figure 11) on the hydric flux of this category.

3.4. Apart from all these structures of different importance and scale described up to now, we have tried to testify, in a very concrete area, where we likewise have sufficient field data, the prominence or mortification of determined and contrastinsg structures depending on the band-ratio. The possible application of the handling of this technique by means of a RAMTEK Terminal in structural geology, is a function of the results obtained in the utilization of different relations of channels, each one of which can visualize in a different way the same structures. This technique was made possible through the IBM-Scientific Center of the Autonomous University of Madrid.

The area selected was Campo Arañuelo, a terciary sub-basin (figure 12) located some 250 kms. to the West of Madrid (see figure 3) and concretely part of its meridional limit, where it has been proved (figure 13) that the granite-metamorphic hercinian basement which forms part of the Mountains of Toledo, is found to be in contact with the non-consolidated sedimentary crust, by means of fractures and robbles of almost the same directions (MUÑOZ, L. 1976, a, b)which delimit three rigid basement units which "penetrate" in the area of the covering, like piano keys. For this reason, we have called them "Naval-moral Key", "Berrocalejo Key", "Oropesa Key" from the West to the East respectively. Using the image E-1228-10325, of 8 May, 1973, with a Solar Elevation of 37º and Azimut of 142º, it was processed in such a way that the color images obtained on the screen were a result of a histogram, made of the radiation levels in each of the bands to be represented and where the levels
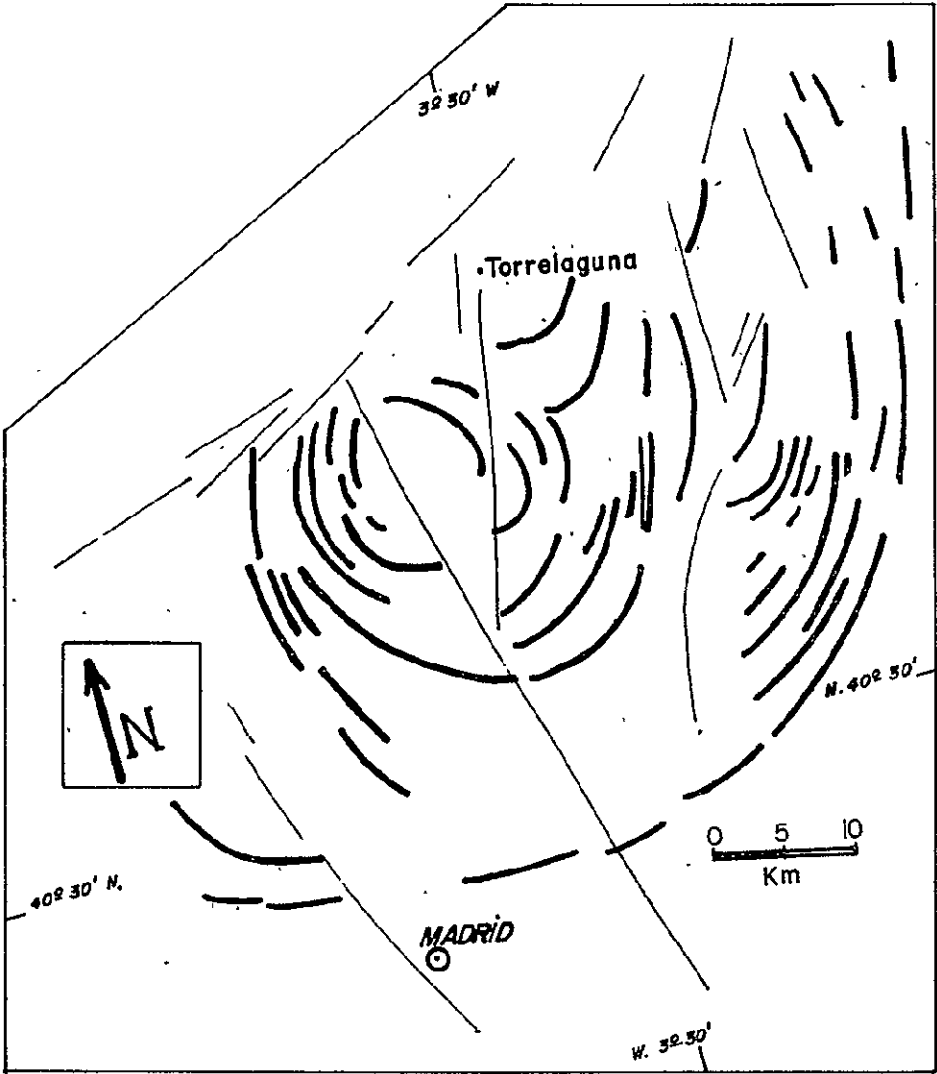
Figure 8

are assembled in 8 grades of intensities for the red and green,
and four grades for the blue. This assembly is made in such
a way that there are approximately the same number of pixels
in each. This condition is imposed for the maximization of
the information.

Some 40 combinations of band-ratios are examined at length,
on the grounds of this determinative.

For false color, we consider as best for the study of the
lithologies and linear structures, the following combinations
of ratios (MUÑOZ, 1976, a):

a) R 4   G 7   B 7/4 which are given

by the following coefficients:

R I'_1 $=$ I_4

G I'_{13} $=$ I_7

B $=$ I'_{14} $=$ $64\ I_7\ /\ (I_4 - 1)$

b) R_4 G 7/4   B 7

given by:

R I'_1 $=$ I_4

G I'_{14} $=$ $64\ I_7\ /\ (I_4 - 1)$

B I'_{13} $=$ I_7

4. INTERPRETATION AND DISCUSSION

The formation of the "Extremenian-Castillian Vault" probably
occurred during the Oligocene-Miocene (ALIA, 1976, a, b),
although in part it must have been influenced by more antique
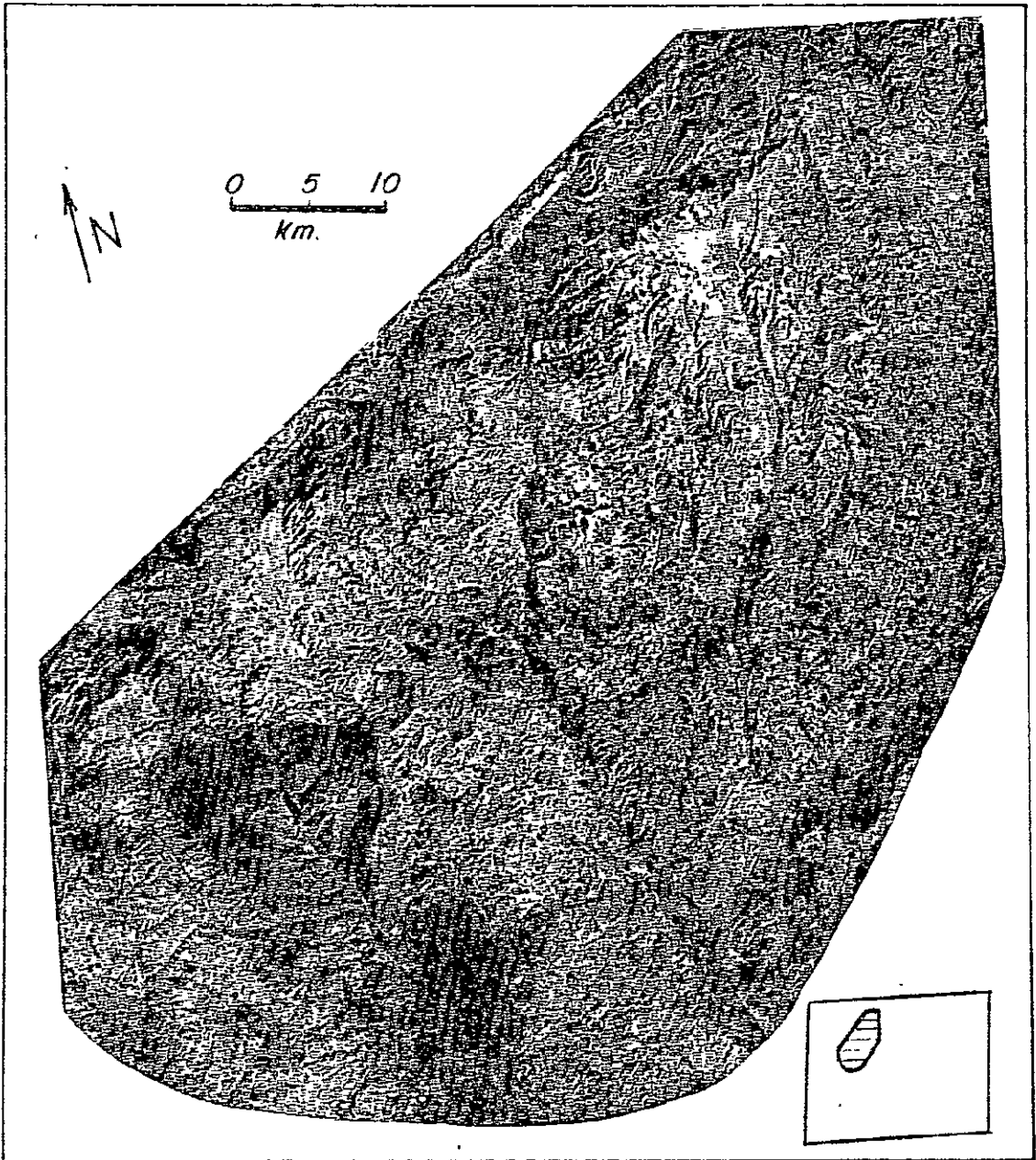structural directrices (Banda Estructural de Toledo, Dique-

Figure 9

and associated fracture of Alentejo-Plasencia, etc.)

During the Oligeocene-Miocene periods and after a generalized elevation phase, another of decompressed collapse followed, along the lengths of the blanks of this megastructure. This collapse would mainly affect the great septentrional unit which would thus be left fractioned in smaller units and blocks. These movements of decompression would individualize the large collateral terciary basins, and within them would, in turn, provoke other movements of blocks of a lesser order which, following lines of weakness parallel to them, would provoke variations of facies and thickness in the correlative sediments, which were then deposited there. Furthermore, the differential movements seem to have kept on up to most recent times, as is deduced for example by the adaption and assymetric morphology which is presented by many of the fluvial courses which are adjusted to the parallel lines to said Vault.

The determination of the "Extremenian-Castillian Vault" by means of the LANDSAT images, also seems to find support in the results obtained in 1966 by the Hawaii Institute of Geophysics, whose map of Anolamies of Bouguer of the Iberian Peninsula is partially reproduced in figure 14. As can be seen by comparing this figure with figure 1, some of the isoano- malies of this map closely correspond to the structures defined in the "Extremenian-Castillian Vault" and the "Banda Estructural de Toledo", and we also observe a greater complexity and irregularity in the distribution of the isoanomalies for the septentrional half of the Vault; on the contrary, in the meridional half, in the LANDSAT images as well as in the map of anomalies of Bouguer, there is less accidentation. These facts and correlations can be interpreted as a consequence of the differential movements continuing up to present times.

Figure 10

The geographical amplitude covered by the megastructure
"Extremenian-Castillian Vault" (its greatest axis is more
than 250 km. long) permits us to suppose that the originating
cause must have affected profoundly not only the continental
crust but also the underlying mantle (ALIA, 1976, a, pag. 236).
It is thus a phenomenon on a lithospheric scale in which we
can hypothetically find two solutions; 1) The lithosphere
submitted to compression forces becomes so deformed that
it becomes vaulted, and then has a passive behavior with the
covering. 2) The mantle is that which vertically pushes the
superincombent lithosphere producing the vaulting.

In the first case the horizontal pushes would possibly come
from the meridional regions of the Béticas, whose greater
structures are at long range, parallel to the greatest axis
of the Vault.

In the second case it could be admitted that the activation
in the mantle of a "plumes" or similar type, could be related
to the generating mechanism of this megastructure.

These ideas on the possible generating mechanisms of the
"Extremenian-Castillian Vault" are on the other hand congruent
with the results obtained in the most localized investigations
made in these regions.

In effect, with the tectonic model explained above, the origin
of an annular structure with concentric rings of dimensions
of 30-40 kms., as in the case of the "Halo Estructural de Gua-
dalix" (MARTIN ESCORZA), 1976, c) could well correspond with
the final sinking phase, by decompression, admitted for the
"Extremenian-Castillian Vault", mainly in its septentrional
half. The fact that the annular alineations of the Halo have
so much effect on the metamorphic rocks of the Cerro de San
Pedro, which belong to the hercinian basement of the Central
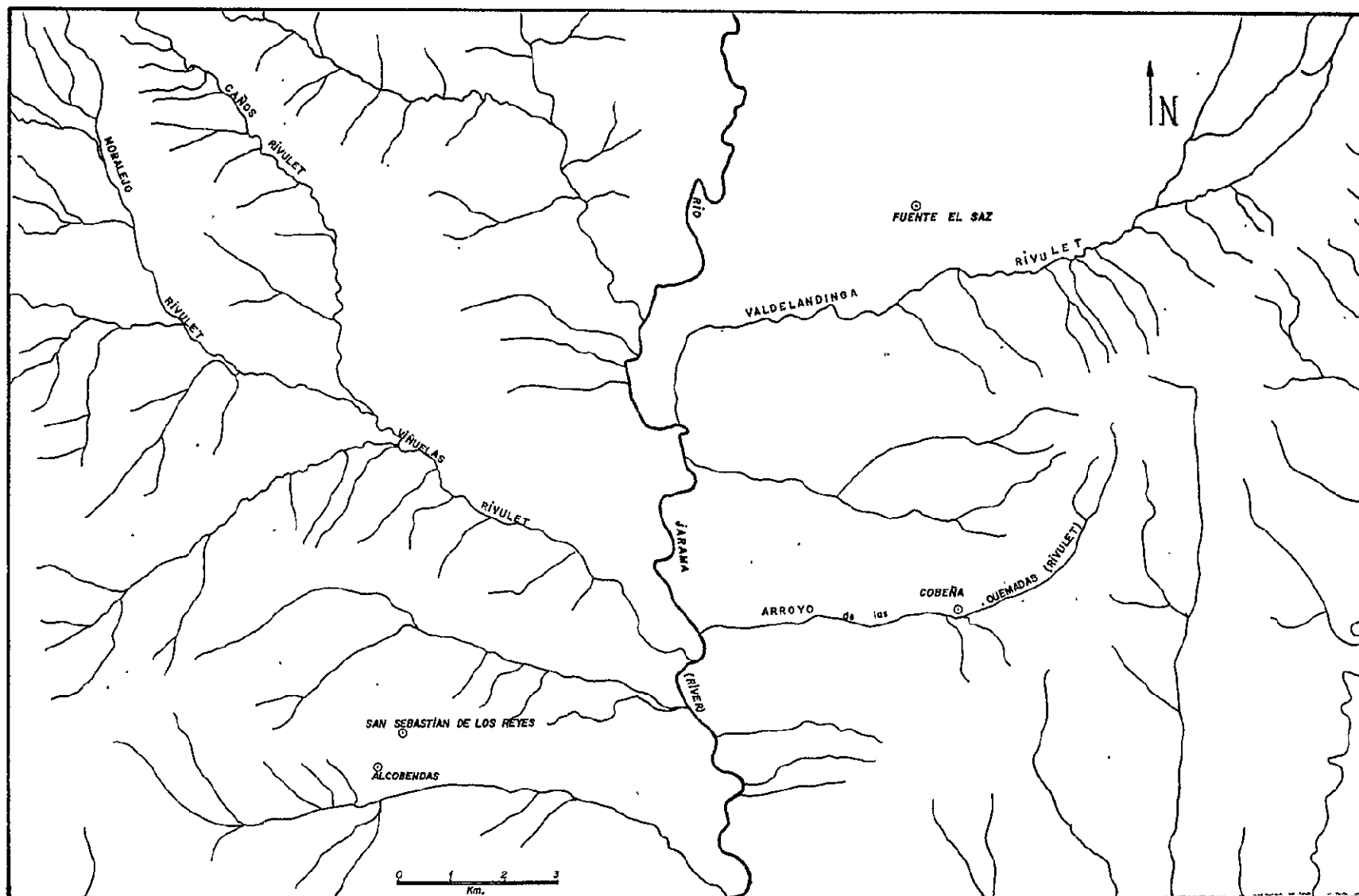System, as well as to the northern zone of Madrid which is

Figure 11

already covered by Neogene sediments and where, furthermore,
by geophysical methods a sedimentary sub-basin has been
discovered (GARCIA SEÑERIZ, J., 1941; CADAVID, S., 1973), with
a greater thickness of neogene deposits (MARTIN ESCORZA, 1976,
b) permits us to relate this sinking of the "Halo Estructural
de Guadalix" with the general collapse of the "Extremenian-
Castillian Vault".

The generating mechanism of this structure could be conceptually
similar to those phenomena which are caused by decompression,
immediately after a subterranean nuclear explosion, which
provokes a crater with concentric circular structures (in BOLT,
1976, fig. 3.3).

As we have already said, the "Halo Extructural de Guadalix" is
not a complete concentric ring (figure 8), but rather almost
half of its septentrional part is cut off by the NE-SW fracture
which limits the meridional edge of the Central System. We
believe that this could be due, or in the case of approximate
contemporaneity of both processes, to the greater fracture
NE-SW absorbing the stresses and would make the penetration
toward the Northwest of the concentric structures of the Halo
more difficult. Or in the case in which it had moved before
as an inverse robble (BENAYAS, et al., 1960; SAN MIGUEL et al.,
1956; MARTIN ESCORZA, 1976, c) cut off in some way the annular
structure leaving only its meridional part visible.

Either way, the complete significance and the total circumstances
which motivated the existence of the "Halo Estructural de Gua-
dalix" must be cleared up more profoundly since, in effect,
the probable sinking which originated them, could have used
or have been favored by pre-existing posthercinian structures.
On the other hand, the present incipient development of the
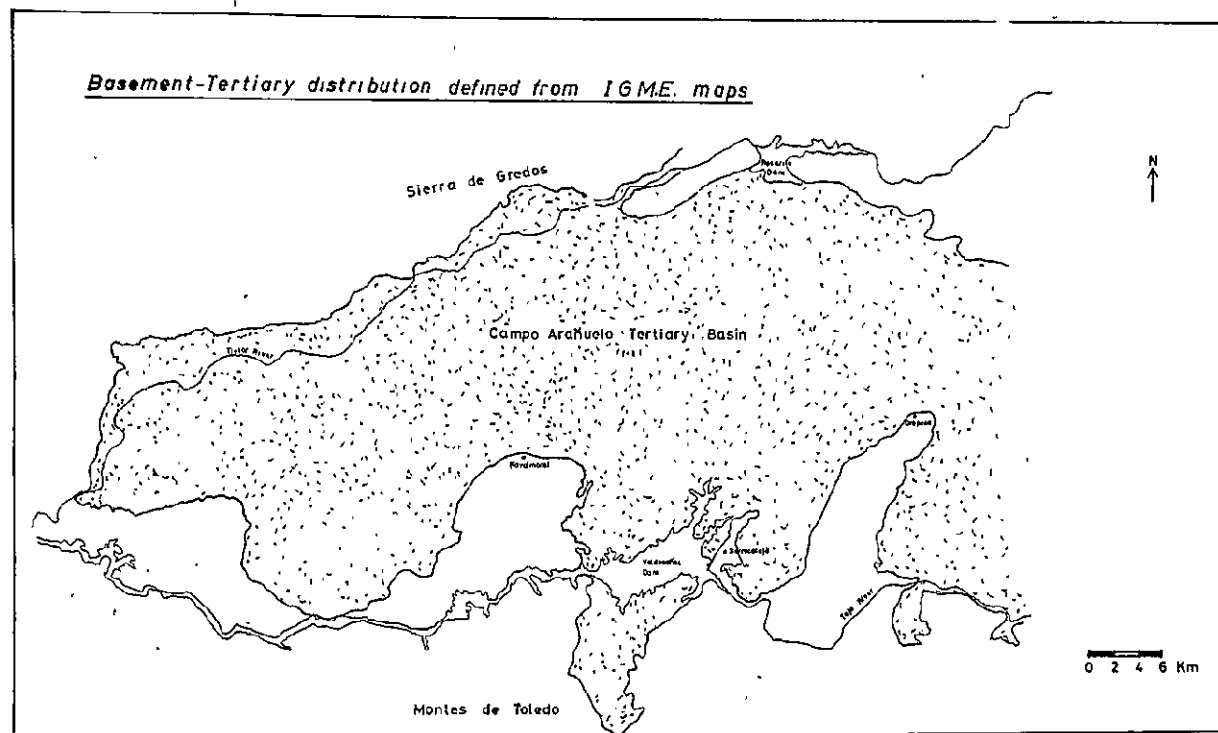fluvial network on the neogene sediments, in accordance with

Figure 12

the e concentric alineations (see figure 10, 11) allows the
log cal supposition taht said Halo remains active in some way
at he present time.

Und ubtedly everything makes us suppose that this structure,
which in its maximum radius reaches the capital of Madrid
affecting a great area in industrial and social expansion,
can have a special significance in the field of construction
as well as in the search for hydric and mining resources.

In figures 5 and 6 all the acknowledged fractures have been
positioned, among which are some which correspond to or have
been activated during the formation of the "Extremenian
Cast llian Vault", and others which, being older, have neverthe-
less not entered into play in this megastructure.

Thus, the NE-SW fractures, whose main alineations are the
Dique of Alentejo-Plasencia and the robble which meridionally
limits the Central System, corresponds to tardi-hercinian
time (PARGA, 1969) and belong to a system of sinistral wrench
faul s (ARTHAUD and MATTE, 1975), in the mentioned NE-SW
dire tion. In the LANDSAT images, they are easily recognizable
for heir folded formations made up of quartz from the lower
Ordovician period (figure 5).

In the case of the fault line associated with the Dique de
Alentejo-Plasencia, the net movement suffered by this formation
of ordovician quartz from one to the other side of the fualt
is 4-7 kms., and even considering the effect of the arching,
this value can be really established as some 23 kms. (UBANELL,
1976).

Another great accident with this same direction is represented
by the meridional edge of the Central System. During thardi-
herci ian times it acted as a dextral wrench fault in a first
stage, and later as a sinistral. It has moved, as we have said

CUENCA DE CAMPO ARAÑUELO

lineaments and Basement-Tertiary distribution as interpreted from the Landsat-1 imagery

E 2170
1! Jul 75
MSS 5

Figure 13

.... Basement - Tertiary contact

——— Fractures and faults

Tajo (with Valdecañas dam) and
Tietar rivers are represented

0   5   10   15   Km

197
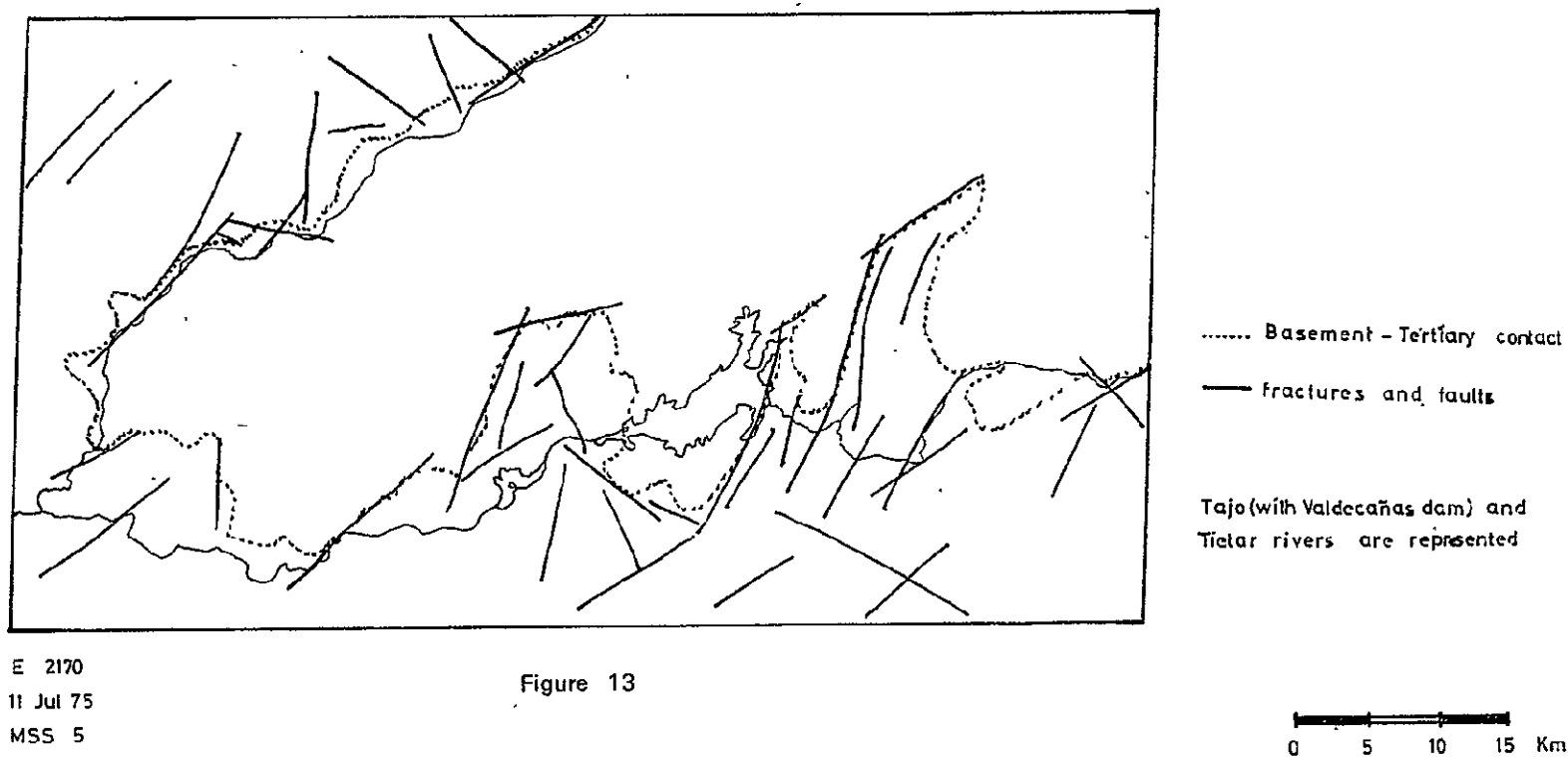
during the Alpine cycle, in accordance with an inverse fault, on top of Miocenean sediments. Finally, movements have been detected during the Quaternary which produced deposits of terraces and variations in the fluvial network (PEDRAZA, 1976)

The NW-SE fractures make up a combined system with the above mentioned NE-SW direction, although they are not as developed.

The sinistral movement of the NE-SW faults provoke phenomena of tension in N-NE, which are frequently taken advantage of by quartz fillings, following numerous but not very long dikes.

The E-W direction alineations should be attributed to the penetration in the Central System of fractures which form part of the tectonic unit known as the "Banda Estructural de Toledo" (ALIA, 1972); and the N-S directions are of special interest since they continue and penetrate into the areas occupied by the sedimentary deposits of the Duero Basin (figure 6).

5. CONCLUSIONS

Making use of the images proportioned by LANDSAT, we have been able to determine:

- A lithospheric megastructure with NE-SW direction of more
  than 350 km. long in its major axis, the "Extremenian-
  Castillian Vault", defined by important structural alineations
  on its flanks and in which it is possible to differentiate
  a large more accidented and complex septentrional area, from
  a meridional area with less structures; both areas are
  delimited by alineations with E-W direction belonging to the
  "Banda Estructural de Toledo".
- We must suppose that the origin of the Extremenian-Castillian

Figure 14

Vault is due, because of its scale, to processes of lithospheric scale, with movements produced by fields of vertical or horizontal stress, but that, in any case, provoked a first stage of arching against gravity, with a later relaxation and differential sinking, in large blocks, during the Oligocenian-Miocenean period.

- Perhaps related to that second stage of generalized decompression of the Extremenian-Castillian Vault, we should inject the process which gave way, in the septentional area of said Vault, to the "halo Estructural de Guadalix" of more reduced dimensions (40 km. of maximum radius).

- The fayed Hercinian Basement of the Central System, is affected by numerous alineations of different sizes among which can be differentiated those which originated in tardi-hercinian periods, from those which originated during the Alpine cycle.

- The attestation in a reduced area in which were found many of the geological characteristics mentioned above has permitted establishing that the best combinations of ratios for the study of lithologies and linear structures in these areas is (MUÑOZ, 1976, a):

R 4   G 7   B 7/4

and

R 4   G 7/4   B 7

Figure 1.- Main defining structural alineations of the "Extremenian-Castillian Vault" which appears practically divided in two by the E-W alineations of the "Banda Estructural de Toledo". In white: main zones of the hercinian basement related to the Vault. The broken lines represent probable structural alineations which are more peripheral.

M = Madrid; TO = Toledo; SA = Salamanca; AV = Avila; SG = Segovia; ZA = Zamora; VA = Valladolid; SO = Soria; GU = Guadalajara; CR = Ciudad Real; CC = Caceres; BA = Badajoz; D.P. = Dique de Plasencia; Ci = Cijara; (according to ALIA, 1976 a, b).

In the upper box we have marked the area covered by this figure on the Iberian Peninsula.

Figure 2.- Image E-1228-10325-7 taken by LANDSAT-1 in March 1973 on the central zone of the Iberian Peninsula. M = Madrid; SA = Salamanca; AV = Avila; SG = Segovia; TO = Toledo. The white areas correspond with the areas of snow in the Mountains of Gredos and Guadarrama.

Figure 3.- Diagrammed representation of some of the visible structures in the figure 2 and which define the septentrional part of the "Extremenian-Castillian Vault". In white: zones of the flayed hercinian basement; in white: covered zones. The thickly drawn lines with an E-W orientation correspond to the so called "Banda Estructural de Toledo". ALIA (1972) (According to ALIA, 1976 a, b) M = Madrid, AV = Avila, TO = Toledo, SG = Segovia, SA = Salamanca. Furthermore: Depresión del Duero= Duero Basin; Depresion del Tajo = Tajo Basin, Meseta Toledana= Meseta of Toledo.

Figure 4.- Mosaic of the LANDSAT images E-1228-10325, E-1229-
10384 and E-1227-10271, on the central parts of the Iberian
Peninsula. M = Madrid, SA = Salamanca.

Figure 5.- Observable alineations in the unit of the hercinian
flayed basement which constitutes the Central System.

Figure 6.- Detailed diagram of the alineations which are visible
on the Hercinian basement of the Central System from E-2170-
10204-7 obtained by LANDSAT-2 in July, 1975. (According to
UBANELL, 1976).

Figure 7.- Geological sketch of the area where the concentric
annular structure named "Halo Estructural de Guadalix" in
inserted (MARTIN ESCORZA, 1976, c). The geological data offered
here have been collected from: APARICIO et al, 1975; APARICIO
et al, 1973; BABIN VICH, 1971; DE LA CONCHA, 1962, 1963; FEBREL
et al, 1958; FUSTER and FEBREL, 1959; HERNANDEZ-PACHECO, F.,
1965; MARTIN ESCORZA, 1976, b.

Figure 8.- Structural lines obtained from the observation of
the zone represented in figure 9, and which define an annular
structural complex of concentric lines which has been named
"Halo Estructural de Guadalix" (according to: MARTIN ESCORZA,
1976, c).

Figure 9.- Section of NASA image E-2367-10122-7 which has been
studied and whose situation in said image is expressed in the
small figure of the lower right hand side.

Figure 10.- Fluvial network of the zone occupied by the section
of figure 9. This fluvial network has been obtained from a
topographical map at scale 1:100.000. As can be observed,

the secondary and terciary networks are those which in some
cases are defining curved alineations, corresponding to the
"Halo Estructural de Guadalix". (According to MARTIN ESCORZA,
1976, c).

Figure 11.- With much greater clarity, the secondary fluvial
network obtained in this case from a map at scale 1:50.000,
which unmistakeably indicates to us in close areas and to the
North of Madrid, the curved structures which define the "Halo
Estructural de Guadalix". (According to MARTIN ESCORZA, 1976,c).

Figure 12.- Tertiary sub-basin of Campo Arañuelo, located 250
kms. West of Madrid.

Figure 13.- Meridional limit of the Campo Arañuelo Tertiary
sub-basin.

Figure 14.- Central Zone of the Map of Anomalies of Bouguer
for the Iberian Peninsula, done by the Hawaii Institute of
Geophysics, 1966. Curve interval = 13 miligals. The same
symbols for the capitals as in the above figures and also
CU = Cuenca.

6. REFERENCES

Alia, M. (1960) "Sobre la tectónica profunda de la Fosa del
Tajo". Notas y Comunicaciónes I.G.M.E., 58, 125-162.

Alia, M. (1972) "Evolution post-hercynienne dans les regions
centrales de la Meseta espagnole". 24 th. Intern. Geol. Cong.
Sect. 3, 265-272.

Alía, M. (1976, a) "Localization of a great structure in Iberian plateau: The Estremenian-Castillian Vault". NASA Project núm. 28760, Second Quarterly Report, 6-9

Alía, M. (1976, b) "Una megaestructura de la Meseta Ibérica: La Bóveda Castellano-Extremeña". Estudios Geol. 32, 229-238.

Alía, M.; Portero, J.M.; Martin Escorza, C. "Evolución geotectónica de la región de Ocaña (Toledo) durante el Neógeno y Cuaternario". Bol. R. Soc. Española Hist. Nat., 71, 9-20.

Aparicio, A.; Casquet, C.; Barrera, J.L. (1973) "Petrogénesis del stock granítico tardi-hercínico de Rascafria-El Paular (Sistema Central español)". Estudios Geológicos, 29, 479-487.

Aparicio, A.; Barrera, J.L.; Caraballo, J.M.; Peinado, M.; Tinao, J.M. (1975) "Los materiales graníticos Hercínicos del Sistema Central español" Mem. I.G.M.E. 85, 145 pags.

Arthaud, F.; Matte, Ph. (1975) "Les decrochements tardi-Hercyniens du Sud-Ouest de l'Europe. Geometrie et essai de reconstitution des conditions de la deformation" Tectonophysics, 25, 139-171

Babin Vich, R. (1971) "Estudio meso y microtectónico del macizo metamórfico de El Vellón". Bol. R. Soc. Española Hist. Nat. (Geol), 69, 5-27.

Banayas, J.; Perez Mateos, J.; Riba, O. (1960) "Asociación de minerales detríticos en los sedimentos de la Cuenca del Tajo". Anal. Edaf. 19, 635-670.

Bischoff, L. (1975) "Das Störungsmuster Zentralspaniens nach Auswerfungen von ERTS-1 Auferahmen". Münster. Forsch. Geol. Paläont. H. 36, 69-79.

Bolt, B.A. (1976) "Nuclear Explosions and Earthquakes". Freeman & Co. San Francisco, 309 pags.

Cadavid, S.; Hernández Fernández, Mª E. (1967) "Estudio magnetométrico del basamento de la Hoja 583, Arganda". Estudios Geológicos, 23, 263-274.

Cadavid, S. (1973) "Estudio geofísico del basamento en la Depresión meridional de la Sierra del Guadarrama". Tesis Doctoral. Facultad Ciencias Geológicas. Universidad Complutense de Madrid.

De la Concha, S. (1962) "Mapa Geológico de España, E. 1:50.000, Hoja núm. 485, Valdepeñas de la Sierra". I.G.M.E.

De la Concha, S. (1963) "Mapa Geológico de España, E. 1:50.000, Hoja núm. 486, Jadraque". I.G.M.E.

Febrel, T.; Fuster, J.M.; De Pedro, (1958) "Mapa Geológico de España, E. 1:50.000, Hoja núm. 484, Buitrago del Lozoya". I.G.M.E.

Fuster, J.M.; Febrel, T. (1959) "Mapa Geológico de España, E. 1:50.000, Torrelaguna". I.G.M.E.

Garcia de Figuerola, L.C. (1963) "El dique diabásico del Norte de Extremadura". Notas y Comunicaciones I.G.M.E., 69, 43-78.

Garcia de Figuerola, L.C. (1965)"La continuación hacia el SW del dique básico de Plasencia (Cáceres)". Notas y Comunicaciones I.G.M.E., 77.

Garcia de Figuerola, L.C.; Corretge, L.G.; Bea, F. (1974) "El dique Alentejo-Plasencia y haces de diques básicos de Extremadura". Boletin Geológico y Minero, 85, 308-337.

García Siñeriz, J. (1941) "Investigación sísmica en El Pardo
(Madrid)". Mem. I.G.M.E., T, 2, 503-547.

Hernández-Pacheco, F. (1965) "La formación de la raña al S. de
Somosierra occidental". Bol. R. Soc. Española Hist. Nat. (Geol),
63, 5-16.

López de Lemos, G. (1975) "La observación de España con sensores
remotos desde el Espacio". Instituto Geográfico y Catastral, 97
pags. Madrid.

Martín Escorza, C. (1976, a) "Un ejemplo de la actividad tectó
nica durante el Mioceno del basamento fracturado de la Fosa del
Tajo". Bol. R. Soc. Española Hist. Nat. (En Prensa)

Martín Escorza, C. (1976, b) "Actividad tectónica durante el Mio
ceno de las fracturas del Basamento de la Fosa del Tajo". Estu-
dios Geológicos, 32, (En Prensa).

Martín Escorza, C. (1976, c) " An Anular structural complex North
of Madrid detected by LANDSAT images". NASA Project núm. 28760,
Third Quarterly Report, 30-44.

Martín Escorza, C.; Hernández Enrile, J.L. (1972) "Contribución
al conocimiento de la geología del Terciario continental de la
Fosa del Tajo". Bol. R. Soc. Española Hist. Nat. 70, 171-190.

Martín Escorza, C; Carbo, A.; Ubanell, A.G. (1973) "Contribu-
ción al conocimiento geológico del Terciario aflorante al N. de
Toledo". Bol. R. Soc. Española Hist. Nat. 71, 167-182.

Muñoz, L. (1976, a) "Possibilities of application of Band-Ratio
technique to the Geological Features of the western limit of the
Tajo Bassins". NASA Project núm. 28760, Second Quarterly Report.
10-20.

Muñoz, L. (1976, b) "Relación basamento-cobertura en un segmento del límite meridional de la Depresión de Campo Arañuelo-Fosa del Tajo Occidental". Tesis de Licenciatura. Facultad de Ciencias Geológicas. Universidad Complutense de Madrid.

Parga, J. R. (1969) "Spätvariszische Bruchsysteme im Hesperichen Massiv". Geol. Rdsch. 59, 1, 323-330.

Pedraza, J. (1976) "Algunos procesos morfogenéticos recientes en el valle del rio Alberche (Sistema Central Español): La Depresión de Aldea del Fresno-Almorox". Bol. Geol. Min. del I.G.M.E., 87, 1-12.

San Miguel, M.; Fuster, J.M.; De Pedro, F. (1956) "Mapa Geológico de España, E. 1:500.000, Hoja núm. 533, San Lorenzo de El Escorial". I.G.M.E.

Ubanell, A.G. (1976) "Fracture pattern in Central Iberian Peninsula from LANDSAT". NASA Project 28760. Second Quarterly Report. 20-23.

Ubanell, A.G. (1975) "Los diques aplíticos de Almorox-Navamorcuende (Sistema Central español) en relación con los "decrochements" destrales tardihercinicos". III Congreso del SW. Huelva-Beja, 1975 (en prensa).

Ugidos, J.M. (1974) "Granitos de dos micas y moscovíticos en la región de Piedrahita-Barco de Avila-Bejar" Studia Geologica, 7, 63-86.

G E O M O R P H O L O G Y

SOME GEOMORPHOLOGICAL ASPECTS OF LANDSAT-2 IMAGES OVER
CENTRAL WESTERN SPAIN.

J. J. Sanz Donaire

Department of Geography
Complutense University
of Madrid.
SPAIN.

G E O M O R P H O L O G Y

SOME GEOMORPHOLOGICAL ASPECTS OF LANDSAT-2 IMAGES OVER CENTRAL
WESTERN SPAIN.

By Juan José Sanz Donaire
Profesor de Geografía
Cátedra de Geografía
Facultad de Geografía e Historia
Universidad Complutense
Madrid.

In this paper is analyzed the geomorphological characteristic
of LANDSAT-2 imagery and, as an example, some photointerpre-
tation work is presented from images no. E-2333-10421, E-2171-
10262 and E-1229-10384 (figure 1).

It has been intended to view relief, taking adjacent images
with 10% overlap as stereoscopic pairs. As this is also
possible with consecutive images taking during a North-South
polar orbit overpassing the country, it can be established
that the necessary relief vision for geomorphological
interpretation can be obtained in 2/3 of the total surface
of an image. Thus, relief has been inferred. Date, hour and
sun angle are important points to consider for viewing an
image with a right relief ilusion.

Another technique possible for geomorphological interpretation
is looking South LANDSAT images from the upper side. That
way, an experienced eye can see relief. Logical thinking is
another aid for relief interpretation: water courses and
barrages (reservoirs) are located in depth; scarped valleys
have less water than open ones; isolated mountains present
a radial drainage pattern; plains may be seen by analyzing
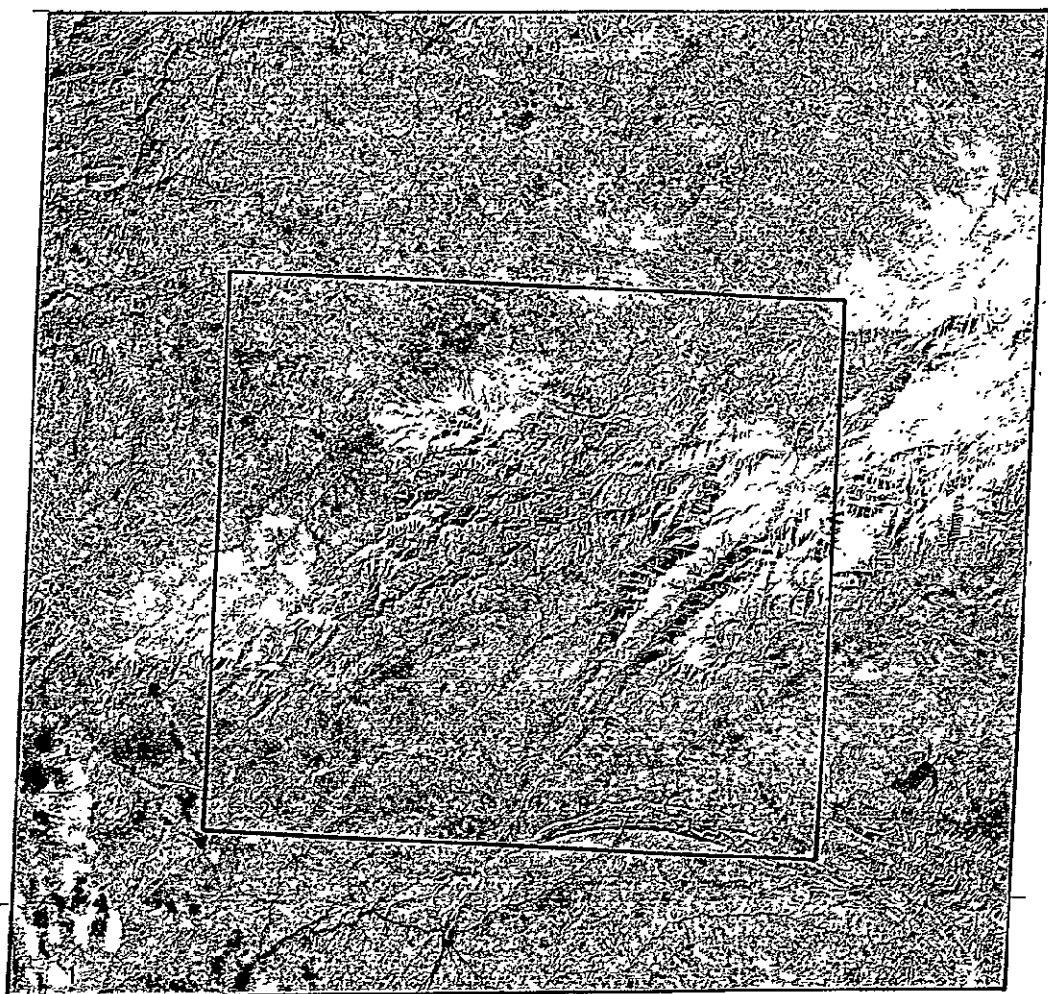
W007-001   W006-301   W006-001   N033-301   W005-301
21DEC75 C N48-25/W006-05 N N48-24/W006-02 MSS   7 R SUN EL20 AZ151 191-4639-A-1-N-D-1L NASA ERTS E-2333-10241-7 01

1 Area of study in Central-Western Spain

2 Bejar Corridor

Figure 1.—LANDSAT image E-2333-10421

land use (cereal cultivated dry land); forests and snow covered
zones, and very dissected land, identify highest mountains, etc.

Photointerpretation of LANDSAT image E-2333-10241, taken
December 21, 1975 shows the planation surface of Las Hurdes
as easely recognized. Morphostructural lines are also pointed
out, so, weakness lines which have depressed Bejar Corridor,
a voussoir between Sierra de Gredos and Las Hurdes, are the
most often appearing NE-SW faults. They follow the same direction
as the Jerte-Aravelle fault, and are responsable for the general
alignment of mountains in this area: Sierra de las Mesas, de
la Cachera, de Francia, are all block-mountains, elevated by
alpine efforts. Locally, the contact between high Tertiary
sediments of the Duero Basin and Paleozoic socle follows the
same orientation. Tectonic "graben" filled by Tertiary rocks
(Moraleja, Coria, Ambroz, Ciudad Rodrigo Basins) are good
examples. It would be interesting to research why "raña" type
sediments (polymyctic quartzitic gravel-red clay conglomerate
of pliocenic-villafranchian age) occupy the Ciudad Rodrigo -
Salamanca Basin.

In the surroundings of Jerte fault many different little
fractures were localized. Snow cover does not allow further
investigation. Long NW-SE lines are only visible on satellite
images, because conventional air photographs do not show them.
Wrench faults in NNW-SSE direction were also recognized. E-W
faults appear mostly in the southern part of image and belong
to the "so called" Structural Band of Toledo. This alignments
close some Miocene basins, so that alpine age is sure.

"Layer lines" are only visible when corresponding to quartzitic
serpentines and "hardlings" (inselberge).

Hydrographic network analysis is also possible in the images.
Encasement is visible as a shadowish company of water courses.

The estremenian and salmantinian peneplains are recognized by means of the superimposed rivers. Fanglomarats of "raña" type look like alluvial fans at the "bajadas" of endorheic basins of Southwestern USA. An arid climate did reign when raña formations were laid.

Bands 5 and 6 are best for the recognition of granitic batholith, like the Garrovillas one, which occupies the Central Southern edge of image. Bands 6 and 7 are best for geomorpho-logical exploring.

214 a

GEOLOGICAL APPROACH TO CENTRAL-WESTERN SPAIN

IMAGE ERTS-2333-10241-7
SCALE 1 : 866.000

DUERO

TORMES

S

CR

BA

P

C

TAJO

Talleres del INSTITUTO GEOGRAFICO Y CATASTRAL *J. J. Sanz Donaire*
Madrid, 1976
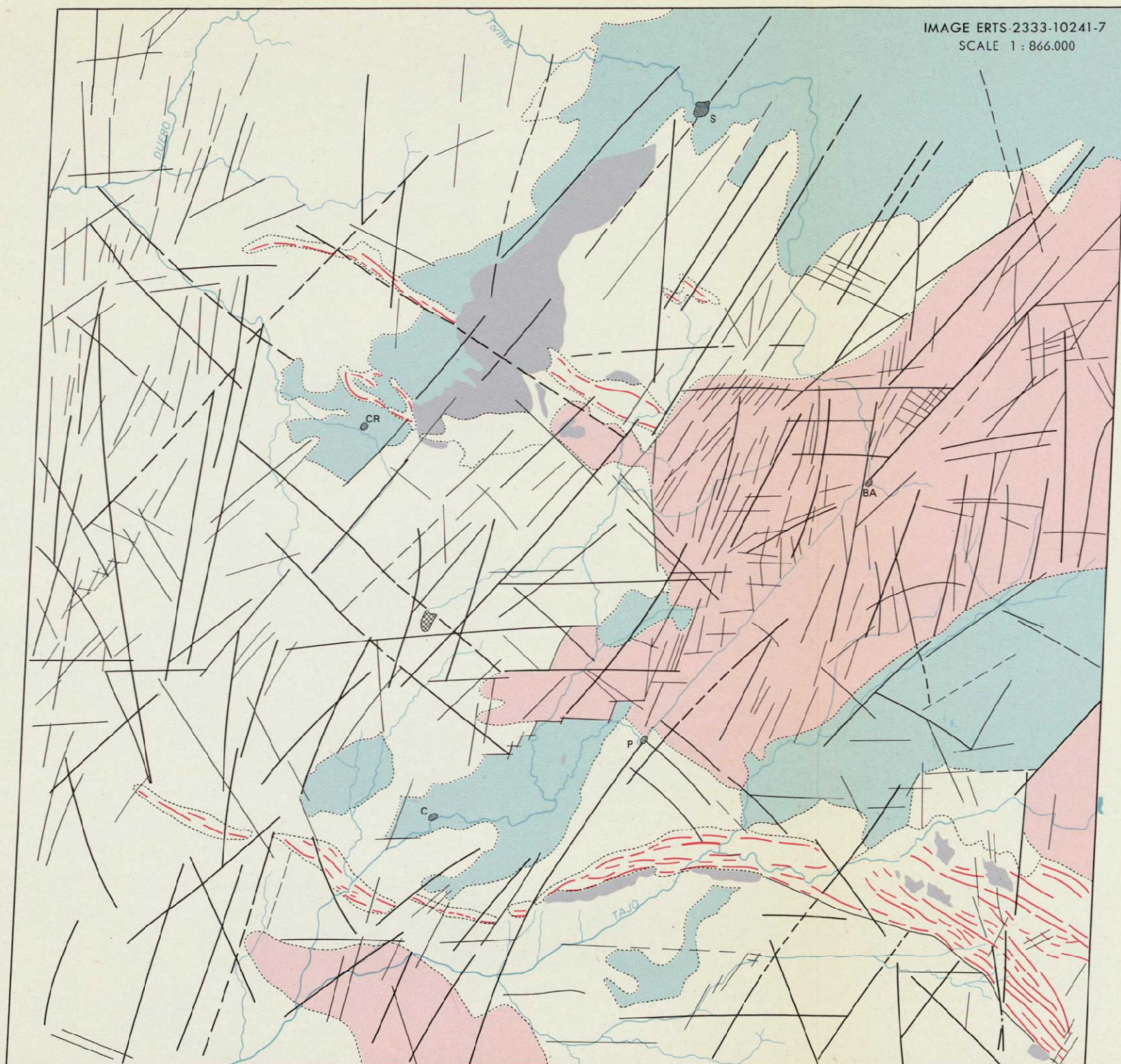
Mainly granitic rocks	Main rivers
Tertiary and quaternary rocks	Contact between geological formations
Quartzitic crests	Faults and weakness lines
Raña type sediments	Hurdes planation surface

S   Salamanca
BA Barco de Avila
CR Ciudad-Rodrigo
C   Coria
P   Plasencia

GEOMORPHOLOGICAL INTERPRETATION OF BEJAR CORRIDOR

IMAGE LANDSAT-1229-10384
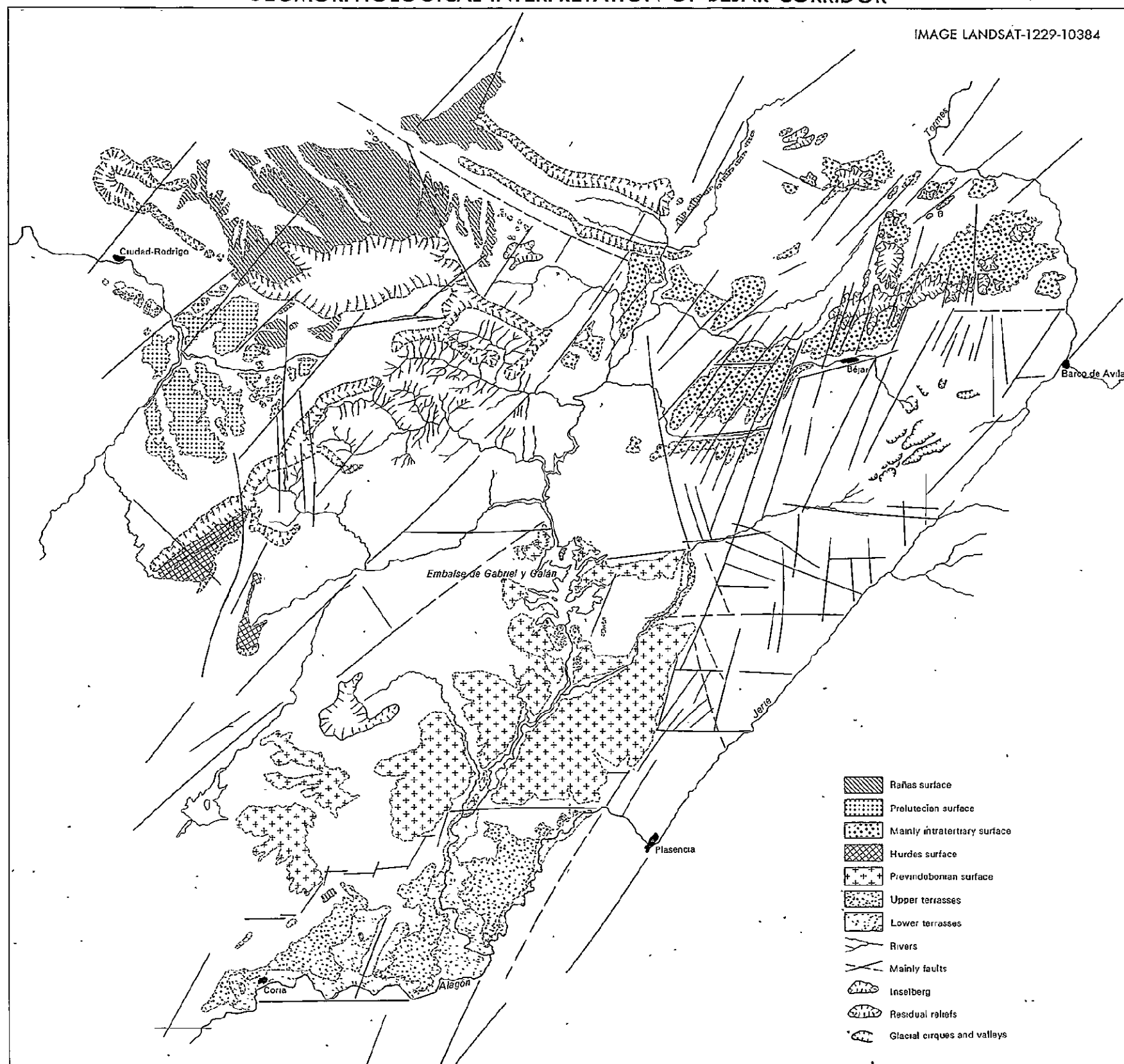
Legend	
	Rañas surface
	Prelutecien surface
	Mainly intratertiary surface
	Hurdes surface
	Previndobonian surface
	Upper terrasses
	Lower terrasses
	Rivers
	Mainly faults
	Inselberg
	Residual reliefs
	Glacial cirques and valleys

Talleres del INSTITUTO GEOGRAFICO Y CATASTRAL

J J Sanz Donaire
Madrid, 1976

216

L A N D   U S E

.

APPLICATION OF LANDSAT-2 DATA TO LAND USE MAPPING IN CENTRAL SPAIN.

Dr. Elena Chicharro Fernández

National University of
Education at Distance
Madrid.
SPAIN.

LAND USE

APPLICATION OF LANDSAT-2 DATA TO LAND USE MAPPING IN CENTRAL
SPAIN.

By Dr. Elena Chicharro Fernández
Universidad Nacional de
Educación a Distancia
Madrid.

1. INTRODUCTION

Two land use maps of an area convering the province of Madrid,
(around 8.000 km^2) have been designed from LANDSAT images. Map
1 has been set up after analysis of black and white photographs
(scale 1:500.000), but map 2 is a result of recording false
color images (scale 1:250.000). Different transparencias (scale
1:1.000.000) of the province of Madrid, have been also taken
into account. Analytic phase has been made with photographs
at scale 1:500.000 and 1:250.000. Images at 1:500.000 were taken
on July 10, 1975; July 11, 1975; July 28, 1975; July 29, 1975;
September 2, 1975 and January 24, 1976, in bands 4, 5, 6 and 7.
While false color images from March, 8 and 9, 1973 (scale
1:250.000) were only available to be used.

Analysis and interpretation were aided by light tables stereos-
copes and magnifying glasses. Conventional airphotographs 1956
(scale around 1:33.000) and 1972 (scale 1:15.000) have also
been observed, and land use mapping of a 2.000 km^2 area, North
of Madrid, was also discussed (Second Quarterly Report).

2. METHODOLOGY

First step was the election of a pilot zone from which it was
possible to have, on one hand, satellite images and, on the other,

important and complementary information. The elected region lies over a surface of 2.000 km^2. Appearence of the highest number of significant land use units was imagined in it. This idea was soon verified (figure 1).

From satellite images, conventional airphotographs, available land use maps and specially with the support of direct field observations, a key for land use was elaborated for analysing the land use in the whole province. The key was directly verified on the spot. With this verification, a great number of problmes were shown by LANDSAT. These problems will be analized later on.

Once with the key and in spite of the photointerpretative difficulties, we proceeded to analyze the rest of the territory confronting different forms of land use appeared, with those ready examined in the pilot area. Finally a later verification was made along chosen ways through the province to confirm the problems shown in the previous inform, and to evaluate the images from LANDSAT in the analysis of land use.

After comparing the black and white photographs, it is considered that for detection of the green cover and culture, bands 4 and 5 give better resolution to the images, and band 5 is the one from which the best results were obtained. Map number 1 has been elaborated form their photointerpretation. Bands 6 and 7 are not ready prepared for our purposes. This is the reason why they have not been used in this work, as the lithological units, tectonic lines and fluvial currents are more clearly shown in spite of their interesting and important notes and observations.

Figure 1.—Selected pilot area for land use classification of Madrid province

3. RESULTS

In a country like Spain, where present land use forms are result of the influence of favorable and adverse conditions of surrondings, and of the modifications suffered through the history, to analyze satellite images is difficult, because for a detailed study is needed the scale 1:50.000 or 1:25.000.

Therefore, these complex reasons do not advise LANDSAT images as the only document to elaborate thematic cartography, since there might be notable errors. It can be pointed out, however, that if auxiliary methods are used, as it was verified in the pilot area 2.000 km^2 analysed; the errors can be reduced to the minimum, while they are alarmingly increasing in the areas photointerpreted by means of selection and comparison.

The images of the satellite have been a very useful way to elaborate quickly maps of land use of provincial and regional groups; much more time would be required with conventional methods to elaborate the synthesis of a province or region. The great quantity of information gathered by the photographs of the satellite is a very important fact when it has to be interpreted the thematic map of land use, as this allows to establish important correlations of the land use with other geographic aspects (forms of relief, structural lines, lithology, etc.). On the other hand, as large stretches of land are shown on each photograph they permit to reach the study of regional geographic groups. On the LANDSAT images of central region, in black and white as well as in colour, it can be distinguished clearly, and with a highly trustworthy index, the following group of land use units:

- Coniferae forest
- Perennial leaf forests (evergreen-oak grove, plantations of juniper trees).

- Dry cereals farming
- Intensive watering
- Big nucleus of population
- Dams

The false colour images of the area at 1:250.000 scale, offer
more possibilities than the black and white ones, in the
detection of medium and small nucleus of population, as well
as in the identification of communications; while it gives
imprecisions in some types of forest limits in relation with
the black and white photogram.

4. ANALYSIS OF THE GENERAL PROBLEM

The problems come from various types of facts; one of the most
important is that the characteristic photographic images, in
false colour, as well as in black and white, obstructs the
stereoscopic sight, except for a small sector, and this makes
impossible to appreciate relief, which has a great influence
in detecting unities of uncertain use. In the same way, the
structure shown by photographs makes difficult to get
satisfactory images on the enlargements made through magnifying
lenses.

The photographs also state problems at scales 1:500.000 and
1:250.000 , as it is impossible to show some of the ways
of using the land which conjugate their scarse superficial
extent with their high economical output, such as the intensive
local watering.

A very important fact in the interpretation of photographs is
the date when images have been taken in the analysis of land
use. On the images taken between July and September, the

contrasts are better defined, whilst in January and March
the tonalities are in general blurred, and this makes the
analytic work enormously difficult, as the Atlantic forests
tend to get mixed with bushed and pasture grounds fenced-in
by trees, and the little intensively irrigated lands get
similar to some dry·lands.

Bush-trees growing (oliveyard an vineyard) are the ways of
land use impossible to recognise, on the black and white
photographs at scale 1:500.000 as well as on the false·colour
ones at scale 1:250.000, because they appear as small parcels
and formations of various kinds.

Bushed can be easily mistaken with atlantic forest, with
pasture lands fenced-in and with some of the uncultivated
lands.

Non-fenced meadows can have tonalities similar to some of the
uncultivated lands. In the same way, it is impossible to
separate species inside each formation, in the coniferae as
well as in the other types of forest; however, under certain
conditions the recently refforested masses, can be distinguished
provided they occupy a considerable surficial extent.

Little intensively irrigated lands are detected if the date
when the photograph has been taken is between July and
September.

REMOTE SENSING TECHNIQUES

REMOTE SENSING TECHNIQUES APPLIED IN A MULTISPECTRAL
SURVEY OF ARANJUEZ TEST SITE.

Germán Lemos (*), Javier Salinas (**) and Manuel Rebollo (***)

(*) Remote Sensing Laboratory
Geographic and Cadastral Institute.

(**) Service of Photogrammetry and
Photointerpretation
Polytechnic University of Madrid.

(***) IBM-Scientific Center
Autonomous University of Madrid.

REMOTE SENSING TECHNIQUES

REMOTE SENSING TECHNIQUES APPLIED IN A MULTISPECTRAL SURVEY OF
ARANJUEZ TEST SITE.

By Germán L.Lemos (*), Javier Salinas (**) and Manuel Rebollo (***)

1. OBJECTIVES

As part of this NASA supported project, the Remote Sensing
Laboratory of Instituto Geográfico y Catastral has participated
in a survey of Aranjuez test-site, with the purpose of obtaining,
by means of remote sensing techniques, basic data to work with
in a multidisciplinary approach. The pilot area of Aranjuez is
located South of Madrid (figure 1), and it has a rectangular
shape of 7 kms x 14 kms.

The survey was conducted at three different stages. In a first
stage, field works were done for acquisition of ground truth
in the pilot area, with the idea of correlating such information
to the data obtained, in a second stage, by means of an airborne
multispectral scanner and photographic cameras. In a third stage
it was analyzed the best existing LANDSAT information over the
area for the purpose of defining how it would correlate to the
data obtained during the aerial mission. The ground data and
the aerial information were obtained simultaneously, while
LANDSAT information available for analysis corresponded to an
image dated several months before the date of flight.

As intention of this operation it was defined the development
of methods and techniques for acquisition of data with remote

(*)   Laboratorio de Teledetección. Instituto Geográfico y Ca-
      tastral.

(**) Servicio de Fotogrametría y Fotointerpretación. Universi_
      dad Politécnica de Madrid.

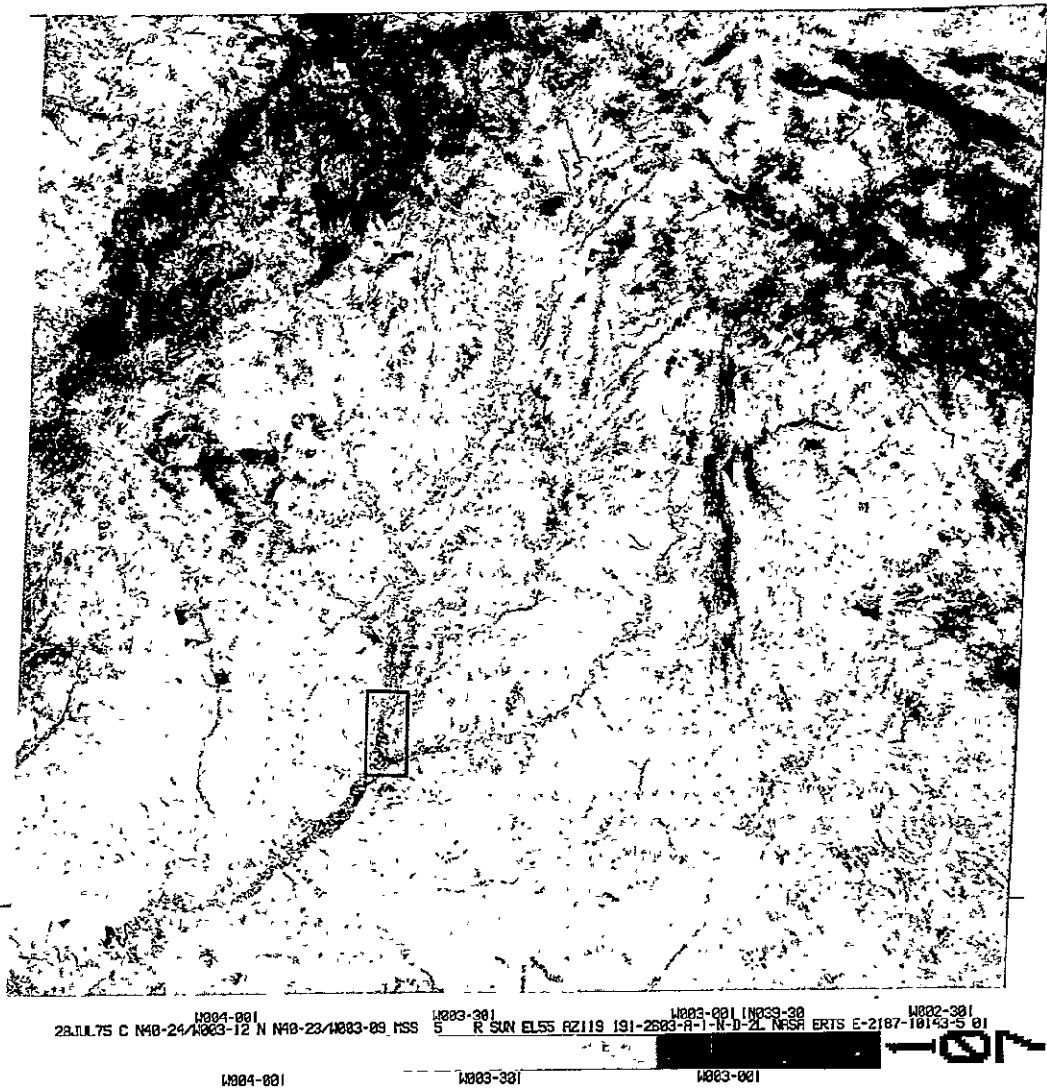(***) Centro de Investigación UAM-IBM. Universidad Autónoma de
      Madrid.

229

28JUL75 C N40-24/W003-12 N N40-23/W003-09 MSS 5 R SUN EL55 AZ119 191-2603-A-1-N-D-2L NASA ERTS E-2187-10143-5 01

Figure 1 —Pilot area of Aranjuez as it is seen in LANDSAT image

sensors, in a mode which was relatively new to spanish inves-
tigators. As secondary objective it was defined the analysis
and scientific application of the information in, several
disciplines. As part of this secondary objective,, it. was
intended the correlation of LANDSAT and airborne MSS data
over the test site. Figure 2 shows the topographic configuration
of the pilot area at approximate scale 1:50.000, with the
position of sites where local measurements have been done, and
the directions of flight. The aerial mission was conducted in
May 15, 1976 under good atmospheric conditions.

2. GROUND SEGMENT

The area of Aranjuez was chosen as test site for the following
reasons:

1 - it is included in the area of. Central Spain under study
for this NASA supported project, and both photographic
and digital LANDSAT data exist on it. Another important
reason for selecting such test site, which has to be taken
into account in a country like Spain, is that Aranjuez is
not subject to limitations in flight imposed by the militar
organizations, nor it is included in any commercial air
traffic corridor. Although LANDSAT satellites provide
digital data over any area of the country, freely
distributed all over the world, when planning a civil
aerial mission in Spain there are military restricted
areas which cannot be flown. Such situation was avoided
in the case of Aranjuez.

2 - the test site presents a land use very clearly defined, with
differentiation of urban areas, crops, bare soils and three
rivers. At the edges are located the city of Aranjuez and
the village of Titulcia, where some archeological deposits
have been found.
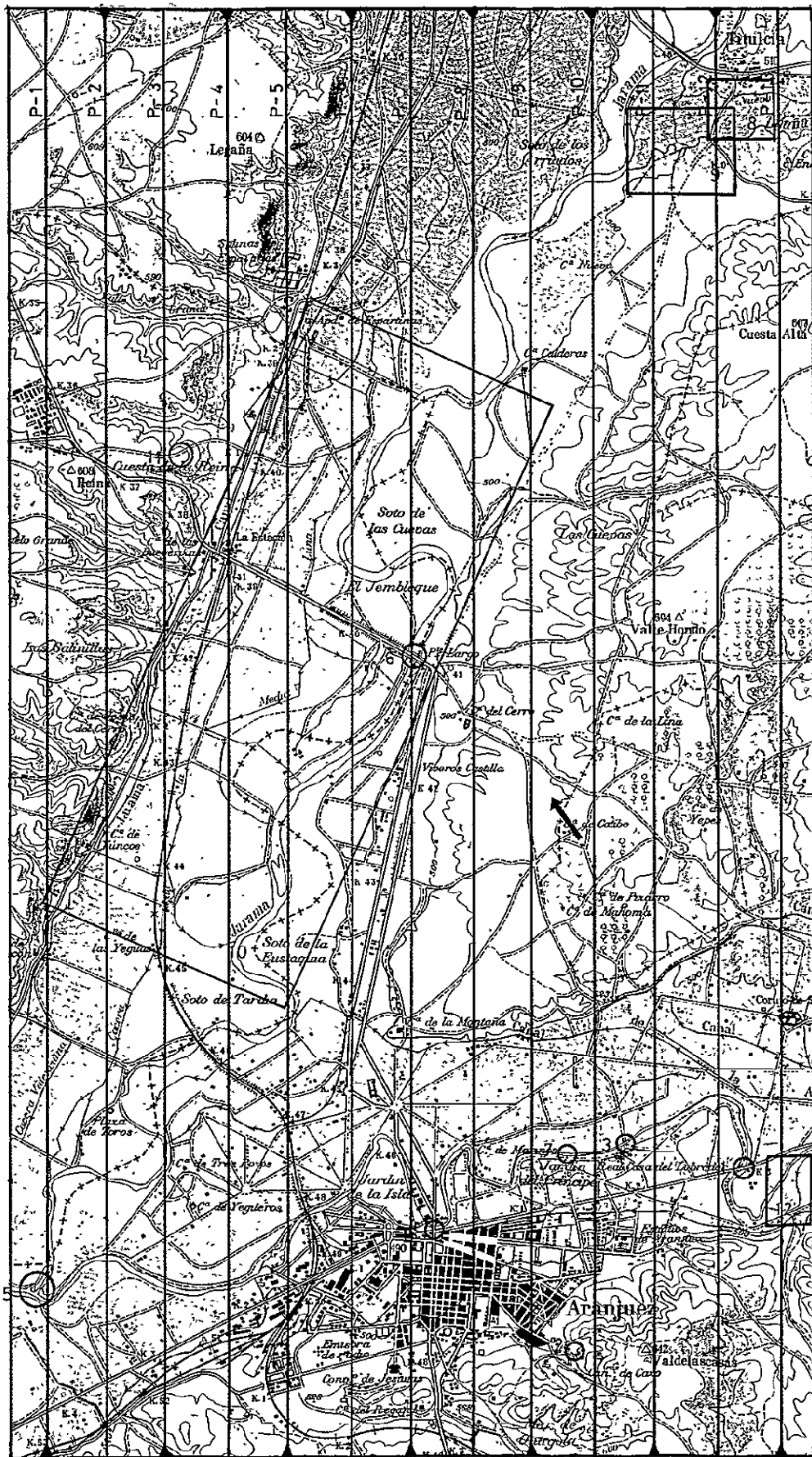
Figure 2.—Topographic map of Aranjuez pilot area with location of sites were ground truth was obtained

Parameter	Units	Tajo river		Jarama river	Confluence
		Site no. 1	Site no. 3	Site no. 6	Site no. 5
Turbidity	F.T.U.	8	8	110	84
Suspended solids	mg/l.	7	6	119	45
Dry residual	(110ºC) mg/l.	965	943	673	872
pH	——	7.35	7.40	7.05	7
Conductivity	(25ºC)	1260	1276	1050	1260
D.Q.O.	mg/l.O	22	18	146	126
Detergents A.B.S.	mg/l.	---	---	2.54	2.5
Chloride	mg/l. Cl^-	70.8	61.9	79.6	90.2
Sulfate	mg/l. $SO_4^=$	510	474	240	384
Carbonate	mg/l. $CO_3^=$	0	0	0	0
Bicarbonate	mg/l. CO_3H^-	158.6	158.6	219.6	176.9
Calcium	mg/l. Ca^{++}	172	172	96	156
Magnesium	mg/l. Mg^{++}	53.5	43.7	31.6	21.8
Sodium	mg/l. Na^+	60	54	71.2	80.4
Potassium	mg/l. K^+	2.1	2.2	14.7	9.6

Table 1.

3 - Tajo, Tajuña and Jarama rivers present in the pilot area a
very different physical pattern because their different
degree of pollution. From airborne MSS data it was expected
to differentiate the pure waters of Tajo and Tajuña rivers
and the polluted flow of Jarama, which receives on its upper
course the detritus of a large city like Madrid, 3 million
inhabitants.

4 - at the irrigation lands along Jarama, Tajo and Tajuña rivers,
an analysis of phenological states of crops could be possible
if the area flown at low altitudes, being interesting to
find out differences in the reflectance of cereals, olive-
groves and bare soils of gypsum.

Aranjuez offered good conditions for flight at low altitude,
with a maximum spot height of 642 m in Valdelascasas vertex.
Furthermore, a rapid access by highway is guaranteed from Madrid
in 45 minutes, and the transportation network into the pilot
area is in good conditions. The terrain is formed by gypsums,
silty loams and lacustrine limestones. As vegetation, broad
areas are cultivated along the irrigated lands of Jarama, Tajo
and Tajuña rivers, while the rest of the zone has olive-groves
or bare soils. In figure 3 it is presented a panoramic view of
the test site with the city of Aranjuez in firt term.

As part of the ground survey it was done photointerpretation
work by experienced personnel of Instituto Nacional de Investi
gaciones Agrarias in sites no.10 and 12, mainly focused to the
identification of different types of crops. Also, around the
city of Titulcia black and white infrared images were taken
for the purpose of identifying archeological sites (number 8
in figure 2).

Multiband photography was also tested during the day of flight
in sites no.1, 2 and 11 (figure 2), with Minolta cameras and

Figure 3.—Panoramic view of the pilot area with the city of Aranjuez in first term
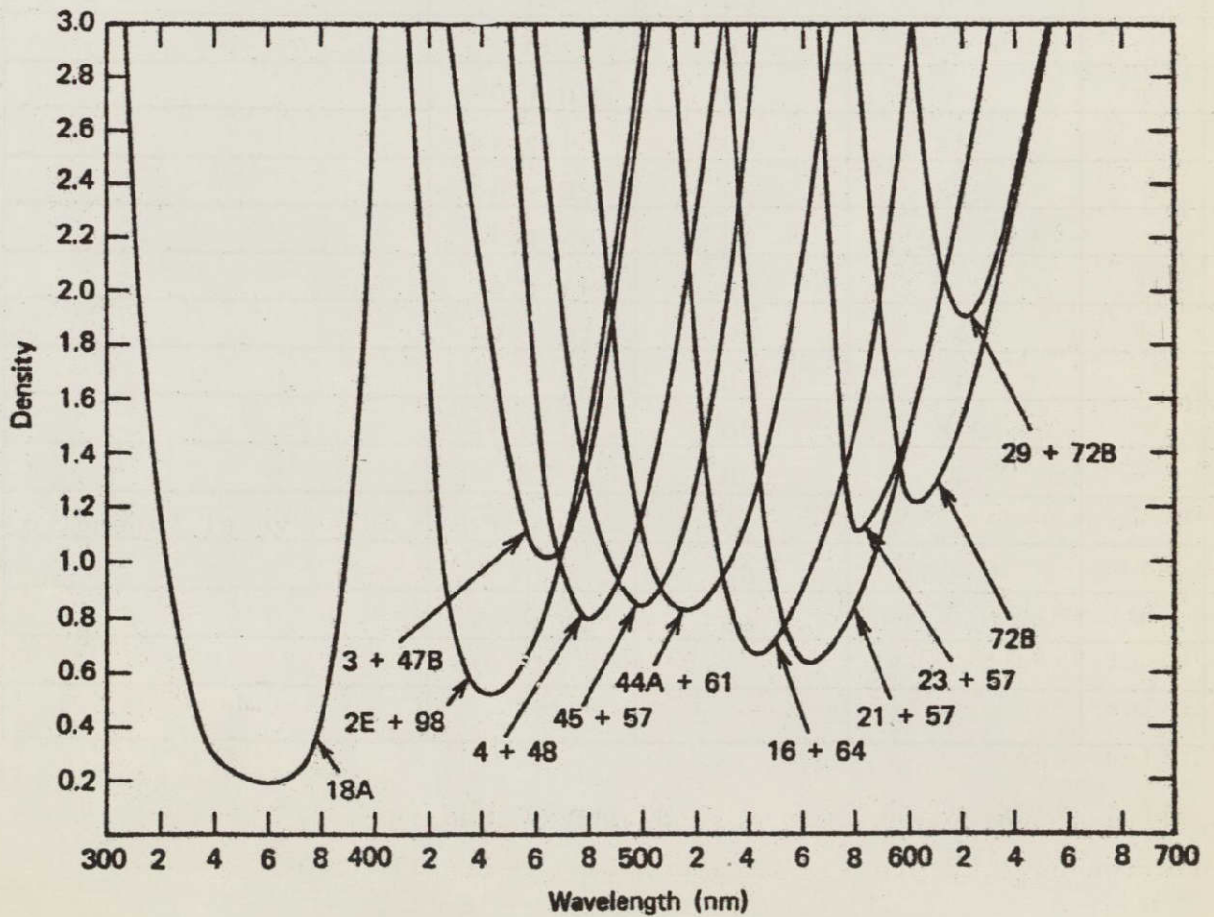
Figure 4.—Bandpass Wratten filter combinations tested

DIRECCION GENERAL DEL INSTITUTO GEOGRAFICO Y CATASTRAL

LABORATORIO DE TELEDETECCION

FOTOGRAFIA MULTIBANDA

LOCALIDAD ARANJUEZ

LUGAR FINCA INIA SOTOMAYOR

MOTIVO VUELO MSS

FECHA 15 - MAYO - 1976

HORA SOLAR; 10'45 - 11'30

PELICULA PANATOMIC

CAMARA MINOLTA

SENSIBILIDAD 32 ASA

CIELO ☒ DESPEJADO
☐ POCO NUBOSO
☐ CUBIERTO

DATOS FOTOGRAFICOS

Nº	FOCAL (mm.)	DIAFRAGMA	EXPOSICION (1/seg)	FILTRO	OBSERVACIONES
1	50	8 - 11	125		panorámica
2	"	8	125	polariz.	"
3	"	1'4 - 2'8	60	18A	
4	"	4 - 5	60	47B	
5	"	5'6	60	25	
6	"	4 - 5	60	58	
7	"	5'6	30	47B + 3	
8	"	2'8	60	4 + 48	
9	"	2'8	60	2E + 48	
10	"	1'4 - 2'8	60	45 + 57	
11	"	2'8	60	44A + 61	
12	"	4	60	16 + 64	
13	"	4	60	21 + 57	
14	"	2'8	60	23 + 57	
15	"	4	30	72B	
16	"	4	15	29 + 72B	no se ve el fotómetro
17	"	4 - 5'6	60	61	
18	"	1'4 - 2'8	60	61 + 25	
19					
20					

EL OBSERVADOR,

Figure 5. Sheet of the survey book filled during field work in site nº 12, called "finca INIA Sotomayor".

several film-filter combinations. The filters used were Wratten
and BDB, while the films tested in the ground have been the
following:
- Panatomic
- Plus-X Pan

Figure 4 shows the filter combinations tested for the purpose
of obtaining narrow bandpasses of sun reflected radiation. Such
single or doble combinations have been tried as assay of future
multiband missions, and for selection of the best bands to be
used in each application. Figure 5 represents one sheet of the
survey book filled during the field work at site no.12, called
"finca INIA Sotomayor".

Simultaneously to the aerial flight, local measurements have
been done of physical parameters in the ground for determining
atmospheric conditions and chemical components of the water.
Samples of Tajo and Tajuña rivers were taken and analyzed by
the Laboratory of Water Analysis of the Center of Hydrographic
Studies, in sites no.1, 3, 4, 5 and 6. Figure 6 corresponds
to site no.3 in Tajo river, while figure 7 was taken in site
no.7.

In table 1 is enclosed the result of the analysis of water
samples.

As ancillary information for acquisition of ground truth in the
test site have been used topographic maps at scale 1:50.000,
geological and forestry charts at scale 1:400.000, and the
Lithologic Map of Spain. Aranjuez is located in the sheet no.
605 of the National Topographic Map at scale 1:50.000.

3. AERIAL SEGMENT

The aerial survey was conducted by Instituto Nacional de Técni-
ca Aeroespacial in an airplane CASA-212 (figures 8 and 9)

Figure 6. Obtaining water samples in Tajo river (site nº 3)

Figure 7. Partial view of Tajo river on its pass by the city of Aranjuez (site nº 7)

equiped with the following sensors:
- 4 Hasselblad cameras 500 EL, f/50
- multispectral scanner Daedalus, 10 channels

The cameras were loaded with the following films and filters:
- Panatomic-X 3410   Wratten 58
- Panatomic-X 3410   Wratten 47B
- Aerochrome IR 2443   Wratten 12
- Kodak black and white IR 2424   Wratten 88

The scanner did not operate in thermal IR wavelengths, being
the bands used indicated in table 2. The MSS Daedalus was
available

channel	spectral band (μ)
1	0,38 - 0,42
2	0,42 - 0,45
3	0,45 - 0,50
4	0,50 - 0,55
5	0,55 - 0,60
6	0,60 - 0,65
7	0,65 - 0,70
8	0,70 - 0,80
9	0,80 - 0,90
10	0,90 - 1,10

Table 2. MSS Daedalus spectral bands.

from the french CNES (Centre National d'Etudes Spatiales), who
supplied the equipment, technical personnel and preprocessing
of the information for this survey, as part of the Scientific
and Technical Cooperation Agreement signed between France and
Spain.

Figure 8.—Airplane CASA-212 used in the multispectral survey

Figure 9.—Interior view of a CASA-212 airplane equiped for aerial photography missions at the Cartographic and Fotographic Service of the Air Force

The MSS Daedalus has the following components:
- optical head of scanning in two channels
- array of multispectral detection in the visible
- electronic console of command and control
- distribution box
- control unit of sources of reference
- system of visualization

The optical head of scanning is composed by a rotating mirror, parabolic optics, dichroic plate for selection of visible or IR radiation, two lamp sources of references and a gyroscopic system of movement compensation. Its major characteristics are indicated in table 3.

Optical head of scanning	characteristics
Spectral band	0,38 - 1'1 μ
Total FOV (geometric)	87º 20'
Scanning rate	80 rps (fixed)
Instantaneous FOV	2,5 mrd.

Table 3.

Both sources of reference are lamps calibrated at the N.B.S. (National Bureau of Standards), giving two squared signals just before and after the video signal obtained from the earth radiation in each rotation of the scanning mirror (figure 10).
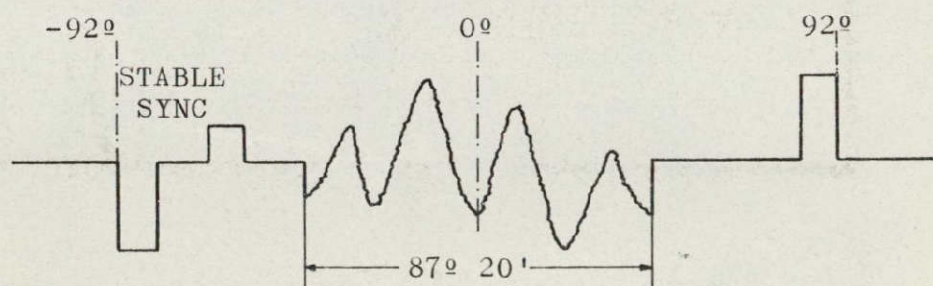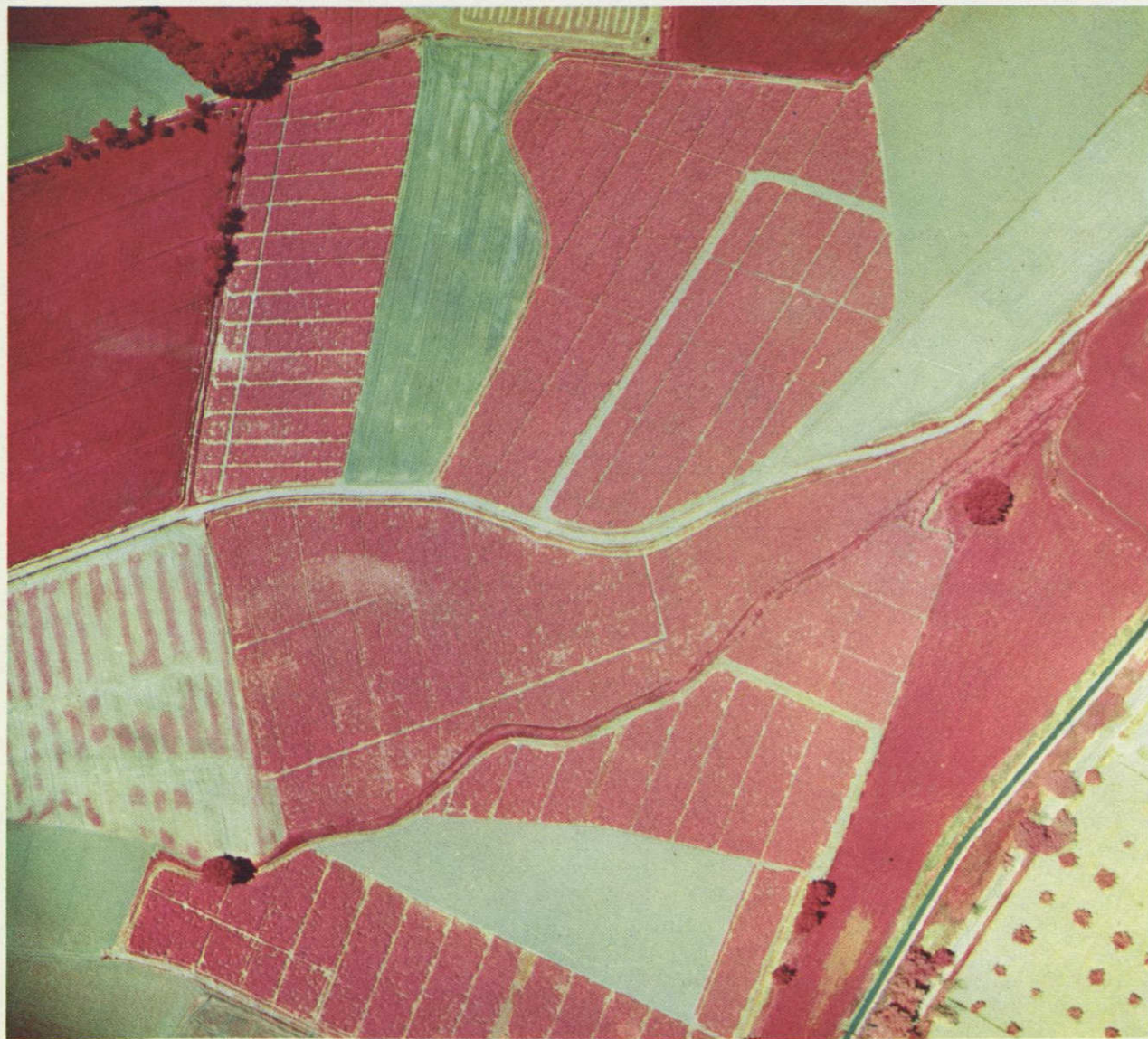

Figure 10. Complex video signal.

Figure 11.—Color infrared image obtained with Hasselblad camera on site no. 10 (original in 70 mm format)
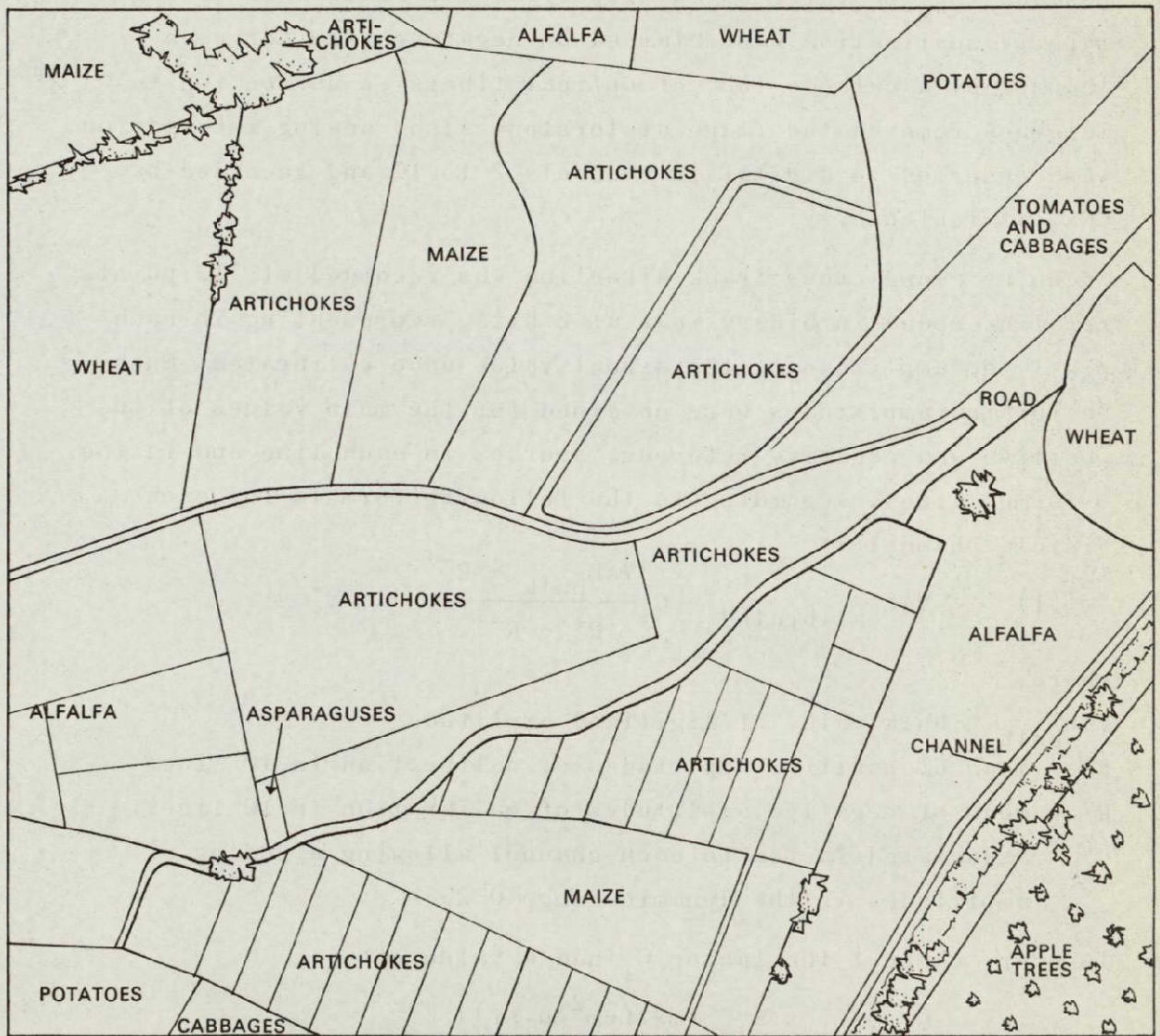
Figure 12.—Photointerpretation of the image shown in figure 11

Calibration lamps give signals of amplitudes, corresponding to the lower and higher video signals received from the earth, whose equivalent spectral radiance is represented by a term L_i in each channel.

Besides the recording of multispectral information in analog tape, visualization was obtained on negative film for each channel by a cathode tube of optical fibers. A correction in tangency removed the image distorsion. Also, analog information was converted to digital in channels 2 to 10 and recorded by CNES at Toulouse.

Scanning along cross-track direction was recorded at 512 points per line coded in binary mode at 8 bits, representing in each pixel the amplitude of the signal value once calibrated. Such calibrated amplitudes were obtained for the mean values of the positive and negative reference sources in each line and in the 9 former lines, according to the following formula for each visible channel i:

$$(1) \qquad VAL_{calibrated} = C_i \frac{VAL_{bulk} - R^-}{R^+ - R^-}$$

where,

VAL_{bulk} = bulk value of digitized amplitude

R^+ = mean of positive amplitudes of calibration in 10 lines

R^- = mean of negative amplitudes of calibration in 10 lines

C_i = associated factor to each channel allowing a coding of amplitudes in the dynamic range 0-255

In every channel the factor C_i had a value of:

$$C_i = L_i \times K_i \quad (mW/(cm^2 \cdot \mu \cdot sr))$$

where L_i represents the above mentioned spectral radiance and K_i is a coefficient which divides the amplitudes for obtaining physical values. The coefficients K_i are available on tape at the beginning of each scene, being different for each channel.

Figure 13.—Black and white image obtained over the confluence of Tajo (lower part) and Jarama (right) rivers. Point indicate densitometric analysis done on the original negative

In the case of Aranjuez test site their value is indicated in table 4.

channel	2	3	4	5	6	7	8	9	10
K_i	23.2	15.7	15.1	14.9	16.9	17	20.9	24.8	32.1

Table 4.

As it can be seen from (1), the "history" of the recorded earth radiation is taken into consideration and the value of pixel amplitudes has a relative significance in each channel, although it is not correlated in different channels.

The aerial mission was conducted on May 15, 1976 at 500 m height with a nominal speed of 54 m/s. The direction of each pass over the test site is indicated in figure 2.

The color IR images obtained with the Hasselblad cameras have allowed a rapid work of photointerpretation based on the existing field data. Because the low height flying altitude, most of the surficial features have been easely identified without ground control. This applies namely to the recognition of different types of crops, which is being carried out, at the date of submission of this final report, by the Service of Photogrammetry and Photointerpretation of the Polytechnic University of Madrid. In figure 11 is shown as example an enlarged image obtained in false color during the aerial mission, while figure 12 represents its photointerpretation.

Black and white multiband photography has also provided valuable data in the analysis of water pollution at Jarama river. Figure 13 represents one of the images obtained over the confluence of Tajo and Jarama rivers (site no.5), with indication of the points where densitometric analysis have been effected on the original
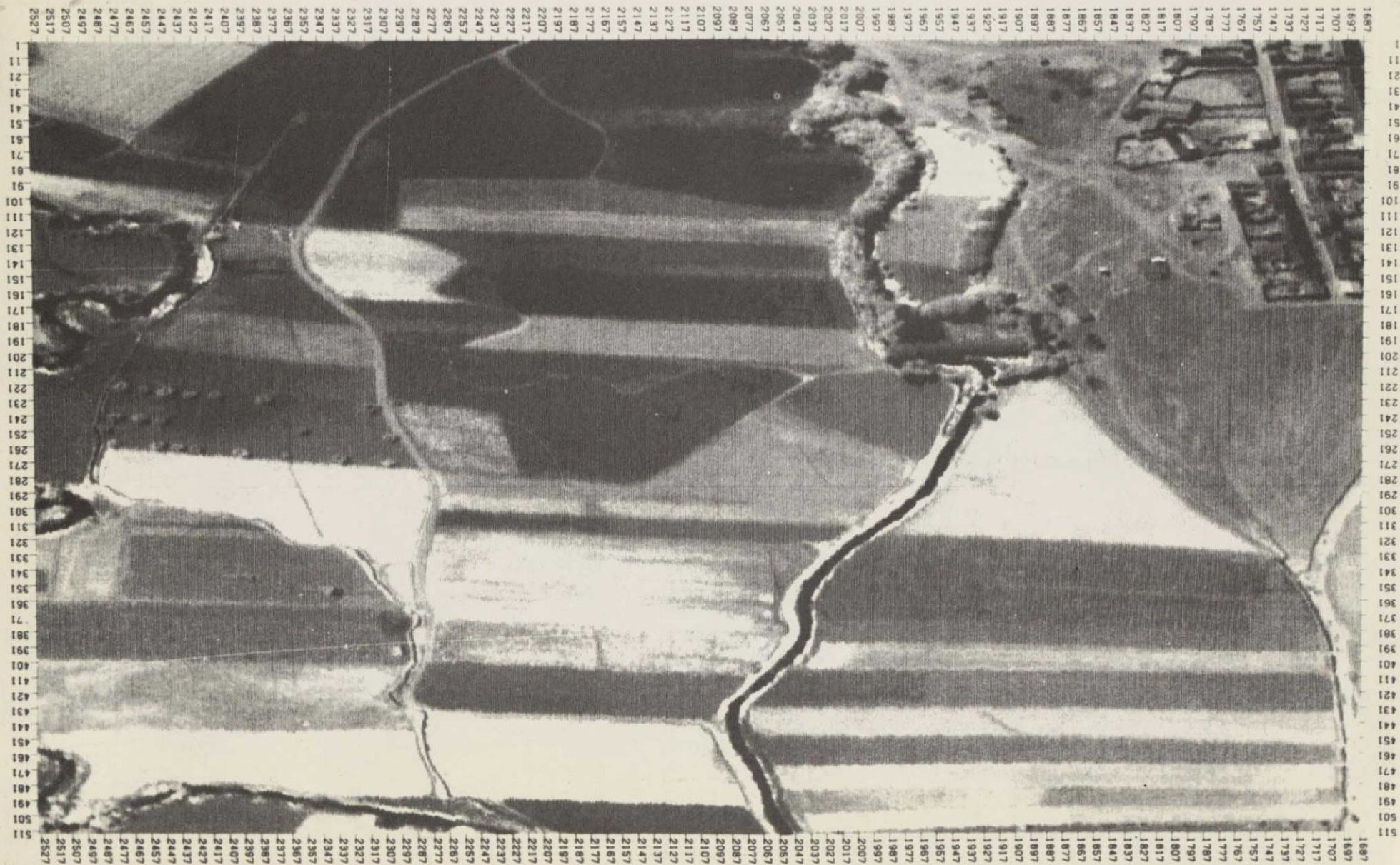
Figure 14.—Photographic recording of a digitized scene obtained by the MSS Daedalus over Titulcia in site no. 8 (Courtesy of CNES)
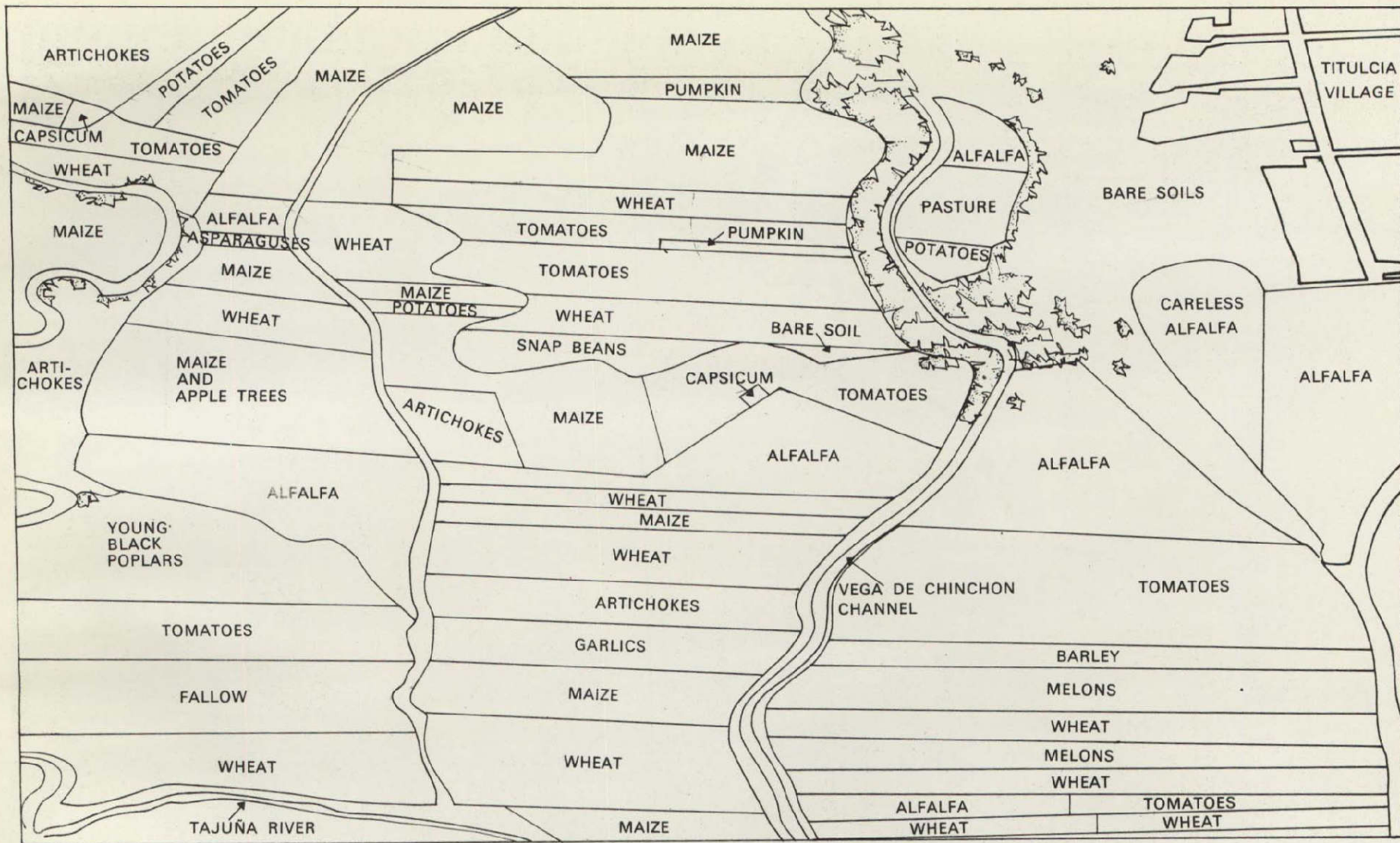
Figure 15.—Photointerpretation of the image shown in figure 14

negative. The filter used in this scene was the wratten 47B.
Measurement of optical densities was done on a Welch densito-
meter by transparency, with the results indicated in table 5.

Point	1T	2T	1J	2J	1C	2C	3C	4C	5C
Density	0.24	0.26	0.36	0.42	0.36	0.32	0.59	0.29	0.19

Table 5.

Although digital processing of the MSS Daedalus magnetic tapes
is undergoing at this moment in cooperation with the IBM-Scien-
tific Center of the Autonomous University of Madrid, some good
quality images have been furnished by the Mathematic Division
of CNES in Toulouse. Figure 14 represents an enlarged copy
of the film recording of digital data done in channel 9 over
Titulcia (site no.8). It can be seen on the image the village
(upper right) and both Tajuña river (left) and the channel of
Vega de Chinchón (center). In figure 15 is shown the photointer-
pretation of figure 14.

During the aerial mission it was avoided the influence of
different sun angle elevations by conducting the flight at noon
(12 a.m. to 2p. m.), with a vertical incidence of light to the
target and vertical reflectance of solar radiation detected by
the scanner.

Processing of photographic films used with the Hasselblad
cameras was done at the Remote Sensing Laboratory of Instituto
Nacional de Técnica Aeroespacial, in Torrejón de Ardoz, Madrid.

4. SPACE SEGMENT

LANDSAT information was included in this survey as a tool for
obtaining an automatic classification of land use in Aranjuez

• 09/56.04 1

1803

CLUSTER REPORT MENU

CLUSTER	POPULATION	CLASS MATCH	DISTANCE	CLUSTER MATCH	DISTANCE	NAME	CANCEL
1	486 0		0 0		0 0	_____	_
2	1648 0		0 0		0 0	_____	_
3	696 0		0 0		0 0	_____	_
4	1236 0		0 0		0 0	_____	_
5	905 0		0 0		0 0	_____	_
6	1132 0		0 0		0 0	_____	_
7	388 0		0 0		0 0	_____	_
8	782 0		0 0		0 0	_____	_
9	372 0		0 0		0 0	_____	_
10	227 0		0 0		0 0	_____	_
11	492 0		0 0		0 0	_____	_
12	543 0		0 0		0 0	_____	_
13	269 0		0 0		0 0	_____	_
14	146 0		0 0		0 0	_____	_
15	42 0		0 0		0 0	_____	_
......	172 UNASSIGNED PIXELS					_____	_

☐ DETAILED REPORT   ☐ DISTANCE TABLE   ☐ CHAINING   ☐ MAP GENERATION

☐ REJECT RESULTS AND RECOVER   ☐ END RUN STORING STATISTICS   ☐ GOODNESS OF FIT

☐ FORCE ITERATIVE SEQUENCE   ☐ HIT STATISTICS

Figure 16.—Cluster menu representing the population in each class

• 09/57 37 1

1805

DETAILED CLUSTERING REPORT

RUN NO 1	CLUSTER 1 C OF 0/ 0 S FROM 0	CLUSTER 2 C OF 0/ 0 S FROM 0	CLUSTER 3 C OF 0/ 0 S FROM 0	CLUSTER 4 C OF 0/ 0 S FROM 0	CLUSTER 5 C OF 0 0 S FROM 0
CHANNELS	MEAN STD	MEAN STD	MEAN STD	MEAN STD	MEAN STD
1	40 25 2 17	38.12 1 67	36 73 1 76	33 19 1 84	33 40 1 74
2	42 63 2 76	29 27 2 09	37 46 2 44	33 39 1 86	32 78 2 00
3	47 14 2.63	31 40 1 82	41 09 2 21	25 60 2.19	42 30 2 04
4	22 63 1.93	14 74 1 51	19 59 1 65	16 80 1 53	21 59 1 43

PB
PF
RET

Figure 17.—Mean and standard deviation values of claster classer

```
                        * 89/59/49 1
1885
        DETAILED  CLUSTERING  REPORT
 RUN      CLUSTER  6     CLUSTER  7     CLUSTER  8     CLUSTER  9     CLUSTER 10
 NO       C OF  0/ 0     C OF  0/ 0     C OF  0/ 0     C OF  0/ 0     C OF  0/ 0
 1        S FROM  0      S FROM  0      S FROM  0      S FROM  0      S FROM  0

 CHANNELS MEAN   STD     MEAN   STD     MEAN   STD     MEAN   STD     MEAN   STD

    1     30.27  1 62    28 45  1 56    29 23  1 72    34 79  2 23    26 29  1 77
    2     28 51  1 89    26 92  1 77    26 47  2 18    34 87  2 76    24 41  2 62
    3     37 69  2 13    -7 00  1 75    44 36  2 05    48 13  2 26    48 37  2 15
    4     19 13  1 44    12 82  1 38    23 97  1 54    24 60  1 56    27 33  1 41
```

Figure 18.—Mean and standard deviation values of cluster classes

```
                        * 10 00 11 1
1885
        DETAILED  CLUSTERING  REPORT
 RUN      CLUSTER 11     CLUSTER 12     CLUSTER 13     CLUSTER 14     CLUSTER 15
 NO       C OF  0/ 0     C OF  0/ 0     C OF  0/ 0     C OF  0/ 0     C OF  0/ 0
 1        S FROM  0      S FROM  0      S FROM  0      S FROM  0      S FROM  0

 CHANNELS MEAN   STD     MEAN   STD     MEAN   STD     MEAN   STD     MEAN   STD

    1     26 86  1 30    26 60  1 58    24 32  1 66    26 95  1 74    25 29  1 80
    2     23 27  1 87    25 56  2 04    20 33  1 94    21 97  2 17    18 69  2 16
    3     38 95  2 10    31 91  2 02    25 64  2 23    20 04  2 15    52 76  2 09
    4     21 03  1 50    16 48  1 50    12 58  1 64    7 40   1 65    22 14  1 69
```

Figure 19.—Mean and standard deviation values of cluster classes

test-site. The aerial flight conducted at low altitude was
intended to provide a knowledge of the area, which could be
correlated and used for a supervised classification of resources
in Aranjuez by means of LANDSAT MSS data.

As a first step in this program, which is undergoing now, a
classification of LANDSAT image no. 2223-10135 was done by
clustering techniques, assuming that none ground truth of the
pilot area existed, in the intent of determining the capability
of the satellite by itself for surveying Aranjuez land uses.

The cluster analysis was done at the IBM-Scientific Center of
the Autonomous University of Madrid, where ERMAN-II program
is available on an IBM 360/65 computer interfaced to an
interactive television terminal RAMTEK. Such powerful software
was used for classifying Aranjuez test site. The area represents
on tape no.2223-10135 a rectangle of 250x256 pixels, being
the upper left corner of the subscene in line 1400 and pixel
1250.

Before any classification was done, a registration was conducted
on the digital tapes for geometrically correcting the subscene
and positioning it by reference to a grid in UTM projection.
Such procedure has been explained in another section of this
final report (reference 1). Coordinates of control points were
extracted from the National Topographic Map at scale 1:50.000,
published by Instituto Geográfico y Catastral (sheet no.605).

After an accurate geometric correction was done, clustering of
the subscene was intended with 15 classes and the same "a priori"
probability $P(Wi)$ for all of them. Figure 16 represents the
population included in each class, and figures 17,18 and 19
indicate the mean and standard deviation values obtained for
each class of cluster. At this point, a plot was effected of

spectral radiance levels versus all four MSS channels for the
15 clustering classes (figure 20). Furthermore, the mean and
standard deviation values of each of the 15 classes was
represented in channels 2(band 5 of LANDSAT MSS sensor) and
4 (band 7 of LANDSAT MSS sensor). Bands 5 and 7 have been
selected for this plot because they show lower correlation of
information than any other two bands of MSS sensor (this subject
is discussed in another section of this final report - see
Digital Processing - reference 2).

As result of this graphic representation, and because the
existing similarities in spectral responses of classes, a
grouping in 8 new classes was intended from the previous
clustering classification. Table 6 summarized the reduction
in classes carried out, with indication of the color assigned
to the new grouping.

GROUPING OF CLUSTERS	NEW CLASS	COLOR
I	I	yellow
G - H	G	light green
A - E - B	A	cyan
C	C	blue
Q - N	Z	violet
F - J - L	Y	white
K - P	X	red
M	M	black

Table 6.

The result of this grouping of clusters in 8 new classes produced
the image shown in figure 21; where one of the classes, corres-
ponding to water, has been separately represented in figure 22.

5. RESULTS AND DISCUSSION

The survey of Aranjuez test site has allowed to the participant organizations in this project an acquisition of know how and apprenticeship in remote sensing techniques applied to several disciplines which promises good result in the future when more systematic surveys of the country will be conducted. This is probably the most important accomplishment that the multidisciplinary survey has produced in all participants.

As part of the field work conducted in Aranjuez it is here dedicated a comment to both types of films tested, Panatomic (32 ASA) and Plus-X Pan (125 ASA).

Although the higher sensitivity of Plus-X Pan film, when an aerial mission is conducted there is in general a need for a good speed photographic film with high resolution. Such requirements are better satisfied by the Panatomic film. In the field, when the camera is mounted on tripod and focused to a fixed objective, being the time of exposure not critical and able to increase as much as needed, Panatomic film provides better results than Plus-X Pan film. This has been observed in Aranjuez, in spite of the better sensitivity of Plus-X Pan film.

The film-filter combinations tested have provided more details and a better contrast of the images when used Panatomic film. As it can be seen in digures 4 and 5, several filters were tested in an effort to select the best spectral bands to be used for each general application. Although results show very similar and none comment can be done until the spectral curves of objectives are determined, some combinations of Wratten filters are rejected because their low transmission of light in the spectral region where film used is sensitive. Such rejected combinations are the following:
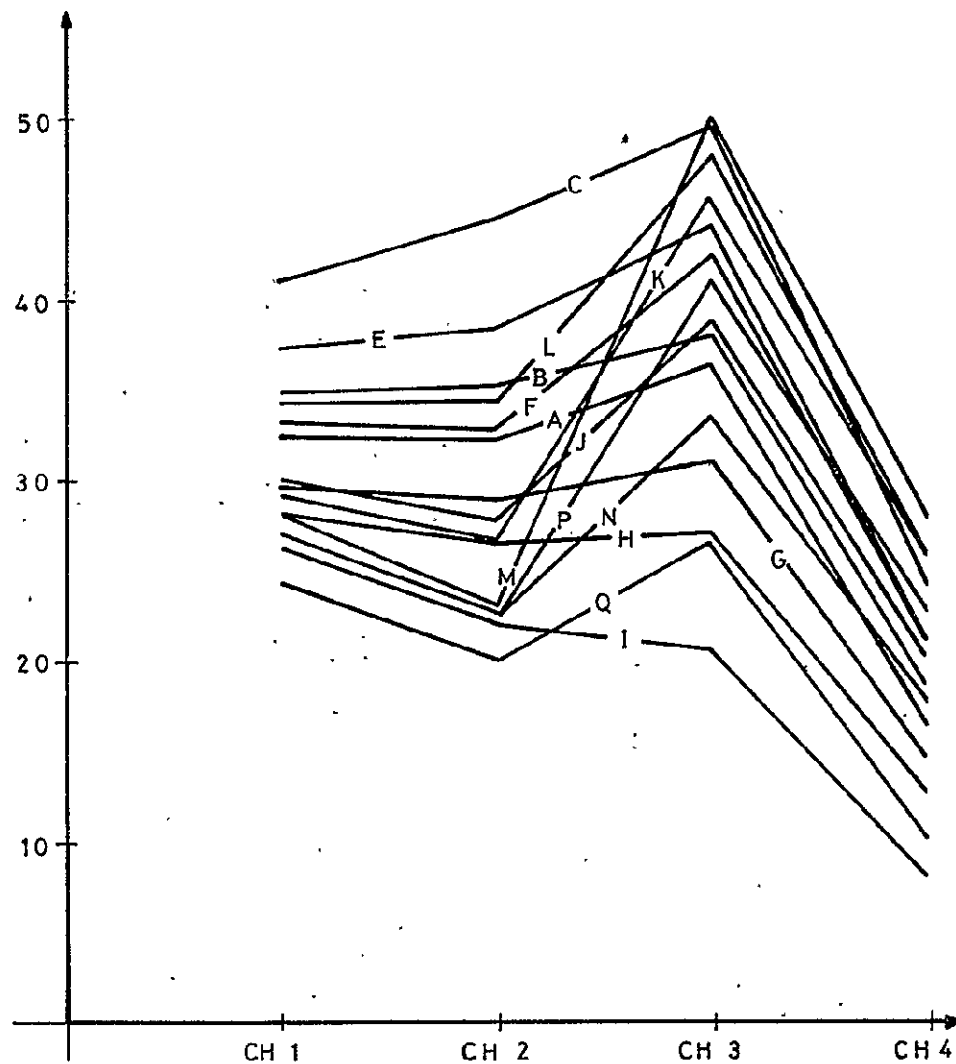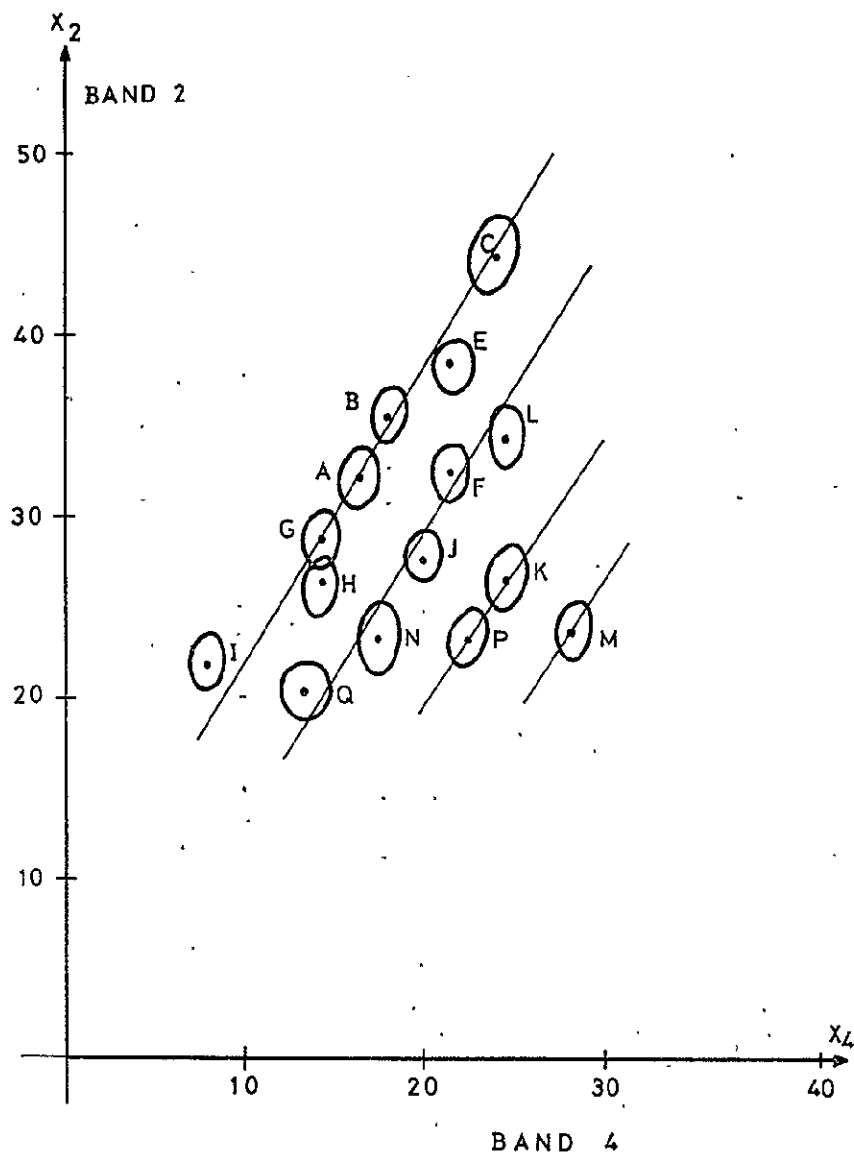
Figure 20.—Spectral radiance levels in LANDSAT MSS bands (right), and mean-standard deviation values of each cluster class in MSS bands 5 and 7 left

- 72 B + 58
- 45 + 16
- 25 + 16

Better results were obtained with the conventional filters
used in multiband aerial photography:

- 47 B (360 nm - 500 nm)
- 58 (465 nm - 620 nm)
- 25 (580nm - limit of film sensitivity)

From the analysis of water samples taken in Jarama and Tajo
rivers (table 1 - sites 1, 3, 4, 5 and 6 of figure 2), it can
be states the high content of suspended solids and turbidity
of Jarama waters, with a D.Q.O. value of 146 mg/l oxygen. The
densitometric analysis of waters in the confluence of Jarama
and Tajo rivers (figure 13 - Table 5), shows that a certain
correlation exists between optical densities in the film versus
turbidity and suspended solids in the waters. These two physical
parameters can be clearly identified on the aerial imagery in
a qualitative mode. Points 3C and 4C do not seem representatives
because the presence of foams on them and the existence of
backwaters. Although some other chemical components of the
waters could be correlated to the optical densities measured,
it seems that the spectral response produced by turbid waters
is much more strong than the one detectable from chemical
pollutants.

The photointerpretation work conducted for identification of
different types of crops and phenological states has shown the .
uniqueness of color infrared aerial photography for these
purposes when taken at low altitudes. As example, it can be
seen in figure 11 and on its interpretation (figure 12), that
photointerpretation of different types of crops is an easy·
and economic way of work. As result of this survey a comparison
has been done of the cost of photointerpretation and field

work, based on an aerial flight at mean scale 1:7.000 (table 7). It can be deduced from the table the economy and convenience that represents to work by means of photointerpretation techniques in Aranjuez test site.

Agronomic photointerpretation results difficult from the information supplied by the MSS Daedalus, once converted to black and white images. As it is shown in figures 14 and 15 different types of crops have a very similar gray tonality, even if densities are controled during the print out process. However, by digital analysis of the data and false color combination of different bands, results could be improved, although the cost of computer processing could never be competitive with the photointerpretation of color IR imagery.

In the analysis of LANDSAT data done by clustering techniques it has been determined that the satellite by itself (without ground support) was not able to discriminate the existing types of land uses in Aranjuez. The identification of cluster classes showed extremely difficult and none result can be anticipated. As example it is indicated here what every grouped spectral class could be, without reasonable possibility of determining their real content (table 8).

From table 8 it was deduced by photointerpreters that the different colors appearing in the images when due to various types of soils had the influence of moisture, erosion, land uses, etc. Even in cases where the identification and location of a pattern was possible, the low extension of parcels in Aranjuez produces a mixed spectral response in every LANDSAT MSS pixel which does not allow any accurate automatic classification. Results could probably be improved when a supervised classification was done, based on well known training fields. Such training fields could be selected based not in

Field work

In Aranjuez with aerial photograms at scale 1:7000 including displacements and the later work in cabinet:

Hectares photoidentified per person and day	270
Cost of displacements: 150 Km. at 8 pts/Km.	1.200
Diets	500
Salary	1.000
	2.700

Price per hectare photoidentified = ·10 pts./Ha.

Photointerpretation

In the same area and the same conditions of imagery:

Price per hectare photointerpreted =   6 pts/Ha.

Table 7. Cost analysis of field work and photointerpretation in Aranjuez test site.

Cluster class	Possibility in the ground
black	water, terrains with moisture
light green	crops in alluvial soils (dry and irrigated)
cyan	dry farming crops, pastures, scarce vegetative cover, bare soils
violet	scrubs, humid areas
red	scrubs, olive-groves
yellow	irrigation lands, not alluvial terrains
blue	dry farming crops, olive-groves, residential areas, industrial and urban land use
white	not identified

Table 8. Possibilities of identification in the 8 classes cluster run on LANDSAT tape over Aranjuez pilot area.

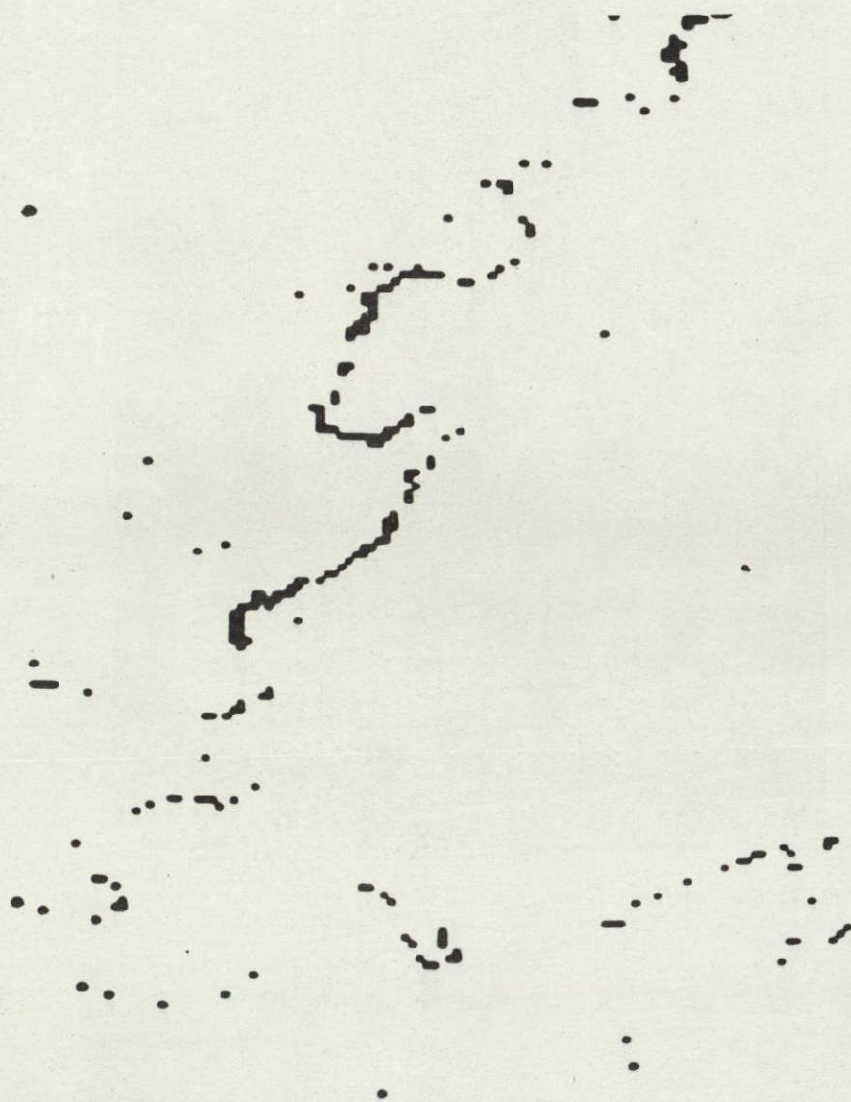Figure 21.—Color representation of 8 cluster classes obtained by digital analysis of LANDSAT data

Figure 22.—Cluster class corresponding to water in Aranjuez test site, showing Jarama and Tajo rivers

the existing information on the ground, but by means of the
aerial images taken during the survey at low altitude, namely
false color photography. Once the images photointerpreted,
their content of information should allow a very accurate
definition of training fields trough the RAMTEK TV terminal.
Furthermore, the higher resolution of the images should guarantee
a correct location of training fields, increasing the accuracy
in selecting their corresponding pixel (s) on the LANDSAT
image, or even their position into the pixel. This transfer
of data from the aerial segment to the space segment should
probably need an intermediate step in the form of aerial images
at small scale (1:60.000 or similar), for carrying out a
generalization of information, which appears necessary because
the low resolution of the MSS pixel (80x80 m on the ground).

Another limitative factor in the malfunction of the cluster
has been the different date of observation with the satellite
and with the airplane, although it does not seem critical in
the case of Aranjuez.

The strongest limitation to the application of LANDSAT data in
Aranjuez, and this is an example of what has been happening
along this project in Central Spain, comes from the small
size of the parcels, which is not the appropiate to the already
low resolution of the MSS sensor. As example of this it was
shown in figure 22 the cluster corresponding to water. It
might represent the course of Jarama river (diagonal in the
image) and the Tajo also (horizontal in the lower part of
the image), but because the reduced width of Tajo river
on its pass by Aranjuez, which does not surpass 40 m (half
of a LANDSAT pixel), it presents a discontinuity. Another
reason for such discontinuity is the vegetative cover along
Tajo margins, with numerous trees of powerful crowns. Such
situation is well represented in figures 6 and 7.

Finally, although in the water class obtained by cluster Jarama river is represented in black color (figure 22), this does not mean that Tajo waters "are not black". In fact, the satellite detects Tajo river as "more black" than Jarama in the IR region, and this is due to the strong pollution of the last, which produces its higher reflectance and its better detection by MSS sensor in band 7. Because the purity of Tajo waters, their absorption of sun radiation is stronger in the infrared band than Jarama waters, which reflect more light due to the presence of surface pollutants (turbidity and suspended solids concentration are good indicators of the spectral response produced).

From the archeological point of view good results have been achieved in the area. Around the village of Titulcia (sites no. 8 and 9) existed in earlier times a celtiberian burying-ground, another one visigothic, and a roman village. As Titulcia was an important point of communications during the roman times, two causeways had their crossing on the village; one going from Toledo to Segovia and the other from Mérida to Zaragoza.

At the time of submission of this final report several archeological sites have been detected, although their real nature cannot be stated until checking work in the ground will be carried out. The location of such sites is positioned around the arrow indicated in figure 2. The Instituto Español de Arqueología Rodrigo Caro is doing the basic research on the ground for determining whether or not an excavation might be conducted.

Aknowledgements

Aknowledgement is given to José Remesal, of Instituto Español de Arqueología Rodrigo Caro, who conducted the archeological recognition of Titulcia.

The cooperation of Dr. García de Nicolas, of Centro de Estudios Hidrográficos, is appreciated for his support in the acquisition of water samples and their analysis in laboratory. It is also recognized the collaboration of Dr. J. Manuel Varela, of Centro de Estudios Hidrográficos, who conducted basic work in the acquisition of ground truth.

The field survey carried out by Dr. Mario Nieves, of Instituto Nacional de Investigaciones Agrarias, is appreciated.

Aknowledgement is given to all personnel of the Department of Avionics and Electro-optics, of Instituto National de Téc nica Aeroespacial, for their dedication to this project and their valuable collaboration.

The participation of the Air Photographic Squadron 403 of Servicio Cartográfico y Fotográfico del Aire, whose pilots conducted this aerial survey, is greatly aknowledged.

References

1 - Germán Lemos. "Evaluation of LANDSAT MSS data for updating cartography at small scales in Central Spain", Final Report, NASA project no.28760, Instituto Geográfico y Catastral, 1976.

2 - A. Santisteban. "Determination of uncorrelated bands in a LANDSAT MSS image", Final Report, NASA project no.28760, IBM-Scientific Center, 1976.

258

WATER RESOURCES

APPLICATION OF LANDSAT-2 DATA TO HYDROLOGY IN CENTRAL SPAIN

Center of Hydrographic Studies
Ministry of Public Works
Madrid
SPAIN.

WATER RESOURCES

APPLICATION OF LANDSAT-2 DATA TO HYDROLOGY IN CENTRAL SPAIN.

By Centro de Estudios Hidrográficos
Ministerio de Obras Públicas
Madrid.

1. INTRODUCTION

As it was stated in the Second Quarterly Report the Centro de Estudios Hidrográficos (C.E.H.) intends to obtain from LANDSAT images useful information on the physical pattern of hydrographic basins from a synoptic point of view and taking into account their evolutive processes.

C.E.H. is in charge of the hydrologic studies and hydraulic acting in the national territory, through the divisions in hydrographic basins of the main rivers and their tributaries. Since many years ago it has inventoried such streams, delimited their basins and measured the length of the currents and the surface of the basins. Furthermore, the Center has determined the discharges of the rivers and the rainfall of the basins, through the corresponding hydrologic network of measurement. However, such quantitative data can be enriched with other qualitative information which, at synoptic scale, can be obtained from satellite images when supported by local measurements of "ground truth" and conventional methods of photointerpretation.

With this purpose, the C.E.H. intended to obtain information on the satellite images focused to:

- a more detailed delineation of drainage networks at synoptic
  scales (1:200.000 and 1:500.000).

- a classification of the terrain surface in hydrographic
  basins.

These two objectives can contribute to define criteria for the
study of runoff in basins and sub-basins, because they provide
parameters which are tied to it and which will be used for
establishing mathematical models of simulation in the different
basins.

In our earlier report it was intended to expand this study
to all Central Region of Spain, as it was proposed in this
multidisciplinary project. For reasons of urgency in the
elaboration of this final report, as well as because the scarce
number of hours-men dedicated to it, the area of analysis was
restricted to only one hydrographic basin; in Guadarrama river,
tributary of the Tajo on its right margin. This study will be
expanded in the future to other areas when the techniques
of analysis will be better known and when more spatial
information will be available.

This study was conducted in four different fronts:
- drainage network
- geology
- vegetation
- farming

In the analysis of drainage network, treatment of the information
was done with the support of D. Luis Montoto, of IBM-Scientific
Center, Autonomous University of Madrid. The hydrographic
interpretation was conducted by D. Jesús Paredes, of C.E.H.

Geology study had the cooperation of D. Manuel Esteras, of
C.E.H.

Fig. 1.—False color image of Gua-
darrama basin at scale 1:500.000
with location of training fields in-
troduced to RAMTEK terminal

M, Timbered
D, Untimbered

Vegetation analysis was directed by D. Javier Luján, in collaboration with D. Carlos Notario and D.J. Antonio García Sánchez, all of them from C.E.H.

The group was coordinated by D. Jesús Cirugeda, and conjunction of these individual workswas carried out by D. Jesús Paredes. The C.E.H. is directed by D. José María Martín Mendiluce, assisted by D. Rafael Heras.

2. TECHNIQUES

2.1. Available information

The following LANDSAT images received from NASA have been used in the works of interpretation:

no.	identification	date	bands	support	tape
1	1228-10325	8-3-73	4,5,6,7	paper	no
2	1228-10325	8-3-73	F.C.	paper	yes
3	2169-10145	10-7-75	4,5,6,7	paper	no
4	2170-10204	11-7-75	4,5,6,7	paper	no
5	2187-10143	28-7-75	4,5,6,7	paper	no
6	2223-10135	2-9-75	4,5,6,7	paper	yes
7	2350-10182	7-1-76	4,5,6,7	paper	no
8	2367-10122	24-1-76	4,5,6,7	paper	no

As ancillary information it was used:

- cartography 1:500.000 of Instituto Geográfico y Catastral (I.G.C.)
- maps of hydrographic basins at scale 1:50.000, based on the National Topographic Maps of I.G.C. at such scale.
- physical data of the basins in spanish rivers (publication by C.E.H.)
- rainfall and flow metering data of the Hydrology Service of C.E.H.

Hydrographic network obtained from
existing cartography at scale 1·500.000

· GAGING STATIONS

■ flood prevention
⊠ Scale and limnigraph
▫ Without limnigraph

METEOROLOGICAL STATIONS

● Thermometric
○ Pluviometric
● Complete station

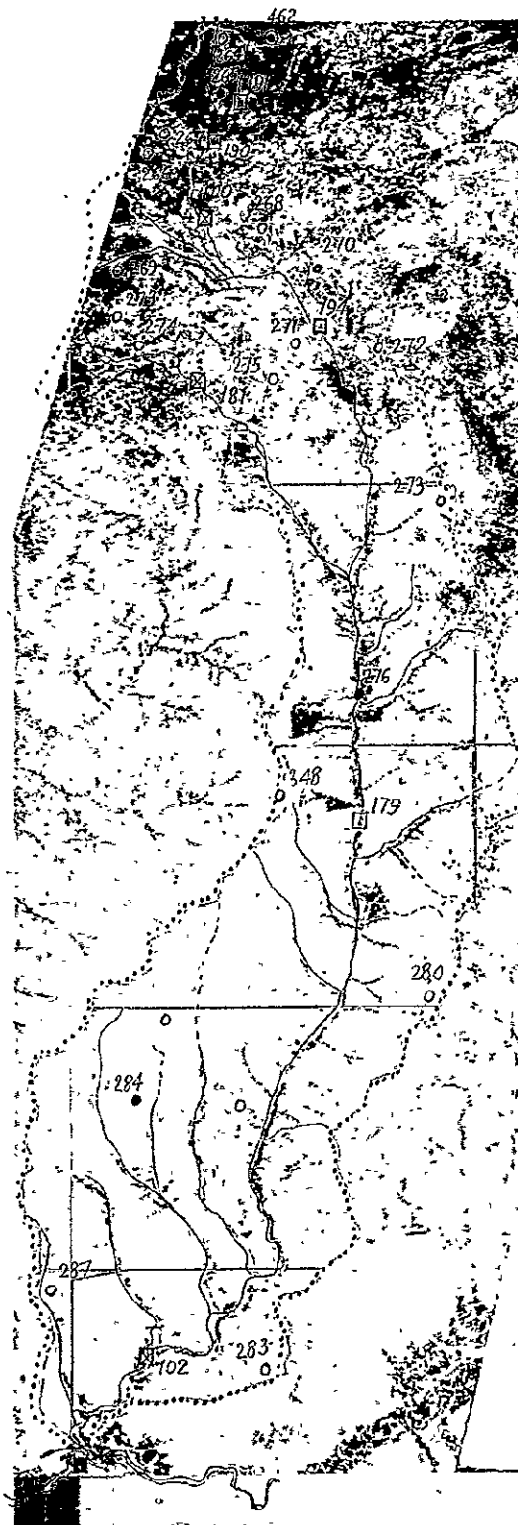Figure 2 —Image obtained by ratio of bands 5/7
Scale 1.500.000

- aerial photogrammetric flight (conducted by the Army Map
  Service in 1956-1957), at approximate scale 1:30.000.
- forestry map at scale 1:400.000 of the Ministry of Agriculture.

2.2. Treatment of the information

From the above mentioned images it was processed the no.2223-
10135 tape for the purpose of obtaining:

- image with band ratio 5/7 at scale 1:500.000 including
  divisory lines of the basin and the sheets corresponding
  to the National Topographic Map at scale 1:50.000 (figures
  2 and 3).
- false color image (4 = blue, 5 = green, 7 = red) at scale
  1:500.000 (figure 1).

The geometric correction of the image was done by means of
control points taken from the maps at scale 1:50.000. For this
process, as it is explained in paragraph 3.1, it was used the
following hardware:

- IBM 360/65 (1024K) computer
- RAMTEK GX 10013 interactive display system with CONRAC
  RHN19 Color TV screen
- Digital color image recorder DICOMED D-47

Digital data concerning to the divisory lines in the basins,
and the limits of the sheets of the maps at scale 1:50.000
were introduced to the system by a digitizer DMAC with output on
paper tape punch; being necessary to elaborate a program for
conversion of the PEGASUS code to the code ASCII of IBM, by
means of a computer NOVA of 32 K.

2.3. Hydrographic interpretation

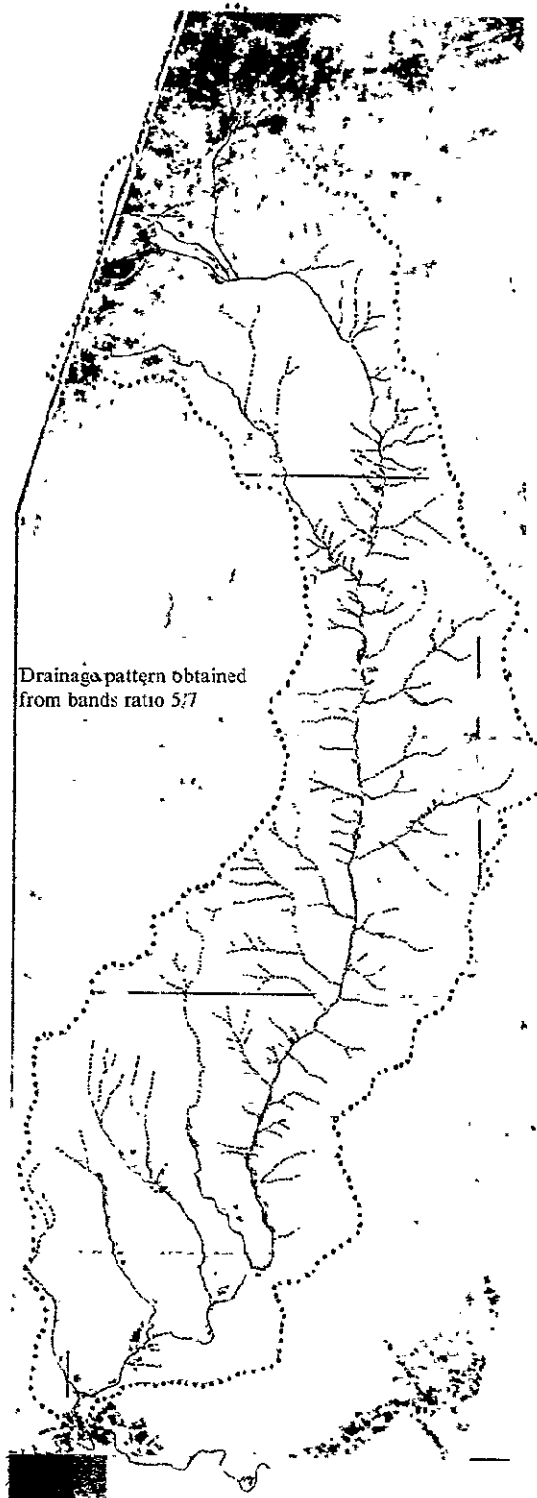For this interpretation it was used image no.6 in band ratio

Figure 3.—Image radiometrically corrected from figure 2
It is clearly identified the hydrographic network of Guada-
rrama river basin Lines indicate borders of the 1:50 000
scale maps included in the basin

5/7 at scale 1:500.000, completed with different black and white images, namely in band 7; being the results compared to the cartography of I.G.C. at scale 1:500.000.

2.4. Geologic interpretation

The geologic interpretation was done in priority on false color image no.2, which was available in digital tape at scale 1:500.000, being also used the rest of images in black and white, namely in band 7. The interpretation was supported by the knowledge of the author, the existence of ground truth and the previous interpretation of conventional aerial images at scale 1:30.000.

2.5. Forestry interpretation

It was used for this purpose the RAMTEK terminal on image no.6 for the selection of areas, evaluation of reflectances and production of histograms (relative radiance - percent resolution elements). Also, some work was done on image no 2. As reference it was available the experience of the photointerpreter in the area and the Forestry Map of Spain at scale 1:400.000.

2.6. Agronomic interpretation

It was used mainly false color image no.2 complemented with other black and white images in bands 5 and 7. The terminal RAMTEK has allowed also some digital processing of image no.6, although this work was conducted only for checking results. The interpretation was based on the current knowledge of terrain on 12 selected sites. The aerial flight at scale 1:30.000 has also been used.

3. ACCOMPLISHMENTS

3.1. Drainage network of Guadarrama basin

This work was conducted in the following stages:

a) From LANDSAT image no.2223-10135 (September 1975), a rectangle
   was selected between lines 540 to 2140 and pixels 1 to 800
   of the original digital tape. This subscene was referred
   to UTM coordinates by means of 8 control points and a
   second order polynomial algorithm, obtaining an image with
   pixels of 80x80 m once geometrically corrected. Table 1 shows
   the geographical coordinates of control points used, their
   corresponding position in the subscene (line and pixel),
   and the errors introduced when registering every control
   point. The errors are given in pixels of displacement along
   X and Y axis, and in radius vector.

Description	Input	Image	Reference		Error		
	Line	Pixel	Latitude	Longitude	X	Y	. R
El Pardo dam	1716	566	N40/32/10.88	W3/47/17.0	−1	0	1.0
Castrejón dam	653	175	N39/50/10:0	W4/17/49.0	1	1	1.4
Navalmedio dam	1954	102	N40/45/4.0	W4/2/7.0	0	0	0.0
Tajo-Guadarra ma junction	746	815	N39/53/5.0	W4/10/56.0	−2	−1	2.2
City of Toledo (center)	742	558	N39/51/30.0	W4/1/26.0	0	0	0.0
Santillana dam	1958	412	N40/43/36.12	W3/48/54.0	1	0	1.0
Aulencia-Guadarrama junction	1547	383	N40/26/10.0	W4/1/46.0	2	2	2.8
Guadarrama-Va llehermoso junction	931	484	N39/59/50.0	W4/1/46.0	2	2	2.8

Table 1.

The registered image can be seen in figure 1, represented in false color. Such image, and all others appearing in this report, are at scale 1:500.000 with North oriented in their vertical direction.

b) Once registered the subscene a new image was created by the following pixel-values transformation:

$$(1) \qquad I = 16 \, \frac{B5}{B7+1}$$

where B5 and B7 represent bands 5 and 7 of the original subscene. The reason why this ratio was selected, instead of the typical B7/B4, is because the closeness of the rivers in the area of study (less than 80 m wide), the existence of vegetation in the margins and the absence of such vegetation in the rest of the image.

c) Image shown in figure 2 represents the ratio above mentioned, once printed through a DICOMED D-47 film recorder. The idea is to discriminate gray levels of more significance in the quotient image by a radiometric adjustement which takes into account the sensitive response of human eye. A histogram was obtained of the ratioed image with the following results:

mean = 29.27

RMS = 29.70

standard deviation = 5.05

being 98% of the pixels with their values comprised between 15 and 38. Then it was done the following transformation:

$$y = \begin{cases} 0 & , \text{ if } gx + b \leqslant 0 \\ gx + b, & \text{ if } gx + b \geqslant 255 \end{cases}$$

where x is the intensity pixel value obtained from (1) and y is the new value on the transformed image I'. The parameters g (gain) and b (bias) were the following:
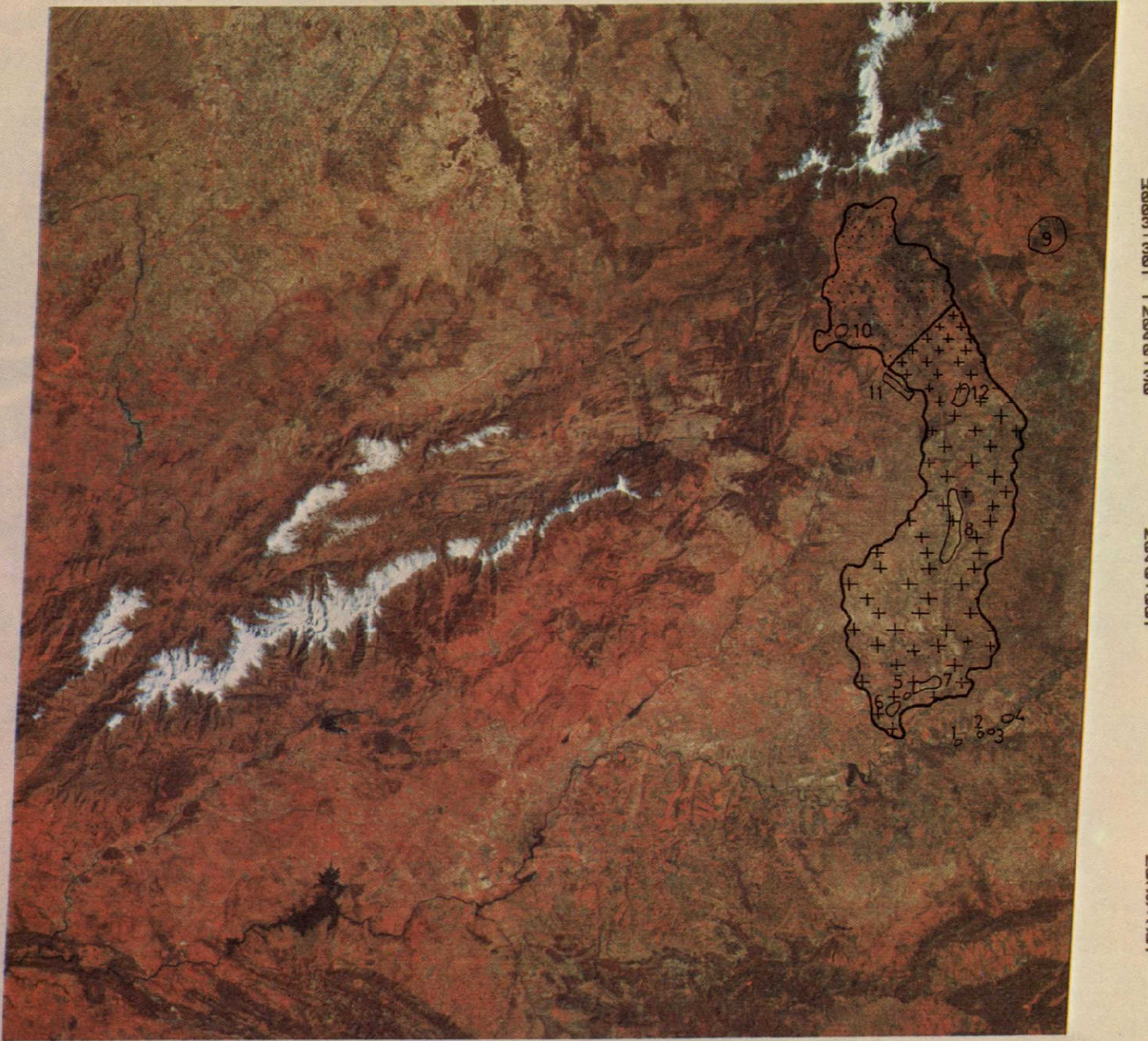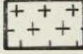
$$g = 12.67 \qquad b = 242.8$$

Crystalline complex

Neogene of Tajo basin

Figure 4.—False colour composite of the Central Region of Spain, indicating the Guadarrama basin and selected test sites where ground truth was obtained

with the resulting characteristic values:

mean = 128.52

RMS = 139.96

standard deviation = 55.40

The new image had 22 gray levels distributed from 0 to 255 radiance values.

d) As a last step this image I' was combined to another image L of identical dimensions, which contained information on the frontiers of the hydrographic basin under study and the limits of the maps at scale 1:50.000. Image L had its pixel values equal to zero, except for those corresponding to the frontier lines, whose values were 255. The process for constructing the combined image was the following:

1 - The limits of the hydrographic basin were digitized from the maps 1:50.000, as well as their corners for a later reference. In this way groups Si of points $(x,y)_i$ are obtained in length units (mm) by reference to the South-West corner of the corresponding map at scale 1:50.000.

2 - The points $(x,y)_i$ of each group Si were converted to geographical coordinates (longitude, latitude), which had been extracted from the maps 1:50.000.

3 - With the image I' registered as reference (once geometrically corrected by control points) it was constructed image L by a trasformation which converted geographical coordinates of the points in the groups Si to coordinates line-pixel. This new image L had the same dimensions than the image I', and its pixels had a null value except for those resulting of the transformation of points $(x,y)_i$ which value 255.

Figure 5.—Band 7 of image 2350-10182, obtained in January 1976
with sun angle elevation of 20°

4 - As a last step, and for a better visualization of the
frontier line in the hydrographic basin on image L,
it was done a process of interpolation between neighbour
pixels resulting from the transformation above mentioned.
Like this it was obtained a continuous line as represen-
tation of the frontier. The algorithm of interpolation
constructed was looking for the necessary points of
the grid in order to obtain a continuous line between
given points Pm and Pn, with the condition that final
points had a minimum distance to the line PmPn.

In the resulting image (figure 3) pixels forming continuous line
do not have the intensity value of 255, as above mentioned, but
their value was chosen for enhancing from the neighbouring pixels.
Like this a better visualization of the frontier line is obtained.
Finally, the discontinuities appearing on such continuous lines
in figure 3 are due to a last process effected on the image,
consisting in a correction by a constant factor $\left[\cos(\text{latitude})\right]$
because during the initial registration the image had been
considered as located in the equator.

3.2. Hydrographic interpretation

Due to the fact that the currents in Guadarrama river and its
tributaries do not attend 80 m in width, the most advantageous
combination was a ratio 5/7, which showed riparian vegetation,
namely on acid terrains, and dry farming crops in light tone.

A different thing happends with the northern part of the basin,
where the presence of prairies and forests in image 5/7 does
not show the drainage network. In this area interpretation was
completed by means of band 7, selecting the black and white
images of higher contrast among those available. Even in such
case the absence of contrast and the closeness of the beds

makes difficult the work, doing it impossible very often.
However, from image no.7(2350-10182) in band 7, taken in
Jannuary 1976 with a "sun elevation" of 20 degrees, the shadow
effect in the North part of the basin (the most mountainous) ·
allows a correct drawing of it in areas where other LANDSAT
images with higher "sun elevation" did not show appropiate.
As example, a comparison can be done of figure 3 with figures 4
and 5.

The ensemble of information extracted on the drainage network
by means of LANDSAT MSS data shows their goodness for producing
synoptic cartography. As comparison are presented here figures
2 and 3 with the hidrographic network superimposed. Figure 2
represents the existing hydrography in Guadarrama basin, as it
appears on the old map at scale 1:500.000 published by I.G.C.
Figure 3 exposes the same drainage network as it is seen from
LANDSAT satellites.

The determination of this network at small scale can be applied
to studies of river bed erosion, problems of solid sediments,
as well as to the study of surficial runoff, from which it is
the major primary exponent. As illustration is presented in
figure 2 the existing network of hydrologic rainfall and flow
metering stations in Guadarrama basin.

3.3. Geologic interpretation

In the basin Guadarrama river exist only two great geological
formations (figure 4). In the upper part of the basin flows
a crystalline system mainly formed by granites and, in a minor
proportion, by metamorphic rocks. In the mouth of Tajo river
and in the opposite margin appear again the granites of Toledo
Mountains. Between both outcrops extends the tectonic basin of
Tajo, occupied by neogene sediments of gravel, arcose, clay,
gypsum and limestone.

The difference between the basement and the deposits of Tajo
basin is very clear in LANDSAT images in all four bands MSS.
However, the limit between both of them is wordy and not precise,
and it can be interpreted only as an extension of the contact
located to the SE, in parallel position to the rivers Alberche
and Perales.

Fracturation of the complex in this basin is not very intense
and the faults, as opposite to the neighbouring basin of Alberche
(to the West), have a scarce length. For this reason they cannot
be interpreted at the scale of LANDSAT images, with the only
exception of one fracture N-S located to the West of Galapagar.

The band of metamophic rocks that, with a general direction
N-S passes by El Escorial, cannot be identified; and the same
happends with the different sediments that form the deposits
of Tajo basin. Geological interpretations of broad areas have
allowed Prof. Alía to define the "Extremenian-Castillian vault"
(1); a megastructure with more than 350 kms length on its major
axis in NE-SW direction. According to such interpretation, the
drainage network of Guadarrama river is related to corresponding
alignements of such vault. One of them should be used by the
Guadarrama itself, experimenting a strong inflexion in the head
waters for attending the city of Avila. The Aulencia river
should likewise follow another essential alignement of the
Extremenian-Castillian vault.

3.4. Forestry interpretation

In a first stage it was intended to evaluate the possibilities
of utilization of the information furnished by LANDSAT satellites,
in relation with the production of forestry thematic cartography

_____

(1) Alía, M.: "Una magaestructura de la meseta ibérica: la bóve
    da Castellano-Extremeña". Estudios Geológicos, 32, 229-238
    (1976).

and its application to the knowledge of several hydrologic variables (runoff, solid contribution, etc).

The Guadarrama basin, from a forestry point of view, has been divided in two areas; one from the river origin (1.800 m) until the spot height of 800 m, the second from 800 m to the mouth of Tajo river. In the first area it can be found the following type of species: Quercus ilex from 800 to 1000 m, Quercus toza from 1200 m to the divisory, Pinus sylvestris and P. pinaster. In the second area the scarce number of trees is represented by Q.ilex.

Initially it was intended the production of cartography of specific masses, and for this purpose it was selected the low area of the basin, South of the axis Brunete-Boadilla del Monte. The reason for this selection was the low influence of relief in the reflectance on that area. Pilot areas have been selected in the holm-oak woods of Batres, Valmojado and Villaviciosa de Odón, and in the reforested pine groves (Pinus pinea) of Naval-carnero and Villaviciosa de Odón. Results, even at level of only one species, do not present any tendency. Histograms, in each MSS band and in their ratios, showed wide intervals of "relative radiance", being superimposed those of different species and without correlation in the case of similar species. As first conclusion it has been established the high influence of the surficial cover of the forest (spread, reforested, etc) in the reflectance. An important factor to consider could be also the small surface of the masses and the rather poor state of them.

Based in such results it was considered a more ample classification which allowed separation of forest masses in conifers and leafy trees. This second possibility was rejected because the low extension of the basin with only a small forest of Q. toza, in the terms of Cercedilla and Navacerrada, which did not

show adequate because its poor vegetative state. In the leafy
trees it can be found the gallery vegetation (vegetation
installed in the riverbed of annual flood), which normally does
not offer a width larger than two pixels and it cannot be used
in training fields.

With such premises, it was intended a classification in two
classes; the first formed by soils covered with trees and the
second formed by soils with farming crops, brushwoods, pastures,
fallow lands and lithosols. In the first class three training
fields of medium vegetation were selected, while in the second
case three others were chosen representing plots of low vegetative
cover, as it can be seen in the enclosed table.

Class	Descriptor	Location	Dominant species
1	M1	)40:14:10:45N) 3:50:50:43W	Q. ilex
1	M2	)40:46:38:07N) 4:03:44:82W	P. pinaster
1	M3	)40:39:15:19N) 4:08:58:20W	P. pinaster
2	D1	)40:33:35:91N) 4:00:17:63W	no vegetative cover
2	D2	)40:09:10:02N) 4:08:29:71W	no vegetative cover
2	D3	)40:11:50:59N) 3:55:01:66W	no vegetative cover

With the purpose of classifying and producing cartography it
was selected an area (Z1) in the lower part of the basin (scarce
influence of relief, which is coincident to the area included
in sheet no.581 of the National Topographic Map at scale 1:50.000),
and another area (Z2) in the upper part (much more influenced by
relief), which is coincident to the area of the basin included
in sheet no.508 of the map.

Results attended with the histograms were positive in all four
bands MSS,.appearing clearly differentiated the "relative
radiances" of soils, with and,without vegetative cover; namely
in band 7, where the reflectance appears comprised between 10%
and 20%. Because the training fields could be spectrally
separated, through the RAMTEK terminal it was done a classifi-
cation of areas Z1 and Z2. Classes 1 and 2 were defined by the
plots M1, M2, M3, and D1, D2 and D3. Blue color was assigned
to class 1, yellow to class 2, and the red was selected for
threshold values.

Results in area Z2 were not enough clear, with a 55% of terrain
not classified, probably due to the influence of relief (high
mountain) and the abundance of pastures (clear mountains).

In the area Z2, results have been satisfactory and in plenty
coincidence with the existing thematic cartography, except in
the mountain of Valmojado; which can be explained because the
poor vegetative state of such area of Quercus ilex. The rest
of the area Z1 appears well classified, with the unique error
of a part of Guadarrama riverside, included as threshold value.
As the trees are holm-oaks an pinus (persistent leafs), this
vegetation of gallery along the river can be defined as Populus,
Salix, Fraxinus, etc).

3.5. Agronomic interpretation

It was intended on image no.2, dated March 8, 1976 to find out
similarities in colors corresponding to identical types of
farming crops. The following working schedule was planned:
a) Selection on the image of spots with identical appearance
   in tonalities.
b) Identification on the ground of the farming crops corresponding
   to such spots.

c) Possible correlation between tonalities and farming crops.

d) Treatment in computer of the acquired information, with the purpose of obtained similar spots of crops existing in the basin.

e) Production of a map representing identical crops to those studied by photointerpretation techniques.

f) Evaluation of the surface occupied by identical crops.

Only steps a) and b) could be accomplished, being phases c) and d) carried out at the moment of submission of this final report. Points selected on the image for identification in the terrain have been indicated in figure 4. The joined table represents their location and description on the National Topographic Map (N.T.M.) at scale 1:50.000 published by I.G.C.

Point	Sheet N.T.M.	Location	Crop
1	629	Western margin Tajo river	Alfalfa
2	629	Western margin Tajo river	Alfalfa
3	629	Eastern margin Tajo river	Alfalfa
4	629	Western margin Tajo river	Alfalfa
5	629	)road Toledo-Torrijos in-)tersection to Guadarrama)river	irrigation land
6	629	dry farming crops	)olive-groves/)vineyards cereals
7	629	dry farming crops	)olive-groves/)cereals
8	604/581	)Eastern margin Guadarra-)ma river	cereals/vineyards
9	534	)around Colmenar Viejo)village	pastures
10	533	El Escorial area	Quercus forests
11	558	)road Villanueva de la)Cañada-Brunete	cereals/stubbles
12	558	mountains	bare soils

The RAMTEK terminal was used with four zones of similar
characteristics as training fields in image no.6. Once obtained
the histograms of the selected areas, it could not be observed
any correlation between them.

4. PROBLEMS

The problems associated to the hydrographic interpretation
depend on the resolution of MSS sensor, which is not the
adequate to the widths of the rivers to be observed in Central
Spain.

Problems in Geological interpretation were related to the small
scale of the images worked with, taking into account the small
area covered by the basin under study.

The agronomic interpretation posed the following problems:

a) None presence of spots with homogeneous color, of size large
   enough for a precise identification.
b) Difficult identification on the terrain of isolated spots,
   unless good points of clear location exist.
c) Difficult location of the corners of training fields when
   selected via cursor through the RAMTEK terminal.

5. DATA QUALITY

The quality of the images furnished by NASA for this project
was, in general, excellent, with good definition and low
presence of cloud cover. Reproduction work of the originals
conducted by I.G.C. showed adequate quality for the purpose
of this work.

The quality of the products obtained through RAMTEK terminal
and DICOMED film recorder was also excellent.

6. CONCLUSIONS

6.1. Treatment of the information

The method for enhancing a geographical accident by means of band ratio techniques applied to LANDSAT images is not new. However, a general knowledge of the area under study allows much better results than by the use of conventional quotients. A radiometric correction of the ratioed image even increases the contrast of the desired geographical accident (2).

It has been explained in this report how a new LANDSAT image was created with known data superimposed. Such data could be ground truth, fields or map borders, etc.

6.2. Hydrography

In the aspect of hydrographic interpretation it can be stated the speed accuracy obtained in the delineation of drainage networks at a synoptic scale from LANDSAT images with adequate processing. It is considered of the maximum interest for C.E.H. the knowledge of such networks, their lengths, densities, and all physical patterns detected by the satellite on this subject.

6.3. Geology

Although conclusions obtained by geological interpretation of the basin are really poor and not spectacular from a lithological point of view, it is recognized the great interest that inter- pretation of other areas could have, even on the same image. In the structural aspect the conclusions of the method are, on the contrary, important from the point of view of the megastructures, although not in the area under study.

_____

(2) A. Santisteban. "Study of radiometric enhancement methods applied to LANDSAT MSS images", Final Report, NASA project no.28760. IBM-Scientific Center, Autonomous University of Madrid.

6.4. Forestry

Because the characteristics of the mediterranean forest masses
of Spain, imposed by the climat and their treatment, it seems
that the closeness has a higher influence than the spectral
properties of reflectance in each species, being still a long
way until the automatic classification of species could be done.

The classification in soils with and without vegetative cover
appears clear in flat terrains, although relief, subalpine
pastures and atlantic pastures produce a masking of the spectral
response of forests. From the point of view of protecting the
terrain (fight against erosion), it is convenient to dispose
of real cartography updated.

In the future it is intended to accomplish the following working
program:

- identification of shrubs
- classification of the different types of forests and thickets
- digitizing of level curves to be introduced through the
  RAMTEK terminal for evaluating the influence of sun elevation
  in areas of strong relief

- automatic classification of species, densities and development
  of them
- evaluation of the flooded surfaces by means of the vegetation
  of gallery and possible profit of them for cultivating species
  of fast growing woods (black poplars)

6.5. Agronomy

The agronomic application of LANDSAT images is considered
important and useful, whenever exists the possibility of checking
the space acquired observations with direct observations on the

ground, namely in real time or as closed as possible to the date of LANDSAT overpass. Concerning the RAMTEK terminal, it is so powerful that even broad areas with the same type of farming crops are displayed in different form, problably due to the following reasons:

a) phenological states of crops

b) density of sowing

c) variety

d) type of soil

These factors make difficult the current application to agronomy of LANDSAT information at the resolution envisaged today by MSS sensor.

6.6. Epilogue

From the point of view of integrating the types of interpretations here exposed, it is considered that a continuous use of LANDSAT images and the processing techniques here considered, should contribute to obtaining, in a short time and at a reasonable cost, the information required for characterizing hydrographic basins. Thus it is desirable to continue the studies here started for a better application in Spain of the LANDSAT information furnished under this project to the multidiscipli-nary group involved.

NASA EARTH RESOURCES TECHNOLOGY SATELLITE